DTU Library

Development and application of measurement techniques for quantifying methane and ammonia emissions from livestock production

Vechi, Nathalia Thygesen

Publication date:
2023

Document Version
Publisher's PDF, also known as Version of record

DTU Sustain
Department of Environmental and Resource Engineering

Development and application of measurement techniques for quantifying methane and ammonia emissions from livestock production

Nathalia Thygesen Vechi

PhD Thesis

Development and application of measurement techniques for quantifying methane and ammonia emissions from livestock production

Nathalia Thygesen Vechi

PhD Thesis
May 2023

DTU Sustain
Department of Environmental and Resource Engineering
Technical University of Denmark

Development and application of measurement techniques for quantifying methane and ammonia emissions from livestock production

Nathalia Thygesen Vechi

PhD Thesis, May 2023

The synopsis part of this thesis is available as a PDF file for download from the DTU research database ORBIT: http://www.orbit.dtu.dk.

Address:	DTU Sustain Department of Environmental and Resource Engineering Technical University of Denmark Bygningstorvet, Building 115 2800 Kgs. Lyngby Denmark
Phone reception:	+45 4525 1600
Homepage:	https://www.sustain.dtu.dk
E-mail:	info@sustain.dtu.dk

Cover:	STEP

Preface

This thesis was completed at the Department of Environmental and Resource Engineering of the Technical University of Denmark (DTU) under the supervision of Professor Charlotte Scheutz and Professor Johan Mellqvist from Chalmers University. The PhD project was conducted from December 2018 to March 2023. The thesis is organised in two parts: the first puts into context the findings of the PhD in an introductive review, whilst the second part consists of the papers listed below. These will be referred to in the text by their paper number, written with the Roman numerals **I-VI**.

I **Vechi, N.T.**, Mellqvist, J., Scheutz, C., (2022). Quantification of methane emissions from cattle farms, using the tracer gas dispersion method. *Agriculture, Ecosystems & Environment*, *330*, 107885. https://doi.org/10.1016/j.agee.2022.107885

II **Vechi, N.T.**, Jensen, N.S., Scheutz, C., (2022). Methane emissions from five Danish pig farms: Mitigation strategies and inventory estimated emissions. *Journal of Environmental Management*, *317*, 115319. https://doi.org/10.1016/j.jenvman.2022.115319

III **Vechi, N.T.**, Scheutz, C., (2023). Measurements of methane emissions from manure tanks using a stationary tracer gas dispersion approach. *Submitted to Biosystems Engineering*

IV **Vechi, N.T.**, Falk, J.M., Fredenslund, A.M., Edjabou, M.E., Scheutz, C., (2023). Methane emission rates averaged over a year from ten farm-scale manure storage tanks. *Submitted to Journal of Environmental Management*

V **Vechi, N.T.**, Mellqvist, J., Samuelsson, J., Offerle, B., Scheutz, C., (2023). Ammonia and methane emissions from dairy concentrated animal feeding operations in California, using mobile optical remote sensing. *Atmospheric Environment*, *293*,119448.https://doi.org/10.1016/j.atmosenv.2022.11948

VI Mellqvist, J., **Vechi, N.T,** Scheutz, C., Durif, M., Gautier, F., Johansson, J., Samuelsson, J., Offerle, B., Brohede, S., (2023). An uncertainty methodology for solar occultation flux measurements: ammonia emissions from agriculture. *Manuscript*

In addition, the following publications, not included in this thesis, were also concluded during this PhD study.

VII **dos Reis Vechi, N.,** Delre, A. and Scheutz, C.: Assessment of methane emissions from Danish livestock production practices using a tracer gas dispersion method, EGU General Assembly 2020, Online, 4–8 May 2020, EGU2020-20405, https://doi.org/10.5194/egusphere-egu2020-20405, 2020.

VIII **Vechi, N.T.,** Mellqvist, J., Offerle, B., Samuelsson, J. and Scheutz, C.: Mobile Optical Remote Sensing for quantification of Ammonia and Methane emissions from Dairy Farms in California., EGU General Assembly 2021, online, 19–30 Apr 2021, EGU21-10911, https://doi.org/10.5194/egusphere-egu21-10911, 2021.

IX Mellqvist, J., Samuelsson, J., Offerle, B., **Vechi, N.T.,** Ericsson, M.,: Characterization of Air Toxics and GHG Emission Sources and their Impacts on Community Scale Air Quality Levels in Disadvantaged Communities, 2020, Report to CARB contract no. 17RD021.2021, https://ww2.arb.ca.gov/sites/default/files/2021-03/17RD021.pdf

Acknowledgements

I would like to express my gratitude to everyone who contributed to this thesis. It has been an intense, gratifying, and interesting journey until here. Thank you to the DTU and the Nordic five tech program for my scholarship and "Mind the Graph" for some of the illustrations. More importantly, thanks goes to my supervisors, Charlotte Scheutz and Johan Mellqvist, for the opportunity to work and learn with them. Thank you for teaching me, sharing your knowledge, keeping me motivated, and always finding time to help and discuss results with me.

Thank you to my colleagues from Fluxsense, Brian, Jerker, John, Pontus, and Samuel. Thank you for being patient and helping me even at a distance. It was great to participate in fieldwork with you.

I should thank my colleagues from DTU, Antonio for teaching me the TDM method, Vincent for assisting me in many measurement campaigns and manure sampling, and Anders and Julie for helping in the field in the results discussions. Thank you to my office mate Konstantinos with whom I could share my frustrations about the instruments and who was always there to help me. Thanks to my other colleagues, which supported me in some form Anastasia, Zhenhan and Nina.

My gratitude also goes to the farmers, which allowed me to investigate the emissions from their farms and kindly replied to questions, which were many. Special thanks go to Lars Kristian Mikkelsen, who helped me find farmrs for the study and showed enthusiasm for my work, and took the picture in this cover of this thesis.

Finally, I would like to thank my family, Mads and Hugo, who have shared me with this thesis this last few months and have always encouraged me to continue. I dedicate this thesis to my parents for all the unconditional support and dedication they have for me.

Summary

Agricultural production is set to grow substantially in the coming years, so reducing its environmental impacts is vital. Agriculture's contribution to ammonia (NH_3) and methane (CH_4) gaseous emissions is significant, especially from livestock production. Investigating these emission sources, using atmospheric measurement techniques, helps gather knowledge about emission rates, the factors driving them and the efficiency of mitigation strategies. However, measuring these sources is still limited to intrusive methods and small-scale experiments or restricted to the type of animal production (e.g., mechanically ventilated barns). Consequently, there is a need to provide alternative methods, especially ones that are easier to apply and can provide accurate emission levels.

Thus, the overall aim of this PhD is to develop and apply methods for quantifying NH_3 and CH_4 emissions from livestock production. CH_4 emissions were measured via the tracer gas dispersion method (TDM) and the indirect flux method (IFM). Emissions from cattle production in Denmark and the USA were studied, while pig farms were investigated only from Denmark. Furthermore, NH_3 emissions were measured from dairy production facilities in the USA. The methods were primarily designed to assess emissions from the entire farm, so a stationary approach to the TDM method was refined, by sampling concentrations downwind from the source at fixed points placed in a field, decreasing dependency on driving along roads.

In Denmark, CH_4 emission rates at nine cattle farms ranged from 0.7 to 28 kg/h. CH_4 rates were then normalised per livestock unit (1 LU = 500 kg of body weight), averaging 23 ± 9 g/LU/h. The farms with the most significant emission factors (EFs) were those with deep litter animal houses with long eating spaces. Moreover, CH_4 emission rates from seven pig farms also ranged across a similar scale (0.2 to 20 kg/h). After converting rates to EFs, farms with no manure treatment averaged between 13 ± 6 and 18 ± 9 g/LU/h, whilst farms storing digested manure averaged an EF of 8 ± 7 g/LU/h. In addition, in-house manure acidification was used at two other farms, with average EFs of 2 ± 1 g/LU/h. Measurements were distributed over the year, and emission fluctuations over the months were more significant at pig than at cattle farms, although emission patterns were the same. Furthermore, measured emissions were higher for all farms than the modelled inventory rates, albeit, for cattle farms, inventory es-

timates and measured rates were within uncertainty levels at most of the studied sites. Conversely, inventory quantifications greatly underestimated pig farms' CH_4 rates.

Furthermore, CH_4 emission rates from ten manure tanks were quantified using mobile and stationary TDMs by running a minimum of six measurement campaigns over the year. Emissions from pig manure were highest, while digested manure had the lowest EFs. The rates varied from 0.01 to 14.3 kg/h. Average annual rates, normalised by manure stored, for all tanks ranged from 0.2 g/m^3/h to 2.7 g/m^3/h, with pig manure storage showing significant variability among the different tanks. Additionally, covered tanks had higher emissions than uncovered tanks.

Moreover, NH_3 and CH_4 emissions were quantified at 14 dairy concentrated animal feeding operations (CAFOs) in California, using SOF and MeFTIR, respectively. An error budget analysis showed that this techniques had an averaged uncertainty of 37% and 53%, for NH_3 and CH_4 quantifications, respectively. Emission rates ranged from 155 to 874 kg/h for CH_4 and 32 to 191 kg/h for NH_3. Average EFs for the dairies were 40 ± 18 g/LU/h for CH_4 and 9 ± 3 g/LU/h for NH_3. Measurements were only performed in May and October, and variations between the measurements were minimal, as the farms operated in similar temperature conditions. NH_3 measurements were limited to the daytime, albeit emissions for this gas still demonstrated diurnal variations over this measurement time. Similarly, we observed NH_3-to-CH_4 ratio diurnal variability. Modelled NH_3 emissions were similar to those measured when a diurnal emissions model was used. For CH_4, modelled emissions were lower than measured emissions; however, a lack of knowledge about manure management at the specific farms influenced the comparison. Finally, the methods employed herein were valuable tools for investigating livestock CH_4 and NH_3 emissions. They captured emission fluctuations over a complete year, as well as the efficiency of two different CH_4 mitigation system, and helped identify factors affecting CH_4 manure emissions.

Dansk sammenfatning

Landbrugsproduktion forventes at vokse betydeligt i de kommende år, derfor er det afgørende at reducere dens miljøpåvirkninger. Landbrugets bidrag til ammoniak (NH_3) og metan (CH_4) gasemissioner er stor, især fra husdyrsproduktion. At undersøge disse emissionskilder ved hjælp af atmosfæriske måleteknikker bidrager med at indsamle viden om emissionsrater, de faktorer der driver dem og effektiviteten af afbødningsstratregier. Måling af disse kilder er stadigt begrænset til tilgængelige metoder og småskalaforsøg, eller begrænset af typen af animalsk produktion (f. eks. Mekanisk ventilerede stalde). Derfor er der behov for finde alternative metoder, især dem, der er lettere at anvende og kan give nøjagtige emissionsniveauer.

Det overordnede formål med denne ph.d. er at udvikle og anvende metoder til at kvantificere NH_3 og CH_4 emissioner fra husdyrproduktion. CH_4 emissioner blev målt via sporgasmetoden (TDM) og den indirekte fluxmetode (IFM). Emissioner fra kvægproduktion i Danmark og USA blev undersøgt, mens kun danske svinefarme blev undersøgt. Desuden blev NH_3 emissioner målt fra mejeriproduktionsanlæg i USA. Metoderne var primært designet til at vurdere emissioner fra hele gårdens drift, så en stationær tilgang til TDM-metoden blev optimeret, gennem prøvetagning af koncentrationer nedvind fra kilden, ud fra faste punkter placeret på en mark, hvilket mindskede afhængigheden af kørsel langs veje.

I Danmark lå CH_4 emissionsraterne på ni kvægbrug fra 0.7 til 28 kg/t. CH_4 rater blev derefter normaliseret pr. husdyrenhed (1 LU = 500 kg kropsvægt), i gennemsnit 23 ± 9 g/LU/t. Bedrifterne med de største emissionsfaktorer var dem med dybstrøelseshuse med lange spisepladser. Desuden varierede CH_4 emissionsraterne fra syv svinebedrifter også over en lignende skala (0.2 til 20 kg/t). Efter omregning til emissionsfaktorer, havde bedrifter uden gødningsbehandling i gennemsnit mellem 13 ± 6 og 18 ± 9 g/LU/t, mens bedrifter, der opbevarede afgasset gylle, i gennemsnit havde en emissionsfaktor på 8 ± 7 g/LU/h. Derudover blev der anvendt egen forsuret gylle på to andre gårde, med gennemsnitlige emissionsfaktorer på 2 ± 1 g/LU/h. Målingerne var fordelt over året, og emissionsudsving over månederne var støre hos svinebedrifter end hos kvægbedrifter, selvom emissionsmønstrene var de samme. Ydermere var de målte emissioner højere for alle bedrifter end de modellerede opgørelsesrater, omend for kvægbrug var opgørelsesestimater og målte rater inden for usikkerhedsniveauer på de fleste af de undersøgte lokaliteter. Omvendt undervurderede lagerkvantificeringer i høj grad svinebedrifternes CH_4 rater.

Endvidere blev CH_4 emissionsraterne fra ti gødningstanke kvantificeret ved hjælp af mobile og stationære TDM'er, ved at køre minimum seks målekampagner i løbet af året. Emissioner fra svinegylle var højest, mens forsuret gylle havde de laveste emissionsfaktorer. Satserne varierede fra 0.01 til 14.3 kg/t. Gennemsnitlige årlige rater, normaliseret efter oplagret gødning, for alle tanke varierede fra 0.2 g/m^3/h til 2.7 g/m^3/h, hvor svinegylleopbevaring viste betydelig variation mellem de forskellige tanke. Derudover havde overdækkede tanke højere emissioner end ikke-overdækkede.

Desuden blev NH_3 og CH_4 emissioner kvantificeret ved 14 mejerikoncentrerede dyrefodringsoperationer (CAFO'er) i Californien ved hjælp af henholdsvis SOF og MeFTIR. En fejlbudgetanalyse viser at denne teknik havde en gennemsnitlig usikkerhed på 37 % og 53 % for henholdsvis NH_3 og CH_4 kvantificeringer. Emissionsraterne varierede fra 155 til 874 kg/t for CH_4 og 32 til 191 kg/t for NH_3. Gennemsnitlige emissionsfaktorer for CAFO'er var 40 ± 18 g/LU/t for CH_4 og 9 ± 3 g/LU/t for NH_3. Målinger blev kun udført i maj og oktober, og variationerne mellem målingerne var minimale, da gårdene bedrifter var under lignende temperaturforhold. NH_3 målinger var begrænset til dagtimerne, selvom emissioner for denne gas stadig viste daglige variationer over denne måletid. Tilsvarende observerede vi i NH_3 til CH_4 forhold daglig variabilitet. Modellerede NH_3 emissioner svarede til dem, der blev målt når en daglige emissionsmodel blev brugt. For CH_4 var modellerede emissioner lavere end målte emissioner; manglende viden om gyllehåndtering på de konkrete bedrifter påvirkede dog sammenligningen. Endelig var de heri anvendte metoder værdifulde værktøjer til undersøgelse af husdyrs CH_4 og NH_3 emissioner. De målte emissionssvingninger over et helt år, såvel som effektiviteten af to forskellige CH_4 reduktionssystemer, og hjalp med at identificere faktorer der påvirker CH_4 gødningsemissioner.

Table of contents

1 Introduction

1.1 Background

About 30 years ago, the first United Nations framework convention on climate change was signed. Since then, the earth's temperature has continued to increase to the point that the threshold of 1.5 °C warming is almost inevitable and set to be reached within the next decades (IPCC, 2022). Agro-food systems account for 31% of total anthropogenic greenhouse gas (GHG) emissions (FAO, 2022), 46 %of which derive from farms. CH_4 is a GHG with a warming potential approximately 28 times worse than carbon dioxide (CO_2) (IPCC, 2022). Moreover, it has a short lifetime in the atmosphere (~ 12 years), so the impact of CH_4 emission reductions is noticed faster than a decrease in CO_2 emissions (IPCC, 2022). CH_4 emissions from livestock production alone correspond to 5.8% of total GHG emissions (Climate watch, 2022). Country-specific contributions vary according to their economic activities; for instance, in the USA, CH_4 emissions from livestock production make up 4% of total GHG emissions (EPA, 2023), while in Denmark, they sum up to 13% (Nielsen et al., 2021). The contribution of each livestock type globally is 35%, 30% and 10% for beef cattle, dairy cattle and pigs, respectively (Herrero et al., 2016).

Likewise, agriculture is a major source of NH_3 emissions (~ 85%) (EDGAR database, 2023) – a process strongly influenced by climate (Sutton et al., 2013). Livestock manure alone corresponds to 13-25% of total NH_3 emissions globally (Sutton et al., 2013), which affect ecosystems by causing eutrophication and by being an indirect GHG. Additionally, NH_3 is a hazard to human health due to the formation of fine particulate matter ($PM_{2.5}$) and its subsequent reaction with acid molecules in the atmosphere. Long-term exposure to $PM_{2.5}$ can affect the lungs and cause premature death (Wyer et al., 2022). Moreover, because NH_3 is a reactive particle, its lifetime in the atmosphere is short (hours to days), depending on atmospheric conditions (Wu et al., 2008). The fate of NH_3 also includes dry and wet deposition, which increases complexity and makes it challenging to model and measure (Zhu et al., 2015a).

NH_3 emissions from livestock are regulated, to some extent, under EU law (NEC 2016/2284) by reporting and monitoring emissions in sensitive habitats and limiting emissions from certain facilities (Wyer et al., 2022). In Denmark, NH_3 legislation is strict, in that farmers must use housing systems and environmental technologies that ensure emissions in this regard are reduced (Bjerg et al., 2019). Additionally, liquid manure storage tanks need to be covered, following recommendations from the Environmental Protection Agency's technology list (Ministeriet for Fødevarer Landbrug og Fiskeri, 2021). Pig manure storage should have a fixed cover, with documented reduction efficiencies relating to NH_3 and odour when located near residential areas (Ministeriet for Fødevarer Landbrug og Fiskeri, 2021).

Climate laws started to emerge in European countries in the last decade, with the intention of achieving short- and long-term goals in relation to carbon neutrality; Denmark was one of the pioneers in this regard (Duwe and Evans, 2020). Particularly in agriculture, there is a new initiative on imposing CO_2 taxes on farms with the aim of reducing GHG emissions, which will further ensure an emission reduction of 55 to 65% of emissions from agriculture and forest sector, by 2030 (Svarer et al., 2022). Additionally, it should be emphasised that Denmark has a quality reporting system for agricultural practices whereby farmers have to document every animal, feed purchase and fertiliser used (Wirsenius et al., 2020). In the USA, the California State Senate recently passed a Bill (SB1383 Lara, Chapter 395, 2016) through the California Air Resources Board (CARB) calling for implementing mitigation strategies to reduce 40% of CH_4 emissions from the livestock sector by 2030 (State of California, 2016).

Nonetheless, research has pointed out that global livestock CH_4 emissions are 11% greater than estimates based on IPCC-modelled emission factors (EFs), with the most significant errors in manure management emissions (~ 36.7%) (Wolf et al., 2017). Similar studies have shown the same model underestimations for NH_3 emissions (Nowak et al., 2012; Van Damme et al., 2018). Models used to predict CH_4 and NH_3 emissions suffer from narrow spatial focus and limited observations (Hristov et al., 2018), which convert to uncertainties about the impact of different factors controlling emissions (Hassouna et al., 2022). Models need to be sharpened to estimate emissions used in legislation and climate agreements, and hence techniques for emissions monitoring should be developed and well-documented to provide models with important data. Moreover, measuring CH_4 and NH_3 livestock emissions is essential for implementing and documenting new management or mitigation strategies. There is no ideal method for these emission quantifications, however, because there are different farm management strategies (e.g., open and closed animal houses), spatial and temporal methodology limitations and measurement uncertainties (Tedeschi et al., 2022). Therefore, there is a need to expand the measurement techniques toolset, and methods not commonly used to quantify livestock emissions should also be tested, in order to determine their suitability for these sources. The focus should thus be on non-intrusive methods that quantify fugitive farm-scale emissions. The mobile tracer gas dispersion method (TDM) has been extensively used to quantify emissions from landfills (Galle et al., 2001; Scheutz et al., 2011), biogas plants (Scheutz and Fredenslund, 2019) and wastewater treatment plants (Delre et al., 2018), and it has been applied in a short-term study at a dairy farm (Arndt et al., 2018). Solar occultation flux (SOF) is another method that has been applied minimally to quantify NH_3 emissions from livestock (Kille et al., 2017), but instead it has been widely used to quantify industrial VOC and alkenes emissions (Johansson et al., 2014; Mellqvist et al., 2010). In addition, SOF combined with ratio measurements results in another method that can be used to simultaneously measure CH_4, known as the indirect flux method (IFM).

Therefore, in this study, we investigate additional applications of TDM, SOF and IFM on livestock emissions. In addition to method development and demonstrations, quality data on livestock emission rates was obtained, which can be further used to expand knowledge about farm-based CH_4 and NH_3 emissions. Measurements were performed in different two countries, namely Denmark and in the USA, and so the results should reveal a broad picture of these emissions.

1.2 Aim of the study

The overall objective of this project was to develop and apply methods to quantify CH_4 and NH_3 emissions from livestock production. It covers whole-farm and manure tank CH_4 emissions from pigs and cattle in Denmark. In addition, NH_3 and CH_4 emissions from dairy-concentrated animal feeding operations (CAFOs) in the USA (California) were studied. The farms' manure management systems and climates are different in both countries. The research questions are as follows:

- Are TDM, IFM and SOF suitable for studying CH_4 and NH_3 emissions from livestock production? (Papers **I-VI**)
- What are the CH_4 emission rates and emission factors (EFs) for Danish cattle and pig farm production, and Californian dairy CAFOs? Additionally, what are the NH_3 emission rates and EFs for Californian dairy CAFOs? (Papers **I**, **II** and **V**)

- What is the CH_4 emissions reduction caused by mitigation methods (biogas and acidification) used Danish farms? (Papers **I**, **II**, **IV** and **V**)
- What are the main factors affecting CH_4 emissions from manure storage tanks? (Paper **IV**)

The method development part of the project is described in Papers **III** and **VI**. The quantification of emissions from manure storage tanks, using TDM, is often restricted by limited road availability; therefore, a study of a new stationary TDM approach was tested (Paper **III**). In paper **VI**, the uncertainty and application of the SOF method for quantifying NH_3 emissions was assessed. Furthermore, method application is the focus of Papers **I**, **II**, **IV** and **V**. The TDM was applied to quantify whole-farm emissions from dairy and beef cattle units in Denmark (Paper **I**). Later, similar work was done for whole-farm emissions at Danish pig farms (Paper **II**), at which point different migration strategies were also investigated. Using the mobile and stationary TDM (Paper **III**) method, ten manure tanks were investigated for a year to verify factors affecting CH_4 emissions (Paper **IV**). Finally, we used the SOF and IFM methods to quantify NH_3 and CH_4 emissions from California dairy CAFOs (Paper **V**).

Based on the measurement methods' characteristics (e.g., medium- spatial coverage, discrete sampling) and limitations (e.g., weather conditions), we defined the approach of our study. In addition, the state of the art lacks measurements of whole-farm emissions from dairy and pig facilities as well as comparisons between units using the same emission measurement methodology. Therefore, in this project, measurements were repeated (six times for TDM and two for SOF and IFM) at several facilities (16 Danish farms, 14 Californian CAFOs) instead of focusing on many more measurements at one or two farms.

2 CH_4 and NH_3 emissions

This chapter provides an overview of CH_4 and NH_3 emissions from cattle (dairy and beef) and pig farms. It summarises the current knowledge on emissions, focusing on management systems used on Danish and Californian farms. Furthermore, the most common methods used to measure these emission sources are discussed.

2.1 CH_4 emissions from livestock production

Livestock CH_4 emissions are produced via two different mechanisms: (1) enteric fermentation and (2) manure degradation. Emissions from the first process come directly from animals' digestive systems, whilst in the second, CH_4 is produced during the anaerobic decomposition of organic matter in the animal manure during storage. The proportion of enteric and manure emissions in a farm varies according to the type of production (e.g., cattle and pig), farms' management choices and climate conditions.

Ruminants have a digestive system that allows for breaking down large carbohydrate molecules into small ones via fermentation (Palangi et al., 2022). CH_4 is produced according to the animal energy feed utilisation, approximately 12% of which is lost as CH_4 (Palangi et al., 2022). Enteric emissions from cattle depend on genetic factors (Løvendahl et al., 2018), age (e.g., calve, heifer, adult cow), production (e.g., milk, beef) (Ellis et al., 2007) and more importantly on dry matter intake (DMI) and diet composition (e.g., amount of fibre and oils) (Ricci et al., 2013).

CH_4 emissions from manure are produced by anaerobic digestion (AD) processes. The magnitude of CH_4 manure emission depends on manure composition (Hilgert et al., 2022; Petersen et al., 2016), environmental conditions (Cárdenas et al., 2021) and the type of management used at the farm (IPCC, 2006; Kupper et al., 2020), all – or a combination – of which are often interconnected.

Regarding environmental conditions, manure temperature is an essential parameter in CH_4 production because it is connected to microbiological activity. However, temperature is a result of local climate, the frequency and time (e.g., autumn, summer) of manure removal and the size and format of storage solutions (Rennie et al., 2018). The relationship between temperature and CH_4

emissions is exponential (Mangino et al., 2001), so a few degrees above a certain threshold can significantly affect CH_4 emissions, whilst changes at low temperatures will have minimal impacts. Sommer et al. (2007) observed that CH_4 emissions for manure temperatures below 15 ºC were insignificant, while at 20 ºC they were almost one magnitude higher. Additionally, Cárdenas et al. (2021) found that CH_4 production was consistently low below the threshold of 13.9 ºC. Other factors associated with manure composition, such as total solids (Qu and Zhang, 2021), volatile solids (Sommer et al., 2004) and pH level, affect CH_4 production and emissions. Inhibition of the microbial community by chemicals, such as hydrogen sulphide (H_2S), might also occur, although research in this area is lacking (Dalby et al., 2021).

Regarding the management of manure, many farms have shifted to liquid manure systems (dry matter < 12%) (Sommer et al., 2013). In Denmark, dairy cattle are placed inside of a house, typically with loose-holding and a slatted floor lined with straw or sand beds. Dairy manure is collected under the animal house and then moved to storage tanks, which are subsequently emptied one or two times a year (Figure 1). Californian dairy CAFOs usually also keep animals in open houses, where the manure is excreted and removed by flushing into anaerobic lagoons (Figure 1). Anaerobic lagoons should be emptied once a year. The described management systems correspond only to lactating cows, and so heifers and calves might be managed differently. Furthermore, on Danish organic farms, milk cows spend part of their day grazing outside during the summer (~ 7 hours over 196 days).

CH_4 emission sources on a farm are animal houses and manure storage units, such as tanks and lagoons. In the former, CH_4 is produced by both enteric fermentation and manure degradation. Most of the research into emissions from livestock production measures emissions from either manure storage units or animal houses, while only a few apply measurements to whole-farm emission studies.

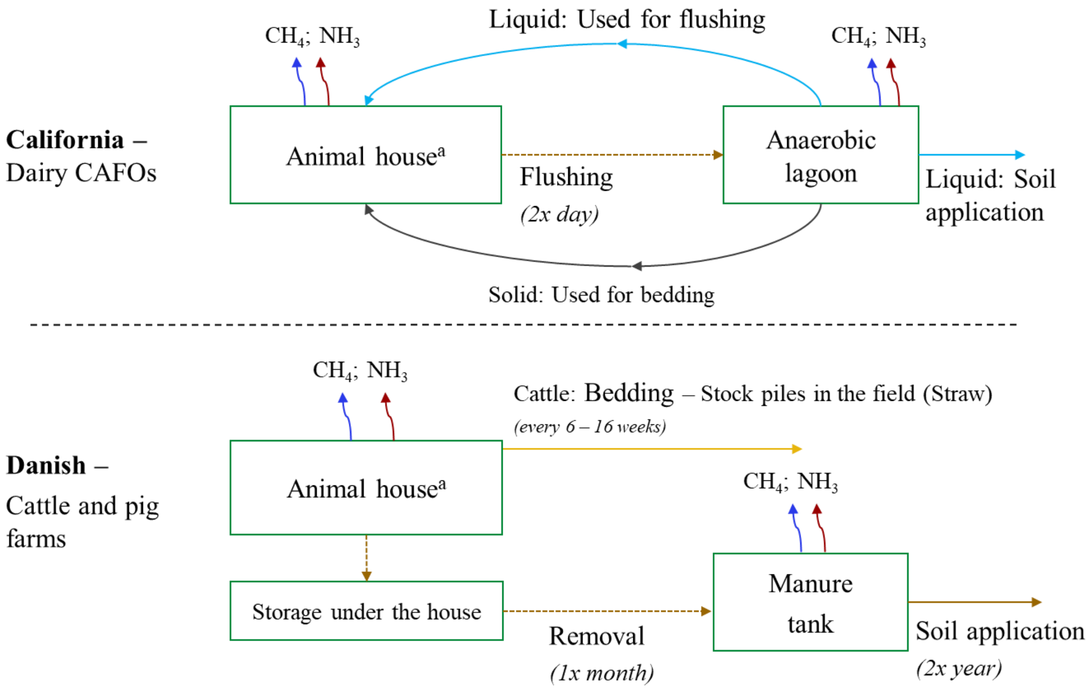

Figure 1: Simplified typical management schemes at Danish pig and cattle farms and Californian CAFOs. On Danish farms, manure is usually stored under the animal house and transferred to an outdoor storage tank once a month. In California, dairy farms recycle water from an anaerobic lagoon to flush the animal house, which is then transferred back to the anaerobic lagoon. [a]Dairy CAFOs animal houses are naturally ventilated, similar to most of the dairy and beef in Denmark, while pig houses are most often mechanically ventilated.

2.1.1 Dairy and beef farm emissions

A recent initiative has created a global database (DATAMAN) of NH_3, N_2O and CH_4 EFs from both animal house and manure storage facilities, collecting approximately 394 CH_4 EFs (Hassouna et al., 2022). For comparison herein, CH_4 EFs covering cattle production normalised by either livestock unit (1 livestock unit = 500 kg of body weight) or by the number of animals were 11.72 ± 5.35 g/LU/h and 21.16 ± 15.13 g/animal/h. These EFs account for enteric and manure emissions in the house, although the contribution from the last one should vary according to the type of floor (e.g., slatted, solid), bedding and climate. Enteric emissions from cattle alone have been reported as varying from 3.2 to 19.6 g/animal/h (Ricci et al., 2013).

The contribution of manure emissions from cattle farms located in temperate regions should be around 15-20% of total emissions (Petersen, 2018). However, in warmer climates, such as in California, manure emissions can be as high as 50% of all farm emissions (Owen and Silver, 2015). In addition to climate conditions, Californian farms are expected to produce higher emissions from manure management due to anaerobic manure lagoons, while in Europe most countries use concrete storage tanks (Wirsenius et al., 2020). Only a few studies have measured CH_4 emissions from whole cattle farms (Arndt et al., 2018; Bjorneberg et al., 2009; Leytem et al., 2011; VanderZaag et al., 2014), and most have focused on North American farms, while only a few have looked at European farms (Amon et al., 2001; Bühler et al., 2021; Hensen et al., 2006); however, measurements over different seasons are still in short supply in some of these studies.

2.1.2 Pig farm emissions

CH_4 emissions from pig farms originate from manure and enteric mechanisms; however, a pig's digestive system is monogastric, so they produce much less CH_4 via enteric fermentation (~ 1.5 g/head/day (IPCC, 2006)) than a ruminant (~ 150 g/head/day (IPCC, 2006)). Similarly to cattle farms, physical CH_4 emission sources at pig farms are animal houses (manure and enteric processes) and manure storage. There are mainly two types of pig farms, namely breeding and growing production. The first involves sows producing piglets, accounting for approximately 14% of Danish pig farms (Danish Agriculture & Food Council, 2020). Piglets are then grown on to become weaners and then transferred to growing farms, where they arrive at approximately 30 kg in body weight and grow up to 110 kg over a 12-week cycle; these are called "fattening pigs" (~ 42% of Danish farms) (Danish Agriculture & Food Council, 2020). Other farms are a blending of both pig types.

Pig animal house emissions have been studied, as pigs are kept in closed housing systems that are often mechanically ventilated, thereby making them easier to measure. The contribution of CH_4 from manure and from enteric emissions will vary according to the animal's age, feed intake (Philippe and Nicks, 2015), house management (e.g., frequency of manure removal), temperature and ventilation rate (Blanes-Vidal et al., 2008; Haeussermann et al., 2006). EFs from animal houses are expected to be approximately 5.0 ± 5.3 g/LU/h (Hassouna et al., 2022, Paper **II**).

After being stored in the animal house, manure is transferred to outdoor storage concrete tanks. CH_4 emissions from these tanks have been studied (Husted, 1994; Kaharabata and Schuepp, 1998; Loyon et al., 2016; VanderZaag et al., 2022), but they are still limited. CH_4 EFs from pig manure tanks are on average 1.39 ± 1.47 g/m^3/h (Hassouna et al., 2022) or 4.29 ± 2.85 g/LU/h (Paper **II**).

Emissions from manure storage at pig farms (animal house and outdoor storage) are expected to contribute to as much as 80% of a farm's total emissions (Paper **II**). Nonetheless, to our knowledge, no study has quantified total fugitive emissions from an entire pig farm.

2.2 Mitigation of CH_4 emissions

Reducing CH_4 emissions from livestock is essential to preventing the effects of climate change. Several strategies can be applied to mitigate emissions from both enteric and manure production. CH_4 manure emission mitigation strategies studied in this thesis (Papers **I**, **II**, **IV** and **V**) are the focus of this subsection, as no enteric or NH_3 mitigation approach was directly studied herein.

Liquid manure management produces CH_4 via AD, and the produced CH_4 can be collected and used as energy. On-site solutions vary from simply covering manure storage facilities (e.g., lagoons (Paper **V**)), to centralised biogas plants, to where manure from several farms is digested with other feedstock. In this last type of setup, the digested manure returns for storage in tanks at the farms providing the manure. This system has been used in Denmark more frequently over the last few years (Papers **I**, **II** and **IV**), and in 2020, 17% of dairy and 14% of pig manure produced in the country was sent to biogas plants (Nielsen et al., 2022). The mitigation efficiency of storing digested manure instead of raw manure has been reported at 85% (Maldaner et al., 2018), while other study has seen a higher CH_4 production from stored digestate than the raw manure (Rodhe et al., 2015).

Manure acidification is one of the most promising mitigation strategies for reducing CH_4 and NH_3 emissions and the capacity to use this systems is installed at 20% of Danish farms (Jensen et al., 2018). The principle consists of reducing the manure's pH, which affects the mechanisms producing both gases. The acid can be added to the storage tank, which is the most common method in Denmark (Foged et al., 2017). Additionally, acidification can be carried out in-house, i.e., when manure stored under the animal barn is transferred to external storage for acidification and then sent back to a storage unit under the animal house or to external tanks. Treatment efficiency in lab- and pilot-scale studies has been reported to vary from 37 to 98% and 17 to 90% for NH_3 and CH_4, respectively (Fangueiro et al., 2015). In a recent study (Lemes et al., 2022), early single-dose acidification in farm-scale manure tanks showed an immediate reduction of 95% in CH_4 emissions. Results on the reduction of CH_4 emissions for in-house acidification are shown in Paper **II**. As a drawback, the treatment might be a health threat to farmers handling the acid and can cause foam formation (Kai et al., 2008); additionally, it is expensive to implement.

Furthermore, frequent slurry removal from manure pits under animal housing can reduce emissions, as manure is moved to a colder environment (indoor vs. outdoor temperature) (Dalby et al., 2022). The effect of this management on CH_4 emissions will be demonstrated in section 4.1.2. In manure storage units, a natural crust on the top of the manure is usually formed. The effects of this crust on CH_4 emissions mitigation, however, are unclear, as when the crust is not homogeneous CH_4 can escape through cracks in the cover (Kupper et al., 2020). Other types of mitigation, such as installing a fixed manure tank cover, have been implemented, but despite generally high efficacy in relation to reducing NH_3 emissions, CH_4 emission mitigation is still poorly documented (Kupper et al., 2020). In Denmark, fixed covers, which are not gas-tight tent structures made of PVC, are used in 24% of pig tanks and 10% of dairy manure tanks (Mikkelsen and Albrektsen, 2020) to reduce NH_3 emissions. The effect of this cover on CH_4 are investigated Paper **IV**.

2.3 NH_3 emissions from livestock production

NH_3 is produced by the decomposition of primarily urea present in animal urine, by enzyme urease, mainly present in faeces (Hristov et al., 2011). The mixture of urine and faeces leads to the production of ammonia (NH_3) and ammonium (NH_4^+), which are in equilibrium in the manure according to certain characteristics (e.g., pH). NH_3 is then volatilised into the atmosphere by mass transfer driven by temperature and wind speed (Olesen and Sommer, 1993) from the surface of the manure. To model NH_3 emissions, differences between NH_4^+/NH_3 concentrations are constrained by turbulent, quasi-laminar and canopy resistances (Sutton et al., 2013). Furthermore, concentrations at the surface are proportional to temperature, based on thermodynamics (Sutton et al., 2013). In pig and cattle farms, sources of NH_3 are animal houses and manure storage.

NH_3 emissions from animal barns can be about 10 to 14% of the nitrogen content in manure, but in extreme circumstances, this figure can reach up to 50% (Hristov et al., 2011). Emissions depend on the house design, nitrogen intake and weather conditions. In a study of San Joaquin Valley (SJV) CAFOs, Miller et al. (2015) measured NH_3 mixing ratios downwind from these animal facilities. NH_3 concentrations were high downwind of the animal area, and they were lower near to anaerobic lagoon areas, while CH_4 concentrations were high in this area, therefore, NH_3 and CH_4 concentrations were poorly correlated downwind the lagoon (Miller et al., 2015).

Average EFs estimated by the US EPA (U.S. Environmental Protection Agency, 2018) for Tulare and Kern county dairy CAFOs are 4.13 g/head/h, varying from 0.52 to 13.03 g/head/h. The same variation of one factor of magnitude's difference between monthly NH_3 emissions has been reported elsewhere (Leifer et al., 2018). In addition to monthly variations, NH_3 emissions have a strong diurnal pattern (Sun et al., 2015; Zhu et al., 2015b) related to temperature and wind speed.

2.4 CH_4 and NH_3 measurement methods

CH_4 and NH_3 have different characteristics. The former is relatively inert and has a lifetime of approximately two decades, whilst the latter is a highly reactive gas and remains in the atmosphere for only a few hours or days (Leifer et al., 2017). Therefore, measuring NH_3 concentrations is difficult, as in close-path instruments, NH_3 will adhere to the tube inlet and instrument interior (Twigg et al., 2022), leading to a delay or inaccuracy in measured concentrations. Hence, open-path instruments are preferable for NH_3 measurements; otherwise, they need to have a special surface coating or heating, to avoid NH_3 adsorption (Sun et al., 2015). Furthermore, CH_4 and NH_3 concentrations can be measured using instruments suited to different platforms. Stationary measurements are often used when the priority is obtaining continuous information. Moreover, instruments can be suited to mobile platforms (Eilerman et al., 2016; Golston et al., 2020), airplanes (Daube et al., 2018), or, more recently, drones (Vinković et al., 2022). One study applied a novel sampling system set up in a drone to quantify emissions from animal houses. The system provides flexibility in terms of measurement, as it does not rely on road availability, albeit measurements are discrete and record for just a few minutes (Vinković et al., 2022). Furthermore, satellite data can be used to investigate emissions over large areas; for instance, historical IASI NH_3 column concentration data has been used to detect and quantify emissions from hotspots around the globe, with most agricultural sources (~33%) related to intensive farming (Van Damme et al., 2018). However, satellite-based detection of farm-scale emission rates is still not possible due to restrictions in spatial resolution.

After concentrations have been measured, they need to be converted to fluxes by using information about the gas flow. Several methods have been used to measure emissions from livestock, each with its own constrains. For instance, for some popular approaches, such as chamber methods (Husted, 1994), during their application they can affect the factors driving emissions (intrusive methods). The design of the facility also plays a role; for instance, emissions from mechanically ventilated houses are often quantified by measuring emission enhancement from an animal house's outlet together with the ventilation rate (Hassouna et al., 2020). This method corresponded to 88% of the EFs from animal houses collected in the DATAMAN dataset (Hassouna et al., 2022), 11% of which were measured using surface chambers and 1% micrometeorological techniques. Regarding storage tanks, Kupper et al. (2020) revealed that 67% of gaseous emissions from manure storage units were quantified using surface chambers, about 30% used micrometeorological techniques, while tracer methods were only used in 1% of the quantifications of lab-, pilot- and farm-scale EFs. Additionally, 46% of the EFs were quantified in farm-scale tanks (Kupper et al., 2020).

Different micrometeorological techniques, such as the inverse dispersion method (IDM), have been used to quantify CH_4 (Bühler et al., 2021; Laubach and Kelliher, 2005) and NH_3 emissions (Flesch et al., 2007). This method estimates emissions using measurements of wind parameters and downwind gas concentrations to derive the emissions-concentration relationship (Flesch et al., 2005). Measurements are continuous, although depending on wind conditions and concentration measurement setup (e.g., open-path, line average), a certain amount of the collected data will be discarded (Bühler et al., 2021; Lemes et al., 2022; McGinn et al., 2006). The method requires certain topographical features (flat terrain) and a lack of interfering sources nearby (Flesch et al., 2005). Recently, IDM was applied to measure emissions from an animal house in Switzerland, revealing a suitable application even at low emission rates and with complex wind conditions (Bühler et al., 2021). The mass balance flux method is another micrometeorological method whereby emissions are estimated based on integration over height in upwind and downwind positions (Wagner-Riddle et al., 2006). Moreover, eddy covariance has also been used to measure emissions from livestock, as long as assumptions on spatial homogeneity are fulfilled (Sun et al., 2015). Since micrometeorological methods rely on assumptions regarding atmospheric dispersion in order to estimate emissions, they can have significant uncertainties. Finally, combining different methods might be the best approach to cover any limitations; however, more research is needed to validate individual methods and apply them in different production scenarios (Tedeschi et al., 2022).

3 Materials and methods

3.1 CH_4 emissions – TDM and IFM

An alternative method for quantifying target gas emissions without relying on atmospheric modelling is to use information from another gas (here, called a tracer) and its correlation to the target gas. The method relies upon both gases dispersing similarly in the atmosphere. The tracer gas can be a synthetic released gas or another naturally released gas from a nearby source, as long as it is ensured that the gases are well mixed. The tracer gas release rate should be deduced through either calculations or measurements. Fluxes from the target gas are calculated by combining the tracer gas's known rate and the target-to-tracer gas ratio. There are a few approaches for estimating emissions using this principle (Galle et al., 2001; Grainger et al., 2007; Roscioli et al., 2015), but herein we focus on two methods, namely the tracer gas dispersion method (TDM) (Mønster et al., 2014; Scheutz et al., 2011) and the indirect flux method (IFM) (Mellqvist et al., 2020), to quantify CH_4 emissions.

3.1.1 Mobile tracer gas dispersion method (TDM)

The first method used acetylene (C_2H_2), an inert synthetic gas, as a tracer gas, as there are no other sources of this gas on a farm. C_2H_2 was released close to the target sources directly from the gas cylinder, using a flowmeter to ensure stable flow. The flow rate was verified by weighing the bottles before and after the release. In order to quantify manure storage tanks, where feasible, the gas was released from the centre of the tank, using an extended tube attached to a floating material. Emission rates were calculated using equation 1:

$$E_{tg} = E_{tr} \frac{\int_{x1}^{x2} (C_{tg} - C_{bg,tg})dx}{\int_{x1}^{x2} (C_{tr} - C_{bg,tr})dx} \cdot \frac{MW_{tg}}{MW_{tr}} \qquad \text{(Eq. 1)}$$

where E represents the emission rate (kg/h) of the tracer (tr) and target (tg) gas, C is the plume concentrations and C_{bg} is the background concentrations of both the target and the tracer gas (ppbv). Finally, MW is the molar weight of both gases. Moreover, the ratios were calculated by integrating the whole plume area through the transect distances (x1 and x2), described by Fredenslund et al. (2019) as the preferred approach.

Concentration measurements were taken from vehicle on which the analytical instruments were installed, with air sampling on the top of the car (~ 2 m). The main instrument used to measure the concentrations was a cavity ring-down spectrometer (CRDS) model G2203 (Picarro Inc., California), measuring both C_2H_2 and CH_4 (Table 1). When this instrument was not available, a combination of two other CRDS was used, namely model G1301 measuring CH_4 and a custom-made CRDS instrument (S/N JADS 2001) for C_2H_2 (more details in Table 1).

Table 1: Characteristics of the instruments used.

Method	Instrument	Gases	Unit	Precision (3σ)	Sampling frequency	Papers
TDM	CSDR- G2203	CH_4	ppbv	2.1	2 s	Paper **I** - **IV**
		C_2H_2		0.3 ppbv	2 s	
	- G1301	CH_4		2.5 ppbv	4 s	
	- JADS	C_2H_2		3.4 ppbv	3 s	
IFM	MeFTIR	NH_3	µg/m^3, ppbv	15 ppbv	9 – 10 s	Paper **V** and **VI**
		CH_4		30 ppbv		
SOF	SOF	NH_3	mg/m^2	2.2 mg/m^2	4 – 5 s	Paper **V** and **VI**

The TDM is applied by following a few steps. First, other potential interfering sources are verified by observation maps and by mobile screening atmospheric CH_4 concentrations in areas surrounding the farm. Further, internal screening of the farm is performed to identify the primary sources of CH_4, thereby allowing for better placement of the tracer gas bottles. Usually, two to three tracer gas bottles are used, whilst their release rates and positions depend on the farm's layout and CH_4 sources. Following the placement of the cylinders, the tracer gas release starts, and measurements of the source's plume concentrations downwind (500 to 2000 m) are taken (Figure 2a). In the case of lack in correlation between the tracer-to-target, adjustments of the release rate or the placement of the cylinders should be done. At least ten transects where the plume is fully covered should be performed, and in this study they were collected within approximately 1 to 2 hours on average. The TDM was used to measure CH_4 emissions from farms in Denmark, including entire farm and manure tank emissions (Paper **I**, **II**, **III** and **IV**). Best practice for measurement campaigns using TDM is presented in Scheutz and Kjeldsen (2019).

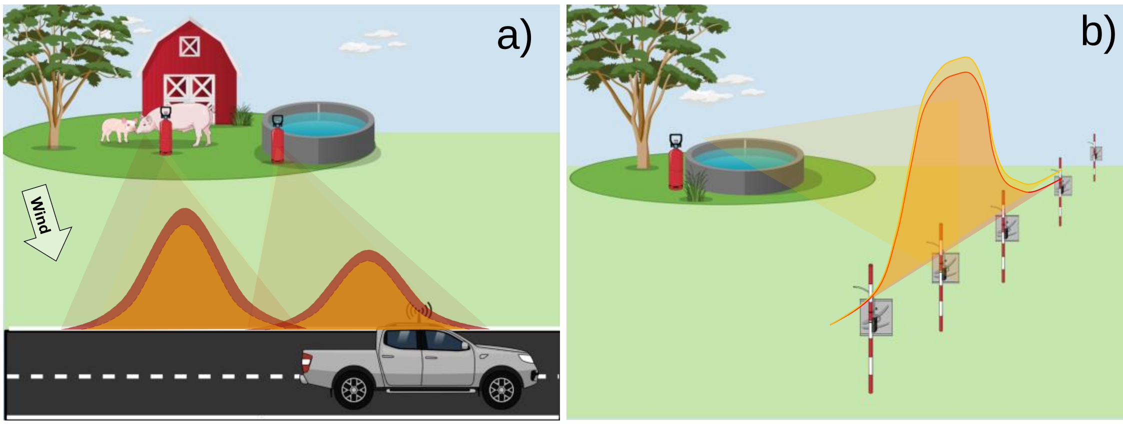

Figure 2: (a) Mobile TDM illustration of measurements performed at a pig farm (b) Stationary TDM illustration, measurements performed at a manure storage tank.

3.1.2 Stationary TDM

Quantifying emissions from manure tanks, using TDM, can be a challenge, as it can be difficult to find roads at appropriate measuring distances and without obstructions, as tanks are often located nearby animal houses. A stationary TDM sampling approach was developed to offer more flexibility to the method, in that concentration measurements could be done in the field without the need for roads.

In the stationary TDM approach, sampling bags were placed downwind of the manure tank, in a field, to sample plume concentrations, instead of driving across the plume with the analytical instrumentation. It is a simple approach and allows for measurements at distances and in places where it is impossible to drive. The procedure consists of five to ten sampling bags (ideally more than seven) placed across the plume downwind from the source at approximately 100 m (Figure 2b). Gas concentration sampling for the campaign in this study occurred for about 30 min at a 150 ml/min air flow sampling rate. After gas sampling, the concentrations were measured in the field using the same analytical platform for mobile measurements (Table 1). After analysing concentrations in the sampling bags, the sampling points could be repositioned in case they were placed outside the plume. The sampling trial should be repeated, ideally three times. According to the analysis comparing mobile and stationary TDM approaches, both methods produced similar results (Figure 3a). The position of the bags within the plume affected the results due to misalignments of the tracer release position and the associated emission plume in regards to the source emission plume. Therefore, according to a comparison between mobile and stationary methods, sampling bags should be placed in the centre of the plume in order to cover the plume peak concentration (and 75% of the tail), which in turn reduces the error rate to 40-60% in comparison to sampling in the tails of the plume (Figure 3b).

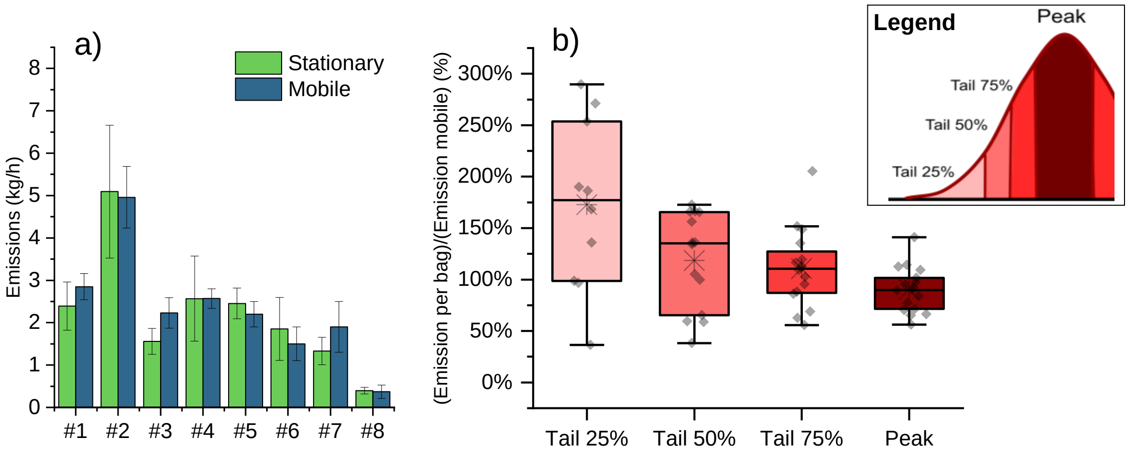

Figure 3: (a) Comparison of emission rates quantified using the mobile TDM and stationary TDM, (b) Difference in emission rates calculated using stationary sampling points at different positions within the plume. The legend indicates each section of the plume correspondent in the graph. (Similar figures used in Paper **III**)

Target source emissions are obtained similarly to the mobile TDM (Eq. 1). The target-to-tracer ratio is calculated by integrating the area under the measured plume, although the plume is often incomplete. A throughout analysis of the best method to estimate the ratio is presented in Paper **III**. More details about the sampling approach, validation experiment and guidelines for data processing and quality assessment are discussed in Paper **III**.

3.1.3 Indirect flux method (IFM)

The IFM method uses a similar principle as the TDM, but instead the quantification of the emission of one target gas is done be measuring the emission of another target gas and then measuring the contraction ratios of the two gases. In this project, CH_4 emission quantification was done by measuring NH_3-to-CH_4 concentration ratios, combined with the independent quantification of NH_3 emissions using the SOF method (Section 3.2). It should be mentioned that SOF is limited to daytime and sunny conditions, and therefore the IFM was also constrained to these conditions. The IFM method was used in Paper **V** to calculate CH_4 emissions at dairy CAFOs. They were calculated using equation 2:

$$E_{CH4} = \frac{1}{n}\sum_n E_{NH3}\left(\frac{kg}{h}\right) / \frac{1}{n}\sum_n \frac{\int_{x1}^{x2}(C_{NH3} - C_{NH3,bg})\left(\frac{\mu g}{m^3}\right)dx}{\int_{x1}^{x2}(C_{CH4} - C_{CH4,bg})\left(\frac{\mu g}{m^3}\right)dx} \quad \text{(Eq. 2)}$$

where E is the respective emission of the two target gases (kg/h), C is concentrations in µg/m^3 and C_{bg} is background concentrations. Measurements were sometimes not performed simultaneously (<25%), as ground concentrations are low in unstable atmospheric conditions because of high convection. Hence, the estimation was done by averaging the measured NH_3 emissions and the NH_3-to-CH_4 ratio, detected between 09:00 and 17:30. Additionally, an assumption adopted was that both CH_4 and NH_3 sources were either the same or collocated at similar distances away from the source. Concentration ratio measurements were done using a mobile extractive FTIR (MeFTIR) (Table 1) (Galle et al., 2001; Samuelsson et al., 2018), with external heating on the air inlet and around the cell to minimise adsorption of the NH_3 in the instrument. The FTIR instrument (Bucker IR cube) was equipped with a dual detector MCT (700-1200 cm^{-1}) and InSb (1800-4000 cm^{-1}) with a resolution of 0.5 cm^{-1}. NH_3 was detected in the fingerprint region (900 to 1000 cm^{-1}), while CH_4 was retrieved in the C-H stretch region (2760 to 3028 cm^{-1}). NH_3 retrieval was achieved by fitting absorption spectra from HITRAN (Rothman et al., 2005), using a least-square fitting routine, while for CH_4 MALT was used (Griffith, 1996). More details on the instrument are shown in Table 1. Both the SOF and MeFTIR instruments were installed in a measurement vehicle. Gas columns and concentrations were measured while driving downwind and upwind of the target sources. A minimum of four to five transects were performed downwind from the source.

3.2 NH_3 measurements – SOF

Solar occultation flux (SOF) measures solar infrared absorption spectra while crossing the gas emission plume (Figure 4). The instrument comprises a solar track made with mirrors that direct a beam of sunlight to an FTIR instrument. The solar track moves and turns according to the driving direction, thereby allowing for measuring concentrations around the target source while driving. An FTIR instrument detects the spectra from which NH_3 column concentrations (mg/m^2) are then obtained (Table 1). To retrieve these column concentrations, reference spectra are fitted to the measured spectra to remove the effects of water, CO_2 and other possible interferences. Therefore, the method measures relative concentrations instead of absolute ones. In addition, due to the The FTIR instrument used for this study was a Bucker IR cube, similar to the one used on the MeFTIR instrument. However, SOF cannot measure CH_4 columns because the absorption lines are almost depleted due to high CH_4 background concentrations in the atmosphere. By crossing the whole NH_3 gas plume, the integrated plume area can then be used to calculate NH_3 emission rates, using equation 3:

$$E_{NH3}\left(\frac{mg}{s}\right) = u_t\left(\frac{m}{s}\right)\int_{x1}^{x2} Column_{NH3}\left(\frac{mg}{m^2}\right)\cdot\cos(\theta)\cdot\sin(\alpha)\,dx(m) \qquad \text{(Eq. 3)}$$

where, in addition to column concentrations ($Column_{NH3}$) along the driving distance (x), we also considered θ, which is the angle of the light path from zenith, and α, which is the angle between the wind direction and driving direction. Furthermore, the accumulated mass flux (mg/m) is multiplied by wind speed parameters in order to derive the emission rate. The assumption used in this method is that the plume is homogenously distributed in the vertical, which is reasonably supported because measurements are done in conditions of high convection. SOF was used in Papers **V** and **VI**

Figure 4: Solar occultation flux method illustration (figure used in Papers **V** and **VI**).

3.2.1 Wind speed

Wind speed is an important factor, as it is used to calculate the emission rate of the SOF method and it should reflect the plume's speed. In order to fulfil this, knowledge of the vertical wind speed profile is needed. Hence, the ideal representation of the plume's wind speed is the integrated wind profile (IWP), from the ground up to the plume's height. To obtain the wind speed profile, a wind Zephyr Lidar (Light Detection Ranging) (Campbell), measuring wind speed between 10 to 300 metres at nine different heights, was used (Paper **V**). Lidar instruments shoot a laser (~ 1.5 µm) which is reflected when it hits atmospheric aerosols. Wind speed is calculated based on the change in frequency of the emitted laser caused by the Doppler shift. Alternatively to Lidar, wind speed can be measured at different heights using wind sensors placed at different heights (Paper **VI**) or GPS tracking radiosondes launched in a balloon. With the wind speed at different heights, the integrated IWP is calculated using equation 4:

$$IWP = \frac{\int_0^H u \cdot dz}{H} \qquad \text{(Eq. 4)}$$

where u is the wind speed at different heights and H is the plume height. To estimate the plume height, column measurements (done by SOF) and simultaneous ground measurements (done by the MeFTIR) are combined, as shown in equation 5:

$$H = \cos(\theta)\ \frac{\int Column_{NH3}\,(x)dx(\frac{mg}{m^2})}{\int Concentration\ _{NH3}(x)dx(\frac{mg}{m^3})} \qquad \text{(Eq. 5)}$$

More details on SOF measurements and the impact of the wind variable are discussed in Paper **VI**.

Wind field experiment – Comparison of measured and modelled transects

A field experiment was designed to quantify the impact of wind variability on emission measurements, using the SOF method. This comprised a controlled release followed by SOF measurements, while wind speeds at 12 locations, distributed between the release and measurement road, were recorded (Figure 5a). At each location wind speed was measured by 2D-sonic wind meters at a height of 3 metres above ground, and at one of the sampling points (ST-3, Figure 5a) a 2D-sonic meter was placed at 15 metres while a 3D-sonic sampled at 3 metres. The purpose was to measure wind speed and then use this information to produce a model representing gas dispersion as close as possible to the true one (Figure 5b). Results from the actual measurements and modelled measurements should have been compared. The aim was to understand how wind variability influences emission rates and to further optimise wind and plume transect measurements (e.g., driving speed, number of wind speed measurements). However, due to time constraints, this part of the project still needs to be completed. Nonetheless, the wind field experiment was performed (Figure 5a) and the model is now ready to be used (Figures 5b). The next step is to compare the modelled transects with the measured ones.

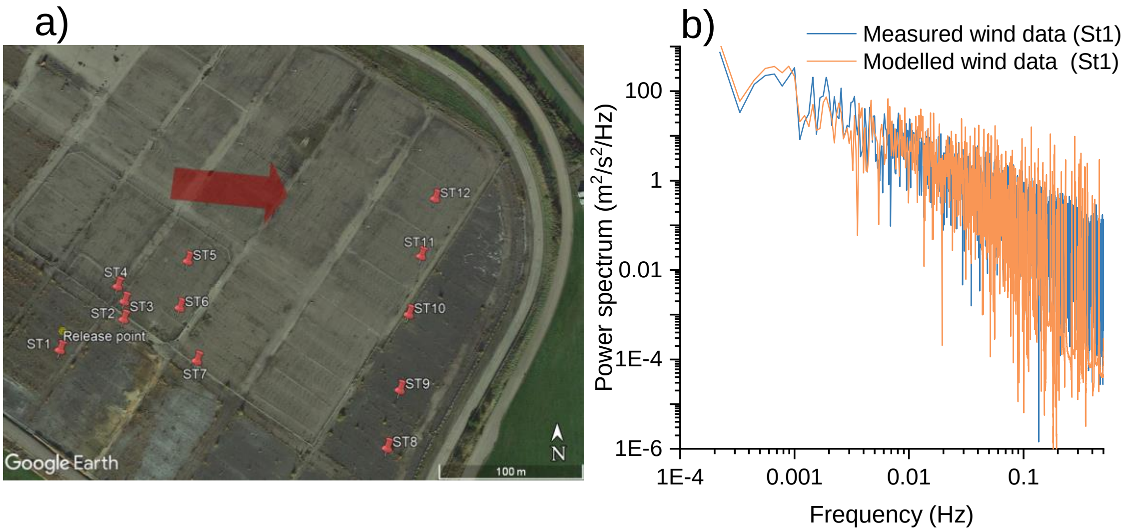

Figure 5: Wind dispersion experiment. (a) Distribution of the wind meters, release point and measurement road. Wind speed was prevailing from the west. Map source: Google Earth © (b) Power spectra density plot comparing real and modelled data.

3.3 Measurement uncertainty – Error budget

A measured emission rate comes with a certain amount of uncertainty, i.e., a range of values where the emission rate is within. Compiling an error budget for a measuring method can provide insights into which variables are critical and have the most significant impact on emission quantification (Gates et al., 2009). Herein, we used the guide to the expression of uncertainty in measurement (GUM) methodology (Joint Committee For Guides In Metrology, 2008) to determine SOF uncertainties (Paper **V** and **VI**) and IFM measurements (Paper **V**). Uncertainty in relation to the SOF method is described in detail in Paper **VI**. In short, there are systematic errors, including an NH_3 absorption cross-section and concentration retrieval (Table 2). Other errors are associated with background delimitation and wind speed measurements. These and random measurement uncertainty were combined to estimate standard (CI 68%) and expanded uncertainties (CI 95%). NH_3 measurement uncertainty averaged 37% (CI 95%), farm specific calculations are shown on Paper **V**. Wind speed is the greatest source of systematic error in SOF measurements. However, vertical profile and plume height measurements help to reduce this uncertainty, as they assist in estimating the actual plume speed. Case studies and more details on this uncertainty estimation are reported in Paper **VI**.

A similar error budget estimation was done for the IFM measurements. The most critical errors for this method related to SOF NH_3 quantification uncertainty, which was calculated as described above, and a mismatch between NH_3 and CH_4 emission sources. CH_4 measurements uncertainties averaged 53%, and farm-specific calculations are shown on Paper **V**. In comparison, for TDM, an uncertainty budget was created in a published study (Fredenslund et al., 2019) comprising estimated – instead of site-specific – uncertainty for the methodology. The method expanded uncertainty for CH_4 quantification ranged from 18 – 24%.

Table 2: Error budget for the uncertainty estimation of SOF, IFM and TDM methods

	SOF (Paper VI and V)		IFM (Paper V)	
Systematic (%)	Spect. Cross section	2	Spect. Cross section	3
	Spect. Retrieval	4.4	Spect. Retrieval	5.6
	Background	1-14	Background NH_3	1-10
			Background CH_4	1-10
			Sources mismatch	5-41
	Wind speed	11-12	SOF NH_3	12-32
Random (%)	Measurement variability	8-31	Measurement variability	5-36
Combined Uncertainty (%)	Standard	17	Standard	25
	Expanded	**37**	**Expanded**	**53**

Furthermore, a controlled release experiment was performed to verify the SOF methodology's accuracy in estimating NH_3 fluxes. Four release rates were tested, varying from 0.48 to 1.1 kg/h (more details in Paper **VI**). The relative error, was a minimum of -31% and a maximum of +14%. Additionally, the calculated standard uncertainty, on average, was 7.5% and the expanded uncertainty 15.1%. The uncertainty interval was close or within 5% of the error range in three out of four release test.

3.4 Quantification of CH_4 emissions from Danish cattle and pig farms

CH_4 emissions from Danish livestock production were measured. The emission rates comprised the whole facility, including animal house and manure storage, without observing rates from single operations. Six measurements distributed equally over a year were completed, allowing for a better comparison of the farms' emissions. Temporal variability coverage by measuring six times over a year is a similar procedure to the Vera protocol for quantifying animal house NH_3 emissions (VERA, 2018).

3.4.1 Danish cattle farms

In the cattle farm study, nine farms (C1-C9) were chosen according to typical farm management practices in the country, the willingness of the farmers to participate and the farms' suitability for a measurement campaign (Paper **I**). Two farms focused on beef production (C8 and C9), while the others were dairy farms (C1-C7). Three farms housed Jersey milk cows (C1-C3), three had Danish Holstein milk cows (C4-C6), whilst the last one had Red Danish milk cows (C7). Regarding house management, three farms had loose-holding with slatted or drained floors (C1, C2 and C4), and two had deep litter with a long eating space (C3 and C6), meaning that 60% of the manure was deposited in the straw beds (Table 3). Some farms had a mix of both systems (C5, C7 and C9), while C8 had deep litter in the whole house. At most farms, the deep litter was retained for two months, except for C5, which retained for only six weeks and C7 for 4 months. Farms sent their removed raw liquid manure and deep litter to centralised biogas plants once or twice a week (biogas) while receiving the digested manure for storage in their tanks, except for C1, C7 and C8. C7 started this practice towards the end of the study period, covering only two out of six measurements. In C8, the deep litter produced when the cows were in the house was stored further away from the farm. Animal numbers were consistent over the year, except for C1, which had seasonal calving in late spring, meaning that cows were inseminated simultaneously. C2 was the only farm where the storage tank had a cover, while the manure tank at C7 had a cover installed halfway through the measurements. Additionally, tanks were completely emptied in spring (C2, C3, C5, C6, C7, C9) and partially in autumn, except for the two organic farms (C1 and C4). In C1 and C4, the tanks were emptied during summer, as manure was more frequently applied to fields and because dairy cows grazed during the day, so less manure was dumped in the house. At the dairy farms, apart from the dairy cows, heifers and calves were also part of the farm, often housed in separate housings with different management systems. They were accounted for in the livestock unit for the EF calculation and in inventory estimates. C4 was an exception, as the measured house had only dairy cows.

In all, 60 quantitative CH_4 emission measurements were completed, with most farms measured every second month. C8 was measured when the animals were inside the house (four times) and once on pasture. Although emission quantification of animals on pasture was done in C8, they were inside the house during all the other campaigns. Emission quantification took approximately 1-2 hours, and 17 to 23 transects were collected on average. Measurement distance away from the target farm varied from 0.7 to 1.5 km. CH_4 EFs were obtained by normalising the emission rates by livestock unit (LU). The average weight of the animals was based on information provided by the relevant farmers, while the number of animals was collected from the animal central database (CHR) for consistency (Table 3). More details are available in Paper **I**.

Table 3: Overview of the farms and measurements characteristics. (Table adapted from Paper **I**)

Farm	Type of animal (Breed)	Livestock unit (LU)[1]	House	Manure management	No. of measurements (transects)	Distance (km)
C1	Dairy cow – Organic (Jersey)	970-1250	Loose-holding drained floor	Slurry	12 (17)	1.5
C2	Dairy cow (Jersey)	330	Loose-holding slatted floor	Biogas	6 (21)	0.7
C3	Dairy cow (Jersey)	540	Deep litter with long eating space	Biogas	6 (21)	1.5
C4	Dairy cow – Organic (Holstein)	230	Loose-holding Slatted Floor	Biogas	6 (21)	1.4

C5	Dairy cow (Holstein)	1055	Loose-holding slatted floor (65%)/deep litter with long eating space (35%)	Biogas	6 (19)	1.3
C6	Dairy cow (Holstein)	305	Deep litter with long eating space	Biogas	7 (21)	1.5
C7	Dairy cow (Red Danish)	320	Loose-holding slatted floor (50%)/deep litter with long eating space (50%)	Slurry (4x) Biogas (2x)	6 (23)	1.1
C8	Beef Cattle (Limousine)	130	Deep litter	Solid piles	4 (17)	0.7
C9	Beef Cattle (Holstein)	545	Loose-holding slatted floor (80%)/deep litter with long eating space (20%)	Biogas	6 (22)	1.1

[1]LU = 500 kg of body weight. Jersey dairy = 0.89 LU; Holstein dairy = 1.2 LU; Jersey heifer 0.65 LU; Holstein heifer 0.78 LU; Jersey bull = 0.68 LU; Holstein bull = 0.85 LU, Jersey calves = 0.16; Holstein calves = 0.21 LU; Limousine cows = 1.6 LU; Limousine heifer or bulls = 0.8-1 LU; Limousine calves 0.3 = LU

3.4.2 Danish pig farms

The pig farm project investigated CH_4 emissions from five farms (P1 – P5), covering conventional management practices (Paper **II**). Furthermore, two additional farms (P6 and P7) were investigated after this project had ended. The results were published (Paper **II**) and are included here to enrich the discussion and statistics. One of the farms (P1) had sows, piglets and weaners, while the others (P2 – P7) had fattening pigs and a few weaners. At farm P1, each pig phase (e.g., farrowing or gestational sows) and type was held in a different house, as described in Table 4. In P2 to P7, the pigs' housing had partly slatted/ drained or partly slatted/solid floors (Table 4). Four farms (P1, P2, P6 and P7) did not treat the produced slurry. Moreover, P3 sent its raw manure to a centralised biogas plant, similar to the cattle farms (biogas). Finally, P4 and P5 acidified manure stored inside the house. P7 removed manure from the animal house every week, unlike P1, P2 and P6, which did this once a month. Furthermore, outdoor tanks were completely emptied in spring and partially emptied in autumn. All the tanks were covered except for P1, which had a natural crust present on a few occasions. The farms had a continuous operation, meaning that a certain amount of pigs entered and left every week, apart from the acidification farms. P4 and P5, during specific periods, had more animals during the same fattening phase; therefore, the number of animals as well as their weight, on each campaign, were considered when normalising the emissions.

Approximately 45 measurement campaigns were performed at the seven farms. Farm emissions were measured six times yearly, following the same approach as the cattle farm study. More information on emission measurements is described in Table 4 and Paper **II**. Once more, EFs were calculated by normalising emissions to LU. Animal weight and their numbers were acquired via interviews with the farmers.

Table 4: Overview of the measured pig farms and measurement characteristics. (Table Adapted from paper **II**)

Farm	Livestock units[1]	Housing	Manure management	No. of measurements (transects)	Distance (km)
P1	452-461[2]	*Farrowing sows* - individual housing and partly slatted floor	*Slurry storage* Uncovered (Natural crust), removal of housing manure - monthly	*8 (20)*	*1.4*
		Gestational sows - loose holding, deep litter, slatted floor			
		Weaners - two climate housing			
		Fattening pigs - partly slatted floor (25-49% solid floor)			
P2	584-695[2]	Partly slatted and drained floor	*Slurry storage* Covered, Removal of housing manure - monthly	*6 (20)*	*1.2*
P3	365-492[2]	Partly slatted floor (50-75% solid floor)	*Biogasification* Covered, removal of housing manure – monthly (complete) or weekly (partially)	*6 (20)*	*1.1*
P4	767-1352[3]	Partly slatted and drained floor	*Acidification* Covered, partial removal of housing manure - daily	*6 (22)*	*1.0*
P5	984-1486[3]	Partly slatted and drained floor	*Acidification* Covered, partial removal of housing manure - daily	*5 (16)*	*1.5*
P6	416-390	Partly slatted and drained floor	*Slurry storage* Covered, Removal of housing manure - monthly	*7 (18)*	*0.8*
P7	700	Partly slatted and drained floor	*Slurry storage* Covered, Removal of housing manure -Weekly	*8 (17)*	*0.9*

[1]For all farms, one livestock unit (LU) equalled 500 kg of body weight. [2]Sows 230 kg; fattening pigs 70 kg; weaners 19.5 kg (Based on farmers' information). [3]LU was calculated based on the weight ranges provided by the farmer (30-60 kg; 60-90 kg; 90-120 kg).

3.5 Quantification of CH_4 emissions from manure storage tanks

CH_4 emissions were quantified from ten liquid manure storage tanks. Two of them stored dairy manure (CN1 and CN2), six had pig manure (PN1, PN2, PC1, PC2, PC3 and PC4) and the last two contained digested manure (DN1, DC1) (Paper **IV**). The tanks were selected according to measurement suitability and that they should comprise a cross-section of manure storage tanks located at Danish farms. The digested manure stored at DN1 and DC1 came from centralised biogas plants. The main difference between these facilities was the retention time, i.e., longer for DC1 (~90 days) than DN1 (~34 days). The biogas plant feedstock was similar, comprising mostly animal manure, energy crops and food waste, although DC1 had a smaller percentage (9%) of chicken manure. Half of the tanks were covered with a PVC tent cover (PC1, PC2, PC3, PC4 and DC1), while the uncovered tanks had a natural crust at certain times. Furthermore, at some farms, there were two tanks close to each other, which were considered as one source, although specific information (e.g., temperature, VS, volume) was collected from each tank.

Following a similar protocol as in the other studies, six measurements distributed over a year were completed; however, more measurements were actually performed on most farms (Table 5). These were primarily done during the day and lasted from 30 minutes to 4 hours. Both the mobile TDM and stationary TDM were used in the quantifications. For the stationary method, two approaches were used. One is described in Paper **III**, namely using bags for atmospheric sampling and in-field concentration analysis, whilst the other way is described elsewhere (Fredenslund et al., 2019) and consists of sampling concentrations at a single point by parking the measurement vehicle near the plume peak. EFs were obtained by normalising emissions by the volume of manure stored in the tank. In addition to the measurements, information on manure volume, manure temperature (at 1 m depth), atmospheric temperature, dry matter (DM) and volatile solids (VS) was obtained to support the emission analysis. However, manure temperature measurements were lacking at CN2 and PC4. Manure was sampled two to three times, except for PC4, from which no samples were taken.

Table 5: Overview of the manure tanks measured in this study and measurement characteristics. (Table adapted from Paper **IV**)

Tank[a]	Manure type (Nr. of animals)	Cover	Tank storage capacity (volume m^3)	No. of measurements	Method[a]
CN1	Cattle (dairy 220)	No	T1 (1300)	7	M, S
CN2	Cattle (dairy 700	No	T1 (5000) T2 (3500)	14	M, B
PN1	Pig (sows 710, piglets 4000)	No	T1 (1640) T2 (3000)	8	M
PN2	Pig (1500)	No	T1 (2200) T2 (2200)	8	M,S
PC1	Pig (2500)	Yes	T1 (4400)	8	M
PC2	Pig (5000)	Yes	T1 (5500)	7	M
PC3	Pig (fattening 1800, piglets 1125)	Yes	T1 (4300)	12	M,S
PC4	Pig (fattening 2300, piglets 1300)	Yes	T1 (5000)	6	M
DC1	Digestate – high HRT	Yes	T1 (7200) T2 (3000)	8	M
DN1	Digestate – low HRT	No	T1 (800) T2 (3100)	8	M,S

[a] "M" stands for mobile TDM, "B" for the stationary TDM using bags for concentration sampling and "S" for stationary TDM measuring concentrations at a single point near the plume peak.

3.6 Quantification of NH_3 and CH_4 emissions from CAFOs

NH_3 and CH_4 were quantified from 14 CAFOs in SJV, California. The farms were located in two main regions, one near Bakersfield (SB2, SB3, SB4, SB5, NB1 and NB2) and the other close to Tulare (WT1, WT3, WT4, WT5, WT6, WT7, ET1 and ET8) (Paper **V**). These are intensive farming areas with a high density of farms, making single-facility measurements rather tricky for some methods but more manageable with a mobile platform. Unlike the other studies, transects were collected downwind of several farms simultaneously, following the wind and weather conditions. For instance, one transect would last about 40 minutes and collect plumes from five farms. This was the chosen approach once the placement of tracer bottles was not necessary, albeit, on the other hand, driving speeds were slow, distances were large and measurement time was limited by sunlight hours. The number of animals (mature cows, heifers and calves) was provided by the San Joaquin Valley air pollution control district (Personal communication, 2020). Knowledge of manure management at the farms was limited to field observations and visualisations of the farms in

GIS tools, e.g., Google Earth. We therefore assumed that farms followed the typical management of Californian farms (US-EPA, 2017), with 60% of the dairy cow manure being managed in anaerobic lagoons. The remaining is managed as liquid/slurry (20%), daily spread (10%), solid storage (9%) and pasture (1%) (Table 6). In some farms, the lagoon was covered in order to collect gas for further energy utilisation (Table 6).

Measurements were performed at two different times of the year, namely in May, comprising 11 measurement days, and in October, covering five days. Different to the TDM, other quality criteria needed to be fulfilled here according to the European standard EN17628:2022 (European standard, 2022) for SOF, at least four plumes should be carried out and wind speed should be higher than 1.5 m/s. EFs were again normalised by LU.

Table 6: Overview of the CAFO study, farm characteristics and measurements. (Table adapted from Paper **V**)

Farm	LU[a]	Manure management	No. of transects for SOF (May - Oct)	No. of transects MeFTIR – Ratio (May - Oct)	Distance (km)
SB2	21626	Anaerobic lagoon (60%)	7	3	2
SB3	14184	Covered lagoon (60%)	15 (9 – 6)	7 (3 – 4)	0.5
SB4	7361	Anaerobic lagoon (60%)	20 (10 – 10)	14 (6 – 8)	0.5
SB5	12748	Anaerobic lagoon (60%)	18 (8 – 10)	13 (7 – 6)	0.6
NB1	10056	Anaerobic lagoon (60%)	18 (7 – 11)	12 (5 – 7)	0.5
NB2	10592	Anaerobic lagoon (60%)	21 (9 – 12)	17 (4 – 13)	0.8
WT1	14883	Covered lagoon (60%)	14	14	0.6
WT3	12618	Anaerobic lagoon (60%)	9	5	0.9
WT4	15241	Anaerobic lagoon (60%)	7	7	0.5
WT5	7111	Covered lagoon (60%)	6	4	0.4
WT6	10308	Anaerobic lagoon (60%)	6	6	0.5
WT7	5503	Covered lagoon (60%)	8	10	0.7
ET1	2678	Anaerobic lagoon (60%)	7	11	0.3
ET8	12368	Covered lagoon (60%)	7	7	0.5

[a] Livestock units (LU): Holstein dairy cow = 1.36 LU, Jersey dairy cow = 0.91 LU, Holstein heifer = 0.81 LU, Jersey heifer = 0.5, Holstein calf = 0.23 LU, Jersey calf = 0.18 LU.

4 Results

4.1 CH_4 emissions from Danish livestock farms – whole-farm emissions

4.1.1 CH_4 emission rates and EFs from cattle farms

Total CH_4 emission rates from the cattle farms varied from 0.7 kg/h to 28 kg/h, i.e., farms C8 and C1, the smallest and biggest, respectively. A smaller rate (0.4 kg/h) was also quantified from a few grazing animals (16 animals) on farm C8. Hence, this demonstrated that the TDM could be used to quantify large whole-farm emissions as well as low emissions from a few animals, as long as suitable roads are available and the animals are located near to each other.

Emission rates were then converted to EFs, for comparison among the farms in this and other studies. EFs varied from 11 to 54 g/LU/h and averaged 23 ± 9 g/LU/h for all farms. The annual average EFs were highest for C3, C6 and C7, with C3 being approximately 75% higher than C1 and C2 (Figure 6). Moreover, C9 had the lowest average EF. The values obtained were comparable to EFs in the literature and generally higher than studies of European farms (Amon et al., 2001; Bühler et al., 2021; Vinković et al., 2022), although seasonal representation is lacking in many of these studies. Emphasis should be given to the fact that our measurements quantified emissions from the whole farm, including barns housing dairy cows, heifers and calves and manure storage units.

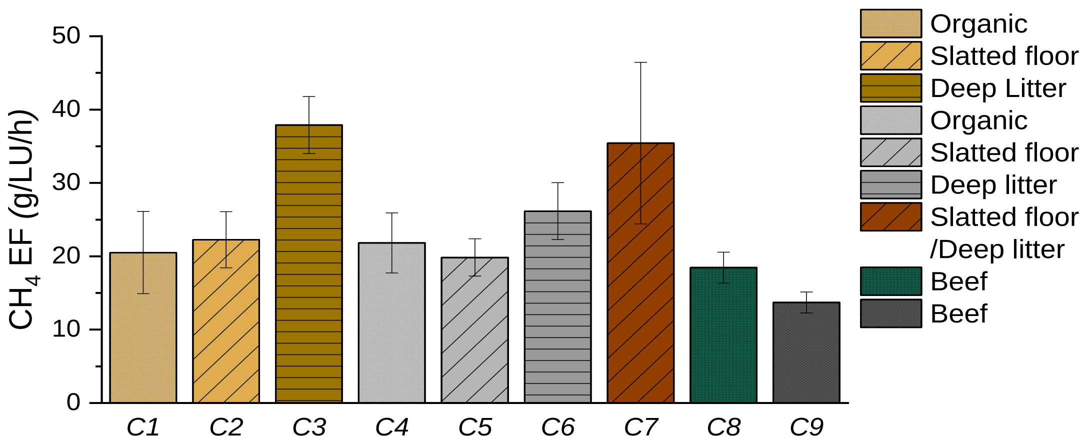

Figure 6: CH_4 EFs for cattle farms in Denmark (Paper **I**)

Farms that used a large percentage of deep litter, with a long retention time, in their housing system had the highest EFs (C3, C6 and C7) (Figure 6). Additionally, although C7 had a lower percentage of deep litter (30%) than the two other farms (60%), retention time was up to 4 months more extensive than the others (~2 months). Deep litter house management, with a long retention time, can produce CH_4 by anaerobic processes when stored for extended periods, and higher emissions from this type of management have been reported before (Edouard et al., 2013; Webb et al., 2012). In addition to deep litter, C7 changed to storing digested manure instead of raw manure in the final two of the six measurement campaigns, which reduced emissions. Jersey and Holstein dairy cows did not display significantly different EFs. Furthermore, beef farms, on average, were 38% lower than dairy cow farms, which might be due to the lower feed intake or the different animals' life stages (Ellis et al., 2007). Most farms (C2, C3, C4, C5, C6 and C9) sent their manure to a centralised biogas plant, but it is difficult to compare the impact of this treatment, as the farms' management systems differed in other ways, such as deep litter and organic farming. Furthermore, the farmers' information on dry matter intake (DMI) was limited because only some farmers shared data on animal diets; therefore, we assumed that they followed national estimations. However, C1, C2 and C3 provided their DMI, and the values were within 10% of national guidelines, namely 6, 7 and 10% higher than the national estimate, respectively.

4.1.2 CH_4 emission rates and EFs from pig farms

CH_4 emissions for pig farms ranged from 0.2 to 20 kg/h, with the lowest rates consistently from farms using acidification treatment. The highest emission rates came from farms that did not treat their manure. Farms P1 to P5 are included in Paper **II**, and farms P6 and P7 were measured after Paper **II** was finalized. Nevertheless, CH_4 emission rates from P6 and P7 tallied with rates previously measured at P1 and P2.

Emission rates were normalised to EFs. To obtain annual average values, instead of averaging all the measurements in a simple average (as in Paper **II**), we used weightings averages proportional to the measurement period (Figure 7). Here, error bars reflect standard deviations of the measurement and not any variability in the emission rates. The EFs ranged from 1.2 g/LU/h to 19g/LU/h. Although P2 and P6 had similar management systems, EFs are different and no clear explanation was found (Figure 7). This supports the need for quantifying several farms in order to derive proper statistics on CH_4 emissions. P7 did not treat its liquid manure, but it did remove it from the animal house more often than the other farms. Furthermore, P1 had no manure treatment and EFs were similar to the other farms, although different types of pigs were housed.

To date, no study has quantified CH_4 emissions from entire pig farms. Summing EFs from the animal house (Hassouna et al., 2022; Kupper et al., 2020; Philippe and Nicks, 2015) and storage tanks from livestock emission databases (Hassouna et al., 2022; Kupper et al., 2020; Philippe and Nicks, 2015), EFs representing whole-farm emissions of 10 ± 6 g/LU/h can be estimated and compared to our values. Based on this comparison, it is clear that the EFs in our study were at the high end, although still within the expected range based on emission databases for some of the farms. In our study, we considered all emission sources at the farm, including those not always considered, such as smaller tanks where manure is stored temporarily.

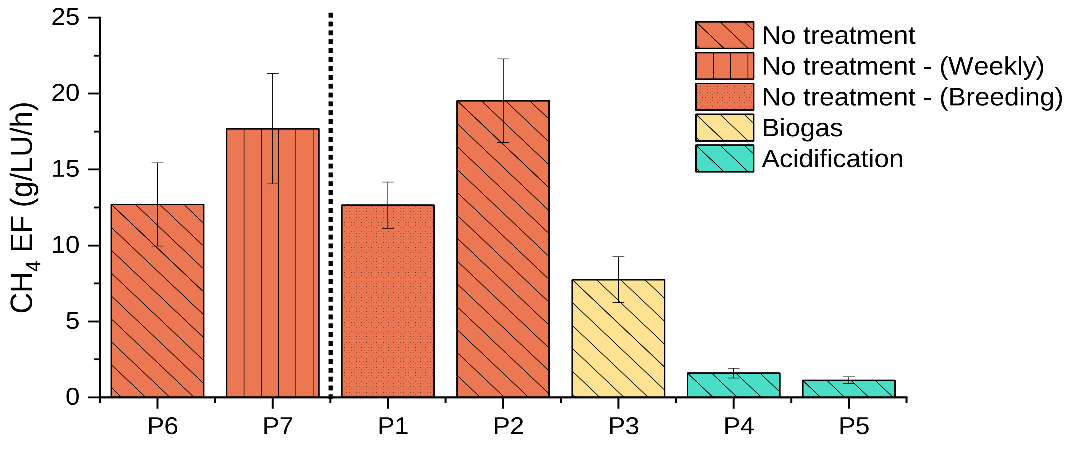

Figure 7: Pig farm CH_4 EFs (adapted from Paper **II**).

EFs significantly differ between farms with and without manure treatment. In contrast to cattle farms, manure emissions are expected to be the highest source of CH_4 emissions at pig farms. Hence, manure emission mitigation has a high impact on EFs from the pig farms. Farm P3, which sent its raw manure for anaerobic digestion and stored digested manure in outdoor tanks, had an EF about 55% lower than the P2 farm. Acidification treatment, however, was the mitigation strategy with the greatest impact on the measured farms. P4 and P5 had, on average, emissions 91 and 93% lower than P2, respectively. In the literature, emission mitigation by manure acidification is also nearly 90%

(Fangueiro et al., 2015; Lemes et al., 2022). The efficiency in emission reduction revealed herein is connected to the manure being acidified daily, which keeps the pH level lower for longer.

4.1.3 Temporal emission variability at pig and cattle farms

CH_4 emissions varied across the year at both pig and cattle farms, with emissions being lower in spring and higher at the end of the summer and into early autumn (Figure 8). Seasonal CH_4 emission variations were more pronounced at pig farms than at cattle farms because at cattle farms the primary emission source is enteric fermentation, which is not expected to vary much over the year (Arndt et al., 2018). In contrast, it is well-established that manure emissions fluctuate due to changes in temperature and the amount of manure stored, in which case seasonal emission variations occur. Consequently, CH_4 emissions from pig farms have higher seasonal variations than cattle farms, as most of the emissions come from manure. This is also supported by the fact that a similar seasonal emission fluctuation pattern has been found in studies of both pig and cattle manure tank CH_4 emissions (Husted, 1994; Kariyapperuma et al., 2018; Maldaner et al., 2018). Manure tank emissions are discussed in section 4.2 and Paper **IV**. Finally, fluctuations of emissions from manure stored in the animal house are expected to be less significant than outdoor storage tank emissions due to more constant temperatures throughout the year (Sommer et al., 2004).

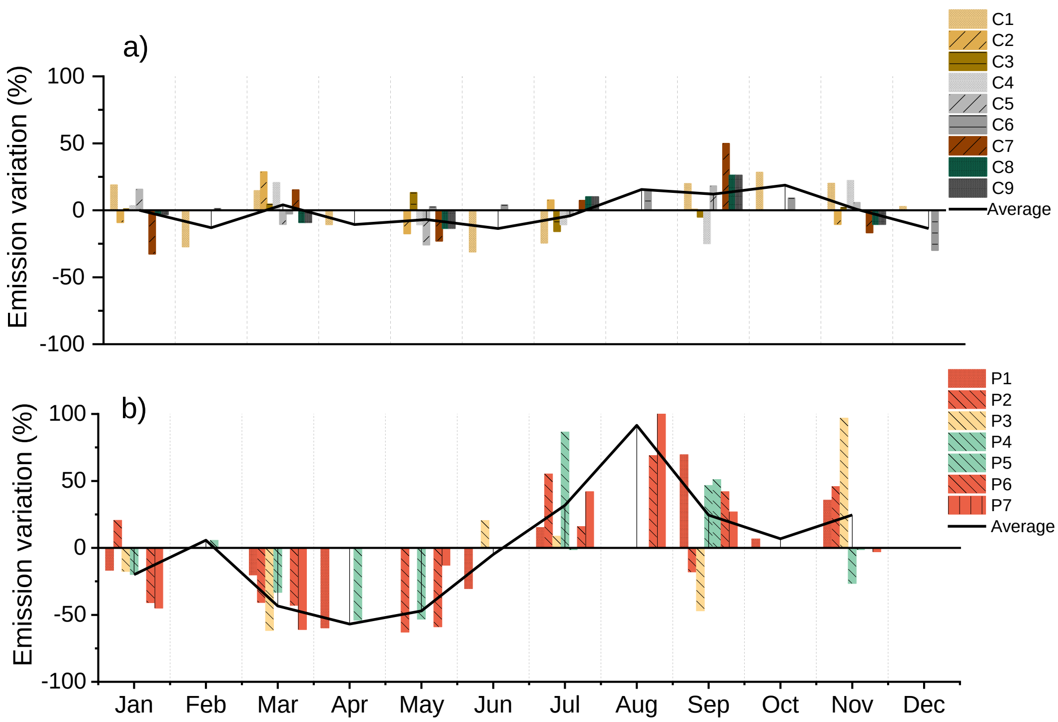

Figure 8: Seasonal CH_4 emissions variations: (a) Pig farms (b) cattle farms. (Adapted from paper **I** and **II**)

The TDM measured discrete emissions, as the measurements covered only a few hours. Of the many emission measurement campaigns performed in this study, only one or two revealed significant emission variations over this sort time period. They occurred when some special activity took place at the farm during measurement, for instance manure removal from the tanks or opening the manure tank's cover. Once they were experienced, an effort was made to avoid this from happening again. Furthermore, the diurnal variability of emissions is not yet completely understood, albeit some studies have not seen diurnal variations in whole-farm emissions (Arndt et al., 2018; Bühler et al., 2021), while others have (Ngwabie et al., 2011; VanderZaag et al., 2014). In our study, measurements were taken mainly at night to avoid diurnal emissions bias due to feeding or a high temperature on the surface of the manure. Diurnal variations in manure emissions are discussed in section 4.2.2.

4.1.4 Inventory comparison

To verify whether inventory models reflect farm-measured emissions, we compared the annually averaged emission rates to estimates found in GHG inventories. However, we acknowledge that these models were made to reflect national-scale practices and might perform poorly on farm-specific data. The IPCC inventory refinement was released during this thesis work; therefore, both older and refined versions of the IPCC guideline (IPCC, 2019, 2006) and national models (Nielsen et al., 2022) were tested. Moreover, the only farm-specific information used was numbers of animals and type of management practices; other parameters, such as DMI and VS excreted, were based on the model estimates and Danish normative (Børsting et al., 2020).

For cattle farms, the models generally underestimated CH_4 emissions by 35% in comparison to measured emissions; however, for most farms (C1, C2, C4, C5 and C6), the measured and modelled emissions were within the uncertainty levels of the two approaches (Figure 9a). C3 and C7 had larger underestimations and EFs, perhaps due to either issues with estimating emissions from deep litter or because emission rates were high at these farms. Emission rates quantified at beef cattle farms were generally higher than the models, which might be associated with uncertainties in the DMI, as they were consistently lower than for dairy cows. However, farm-specific DMI was not made available by the farmers housing beef cows and bulls.

In contrast, for pig farms, models underestimated measured emissions by 51% in comparison to measured emissions. Only the IPCC refinement performed well on the P1 farm, while the other models applied generally provided lower emissions, as was also the case for the IPCC refined models when applied at P2 and P3 (Figure 9b). Uncertainties on manure emission measurements could play a role here. According to Wolf et al. (2017), underestimations of enteric emissions are expected to be lower (~8%) than manure emissions (~37%). This notion supports the higher underestimation of pig farms, whose CH_4 emissions derive mainly from manure. Conversely, lower underestimations of emissions from cattle farms were revealed, as CH_4 is mostly produced via enteric fermentation. Furthermore, knowledge about the dynamics of and contribution to emissions from the animal house and outdoor storage tanks is still limited (Petersen et al., 2016). The model was done in Paper **II** study, therefore the two other farms added later (P6 and P7) where not added here, and the farms with acidification treatment (P4 and P5) could also not be analysed because this management is not included in inventories. More about emissions from pig and cattle farm manure storage units is discussed in section 4.2.

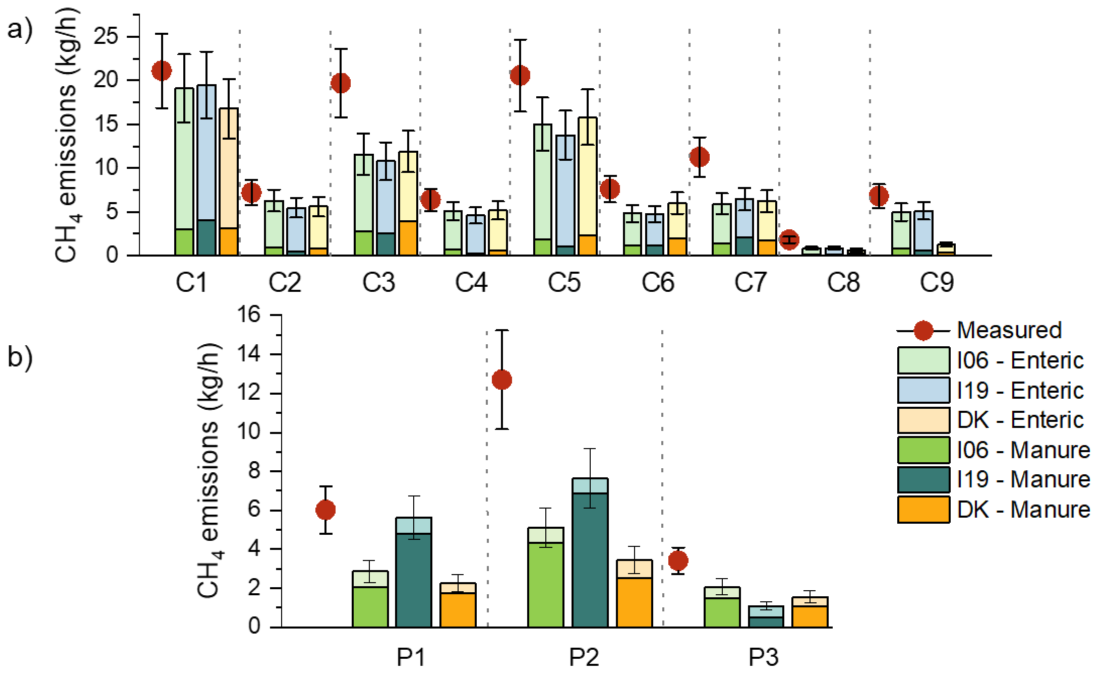

Figure 9: Comparison of average measured and modelled farm emissions. a) Cattle b) Pig farms. (Adapted from Paper **I** (a) and **II** (b))

4.2 CH_4 emissions from Danish livestock farms – manure storage emissions

Measurements of farm-scale manure tanks are essential to closing knowledge gaps about the dynamics and magnitude of CH_4 emissions in actual farm practices. In this study (Paper **IV**), CH_4 emissions from ten manure storage tanks were quantified, using the TDM.

4.2.1 CH_4 emission rates and EFs from manure storage tanks

The measured annual average CH_4 emission rates varied from 0.01 to 14.3 kg/h, while the annual average manure temperature among the tanks varied from 10.6 to 16.4 ºC and averaged 13.8 ºC. The VS% was higher for cattle (3.1 to 4.4%) than for pig-stored manure (1.2 to 3.6%). Furthermore, emission rates (kg/h) were normalised by the amount of manure stored (g/m^3/h). EFs for tanks storing cattle (CN1 and CN2) and digested manure (DN1 and DC1) were similar, averaging 0.63 ± 0.09 g/m^3/h and 0.50 ± 0.02 g/m^3/h, respectively (Figure 10). The average EF for pig manure tanks was 1.56 ± 0.93 g/m^3/h; however, there was a considerable variation between the tanks (from 0.20 to 2.75 g/m^3/h) (Figure 10).

Emissions were also normalised by LU, resulting in EFs of 1.6 ± 0.4 g/LU/h and 8.9 ± 7.1 g/LU/h for cattle and pig manure, respectively. Comparing EFs obtained from the entire farm with EFs from manure tanks, the latter represented approximately 60% of all emissions from pig farms (8.9 g/LU/h out of 15 g/LU/h) and 7% at cattle farms. In Paper **III**, a comparison of whole-farm (C1) and manure tank emissions (CN2) suggests that the measured tanks contributed 14% of total farm emissions at the studied farms.

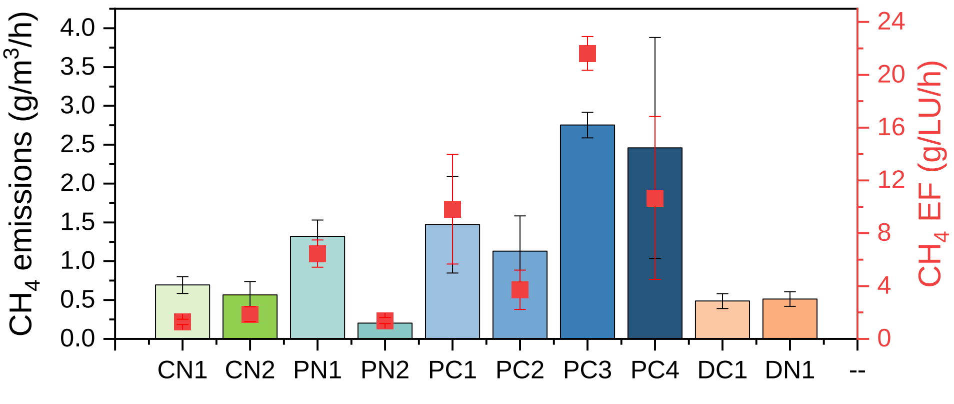

Figure 10: Annually averaged emission rates from ten manure tanks (Left) normalised by amount of manure and (Right) normalised by livestock unit. Bars and dots represent the average emission rate, while the error bar shows averaged variability on the measured transect. Green bars represent manure tanks storing cattle manure, blue for pig manure and orange for digested manure. (Adapted from Paper **IV**)

4.2.2 Temporal emission variability in manure tanks

Seasonal variability in CH_4 emissions from manure tanks was high, as the emissions in some tanks varied by around ±100% of their average (Figure 11). The pattern of emission fluctuations is similar to observations in whole-farm emissions studies, with emissions being lower in spring and high in late summer and early autumn (Figure 11). This hysteresis in emissions dynamics (Kariyapperuma et al., 2018), meaning lower emissions in the warming phase (spring) than in the cooling phase (autumn), is related to the amount of manure stored and e manure temperature history (Cárdenas et al., 2021). The magnitude of these variations is more like the seasonal emission variations observed at pig farms than at the cattle farms, because the large proportion of pig farm emissions emanates from external storage tanks.

Significant diurnal variations in CH_4 emissions from storage tanks have been observed in some studies (Maldaner et al., 2018; VanderZaag et al., 2014), while in others the fluctuation range was smaller (Baldé et al., 2016). These studies focused on measuring emissions from tanks without a cover. Covered tanks do not have direct surface heating caused by solar radiation incidence. On the other hand, the cover can also warm the manure surface by keeping the heat in the cover headspace for a long time, which might affect emissions dynamics differently than open tanks. Therefore, at one of the covered tanks, emissions were measured continuously by pumping air from the tank's headspace while measuring the flow rate, gas concentrations and temperature. No strong diurnal variation (< 20%) in daily average emissions was observed when averaging the measured emissions over the four seasons. More details are described in Paper **IV**.

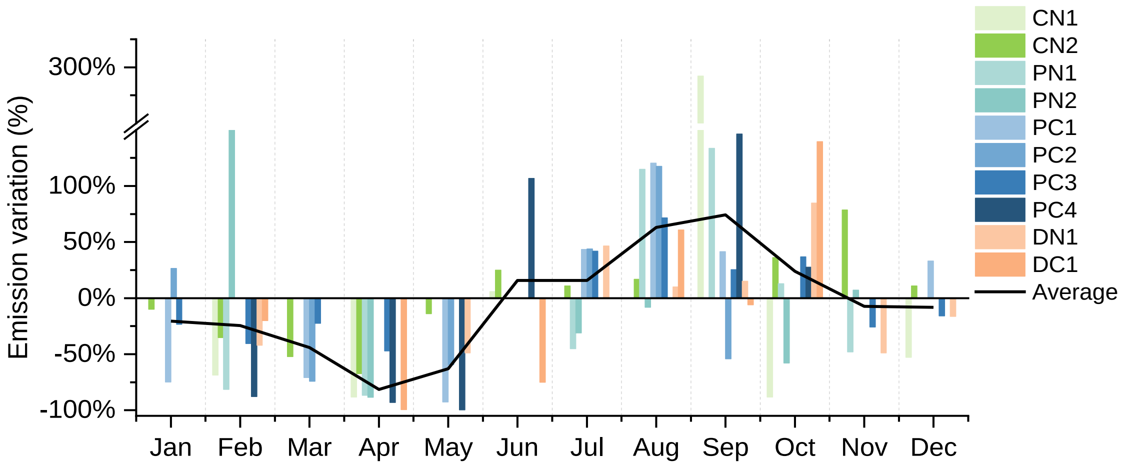

Figure 11: Seasonal variability of measured manure tank emission rates.

4.2.3 Factors affecting emissions

Other supporting information was collected to support the analysis of the measured emission rates (kg/h) and to evaluate which factors significantly affected manure CH_4 emissions. The results for this analysis aligned with other studies showing that manure temperature is the primary explanatory variable, thus demonstrating an exponential relationship with emissions.

Manure type (e.g., cattle, pig and digested manure) also significantly influences emissions. As previously mentioned, raw pig manure had higher emissions than cattle raw manure (Figure 12a). On the other hand, cattle raw manure EFs were only slightly higher than digested manure EFs. However, manure temperature was higher in the digested manure than in cattle manure. On the other hand, CH_4 potential in the digested manure was expected to be lower than in raw cattle manure cattle (Elsgaard et al., 2016), albeit the higher temperature in the digestate might have led to similar emissions (Figure 12a).

Furthermore, the tank's cover was another explanatory variable with a significant impact on emissions (Figure 12b). Covered tanks produced greater emissions than the uncovered tanks (Figure 12b), possibly due to the combination of two different factors. First, anaerobic digestion can produce a small but positive amount of heat (Im et al., 2022), which cannot easily escape into the atmosphere in covered tanks. We observed a slight difference in the temperature offset (manure temperature minus atmospheric temperature) between covered and uncovered tanks; however, more measurements following these two types of tanks are needed to understand if this is the main explanation. Second, when a homogeneous crust is established, CH_4 emissions might be lower due to CH_4

oxidation in the crust (Wood et al., 2013). Covered tanks, though, seldom form a crust, in which case emission mitigation due to CH_4 oxidation is not likely.

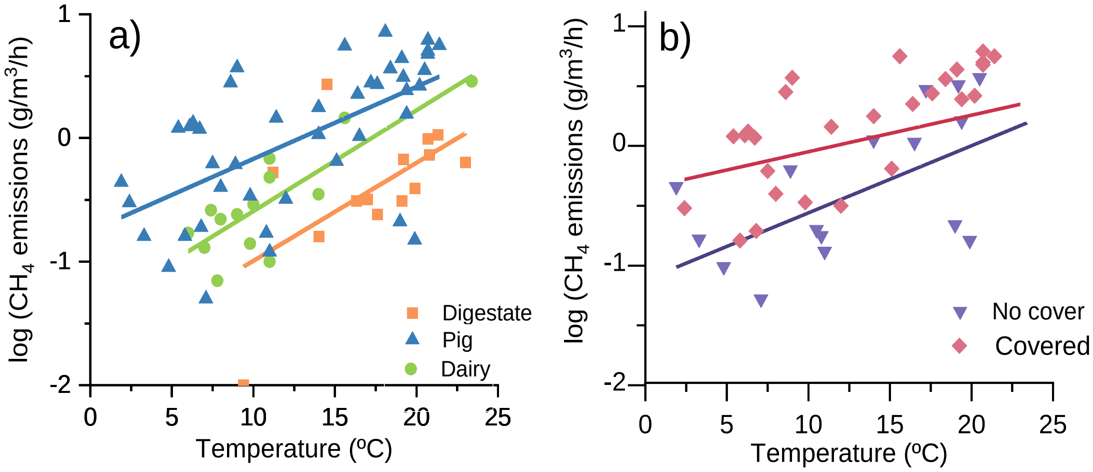

Figure 12: Emissions versus temperature: (a) Effect of manure type, (b) effect of cover. (Adapted from Paper **IV**)

4.3 CH_4 and NH_3 emissions from concentrated animal feedlot operations in the US

This study used two other methods to quantify CH_4 and NH_3 from dairy CAFOs in California (Paper **V**). SOF was used to measure NH_3, while CH_4 was estimated using the IFM.

4.3.1 CH_4 and NH_3 emission rates and EFs from dairy CAFOs

Average NH_3 emission rates varied from 32 kg/h to 191 kg/h, while CH_4 varied from 155 to 874 kg/h, measured at the smallest and largest farms, respectively. Considering NH_3 EFs, they varied from 4.8 to 12.6 g/LU/h and averaged at 9.1 g/LU/h. For CH_4, EFs varied from 13.1 to 68.5 and averaged at 40 g/LU/h (Figure 13).

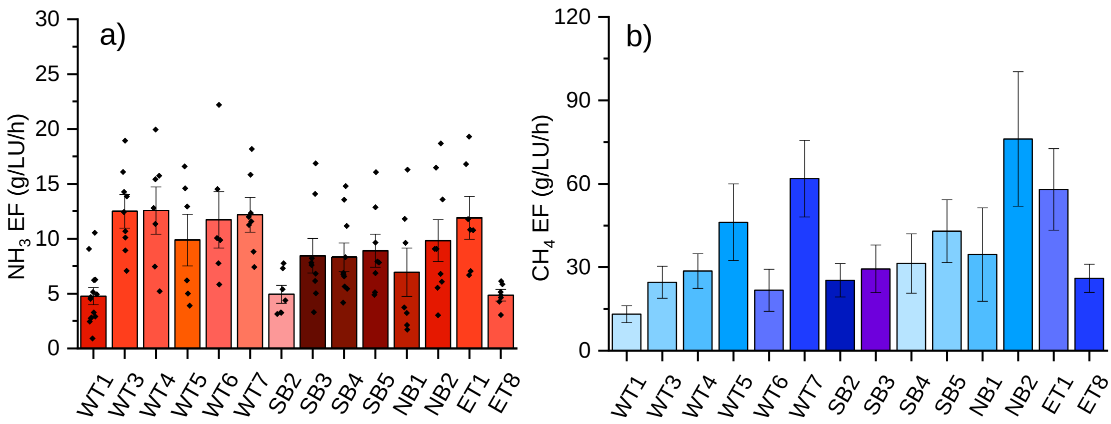

Figure 13: EFs of (a) NH_3 and (b) CH_4 emissions from Californian CAFOs measured in May. (Paper **V**)

Elevated ground concentrations of ethanol were detected at three farms during daytime hours in May. Measurements were performed immediately downwind of the feed storage units and correlated with the smell of alcohol. Concentrations were only observed at facilities where measurements could be done close to the source. Ethanol emissions from feed storage have been reported elsewhere (Yuan et al., 2017). In addition, acetic acid was detected in one of the facilities, most likely also associated with the feeding storage area. Moreover, ground concentrations of nitrous oxide (N_2O) were detected, albeit these were mostly associated with soil emissions from surrounding agricultural fields rather than the animal feedlots.

4.3.2 Temporal emission variability at dairy CAFOs

Unlike the Danish farm studies, measurements were performed only two times during the year in California. NH_3 emissions were similar in both campaigns. This emission can vary by a factor of 10 over the year (Paper **V**, Supplementary information), but May and October had similar rates, most likely because the temperature in this region is similar in both months and is close to the annual average. This is due to NH_3 emissions mainly being driven by short-term changes to manure surface temperature. On the other hand, CH_4 manure emissions are influenced by changes to temperature on a scale of several days to months, as well as manure management, e.g., removal of manure from storage. Two of the farms had different CH_4 emission readings in October and May, but we had no information about the manure management system, which could potentially be used to explain the variations.

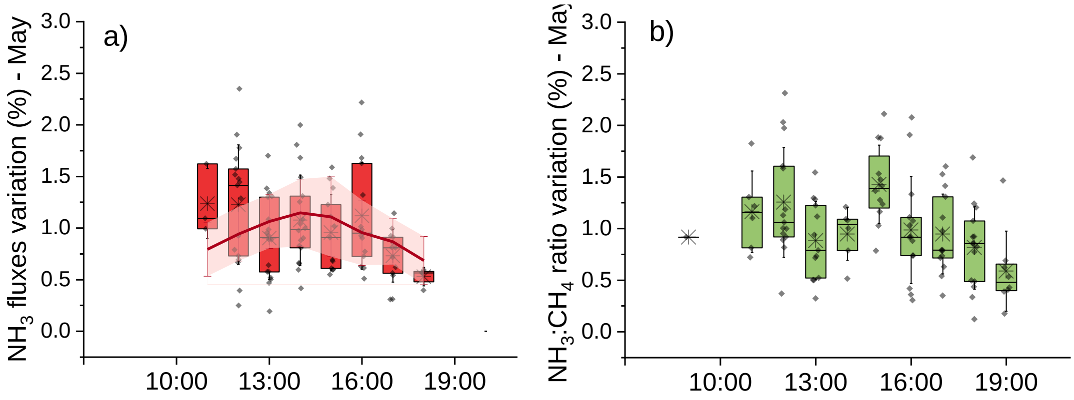

Figure 14: Diurnal variation in emissions: a) NH_3 diurnal variation in May, solid lines correspond to the average of the modelled values from the same measurement period. b) NH_3:CH_4 ratio diurnal variation in May. Figure representing also the October campaign is on Paper **V**. (Adapted from Paper **V**)

Since short-lived temperature variations affect NH_3 rates, diurnal variations in temperature and wind speed will cause a diurnal pattern in emissions. This variation in emissions was observed when the EFs were plotted versus the time of the day, whilst it was also noticed in the NH_3:CH_4 ratios. Other studies have also detected these emission fluctuations (Golston et al., 2020; Lonsdale et al., 2017; Miller et al., 2015). The SOF method is only applicable in sunny weather and daytime conditions; therefore, when investigating NH_3 emissions from farm sources, diurnal variations in rates must be considered. The NH_3:CH_4 ratios also followed a similar pattern, but it is more challenging to establish if such a fluctuation is due to only diurnal NH_3 variations or CH_4 also. As discussed earlier, CH_4 diurnal emission variations have been observed in some studies and not in others. It is also relevant to mention that Californian CAFOs manure management practice is to use anaerobic lagoons instead of concrete manure tanks as in most Danish farms.

4.3.3 Comparison with the inventory and other literature

On average, measured NH_3 was 28% higher than NEI inventory estimates (Figure 15a). Inventory calculations considered the diurnal variation model. However, an overestimation of 71% for diurnal bias was not considered. When comparing the EFs obtained in this study with other measurements at similar farms, the quantified emissions were at the high end of EF because they corresponded to daytime emissions only. These were also in line with other works using SOF to quantify NH_3 emissions (Kille et al., 2017).

For CH_4, the measured emissions were higher than the CARB inventory by 60% (Figure 15b). Additionally, these measurements were similar to estimations done using airborne mass balance flux measurements at the same facilities (Thompson et al., 2019). A recent study (Amini et al., 2022) compared measured emissions in the same area with the CARB inventory and airborne quantifications. Unlike our study, they determined that measurements were only 8% higher than the inventory. However, they assumed that manure was 100% managed in anaerobic lagoons, which was higher than the percentage used in our study (60%). On the other hand, our estimations also align with other studies discussing manure management representativeness in the SJV (Marklein et al., 2021). Furthermore, 40% of the measured farms had a cover on the anaerobic lagoons, and several facilities had solid-liquid separator machines. Therefore, assuming that 100% of the manure was treated in an anaerobic lagoon would not be suitable in our study. Conversely, the comparison of emissions between farms with and without a cover with the anaerobic lagoon did not show significantly different CH_4 EFs; it is uncertain, however, whether they were complete or collecting CH_4 for energy production at all farms.

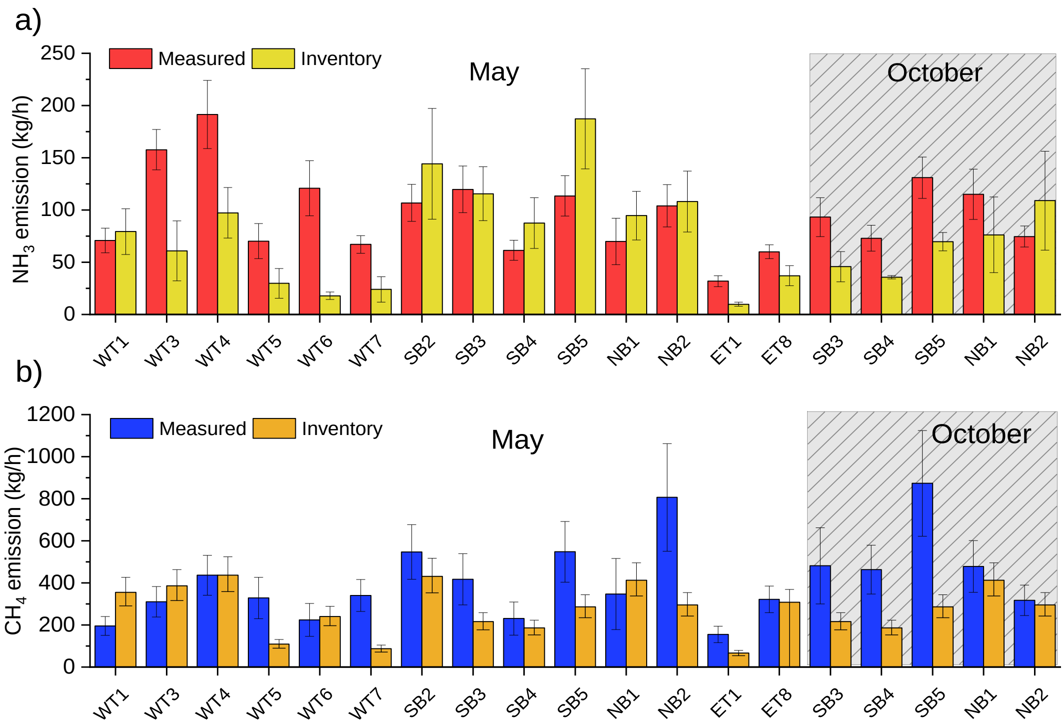

Figure 15: Comparison of measured emissions and inventory estimated emissions: (a) NH_3 and (b) CH_4. (Adapted from Paper **V**)

5 Discussion

A full understanding of farm-scale CH_4 and NH_3 emissions is scarce. Therefore, in this thesis, we investigated several operational farms, using a systematic methodology for comparison within different practices. The results revealed a good deal of variability among similarly managed farms, indicating that minor practices largely influence emissions. Therefore, using single EFs to estimate farm emissions is insufficient, so a large dataset on farm emission rates and emission factors across several farms, considering different management practices and mitigation, is essential.

5.1 Suitability of the methods to study CH_4 and NH_3 emissions from livestock production

The results illustrated that all the methods were applicable to quantifying farm emissions. The TDM was adequate in relation to the strength of the emissions at the studied sites (0.5 to 20 kg/h) (Paper **I** and **II**); for instance, despite low CH_4 emissions from pig farms carrying out acidification treatment, emission rates were obtained (Paper **II**). The TDM method can also be applied to measure whole-farm emissions from several farms, due to low requirements for site selection and no reliance on wind information. In addition, the method was further developed to allow for higher flexibility in quantifying single manure tank emissions when road accessibility was limited (Paper **III**). Moreover, although method comparison was not performed in the project, this has been done in another study (Arndt et al., 2018), which obtained similar rates for IDM, TDM and airborne measurements.

NH_3 is a reactive gas and difficult to quantify, so instrument limitations often challenge emissions measurements methodology (Twigg et al., 2022). SOF performed well in the validation test (Pape **VI**), and uncertainty calculations were approximately 30%, thus demonstrating as reliable method to obtain NH_3 emissions. The method was also suitable for quantifying NH_3 emission measurements from small (1 kg/h) to large sources (100 kg/h) (Paper **VI**). Additionally, the method had the flexibility to measure individual facilities in areas with a high farm density because measuring upwind and downwind plumes allowed for isolating individual sources (Paper **VI**). The indirect flux method (IFM) also detected CH_4 rates at the typical range of farm emissions with an uncertainty of approximately 50%.

All of the studied methods are non-intrusive and can quantify direct emissions from the entire facility, as they were not initially designed to discern single sources. In addition, their setup is flexible, allowing for significant spatial cover; consequently, several facilities can be investigated quickly using single instrumentation. They are rather accurate and precise, as shown in the uncertainty analysis, as they do not rely upon wind modelling, which can add uncertainty to the quantifications. The advantages of the methods applied in this project, compared to commonly used methods such as surface chambers, for instance, is that they are non-intrusive and measure fluxes from the whole source (Tedeschi et al., 2022). Furthermore, micrometeorological techniques are often stationary, and although continuous data is obtained, they lose 50 to 80% of this data due to wind direction coverage (Bühler et al., 2021; Lemes et al., 2022).

TDM, SOF or IFM are not designed for continuous measurements. Additionally, perhaps their main limitation is caused by weather conditions. SOF quantifications are restricted to sunny daytime conditions, as IFM is limited to SOF quantification; in this case, the same limitation applies to it. On the other hand, TDM is more challenging to use on days with strong convection, as the concentration will be low at ground level. Therefore, TDM is better for neutral or stable atmospheric conditions, allowing for concentration measurements at greater distances. In addition, the bias introduced by diurnal variations in manure emissions is minimised in these conditions (night time, cloudy) (Wood et al., 2013).

5.2 CH_4 and NH_3 emission rates and EFs from different production systems

Direct CH_4 emission rates and EFs from whole farms were reported for the first time for Danish cattle and pig production facilities in Papers **I** and **II**, respectively. Direct NH_3 and CH_4 emission rates from dairy CAFOs in California were reported in Paper **V**. Dairies in the USA averaged CH_4 emissions of 40±18 g/LU/h, and there was a large variation between EFs, as farms were quantified, ranging from approximately 13 to 68 g/LU/h. Dairy farms in Denmark averaged 26±8 g/LU/h varying from 20 to 38 g/LU/h. Several factors can justify the difference in emissions between farms located in these two countries, most likely linked to manure management emissions (Wirsenius et al., 2020). The climate of the two regions is quite different, with the annual average temperature for Denmark being 9.4 ºC, whilst it is 19.4 ºC for SJV, California. Furthermore, the management system adopted by each farm might also have influenced emission differences, as anaerobic lagoons are expected to produce more emissions than slurry pits (Wirsenius et al., 2020). Furthermore, Arndt et al. (2018) measured emission contributions from manure management (Lagoons) of 70% in summer and 35% in winter, while at a cattle farm (Paper **III**), we saw contributions of 15% and 8% in summer and winter, respectively.

Measurements showed that modelled emissions are underestimated compared to single-farm emissions (Papers **I**, **II** and **V**). The underestimation was lower for Danish dairy farms, as enteric emissions are the biggest contributor to farm emissions, and better knowledge about this source makes it easier to model them (Hristov et al., 2018). Most farm emission rates were within the models and measurement uncertainty levels. On the other hand, manure emissions are more difficult to model, and so the model perform poorly in farms where manure emissions are dominant. In this study, these were the Danish pig farms and Californian CAFOs. For the Danish pig farms, model revision could benefit manure emissions modelling, as well as revision of the main emissions parameters such as manure temperature. The measured temperatures were higher than those used in the models (Nielsen et al., 2022) and found in previous studies on northern European conditions (Husted, 1994; Rodhe et al., 2015). The manure tank cover also increases emissions, which was used more in pig manure tanks and at most of the pig farms studied herein. Additionally, more data should be collected to improve statistics. The measurements show that emissions can vary greatly among farms and tanks with similar characteristics. Apart from manure modelling uncertainties, the underestimation of American farms is also linked to limited information on their management.

5.3 Factors affecting CH_4 emissions

For all Danish farms, emissions were high at the end of summer and in early autumn, and lower during spring. Cattle farm emissions varied less across the year, which is different from the pig farms, due to manure being the dominant emission source on the latter. Studies measuring whole-farm emissions, or even single sources, several times a year are scarce in the literature.

Furthermore, for diurnal variations, CH_4 emissions from manure are not well documented. Wood et al. (2013) concluded that the reason for daily variations in emissions is the overnight accumulation of gas bubbles in the manure and their release in the early morning, caused by surface heating, coinciding with periods of high gas production. This warming allows for both a decrease in surface tension and gas expansion. These gas bubble bursts are lower on cloudy days, because of lower surface heating, or when there is a presence of a natural crust on the surface of the manure (Wood et al., 2013). Therefore, Wood et al. (2013) recommended discrete night-time sampling over a maximum interval of seven days. On the other hand, Wood et al. (2013) highlighted an overestimation of only 15% when not following the recommended sampling (~ 21days sampling interval). The presented studies (Danish cattle and pig whole farms) mostly fulfilled this time-of-day requisite. The same is not valid for the manure tank measurements, but since diurnal overestimation is small, the bias in our dataset should be minimal. In contrast, diurnal variations in ammonia emissions have been better documented (Lonsdale et al., 2017; Sun et al., 2015), and models have been developed to estimate these fluctuations (Zhu et al., 2015a). Therefore, due to the SOF weather conditions limitation, the quantified emissions only reflect daytime conditions, and in order to obtain total emissions during the day, a model of the expected diurnal fluctuation or measurements using another methodology are needed.

Results from the TDM method demonstrated that manure temperature was an important factor affecting emissions (Paper **IV**). This correlation is not a new finding (Husted, 1994; Maldaner et al., 2018) but it does confirm the method's suitability in terms of identifying factors affecting CH_4 rates. Furthermore, pig manure emissions were higher than cattle emissions, which were then greater than digested manure. A few studies have noted that pig manure produces more CH_4 (Kupper et al., 2020) because of the higher content on easily degradable VS when compared to cattle manure (Petersen et al., 2016). The most exciting finding here was the impact of the manure tank cover in CH_4 emissions, i.e., higher EFs for covered than uncovered tanks. The suggested reason is both the preservation of heat by the cover (Im et al., 2022), leading to a higher manure temperature, and the lack of crust formation. However, this hypothesis still needed to be proven. CH_4 emissions from pig manure tanks also showed considerable variability among the studied tanks, potentially due to small differences in farm management practices, such as the use of intermediary tanks.

5.4 CH_4 mitigation strategies' impact on emissions

TDM can be used to quantify emission mitigation efficiencies from biogas and acidification strategies. Mitigation efficiencies need to be documented in order to be implemented in inventory methods, especially results from farm-scale practices.

This was the first study to quantify CH_4 emissions mitigation from an entire pig farm using acidification treatment. Emissions were 91-93% lower than from pig farms without a manure treatment (P2) (Paper **II**). High mitigation efficiency was expected once it was reported that acidification could reduce CH_4 manure emissions by up to 95% (Fangueiro et al., 2015; Lemes et al., 2022). The percentage of enteric emissions from the pig farms should be low and also be in accordance with the measured rates.

In Denmark, delivering raw manure to centralised biogas plants, and then storing digested manure, is the most common practice, instead of farms having their own biogas reactors (Nielsen et al., 2022). Furthermore, emissions from the cattle manure tanks were similar to tanks storing digested manure (~ 20% difference) (Paper **IV**), and also in farms with and without anaerobic lagoon covers (Paper **V**). In contrast, there was a significant difference between pig manure and digested manure (~ 68%) (Paper **IV**), thus supporting the lower emissions from pig farms storing digested manure (~ 55%, P3) (Paper **II**) compared with farms where manure was not treated (P2). For the whole cattle farms, differences in emissions caused by biogas treatment could not be evaluated, as mentioned previously (Paper **I**). Studies looking at emissions from digested manure have focused on dairy manure (Maldaner et al., 2018; Rodhe et al., 2015)

6 Conclusions

CH_4 emission rates and factors were quantified from livestock production facilities in Denmark and California. The tracer gas dispersion method (TDM) was used in Denmark, while the indirect flux method (IFM) was used in the USA. Furthermore, NH_3 emission rates were also measured at dairy farms in California via the solar occultation flux method (SOF). CH_4 emission rates from cattle farms in Denmark varied from 0.7 to 28 kg/h, while in the USA they ranged from 155 to 874 kg/h. Californian farms were much larger (~ 2000 to 20000 LU) compared to Danish farms (~150 to 1200 LU). Average EFs were 40 and 26 g/LU/h for American and Danish cattle, respectively, due to differences in both management and climate. Additionally, NH_3 emission rates varied from 32 to 199 kg/h, and EFs averaged 9 g/LU/h.

Uncertainty for the SOF NH_3 measurements was 37% on average, and for IFM it was 53% when quantifying CH_4. All three tested methods measured discrete emissions, which lasted a couple of hours. Additionally, in Denmark, measurements were taken a minimum of six times a year, while in the USA, only two quantifications were performed. The techniques were suitable for this source, covering emission rates and showing the expected temporal variability over the year. CH_4 emissions from Danish cattle did not broadly fluctuate during the year, as enteric fermentation is the primary CH_4 production mechanism and remains rather constant over the year. On the contrary, CH_4 emissions from pig farms showed significant variability over the year, and manure was its primary CH_4 source, which is dependent on temperature and organic matter availability.

All comparisons between measured CH_4 and inventory emissions calculations exhibited an underestimation by modelled emissions. The smallest difference was found for Danish cattle, again likely due to enteric emissions being an easier source to predict emissions. For the Danish pig farms, however, where manure emissions dominate, it is more challenging for the model to perform. This is similar to results for American cattle farms, where manure also dominates due to climate and management choices. For NH_3 emissions, the models performed well, as long as the diurnal variation in emissions was considered.

Furthermore, a stationary TDM approach was developed in order to offer more flexibility for manure tank measurement. The stationary TDM uses the same principles as a mobile TDM, ensuring accuracy but sampling at stationary sampling points placed in a field where a vehicle cannot drive. Combining mobile and stationary TDM, CH_4 emission measurements of ten manure tanks were performed at least six times over the year. Pig manure had the greatest CH_4 emissions, while digested manure had the lowest. Additionally, covered tanks showed higher emissions than non-covered tanks.

Moreover, the impact of mitigation strategies on CH_4 emissions was investigated. Using centralised biogas plants to collect raw manure at farms and returned digested manure is efficient for mitigating CH_4 from pig manure. In California, anaerobic digestion treatment was done by covering anaerobic lagoons in order to collect CH_4 gas, thus avoiding its release into the atmosphere. However, emission reduction by this type of system was not observed. Farms employing in-house acidification of manure exhibited emissions approximately 90% lower than a farm with no manure treatment.

Finally, this study provided annual rates and EFs from whole-farm emissions for the first time (cattle and pig northern European farms and dairy CAFOs in SJV). Furthermore, we developed and investigated methods to enrich the toolset for further research into emissions at this type of facility.

7 Future research

The methods developed and applied in this thesis can continue to be used to study CH_4 and NH_3 emissions from livestock farms in the following ways:

- There is a need to understand how the dispersion of the gases by wind affects the measurement of plume concentrations. Finalisation of the wind modelling experiment to better evaluate wind parameters in the SOF method, thus reducing uncertainty, so that the method becomes more accurate and precise. Initial steps in this regard were taken in this study, albeit they were not concluded before the end of this thesis.
- The use of the TDM, SOF or IFM, in combination with a method measuring continuous emissions (e.g., IDM and eddy covariance), should be studied. Although the results of this thesis established the good reliability of discrete method sampling, it would be relevant to combine it with a continuous method. This setup could be used to look further at the variability of emissions and how daily practices influence emissions.
- For Danish cattle farms, the impact on emissions of a few inconclusive factors herein, such as deep litter usage and beef farm underestimations, could be studied. Additionally, for cattle farms it would be interesting to investigate the biogas mitigation of manure emissions.
- Evaluate the contribution of different sources (animal housing and manure) on the same farm with simultaneous measurements, for instance to understand emission dynamics and pig animal house and manure tanks. Such information could be used, for example, to improve inventory calculations of pig farms.
- Once NH_3 has been quantified at pig and cattle manure farms in Denmark, the method could then be used to investigate further emissions from this source, also in combination with the TDM, so that night-time emissions can be quantified.

8 References

Amini, S., Kuwayama, T., Gong, L., Falk, M., Chen, Y., Mitloehner, Q., Weller, S., Mitloehner, F.M., Patteson, D., Conley, S.A., Scheehle, E., FitzGibbon, M., 2022. Evaluating California dairy methane emission factors using short-term ground-level and airborne measurements. Atmos. Environ. X 14, 100171. https://doi.org/10.1016/j.aeaoa.2022.100171

Amon, B., Amon, T., Boxberger, J., Alt, C., 2001. Emissions of NH3, N2O and CH4 from dairy cows housed in a farmyard manure tying stall (housing, manure storage, manure spreading). Nutr. Cycl. Agroecosystems 60, 103–113. https://doi.org/10.1023/A:1012649028772

Arndt, C., Leytem, A.B., Hristov, A.N., Zavala-Araiza, D., Cativiela, J.P., Conley, S., Daube, C., Faloona, I., Herndon, S.C., 2018. Short-term methane emissions from 2 dairy farms in California estimated by different measurement techniques and US Environmental Protection Agency inventory methodology: A case study. J. Dairy Sci. 101, 11461–11479. https://doi.org/10.3168/jds.2017-13881

Baldé, H., VanderZaag, A.C., Burtt, S.D., Wagner-Riddle, C., Crolla, A., Desjardins, R.L., MacDonald, D.J., 2016. Methane emissions from digestate at an agricultural biogas plant. Bioresour. Technol. 216, 914–922. https://doi.org/10.1016/j.biortech.2016.06.031

Bjerg, B., Demeyer, P., Hoyaux, J., Didara, M., Grönroos, J., Hassouna, M., Amon, B., Bartzanas, T., Sándor, R., Fogarty, M., Klas, S., Schiavon, S., Juskiene, V., Radeski, M., Attard, G., Aarnink, A., Gülzari, Ş.Ö., Kuczyński, T., Fangueiro, D., Marin, M.P., Mihina, S., Verbič, J., Calvet, S., Jeppsson, K.H., Menzi, H., Sizmaz, O., Norton, T., 2019. Review of legal requirements on ammonia and greenhouse gases emissions from animal production buildings in european countries. 2019 ASABE Annu. Int. Meet. https://doi.org/10.13031/aim.201901070

Bjorneberg, D.L., Leytem, a B., Westermann, D.T., Griffiths, P.R., Shao, L., Pollard, M.J., 2009. Measurement of atmospheric ammonia, methane, and nitrous oxide at a concentrated dairy production facility in southern Idaho using open-path FTIR spctrometry. Transcations Am. Soc. Agric. Biol. Eng. 52, 1749–1756. https://doi.org/10.13031/2013.29137

Blanes-Vidal, V., Hansen, M.N., Pedersen, S., Rom, H.B., 2008. Emissions of ammonia, methane and nitrous oxide from pig houses and slurry: Effects of rooting material, animal activity and ventilation flow. Agric. Ecosyst. Environ. 124, 237–244. https://doi.org/10.1016/j.agee.2007.10.002

Børsting, C.F., Hellwing, A.L.F., Lund, P., 2020. Normative figures 2020.

Bühler, M., Häni, C., Ammann, C., Mohn, J., Neftel, A., Schrade, S., Zähner, M., Zeyer, K., Brönnimann, S., Kupper, T., 2021. Assessment of the inverse dispersion method for the determination of methane emissions from a dairy housing. Agric. For. Meteorol. 307. https://doi.org/10.1016/j.agrformet.2021.108501

Cárdenas, A., Ammon, C., Schumacher, B., Stinner, W., Herrmann, C., Schneider, M., Weinrich, S., Fischer, P., Amon, T., Amon, B., 2021. Methane emissions from the storage of liquid dairy manure: Influences of season, temperature and storage duration. Waste Manag. 121, 393–402. https://doi.org/10.1016/j.wasman.2020.12.026

Climate watch, 2022. Washington, DC: World Resources Institute. [WWW Document]. URL https://www.climatewatchdata.org.

Dalby, F.R., Hafner, S.D., Petersen, S.O., VanderZaag, A.C., Habtewold, J., Dunfield, K., Chantigny, M.H., Sommer, S.G., 2021. Understanding methane emission from stored animal manure: A review to guide model development. J. Environ. Qual. 50, 817–835. https://doi.org/10.1002/jeq2.20252

Dalby, F.R., Hansen, M.J., Guldberg, L.B., Hafner, S.D., Feilberg, A., 2022. Simple Management Changes Drastically Reduce Pig House Methane Emission in Combined Experimental and Modeling Study. Environ. Sci. Technol. https://doi.org/10.1021/acs.est.2c08891

Danish Agriculture & Food Council, 2020. Statistics - pig meat. Copenhagen.

Daube, C., Conley, S., Faloona, I.C., Arndt, C., Yacovitch, T.I., Roscioli, J.R., Herndon, S.C., 2018. Using the tracer flux ratio method with flight measurements to estimate dairy farm CH4 emissions in central California 1–20. https://doi.org/10.5194/amt-2018-356

Delre, A., Mønster, J., Samuelsson, J., Fredenslund, A.M., Scheutz, C., 2018. Emission quantification using the tracer gas dispersion method: The influence of instrument, tracer gas species and source simulation. Sci. Total Environ. 634, 59–66. https://doi.org/10.1016/j.scitotenv.2018.03.289

Duwe, M., Evans, N., 2020. Climate Laws in Europe: Good Practices in Net-Zero Management. Berlin, Den Haag.

EDGAR database, 2023. EDGAR - Emissions Database for Global Atmospheric Research Air and Toxic pollutants [WWW Document]. URL https://edgar.jrc.ec.europa.eu/air_pollutants

Edouard, N., Charpiot, A., Hassouna, M., Faverdin, P., Robin, P., Dolle, J.B., 2013. Ammonia and grenhouse gases emissions from dairy cattle buildings: slurry vc. farm yard manure management systems. Emiss. gas dust from Livest. 122–125.

Eilerman, S.J., Peischl, J., Neuman, J.A., Ryerson, T.B., Aikin, K.C., Holloway, M.W., Zondlo, M.A., Golston, L.M., Pan, D., Floerchinger, C., Herndon, S., 2016. Characterization of Ammonia, Methane, and Nitrous Oxide Emissions from Concentrated Animal Feeding Operations in Northeastern Colorado. Environ. Sci. Technol. 50, 10885–10893. https://doi.org/10.1021/acs.est.6b02851

Ellis, J.L., Kebreab, E., Odongo, N.E., McBride, B.W., Okine, E.K., France, J., 2007. Prediction of methane production from dairy and beef cattle. J. Dairy Sci. 90, 3456–3466. https://doi.org/10.3168/jds.2006-675

Elsgaard, L., Olsen, A.B., Petersen, S.O., 2016. Temperature response of methane production in liquid manures and co-digestates. Sci. Total Environ. 539, 78–84. https://doi.org/10.1016/j.scitotenv.2015.07.145

EPA, 2023. Inventory of U.S. Greenhouse Gas Emissions and Sinks [WWW Document]. URL https://crsreports.congress.gov

European standard, 2022. EN 17628:2022 [WWW Document]. URL https://www.sis.se/api/document/preview/80034943/

Fangueiro, D., Hjorth, M., Gioelli, F., 2015. Acidification of animal slurry– a review. J. Environ. Manage. https://doi.org/10.1016/j.jenvman.2014.10.001

FAO, 2022. Greenhouse gas emissions from agrifood systems - Global, regional and country trends, 2000-2020. Rome.

Flesch, T.K., Wilson, J.D., Harper, L.A., Crenna, B.P., 2005. Estimating gas emissions from a farm with an inverse-dispersion technique. Atmos. Environ. 39, 4863–4874. https://doi.org/10.1016/j.atmosenv.2005.04.032

Flesch, T.K., Wilson, J.D., Harper, L.A., Todd, R.W., Cole, N.A., 2007. Determining ammonia emissions from a cattle feedlot with an inverse dispersion technique. Agric. For. Meteorol. 144, 139–155. https://doi.org/10.1016/j.agrformet.2007.02.006

Foged, H.L., Lyngvig, H.S., Toft, M., Jacobsen, B.H., 2017. Scenarie for forsuring af halvdelen af gyllen i Danmark 1–39.

Fredenslund, A.M., Rees-White, T.C., Beaven, R.P., Delre, A., Finlayson, A., Helmore, J., Allen, G., Scheutz, C., 2019. Validation and error assessment of the mobile tracer gas dispersion method for measurement of fugitive emissions from area sources. Waste Manag. 83, 68–78. https://doi.org/10.1016/j.wasman.2018.10.036

Galle, B.O., Samuelsson, J., Svensson, B.H., Borjesson, G., 2001. Measurements of methane emissions from landfills using a time correlation tracer method based on FTIR absorption spectroscopy. Environ. Sci. Technol. 35, 21–25. https://doi.org/10.1021/es0011008

Gates, R.S., Casey, K.D., Xin, H., Burns, R.T., 2009. Building Emissions Uncertainty Estimates. Trans. ASABE 52, 1345–1351.

Golston, L.M., Pan, D., Sun, K., Tao, L., Zondlo, M.A., Eilerman, S.J., Peischl, J., Neuman, J.A., Floerchinger, C., 2020. Variability of Ammonia and Methane Emissions from Animal Feeding Operations in Northeastern Colorado. Environ. Sci. Technol. 54, 11015–11024. https://doi.org/10.1021/acs.est.0c00301

Grainger, C., Clarke, T., McGinn, S.M., Auldist, M.J., Beauchemin, K.A., Hannah, M.C., Waghorn, G.C., Clark, H., Eckard, R.J., 2007. Methane Emissions from Dairy Cows Measured Using the Sulfur Hexafluoride (SF6) Tracer and Chamber Techniques. J. Dairy Sci. 90, 2755–2766. https://doi.org/10.3168/jds.2006-697

Griffith, D.W.T., 1996. Synthetic calibration and quantitative analysis of gas-phase FT-IR spectra. Appl. Spectrosc. 50, 59–70. https://doi.org/10.1366/0003702963906627

Haeussermann, A., Hartung, E., Gallmann, E., Jungbluth, T., 2006. Influence of season, ventilation strategy, and slurry removal on methane emissions from pig houses, in: Agriculture, Ecosystems and Environment. pp. 115–121. https://doi.org/10.1016/j.agee.2005.08.011

Hassouna, M., Calvet, S., Gates, R.S., Hayes, E., Schrade, S., 2020. Measurement of Gaseous Emissions from Animal Housing, in: In Holden, N.M., Wolfe, M.L., Ogejo, J.A., Cummins, E.J. (Eds.), Introduction to Biosystems Engineering. American society of Agriculture and Biological Engineers - ASABE. https://doi.org/10.21061/introbiosystemsengineering/gaseous_emissions

Hassouna, M., van der Weerden, T.J., Beltran, I., Amon, B., Alfaro, M.A., Anestis, V., Cinar, G., Dragoni, F., Hutchings, N.J., Leytem, A., Maeda, K., Maragou, A., Misselbrook, T., Noble, A., Rychła, A., Salazar, F., Simon, P., 2022. DATAMAN: A global database of methane, nitrous oxide, and ammonia emission factors for livestock housing and outdoor storage of manure. J. Environ. Qual. 52, 1–17. https://doi.org/10.1002/jeq2.20430

Hensen, A., Groot, T.T., Van Den Bulk, W.C.M., Vermeulen, A.T., Olesen, J.E., Schelde, K., 2006. Dairy farm CH4 and N2O emissions, from one square metre to the full farm scale. Agric. Ecosyst. Environ. 112, 146–152. https://doi.org/10.1016/j.agee.2005.08.014

Herrero, M., Henderson, B., Havlík, P., Thornton, P.K., Conant, R.T., Smith, P., Wirsenius, S., Hristov, A.N., Gerber, P., Gill, M., Butterbach-Bahl, K., Valin, H., Garnett, T., Stehfest, E., 2016. Greenhouse gas mitigation potentials in the livestock sector. Nat. Clim. Chang. 6, 452–461. https://doi.org/10.1038/nclimate2925

Hilgert, J.E., Amon, B., Amon, T., Belik, V., Dragoni, F., Ammon, C., Aura, C., Petersen, S.O., Herrmann, C., 2022. Methane Emissions from Livestock Slurry : Effects of Storage Temperature and Changes in Chemical Composition.

Hristov, A.N., Hanigan, M., Cole, A., Todd, R., McAllister, T.A., Ndegwa, P.M., Rotz, A., 2011. Review: Ammonia emissions from dairy farms and beef feedlots. Can. J. Anim. Sci. 91, 1–35. https://doi.org/10.4141/CJAS10034

Hristov, A.N., Kebreab, E., Niu, M., Oh, J., Bannink, A., Bayat, A.R., Boland, T.M., Brito, A.F., Casper, D.P., Crompton, L.A., Dijkstra, J., Eugène, M., Garnsworthy, P.C., Haque, N., Hellwing, A.L.F., Huhtanen, P., Kreuzer, M., Kuhla, B., Lund, P., Madsen, J., Martin, C., Moate, P.J., Muetzel, S., Muñoz, C., Peiren, N., Powell, J.M., Reynolds, C.K., Schwarm, A., Shingfield, K.J., Storlien, T.M., Weisbjerg, M.R., Yáñez-Ruiz, D.R., Yu, Z., 2018. Symposium review: Uncertainties in enteric methane inventories, measurement techniques, and prediction models, in: Journal of Dairy Science. pp. 6655–6674. https://doi.org/10.3168/jds.2017-13536

Husted, S., 1994. Seasonal Variation in Methane Emission from Stored Slurry and Solid Manures. J. Environ. Qual. 23, 585–592. https://doi.org/10.2134/jeq1994.00472425002300030026x

Im, S., Mostafa, A., Lim, K.H., Kim, I., Kim, D.H., 2022. Automatic temperature rise in the manure storage tank increases methane emissions: Worth to cool down! Sci. Total Environ. 823, 153533. https://doi.org/10.1016/j.scitotenv.2022.153533

IPCC, 2022. Climate Change 2020: Impact, Adaptation, and Vulnerability, Contributi. ed. United Kingdom and New York, NY, USA.

IPCC, 2019. 2019 Refinement to the 2006 IPCC Guidlines for National Greenhouse Gas Inventories, Volume 4: Agriculture, forestry and other land use.

IPCC, 2006. IPCC Guidelines for National Greenhouse Gas Inventories, Agriculture, forestry and other land use, Prepared by the National Greenhouse Gas Inventories Programme. CIGES, Japan.

Jensen, J., Krogh, P.H., Sørensen, P., Petersen, S.O., 2018. Potentielle miljøeffekter ved anvendelse af forsuret gylle på landbrugsjord, Videnskabelig rapport fra DCE.

Johansson, J., Mellqvist, J., Samuelsson, J., Offerle, B., Lefer, B., Rappenglück, B., Flynn, J., Yarwood, G., 2014. Emission measurements of alkenes, alkanes, SO2 and NO2 from stationary sources in southeast Texas over a 5 year period using SOF and Mobile DOAS. J. Geophys. Res. 1–8. https://doi.org/10.1002/2013JD021350.Received

Joint Committee For Guides In Metrology, 2008. Evaluation of measurement data — Guide to the expression of uncertainty in measurement. Int. Organ. Stand. Geneva ISBN 50, 134.

Kaharabata, S.K., Schuepp, P.H., 1998. Methane emissions from aboveground open manure slurry tanks oxygen demand z 218. Global Biogeochem. Cycles 12, 545–554.

Kai, P., Pedersen, P., Jensen, J.E., Hansen, M.N., Sommer, S.G., 2008. A whole-farm assessment of the efficacy of slurry acidification in reducing ammonia emissions. Eur. J. Agron. 28, 148–154. https://doi.org/10.1016/j.eja.2007.06.004

Kariyapperuma, K.A., Johannesson, G., Maldaner, L., VanderZaag, A., Gordon, R., Wagner-Riddle, C., 2018. Year-round methane emissions from liquid dairy manure in a cold climate reveal hysteretic pattern. Agric. For. Meteorol. 258, 56–65. https://doi.org/10.1016/j.agrformet.2017.12.185

Kille, N., Baidar, S., Handley, P., Ortega, I., Sinreich, R., Cooper, O.R., Hase, F., Hannigan, J.W., Pfister, G., Volkamer, R., 2017. The CU mobile Solar Occultation Flux instrument: Structure functions and emission rates of NH3, NO2 and C2H6. Atmos. Meas. Tech. 10, 373–392. https://doi.org/10.5194/amt-10-373-2017

Kupper, T., Häni, C., Neftel, A., Kincaid, C., Bühler, M., Amon, B., VanderZaag, A., 2020. Ammonia and greenhouse gas emissions from slurry storage - A review. Agric. Ecosyst. Environ. 300. https://doi.org/10.1016/j.agee.2020.106963

Laubach, J., Kelliher, F.M., 2005. Methane emissions from dairy cows: Comparing open-path laser measurements to profile-based techniques. Agric. For. Meteorol. 135, 340–345. https://doi.org/10.1016/j.agrformet.2005.11.014

Leifer, I., Melton, C., Tratt, D.M., Buckland, K.N., Chang, C.S., Frash, J., Hall, J.L., Kuze, A., Leen, B., Clarisse, L., Lundquist, T., Van Damme, M., Vigil, S., Whitburn, S., Yurganov, L., 2018. Validation of mobile in situ measurements of dairy husbandry emissions by fusion of airborne/surface remote sensing with seasonal context from the Chino Dairy Complex. Environ. Pollut. 242, 2111–2134. https://doi.org/10.1016/j.envpol.2018.03.078

Leifer, I., Melton, C., Tratt, D.M., Buckland, K.N., Clarisse, L., Coheur, P., Frash, J., Gupta, M., Johnson, P.D., Leen, J.B., Van Damme, M., Whitburn, S., Yurganov, L., 2017. Remote sensing and in situ measurements of methane and ammonia emissions from a megacity dairy complex: Chino, CA. Environ. Pollut. 221, 37–51. https://doi.org/10.1016/j.envpol.2016.09.083

Lemes, Y.M., Garcia, P., Nyord, T., Feilberg, A., Kamp, J.N., 2022. Full-Scale Investigation of Methane and Ammonia Mitigation by Early Single-Dose Slurry Storage Acidification. https://doi.org/10.1021/acsagscitech.2c00172

Leytem, A.B., Dungan, R.S., Bjorneberg, D.L., Koehn, A.C., 2011. Emissions of Ammonia, Methane, Carbon Dioxide, and Nitrous Oxide from Dairy Cattle Housing and Manure Management Systems. J. Environ. Qual. 40, 1383. https://doi.org/10.2134/jeq2009.0515

Lonsdale, C.R., Hegarty, J.D., Cady-pereira, K.E., Alvarado, M.J., Henze, D.K., Turner, M.D., Capps, S.L., Nowak, J.B., Neuman, J.A., Middlebrook, A.M., Bahreini, R., Murphy, J.G., Markovic, M.Z., Vandenboer, T.C., Russell, L.M., 2017. Modeling the diurnal variability of agricultural ammonia in Bakersfield , California , during the CalNex campaign 3, 2721–2739. https://doi.org/10.5194/acp-17-2721-2017

Løvendahl, P., Difford, G.F., Li, B., Chagunda, M.G.G., Huhtanen, P., Lidauer, M.H., Lassen, J., Lund, P., 2018. Review : Selecting for improved feed ef fi ciency and reduced methane emissions in dairy cattle. https://doi.org/10.1017/S1751731118002276

Loyon, L., Guiziou, F., Picard, S., Saint-Cast, P., 2016. Farm-Scale Applicability of Three Covers (Peat, Polystyrene Balls and Synthetic Sheet Roof) to Reduce Ammonia Emissions from Pig Slurry Storage. Agric. Sci. 07, 396–406. https://doi.org/10.4236/as.2016.76041

Maldaner, L., Wagner-Riddle, C., VanderZaag, A.C., Gordon, R., Duke, C., 2018. Methane emissions from storage of digestate at a dairy manure biogas facility. Agric. For. Meteorol. 258, 96–107. https://doi.org/10.1016/j.agrformet.2017.12.184

Mangino, J., Bartram, D., Brazy, A., 2001. Development of a methane conversion factor to estimate emissions from animal waste lagoons, in: US EPA’s 17th Annual Emission Inventory Conference. Atlanta, Georgia.

Marklein, A.R., Meyer, D., Fischer, M.L., Jeong, S., Rafiq, T., Carr, M., Hopkins, F.M., 2021. Facility-scale inventory of dairy methane emissions in California: Implications for mitigation. Earth Syst. Sci. Data 13, 1151–1166. https://doi.org/10.5194/essd-13-1151-2021

McGinn, S.M., Flesch, T.K., Harper, L.A., Beauchemin, K.A., 2006. An Approach for Measuring Methane Emissions from Whole Farms. J. Environ. Qual. 35, 14–20. https://doi.org/10.2134/jeq2005.0250

Mellqvist, J., Samuelsson, J., Johansson, J., Rivera, C., Lefer, B., Alvarez, S., Jolly, J., 2010. Measurements of industrial emissions of alkenes in Texas using the solar occultation flux method. J. Geophys. Res. 115, D00F17. https://doi.org/10.1029/2008JD011682

Mellqvist, J., Samuelsson, J., Offerle, B., Vechi, N.T., Ericsson, M., 2020. Characterization of Air Toxics and GHG Emission Sources and their Impacts on Community Scale Air Quality Levels in Disadvantaged Communities.

Mikkelsen, M.H., Albrektsen, R., 2020. Forbedring af datagrundlaget for opgørelse af ammoniakemissionen fra landbruget.

Miller, D.J., Sun, K., Tao, L., Pan, D., Zondlo, M.A., Nowak, J.B., Liu, Z., Diskin, G., Sachse, G., Beyersdorf, A., Ferrare, R., Scarino, A.J., 2015. Ammonia and methane dairy emission plumes in the San Joaquin valley of California from individual feedlot to regional scales. J. Geophys. Res. 120, 9718–9738. https://doi.org/10.1002/2015JD023241

Ministeriet for Fødevarer Landbrug og Fiskeri, 2021. Bekendtgørelse om miljøregulering af dyrehold og om opbevaring og anvendelse af gødning.

Mønster, J., Samuelsson, J., Kjeldsen, P., Rella, C., Scheutz, C., 2014. Quantifying methane emission from fugitive sources by combining tracer release and downwind measurements - A sensitivity analysis based on multiple field surveys. Waste Manag. 34, 1416–1428. https://doi.org/10.1016/j.wasman.2014.03.025

Ngwabie, N.M., Jeppsson, K.H., Gustafsson, G., Nimmermark, S., 2011. Effects of animal activity and air temperature on methane and ammonia emissions from a naturally ventilated building for dairy cows. Atmos. Environ. 45, 6760–6768. https://doi.org/10.1016/j.atmosenv.2011.08.027

Nielsen, O.-K., Plejdrup, M.S., Winther, M., Nielsen, M., Gyldenkærne, S., Mikkelsen, M.H., Albrektsen, R., Thomsen, M., Hjelgaard, K., Fauser, P., Brunn, H.G., Johanssen, V., Nord-Larsen, T., Vesterdal, L., Stupak, I., Scott-Bentsen, N., Rasmussen, E., Petersen, S.B., Baunbæk, L., Hansen, M.G., 2022. DENMARK ’ S NATIONAL INVENTORY REPORT 2022.

Nielsen, O.-K., Plejdrup, M.S., Winther, M., Nielsen, M., Gyldenkærne, S., Mikkelsen, M.H., Albrektsen, R., Thomsen, M., Hjelgaard, K., Fauser, P., Bruun, H.G., Johanssen, V., Nord-Larsen, T., Vesterdal, L., Stupak, I., Scott-Bentsen, N., Rasmussen, E., Petersen, S.B., Olsen, T.M., Hansen, M.G., 2021. Denmark's national inventory report 2021. Emission Inventories 1990-2019 - Submitted under the United Nations Framework Convention on Climate Change and the Kyoto Protocol.

Nowak, J.B., Neuman, J.A., Bahreini, R., Middlebrook, A.M., Holloway, J.S., McKeen, S.A., Parrish, D.D., Ryerson, T.B., Trainer, M., 2012. Ammonia sources in the California South Coast Air Basin and their impact on ammonium nitrate formation. Geophys. Res. Lett. 39, 6–11. https://doi.org/10.1029/2012GL051197

Olesen, J.E., Sommer, S.G., 1993. Modelling effects of wind speed and surface cover on ammonia volatilization from stored pig slurry. Atmos. Environ. Part A, Gen. Top. 27, 2567–2574. https://doi.org/10.1016/0960-1686(93)90030-3

Owen, J.J., Silver, W.L., 2015. Greenhouse gas emissions from dairy manure management: A review of field-based studies. Glob. Chang. Biol. 21, 550–565. https://doi.org/10.1111/gcb.12687

Palangi, V., Taghizadeh, A., Abachi, S., Lackner, M., 2022. Strategies to Mitigate Enteric Methane Emissions in Ruminants : A Review 1–15.

Petersen, S.O., 2018. Greenhouse gas emissions from liquid dairy manure: Prediction and mitigation. J. Dairy Sci. 101, 6642–6654. https://doi.org/10.3168/jds.2017-13301

Petersen, S.O., Olsen, A.B., Elsgaard, L., Triolo, J.M., Sommer, S.G., 2016. Estimation of methane emissions from slurry pits below pig and cattle confinements. PLoS One 11, 1–16. https://doi.org/10.1371/journal.pone.0160968

Philippe, F.X., Nicks, B., 2015. Review on greenhouse gas emissions from pig houses: Production of carbon dioxide, methane and nitrous oxide by animals and manure. Agric. Ecosyst. Environ. 199, 10–25. https://doi.org/10.1016/j.agee.2014.08.015

Qu, Q., Zhang, K., 2021. Effects of pH , Total Solids , Temperature and Storage Duration on Gas Emissions from Slurry Storage : A Systematic Review 1–16.

Rennie, T.J., Gordon, R.J., Smith, W.N., VanderZaag, A.C., 2018. Liquid manure storage temperature is affected by storage design and management practices—A modelling assessment. Agric. Ecosyst. Environ. 260, 47–57. https://doi.org/10.1016/j.agee.2018.03.013

Ricci, P., Rooke, J.A., Nevison, I., Waterhouse, A., 2013. Methane emissions from beef and dairy cattle : Quantifying the effect of physiological stage and diet characteristics 1 5379–5389. https://doi.org/10.2527/jas2013-6544

Rodhe, L.K.K., Ascue, J., Willén, A., Persson, B.V., Nordberg, Å., 2015. Greenhouse gas emissions from storage and field application of anaerobically digested and non-digested cattle slurry. Agric. Ecosyst. Environ. 199, 358–368. https://doi.org/10.1016/j.agee.2014.10.004

Roscioli, J.R., Yacovitch, T.I., Floerchinger, C., Mitchell, A.L., Tkacik, D.S., Subramanian, R., Martinez, D.M., Vaughn, T.L., Williams, L., Zimmerle, D., Robinson, A.L., Herndon, S.C., Marchese, A.J., 2015. Measurements of methane emissions from natural gas gathering facilities and processing plants: Measurement results. Atmos. Meas. Tech. 8, 2017–2035. https://doi.org/10.5194/amt-8-2017-2015

Rothman, L.S., Jacquemart, D., Barbe, A., Benner, D.C., Birk, M., Brown, L.R., Carleer, M.R., Chackerian, C., Chance, K., Coudert, L.H., Dana, V., Devi, V.M., Flaud, J.M., Gamache, R.R., Goldman, A., Hartmann, J.M., Jucks, K.W., Maki, A.G., Mandin, J.Y., Massie, S.T., Orphal, J., Perrin, A., Rinsland, C.P., Smith, M.A.H., Tennyson, J., Tolchenov, R.N., Toth, R.A., Vander Auwera, J., Varanasi, P., Wagner, G., 2005. The HITRAN 2004 molecular spectroscopic database. J. Quant. Spectrosc. Radiat. Transf. 96, 139–204. https://doi.org/10.1016/j.jqsrt.2004.10.008

Samuelsson, J., Delre, A., Tumlin, S., Hadi, S., Offerle, B., Scheutz, C., 2018. Optical technologies applied alongside on-site and remote approaches for climate gas emission quantification at a wastewater treatment plant. Water Res. 131, 299–309. https://doi.org/10.1016/j.watres.2017.12.018

Scheutz, C., Fredenslund, A.M., 2019. Total methane emission rates and losses from 23 biogas plants. Waste Manag. 97, 38–46. https://doi.org/10.1016/j.wasman.2019.07.029

Scheutz, C., Kjeldsen, P., 2019. Guidelines for landfill gas emission monitoring using the tracer gas dispersion method. Waste Manag. 85, 351–360. https://doi.org/10.1016/j.wasman.2018.12.048

Scheutz, C., Samuelsson, J., Fredenslund, A.M., Kjeldsen, P., 2011. Quantification of multiple methane emission sources at landfills using a double tracer technique. Waste Manag. 31, 1009–1017. https://doi.org/10.1016/j.wasman.2011.01.015

Sommer, S.G., Christensen, M.L., Schmidt, T., Jensen, L.S., 2013. Animal manure recycling: Treatment and management. John Wiley & Sons.

Sommer, S.G., Petersen, S.O., Møller, H.B., 2004. Algorithms for calculating methane and nitrous oxide emissions from manure management. Nutr. Cycl. Agroecosystems 69, 143–154. https://doi.org/10.1023/B:FRES.0000029678.25083.fa

Sommer, S.G., Petersen, S.O., Sørensen, P., Poulsen, H.D., Møller, H.B., 2007. Methane and carbon dioxide emissions and nitrogen turnover during liquid manure storage. Nutr. Cycl. Agroecosystems 78, 27–36. https://doi.org/10.1007/s10705-006-9072-4

State of California, 2016. Senate Bill No.1383.

Sun, K., Tao, L., Miller, D.J., Zondlo, M.A., Shonkwiler, K.B., Nash, C., Ham, J.M., 2015. Open-path eddy covariance measurements of ammonia fluxes from a beef cattle feedlot. Agric. For. Meteorol. 213, 193–202. https://doi.org/10.1016/j.agrformet.2015.06.007

Sutton, M.A., Reis, S., Riddick, S.N., Dragosits, U., Nemitz, E., Theobald, M.R., Tang, Y.S., Braban, C.F., Vieno, M., Dore, A.J., Mitchell, R.F., Wanless, S., Daunt, F., Fowler, D., Blackall, T.D., Milford, C., Flechard, C.R., Loubet, B., Massad, R., Cellier, P., Personne, E., Coheur, P.F., Clarisse, L., Van Damme, M., Ngadi, Y., Clerbaux, C., Skjøth, C.A., Geels, C., Hertel, O., Kruit, R.J.W., Pinder, R.W., Bash, J.O., Walker, J.T., Simpson, D., Horváth, L., Misselbrook, T.H., Bleeker, A., Dentener, F., de Vries, W., 2013. Towards a climate-dependent paradigm of ammonia emission and deposition. Philos. Trans. R. Soc. B Biol. Sci. 368. https://doi.org/10.1098/rstb.2013.0166

Svarer, M., Sørensen, P.B., Kreiner, C.T., Termansen, M., Cordtz, J.F., Juhl, S., 2022. Grøn skattereform Indhold.

Tedeschi, L.O., Abdalla, A.L., Álvarez, C., Anuga, S.W., Arango, J., Beauchemin, K.A., Becquet, P., Berndt, A., Burns, R., De Camillis, C., Chará, J., Echazarreta, J.M., Hassouna, M., Kenny, D., Mathot, M., Mauricio, R.M., McClelland, S.C., Niu, M., Onyango, A.A., Parajuli, R., Pereira, L.G.R., del Prado, A., Tieri, M.P., Uwizeye, A., Kebreab, E., 2022. Quantification of methane emitted by ruminants: A review of methods. J. Anim. Sci. 1–22. https://doi.org/10.1093/jas/skac197

Thompson, C., Stockwell, C., Smith, M., Conley, S., 2019. Statewide airborne methane emissions measurement survey - Final summary report 69.

Twigg, M.M., Berkhout, A.J.C., Cowan, N., Crunaire, S., Dammers, E., Ebert, V., Gaudion, V., Haaima, M., Häni, C., John, L., Jones, M.R., Kamps, B., Kentisbeer, J., Kupper, T., Leeson, S.R., Leuenberger, D., Lüttschwager, N.O.B., Makkonen, U., Martin, N.A., Missler, D., Mounsor, D., Neftel, A., Nelson, C., Nemitz, E., Oudwater, R., Pascale, C., Petit, J.E., Pogany, A., Redon, N., Sintermann, J., Stephens, A., Sutton, M.A., Tang, Y.S., Zijlmans, R., Braban, C.F., Niederhauser, B., 2022. Intercomparison of in situ measurements of ambient NH3: Instrument performance and application under field conditions. Atmos. Meas. Tech. 15, 6755–6787. https://doi.org/10.5194/amt-15-6755-2022

U.S. Environmental Protection Agency, 2018. 2014 National Emissions Inventory (NEI) data [WWW Document]. URL https://gispub.epa.gov/neireport/2014/ (accessed 8.18.20).

US-EPA, 2017. Annexes to the inventory of U.S. GHG emissions and sinks. U.S. Environmental Protection Agency. Inventory of U.S. Greenhouse gas emissions and sinks: 1990-2015. 1–458.

Van Damme, M., Clarisse, L., Whitburn, S., Hadji-Lazaro, J., Hurtmans, D., Clerbaux, C., Coheur, P.F., 2018. Industrial and agricultural ammonia point sources exposed. Nature 564, 99–103. https://doi.org/10.1038/s41586-018-0747-1

VanderZaag, A.C., Flesch, T.K., Desjardins, R.L., Baldé, H., Wright, T., 2014. Measuring methane emissions from two dairy farms: Seasonal and manure-management effects. Agric. For. Meteorol. 194, 259–267. https://doi.org/10.1016/j.agrformet.2014.02.003

VanderZaag, A.C., Glenn, A., Balde, H., 2022. Manure methane emissions over three years at a swine farm in western Canada. J. Environ. Qual. 1–11. https://doi.org/10.1002/jeq2.20336

VERA, 2018. Test Protocol for Livestock Housing and Management Systems. VERA – Verif. Environ. Technol. Agric. Prod. 2, 1–55.

Vinković, K., Andersen, T., de Vries, M., Kers, B., van Heuven, S., Peters, W., Hensen, A., van den Bulk, P., Chen, H., 2022. Evaluating the use of an Unmanned Aerial Vehicle (UAV)-based active AirCore system to quantify methane emissions from dairy cows. Sci. Total Environ. 831. https://doi.org/10.1016/j.scitotenv.2022.154898

Wagner-Riddle, C., Park, K.H., Thurtell, G.W., 2006. A micrometeorological mass balance approach for greenhouse gas flux measurements from stored animal manure. Agric. For. Meteorol. 136, 175–187. https://doi.org/10.1016/j.agrformet.2004.11.014

Webb, J., Sommer, S.G., Kupper, T., Groenestein, K., Hutchings, N.J., Eurich-Menden, B., Rodhe, L., Misselbrook, T.H., Amon, B., 2012. Emissions of ammonia, nitrous oxide and methane during the management of solids manures, Volume 8. ed, Agroecology and Strategies for Climate Change. Sustainable Agriculture Reviews.

Wirsenius, S., Searchinger, T., Zionts, J., Peng, L., Beringer, T., Dumas, P., 2020. Comparing the Life Cycle Greenhouse Gas Emissions Land-Use Carbon Opportunity Costs.

Wolf, J., Asrar, G.R., West, T.O., 2017. Revised methane emissions factors and spatially distributed annual carbon fluxes for global livestock. Carbon Balance Manag. https://doi.org/10.1186/s13021-017-0084-y

Wood, J.D., Gordon, R.J., Wagner-Riddle, C., 2013. Biases in discrete CH4 and N2O sampling protocols associated with temporal variation of gas fluxes from manure storage systems. Agric. For. Meteorol. 171–172, 295–305. https://doi.org/10.1016/j.agrformet.2012.12.014

Wu, S.Y., Hu, J.L., Zhang, Y., Aneja, V.P., 2008. Modeling atmospheric transport and fate of ammonia in North Carolina-Part II: Effect of ammonia emissions on fine particulate matter formation. Atmos. Environ. 42, 3437–3451. https://doi.org/10.1016/j.atmosenv.2007.04.022

Wyer, K.E., Kelleghan, D.B., Blanes-Vidal, V., Schauberger, G., Curran, T.P., 2022. Ammonia emissions from agriculture and their contribution to fine particulate matter: A review of implications for human health. J. Environ. Manage. 323, 116285. https://doi.org/10.1016/j.jenvman.2022.116285

Yuan, B., Coggon, M.M., Koss, A.R., Warneke, C., Eilerman, S., Peischl, J., Aikin, K.C., Ryerson, T.B., De Gouw, J.A., 2017. Emissions of volatile organic compounds (VOCs) from concentrated animal feeding operations (CAFOs): Chemical compositions and separation of sources. Atmos. Chem. Phys. 17, 4945–4956. https://doi.org/10.5194/acp-17-4945-2017

Zhu, L., Henze, D., Bash, J., Jeong, G.R., Cady-Pereira, K., Shephard, M., Luo, M., Paulot, F., Capps, S., 2015a. Global evaluation of ammonia bidirectional exchange and livestock diurnal variation schemes. Atmos. Chem. Phys. 15, 12823–12843. https://doi.org/10.5194/acp-15-12823-2015

Zhu, L., Henze, D.K., Bash, J.O., Cady-Pereira, K.E., Shephard, M.W., Luo, M., Capps, S.L., 2015b. Sources and Impacts of Atmospheric NH3: Current Understanding and Frontiers for Modeling, Measurements, and Remote Sensing in North America. Curr. Pollut. Reports 1, 95–116. https://doi.org/10.1007/s40726-015-0010-4

9 Papers

I **Vechi, N.T.**, Mellqvist, J., Scheutz, C., (2022). Quantification of methane emissions from cattle farms, using the tracer gas dispersion method. *Agriculture, Ecosystems & Environment*, *330*, 107885. https://doi.org/10.1016/j.agee.2022.107885

II **Vechi, N.T.**, Jensen, N.S., Scheutz, C., (2022). Methane emissions from five Danish pig farms: Mitigation strategies and inventory estimated emissions. *Journal of Environmental Management*, *317*, 115319. https://doi.org/10.1016/j.jenvman.2022.115319

III **Vechi, N.T.**, Scheutz, C., (2023). Measurements of methane emissions from manure tanks using a stationary tracer gas dispersion approach. *Submitted to Biosystems Engineering*

IV **Vechi, N.T.**, Falk, J.M., Fredenslund, A.M., Edjabou, M.E., Scheutz, C., (2023). Methane emission rates averaged over a year from ten farm-scale manure storage tanks. *Submitted to Journal of Environmental Management*

V **Vechi, N.T.**, Mellqvist, J., Samuelsson, J., Offerle, B., Scheutz, C., (2023). Ammonia and methane emissions from dairy concentrated animal feeding operations in California, using mobile optical remote sensing. *Atmospheric Environment*, *293*,119448.https://doi.org/10.1016/j.atmosenv.2022.11948

VI Mellqvist, J., **Vechi, N.T,** Scheutz, C., Durif, M., Gautier, F., Johansson, J., Samuelsson, J., Offerle, B., Brohede, S., (2023). An uncertainty methodology for solar occultation flux measurements: ammonia emissions from agriculture. *Manuscript*

I

Quantification of methane emissions from cattle farms, using the tracer gas dispersion method.

Vechi, N.T., Mellqvist, J., & Scheutz, C.

Agriculture, Ecosystems and Environment, *330*, 107885

https://doi.org/10.1016/j.agee.2022.107885

Agriculture, Ecosystems and Environment 330 (2022) 107885

Contents lists available at ScienceDirect

Agriculture, Ecosystems and Environment

journal homepage: www.elsevier.com/locate/agee

Quantification of methane emissions from cattle farms, using the tracer gas dispersion method

Nathalia T. Vechi[a,b,*], Johan Mellqvist[b], Charlotte Scheutz[a]

[a] Department of Environmental Engineering, Technical University of Denmark, Kongens Lyngby, Denmark
[b] Department of Space, Earth and Environment, Chalmers University, Göteborg, Sweden

ARTICLE INFO

Keywords:
Dairy cows
Beef cattle
GHG inventory models
Enteric fermentation
Manure management

ABSTRACT

In Denmark, agriculture is the largest source of anthropogenic methane emissions (81%), mainly from cattle (dairy and beef) farms. Whole-farm methane emissions were quantified at nine Danish cattle farms, using the tracer gas dispersion method. Five to six measurement campaigns were carried out at each farm, covering a full year. Of the nine cattle farms, seven were home to dairy cows and two to beef cattle. The farms represented typical breeds, housing and management systems used in Denmark. Whole-farm methane emission rates ranged from 0.7 to 28 kg h^{-1}, with the highest measurements seen at locations with the highest number of animals. Emissions tended to be higher from August to October, due to elevated temperatures and high amounts of stored manure during this period of the year. The average emission factor (EF) for dairy cow farms was 26 ± 8.5 g Livestock Unit $(LU)^{-1}$ h^{-1}, whereas it was 16 ± 4.1 LU^{-1} h^{-1} for beef cattle farms, i.e. 38% lower for the latter. The use of deep litter house management explained some of the differences found in the EFs for dairy cows. Methane emission rates estimated using IPCC models and national guidelines tended, on average for all farms and measurements, to be underestimated by 35% in comparison with the measured methane emissions, for all models and farms. The results suggest that future improvements to inventory models should focus on enteric methane emissions from beef cattle and manure methane emissions for both dairy cows and beef cattle, especially from deep litter management.

1. Introduction

Many countries have strengthened their greenhouse gas (GHG) reduction targets and are putting efforts into reducing associated emissions with the goal of minimising climate change impacts. Globally, methane is the second most important emitted GHG and constitute 19% of the combined effective radiative forcing (relative to 1750) of the well-mixed GHGs (Forster et al., 2021). Atmospheric methane concentrations are increasing and reached 1.89 ppm in 2020, corresponding to an increase of 16% since 1985 (NOAA, 2021). Due to the relatively short atmospheric lifetime of methane (IPCC, 2013), reducing its emissions will lead to cost-effective mitigation of climate change impacts in the short term (Johansson et al., 2008). In Denmark, 81% of all anthropogenic methane emissions come from agriculture, produced by both enteric fermentation and manure management (Nielsen et al., 2021). Of the methane emitted from cattle livestock, about 76% is due to enteric emissions from the ruminant digestive system and about 24% comes from degradation of animal manure, stored either under the animals' house or at outside tank storages (Nielsen et al., 2021). Approximately 1.5 million cattle (dairy and non-dairy), accounting for about 20% of total agricultural exports (Danish Agriculture and Food Council, 2018), contribute 59% of all national methane emissions, which is a reflection of the large dairy industry in the country.

At the Danish national level, methane emissions from livestock production are estimated by using the empirical models provided in the International Panel on Climate Change (IPCC) 2006 guidelines for national inventory GHG emission reporting (IPCC, 2006). However, these models lack spatial resolution, and many of their parameters are based on limited or outdated research (Hristov et al., 2018). In order to improve them, the IPCC recently published a refined version of their guidelines, updating and supplementing some of the calculations and factors and using more actual research (IPCC, 2019). Where available, nations are encouraged to apply national models and emission factors, with the justification that they will better reflect their animal management policies.

Few studies have compared estimated methane emissions using these

* Corresponding author at: Department of Environmental Engineering, Technical University of Denmark, Denmark.
E-mail address: navei@env.dtu.dk (N.T. Vechi).

https://doi.org/10.1016/j.agee.2022.107885
Received 18 August 2021; Received in revised form 19 January 2022; Accepted 23 January 2022
Available online 10 February 2022

IPCC models with emissions based on whole-farm scale measurements representing real management conditions. This form of study is important for evaluating model accuracy and consequently improving emission predictions. Additionally, for models to achieve reliable predictions, a large dataset with a wide range of feed compositions and management systems across different regions remains to be built (Hristov et al., 2018).

Methods for quantifying enteric emissions from a single cow have mostly used respiratory chambers (Hammond et al., 2015), SF_6 tracer flux (Grainger et al., 2007) and, head-chamber systems (Sorg et al., 2018), albeit these are difficult to apply in real farm-scale measurements. Similarly, studies on methane emissions from farm-scale manure tanks are scarce, but they are still needed in order to obtain emission rates that reflect real conditions, preferably using non-intrusive methods (Kupper et al., 2020). Flux chambers (Amon et al., 2006), inversion dispersion models such as backward Lagrangian Stochastic (bLS) dispersion modelling (Baldé et al., 2016) and micrometeorological mass balance methods (Wagner-Riddle et al., 2006) are commonly used to measure emissions from manure tanks. Quantifying whole-farm CH_4 emissions is useful in understanding mitigation efforts. In addition, inventory models have been reported to underestimate livestock emissions (Owen and Silver, 2015; Wolf et al., 2017), therefore farm measurements representing real management conditions can help to improve model accuracy for the whole-farm system; however, they are few in number and mostly focused in North America (Arndt et al., 2018; Hensen et al., 2006; McGinn and Beauchemin, 2012; VanderZaag et al., 2014). The mobile tracer gas dispersion method (sometimes also referred to as the tracer correlation method or tracer flux ratio method) is a ground-based remote method that has been used to quantify emissions from many different area sources, such as landfills (Börjesson et al., 2009; Scheutz et al., 2011; Mønster et al., 2015), wastewater treatment plants (Delre et al., 2017; Samuelsson et al., 2018), biogas plants (Scheutz and Fredenslund, 2019) and livestock production facilities in North America (Arndt et al., 2018; Daube et al., 2019). This method has been described elsewhere (Galle et al., 2001; Roscioli et al., 2015; Scheutz and Kjeldsen, 2019) and can be used to quantify whole-farm emissions and, in some cases, emissions from physically well-separated farm operations such as manure tanks and cattle barns (Arndt et al., 2018). The tracer gas dispersion method uses a tracer gas to mimic the source methane release, which it is a principle also used in other techniques such as the SF_6 tracer flux method where it has been used to measure enteric methane emissions from individual cows (Grainger et al., 2007), and from manure tanks (Kaharabata and Schuepp, 1998) by performance of stationary plume sampling. The mobile tracer gas dispersion method applies an easier approach using a mobile analytical platform and measures multiple complete plume transects at a greater distance to the emission source securing sufficient mixing and source simulation thus reducing measurement uncertainty.

The objective of this study was to quantify whole-farm methane emissions from cattle farms, using a mobile tracer gas dispersion method, and to compare measured emissions with estimated methane emissions, using IPCC guidelines and national inventory models. We directly measured methane emissions consistently over one year for nine farms, which were selected to represent the different housing systems, manure management systems and breeds currently used in Danish agriculture. This study targets the lack of studies assessing whole-farm direct CH_4 emissions from cattle livestock and the need for IPCC model validation.

2. Materials and methods

2.1. Investigated sites

Nine cattle farms (C1-C9) were chosen for this study (Table 1). Seven of them were dairy farms, while the other two focused on beef production. Their selection was based on wishing to represent typical breeds, housing systems and manure management methods used in Denmark, where three dairy cow breeds predominate: the Danish Holstein (70%), Danish Jersey (12%) and Red Danish (5%) (Danish agriculture and Food Council, 2020a). Among beef cattle, the Limousine is the most common breed, accounting for 18% of all beef animals (SEGES, 2021). Considering these statistics, we selected at least one farm for each breed. Regarding manure management, 28% of the manure produced by cattle (dairy and non-dairy) is treated by anaerobic digestion, while 8% of the farms use deep litter and 60% have loose-holding housing systems for dairy cows (Nielsen et al., 2021). Therefore, three farms with loose-holding and different floor types (drained or slatted floor) (C1, C2 and C4), two with deep litter with a long eating space (C3 and C6), three with a mix of both systems (C5, C7, and C9) and one with deep litter only (C8) were selected. For the farms applying deep litter with a long eating space (C3 and C6), 60% of the excreted manure is deposited in straw beds, forming the deep litter, while 40% is collected as liquid/slurry. The anaerobic digestion of manure at the studied farms is performed in centralised biogas plants, i.e. raw manure is collected from pits under

Table 1
Overview of the investigated farms. For more detailed information, refer to Table A1 in Appendix A.

Farm Name	Type of animal	Numbers of animals			Livestock unit (LU)[a]	Animal breed	House	Manure handling
		Dairy	**Heifer/young bulls**	**Calves**				
C1	Dairy cow - Organic	600 – 745	289–765	0–643	970–1250	Jersey	Loose-holding drained floor	Liquid/slurry manure
C2	Dairy cow	250	110	100	330	Jersey	Loose-holding slatted floor	Biogas
C3	Dairy cow	420	180	150	540	Jersey	Deep litter with long eating space	Biogas
C4	Dairy cow - Organic	240	180	70	230	Holstein	Loose-holding slatted floor	Biogas
C5	Dairy cow	526	405	212	1055	Holstein	Loose-holding slatted floor (65%)/deep litter with long eating space (35%)	Biogas
C6	Dairy cow	160	110	40	305	Holstein	Deep litter with long eating space	Biogas
C7	Dairy cow	190	103	44	320	Red Danish	Loose-holding slatted floor (50%)/deep litter with long eating space (50%)	Liquid/slurry manure (3/20 – 9/20) Biogas (9/20–1/21)
C8	Beef cattle	30	40	20[b]	130	Limousine	Deep litter	Solid piles
C9	Beef cattle		560	143	545	Holstein	Loose-holding slatted floor (80%)/deep litter with long eating space (20%)	Biogas

[a] LU = 500 kg of body weight. Jersey dairy = 0.89 LU; Holstein and Red Danish dairy = 1.2 LU; Jersey heifer 0.65 LU; Holstein and Red Danish heifer 0.78 LU; Jersey bull = 0.68 LU; Holstein bull = 0.85 LU, Jersey calves = 0.16; Holstein and Red Danish calves = 0.21 LU; Limousine cows = 1.6 LU; Limousine heifer or bulls = 0.8–1 LU; Limousine calves 0.3 = LU.

[b] On average, farm C8 had 26 heifers and 13 bulls.

the barn one or more times a week and then taken to a biogas plant, which in turn returns degassed biomass to the farm's manure tanks. The amount of degassed manure received is around 90% of the initial volume; however, the composition largely differs, since biogas plants employ a mix of manure, deep litter, organic industrial waste and energy crops. Six farms send their manure for anaerobic digestion, while C7 only started sending it after September. For the other two farms, the manure was not treated and was instead either stored in liquid/slurry form (C1) or as a solid in deep litter piles (C8). Organic farms account for 14% of Danish dairies (Danish agriculture and Food Council, 2020b); hence, two organically managed farms were selected (C1, and C4). Among other things, milk cows spend part of their day grazing during the summer (~7 h over 196 days) and are fed with a high percentage of organic fodder. Enteric methane emissions vary according to the animal feed intake and the energy used, therefore different breed with differences in weight will produce distinctive emissions. As for manure emissions, the amount of manure stored in the house, the use of straw in the house or any other treatment the manure is subjected to can affect the strength of emissions.

The farms had a constant number of animals during the year. One exception was C1, which has seasonal calving in late spring, as all cows are inseminated at the same time, thereby affecting milk production and especially the amount of heifers and calves during the year. Methane emission factors (EFs) were calculated by normalising measured emission rates to the body weight base unit, whereby one livestock unit (LU) corresponded to 500 kg of body weight (Table 1). The animal weights used and other information on the farm's management were obtained by interviewing the farmers (Table A1 in Appendix A). Animal numbers used to model annual farm emissions were obtained from the animal central database (Centrale Husdyrbrugsregister (CHR)), to ensure consistency among the farms and to account for monthly variations. At the dairy farms, in addition to dairy cows, the numbers of heifers and calves were also included in the assessment of whole-farm emissions. These animals are sometimes managed at individual housing systems apart from the dairy cows' housing, which was taken into consideration when calculating inventory emissions. The only exception was farm C4, where measurements included only dairy cows, while heifers and calves were located at a building further away from the main farm, in which case they were not included in neither the measurements nor the modelling.

2.2. The tracer dispersion method

Methane emissions were quantified using the mobile tracer gas dispersion method, which has been employed previously to quantify methane emissions from dairy livestock in the USA (Arndt et al., 2018; Daube et al., 2019). The method involved the controlled release of tracer gas and simultaneous measurements of methane and tracer gas concentrations downwind of the farms, using high-precision instruments installed on a mobile platform (Galle et al., 2001; Mønster et al., 2014; Scheutz et al., 2011). Although the method has limited temporal resolution, it has a short setup time and can cover more than one facility in a single day; additionally, it is independent of weather conditions and atmospheric modelling. The method is based on the assumption that the source and tracer gas disperse similarly (Mønster et al., 2014), and therefore the tracer gas can be used to simulate target gas (methane) emissions, which can then be calculated by considering the ratio between the target and the tracer gas, and the known constant emission rate of the tracer gas (Eq. 1)

$$E_{tg} = Q_{tr}\frac{\int_{x1}^{x2}\left(C_{tg} - C_{tg\text{-}bg}\right)dx}{\int_{x1}^{x2}\left(C_{tr} - C_{tr\text{-}bg}\right)dx}\cdot\frac{MW_{tg}}{MW_{tr}} \quad (1)$$

where E_{tg} (kg h^{-1}) is the target gas emission, Q_{tr} (kg h^{-1}) is the known tracer gas flux, C_{tg} and $C_{tg\text{-}bg}$ (ppb as mass mixing ratio) are target gas concentrations measured inside the plume and in the background, respectively, similar to C_{tr} (ppb) and $C_{tr\text{-}bg}$ (ppb) for the tracer gas. MW_{tg} (g/mol) and MW_{tr} (g mol^{-1}) are the molecular weights for the target and the tracer gas, respectively. X2 (m) and X1 (m) represent the end and the beginning of the plume, respectively. The ratio is estimated by integrating the plume concentration of each gas, because this has been demonstrated as the best approach for minimising minor tracer gas misplacement (Fredenslund et al., 2019; Mønster et al., 2014). A number of transects provided average emissions, and in order to be considered a measurement, a minimum of 10 transects should be performed (Fredenslund et al., 2019). Acetylene (C_2H_2) was selected as the tracer gas, due to its negligible atmospheric background concentrations and long atmospheric lifetime. Recent studies, using the tracer gas dispersion method by performing controlled releases, have shown that method uncertainty is no higher than ± 20% in a 95% confidence interval (Fredenslund et al., 2019; Mønster et al., 2014).

The present study used a mobile analytical platform equipped with fast-response and sensitive gas analysers and a global positioning system (GPS) connected to the van. Air was sampled from the car's roof (two meters above ground) with the help of an external pump, and measured concentrations were shown in real time. Three different gas analysers (based on cavity ring-down spectroscopy) were used, based on instrument availability. The instrument used most during the measurement campaigns was a methane and acetylene analyser (G2203, Picarro Inc., CA), with a measurement frequency of two seconds and a precision (3σ) of 2.14 and 0.34 ppb for methane and acetylene, respectively. In addition, two other instruments were used in combination during the campaigns carried out from January 2020 to June 2020. One instrument measured acetylene (S/N JADS 2001, Picarro Inc., CA), with a response on average every three seconds and a precision (3σ) of 2.5 ppb, while the other instrument measured methane (G1301, Picarro Inc., CA), with a response time of four seconds and a precision (3σ) of 3.4 ppb. Acetylene (≥ 99.5%) was released from gas cylinders (at one to two locations usually close to the animal house and manure tanks), using constant flow rates set with calibrated high-precision flowmeters. In addition, the cylinders were weighed before and after each measurement campaign, in order to determine the precise mass of the released tracer. The tracer release rates varied from 0.6 to 2 kg h^{-1}.

Prior to the measurements, a desktop study was performed in order to evaluate the best weather conditions for optimal measurement performance, especially with regards to interfering methane sources and road availability. During the field campaign, the measurements can be described in three phases – as defined earlier (Scheutz and Kjeldsen, 2019). First, an on-site screening of the farm was performed to identify the main methane emission sources, which were mainly the animals' barns and manure tanks. Second, the farm's surroundings were screened by driving along available roads, in order to identify any interfering sources located in the area. Lastly, tracer gas was released and plume measurements performed. If the tracer and target gas plumes did not correlate well, meaning that they did not start and finish at the same time, the tracer gas bottles were repositioned. Crossing the whole plume downwind is important, to define baselines for the integrated plume calculations and assuring that the whole emission from the target source is measured.

2.3. Measurement campaigns

Table 2 provides an overview of the performed measurement campaigns. In total, 60 quantitative emission measurement campaigns were taken, all fulfilling the requirement of at least 10 plume transects carried out over 1–2 h. Most quantifications were performed on roads more than 1 km away from the target source, to ensure sufficient plume mixing.

Whole-farm methane emission rates were measured every second month, covering all seasons over one year. However, C1 was measured over a period of two years. Since the measurements were distributed equally around the year, the simple average of all measurements was considered as the annual average emissions. One exemption was beef farm C8, on which the animals grazed during the summer, and so

Table 2
Summary of the quantitative emission measurements.

Farm	Date	Time interval	Wind speed (m s^{-1}) and direction[a]	T (°C)	Road distance (km)	Number of transects	Methane emission ± SD (kg h^{-1})	Emission factor ± SD (g LU^{-1} h^{-1})
C1	07–02–19	11:00–13:20	4.5, SSW	3	1.1 (10) 2.1 (14)	24	15.3 ± 4.3	15.9 ± 4.5
	11–04–19	17:57–19:10	4, ENE	7	1.5	11	18.8 ± 1.4	20.4 ± 1.5
	28–06–19	22:09–23:15	2, WSW	18	1.5	20	13.0 ± 1.6	13.5 ± 1.7
	25–09–19	16:00–18:00	6, ENE	15	1.5	12	25.2 ± 4.1	25.9 ± 4.1
	14–11–19	17:00–18:40	1.5, ESE	4	2.4	11	28.5 ± 4.0	30.5 ± 4.3
	22–01–20	20:00–22:00	6, W	6	1.4	12	25.1 ± 4.2	26.8 ± 4.7
	04–03–20	16:00–18:00	2.5, WSW	7	1.4	20	24.1 ± 3.3	20.3 ± 2.9
	23–06–20	18:00–19:00	2, WSW	20	1.4	13	16.6 ± 4.2	13.5 ± 3.5
	13–07–20	17:30–19:00	2.5, W	18	1.4	20	15.9 ± 1.8	13.9 ± 1.6
	02–10–20	14:45–16:00	2.5, ESE	16	0.95	18	27.6 ± 4.2	24.9 ± 3.8
	05–11–20	14:45–15:45	5, W	11	1.4	17	22.1 ± 2.2	20.2 ± 2.0
	12–12–20	14:00–15:30	2, E	3	0.95	22	21.6 ± 1.7	20.0 ± 1.6
C2	05–03–20	19:00–21:00	1.5, ENE	3	0.7 (14) 1.0 (4)	18	9.2 ± 1.9	28.5 ± 5.9
	12–05–20	20:00–22:00	3.5, NW	5	0.4	17	5.9 ± 0.5	17.8 ± 1.5
	08–07–20	16:00–18:00	4, NW	14	0.4	25	7.7 ± 1.1	24.1 ± 3.4
	09–09–20	07:00–08:30	3, SW	17	1.0	20	7.2 ± 1	23.0 ± 3.2
	10–11–20	11:00–13:00	2.5, SE	7	1.1	22	6.4 ± 0.6	19.9 ± 1.9
	04–01–21	13:00 – 14:15	5, ESE	2	0.6 (22) 1.0 (3)	25	6.5 ± 1.0	20.2 ± 3.1
C3	06–03–20	15:30–17:30	4, NE	5	1.4	14	23.7 ± 4.1	40.6 ± 7.5
	08–05–20	17:30–19:00	3, W	16	1.2	17	22.3 ± 5.5	43.5 ± 11.3
	07–07–20	21:00–22:30	1.5, W	14	1.2	30	16.6 ± 1.1	32.3 ± 2.1
	08–09–20	10:00–12:00	3.5, W	18	1.2	27	18.7 ± 3.6	35.6 ± 6.8
	12–11–20	13:00–15:00	2.5, SSE	9	1 (9) 2.2 (14)	23	20.1 ± 2.8	38.0 ± 5.3
	05–01–21	09:00 – 11:00	1, NE	3	2	17	19.9 ± 2.4	37.4 ± 4.5
C4	17–03–20	13:30–15:30	5, SW	9	1.6	19	7.7 ± 1.3	26.4 ± 4.5
	14–05–20	16:00–18:00	1.5, NW	13	0.8	24	5.7 ± 1.0	19.5 ± 3.4
	07–07–20	15:00–16:30	4.5, WSW	17	1.6	18	5.6 ± 1.2	19.5 ± 4.2
	07–09–20	17:30–18:45	2, WSW	15	1.6	24	4.8 ± 0.6	16.9 ± 2.1
	10–11–20	14:30–18:00	1.5, SSE	6	0.9	21	7.8 ± 1.5	27.2 ± 5.2
	04–01–21	16:00 – 18:00	4.5, NE	1	1.7	21	6.6 ± 0.8	21.3 ± 2.6
C5	05–03–20	16:00–18:00	2.5, ENE	5	1.4	19	18.1 ± 2.9	18.2 ± 3.1
	12–05–20	12:00–16:00	3.5, W	7	1.8 (10) 0.4 (3)	13	17 ± 3.3	17.2 ± 3.2
	07–07–20	17:20–18:45	2.5, W	14	1.8	20	19.6 ± 1.8	20.1 ± 1.8
	07–09–20	16:00–15:30	4.5, SW	17	1.8	21	23.9 ± 3.6	24.1 ± 3.6
	11–11–20	17:00–18:30	1.5, ESE	7	1.2 (19) 0.6 (2)	21	21.3 ± 2.7	21.3 ± 2.7
	05–01–21	16:30 – 18:30	2, ENE	1	1.1	19	23.4 ± 1.6	23.3 ± 1.6
C6	29–03–19	20:15–22:30	4, SW	10	1.4	29	7.5 ± 1.2	26.0 ± 4.2
	20–08–19	21:00–23:00	2, SW	13	1.4	32	8.9 ± 1.0	30.0 ± 3.4
	13–02–20	10:00–13:00	2.5, S	3	1.5	11	7.8 ± 1.9	27.9 ± 6.8
	18–05–20	16:30–18:30	1.5, WSW	11	1.4	20	7.3 ± 1.2	24.7 ± 4.1
	27–06–20	21:30–23:30	1, S	20	1.5	16	8.0 ± 1.5	27.1 ± 5.1
	10–10–20	15:00–17:00	1.5, WSW	10	1.5	20	8.4 ± 1.1	29.0 ± 3.8
	18–12–20	10:45: 12:15	3.5, SSW	8	1.8	19	5.4 ± 0.8	18.3 ± 2.7
C7	16–03–20	11:00–13:00	3.5, W	8	1.0	19	13 ± 1.8	39.6 ± 5.5
	07–05–20	19:45–22:15	3.5, W	14	1.0	18	8.7 ± 0.9	27.0 ± 2.8
	06–07–20	20:30–22:00	4.5, W	13	1.0	30	12.1 ± 1.3	37.2 ± 4.0
	09–09–20	15:30–17:30	3.5, W	18	1.0	26	16.9 ± 1.7	54.4 ± 5.5
	12–11–20	14:00–15:30	2.5, ESE	7	1.8	20	9.3 ± 1.1	30.2 ± 4.8
	12–01–21	10:00 – 12:00	3, WSW	1	1.0	23	7.6 ± 0.8	24.2 ± 2.5
C8 - House	16–03–20	18:00–19:30	1.5, WSW	7	0.7	20	1.2 ± 0.2	11.6 ± 1.9
	07–05–20	21:30–23:45	1, WSW	8	0.7	13	1.9 ± 0.5	16.9 ± 4.5
	11–11–20	07:30–09:00	1, SE	7	0.7	17	1.1 ± 0.3	17.9 ± 4.9
C8 - Grazing	11–11–20	10:30–12:00	1, SE	7	0.5	19	0.4 ± 0.1	23.5 ± 5.9
C8 - House	06–01–21	08:00 – 10:00	4, NE	1	1.0	16	2.7 ± 0.6	22.3 ± 3.6
C9	17–03–20	17:30–19:30	4.5, WSW	7	0.8	16	6.2 ± 1.1	11.5 ± 2.0
	08–05–20	20:00–22:00	2.5, W	11	0.8	18	5.9 ± 0.8	10.6 ± 1.4
	08–07–20	20:00–21:30	1, WNW	14	1.5	29	7.4 ± 0.7	18.0 ± 1.7
	08–09–20	13:30–14:45	0.5, WNW	21	1.2	21	8.6 ± 1.3	18.4 ± 2.8
	12–11–20	17:00–18:15	1, S	8	0.6	24	6.1 ± 0.7	11.8 ± 1.4
	05–01–21	13:00 – 15:00	2.5, NE	2	1.5	21	6.6 ± 0.7	11.9 ± 1.3

[a] Wind speed measured by a vane anemometer at a height of 1.5 m.

measurements were only taken during the winter season (from November to May). However, in the November measurement campaign, about two-thirds of the animals were housed inside while the others grazed on a nearby field. Emissions from both groups of cows were therefore measured in this campaign. For the dairy farms and beef farm C9, measurements were only taken when animals were inside, although cows did graze outside for part of the day (~7 h) at the organic farms (C1, C4).

2.4. Methane emission estimation, following the IPCC and Danish inventories

Measured methane emission rates were compared to modelled emission rates, following the IPCC's inventory guidelines and the Danish national guideline. The IPCC guidelines are divided into Tier 1, 2, and 3, differing on the level of information used in the calculation (IPCC, 2006); for this study, Tier 2 was adopted. Additionally, the IPCC recently published a refined version of their models, which included improvements to the estimations of methane emissions from cattle production (IPCC, 2019); therefore, for comparison, both the 2006 IPCC model (I06) and its 2019 refined version (I19) were used here. The Danish GHG inventory uses a similar approach to the IPCC (2006), applying extra information and models, which should reflect better the management systems used at Danish farms (Nielsen et al., 2021). Both the IPCC guidelines (I06 and I19) and the Danish guideline (DK) calculate EFs for enteric fermentation and manure management, and each uses similar equations (Eq. A1 and A2 in Appendix A).

Farm-specific information obtained from the farmers was used in the modelling, such as type of housing system, manure treatment, frequency of manure removal (when applicable in IPCC, 2019), milk production and animal body weight (Table A1). The calculations resulted in estimated EFs per animal head (Table A5), which were then converted to annual emissions by multiplying the EFs by the number of animals in that month (the same month as the measurement was done) and then averaged over all months to get an average annual emission rate. The estimated annual emissions were compared to the measured annual emissions, which was the average of all measurements.

As values for animal feed intake were not available or unknown for some of the farms, enteric emissions were calculated for consistency by following the indicated approach for each of the models. Gross energy (GE) is the main parameter used to estimate enteric emissions. The IPCC calculates GE based on animal used net energy (NE) and digestible energy (DE) (IPCC, 2006) (Fig. 1), while the Danish guideline uses GE per feed intake for dairy cows, or feeding units (FU) for other cattle (Nielsen et al., 2021). Standardised GE values for the different livestock and breeds in the country (Table A2) (Børsting et al., 2020) are provided based on national feeding plans for 15–18% of Danish dairy production (Nielsen et al., 2021). For three of the farms (C1, C2 and C3), feeding plans were known; however, the difference between real feeding and standardised values were minimal and did not affect the models' results.

Manure emissions are estimated by the models using information on volatile solid contents (VS), the methane conversion factor (MCF) (Table A3) and maximum methane-producing capacity (B_0) (for more information, see Appendix A). The IPCC calculates the quantity of VS excreted based on energy intake, while the Danish guideline provides standard values for excreted manure based on information on typical animal characteristics (Børsting et al., 2020) and according to the types of housing systems most frequently used in the country (Table A4) (Fig. 1). The estimation of VS by the Danish inventory approach results in higher values than the VS based on GE, mainly due to the inclusion of bedding material in the first option (Nielsen et al., 2021). The IPCC 2019 refinement contains updated model parameters and improvements to the way the methane conversion factor (MCF) for liquid manure is estimated. The newest version applies a more detailed sub-model, using temperature-dependent degradation functions, and considers manure storage time. A similar sub-model is also applied in the Danish national guidelines, following the most common practices and data available for the country, resulting in recommended values for annual MCF for cattle manure handled as liquid slurry or treated biogas (Table A3) (Nielsen et al., 2021). For deep litter, the Danish model adopts the MCF provided in the IPCC 2006 model. Additionally, the Danish model considers different temperatures for the storage of manure in barns and for external manure tanks in order to calculate MCF factors (Nielsen et al., 2021). According to the IPCC guidelines and the Danish national inventory the uncertainty on the EF estimates using Tier 2 is on the order of 20%, which is a reflection of the level of information available.

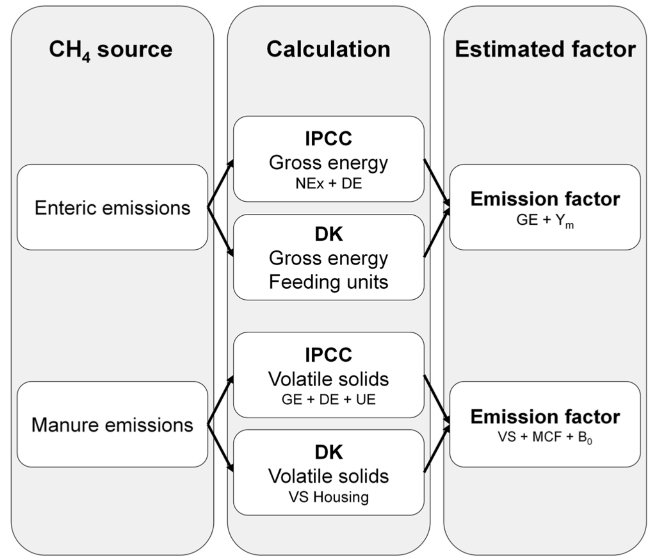

Fig. 1. The IPCC and Danish inventory models estimate enteric and manure methane emissions, using similar equations (Appendix A). NEx = Net energy for each type of activity (Maintenance, growth, activity, pregnancy and lactation). DE = Digestible energy; GE = Gross energy, UE = urinary energy fraction. VS = Volatile solids. MCF = Methane conversion factor. Ym = Methane yield. The most important parameters for enteric fermentation are GE and Y_m, while manure emissions are based on VS, MCF and B_0. Both methods differ in the calculation of.

3. Results and discussion

3.1. Methane emission rates

Whole-farm methane emissions were quantified at nine farms, and during all quantitative measurement campaigns, well-confined methane and tracer gas plumes were obtained, thus avoiding any influence of methane plumes from neighbouring sources. Fig. 2 shows a representative example of an on-site and off-site methane screening campaign as well as plume concentration transects. The average measurement time was ~ 90–120 min, and within this time interval no temporal emission variations were observed, not even for longer measurement periods (> 4 h). Whole-farm emissions rates ranged from 0.7 kg h^{-1} to 28 kg h^{-1} (Table 2). The highest emission rates were measured at the three dairy farms C1, C3 and C5, which were also home to the highest number of animals. The lowest emission rates were recorded at beef cattle farm C8, which had only approximately 100 animals (including animals at different life stages). During one of the campaigns at C8, methane emissions of 0.4 kg h^{-1} from 16 cattle grazing in the field were measured.

Methane emissions fluctuated throughout the year, but these oscillations were small, with emissions varying on average between − 16% and + 13% of the mean annual emission measured at the individual farm (Fig. 3). The measured emission rates contained both enteric and manure methane emissions. Enteric emissions were expected to be

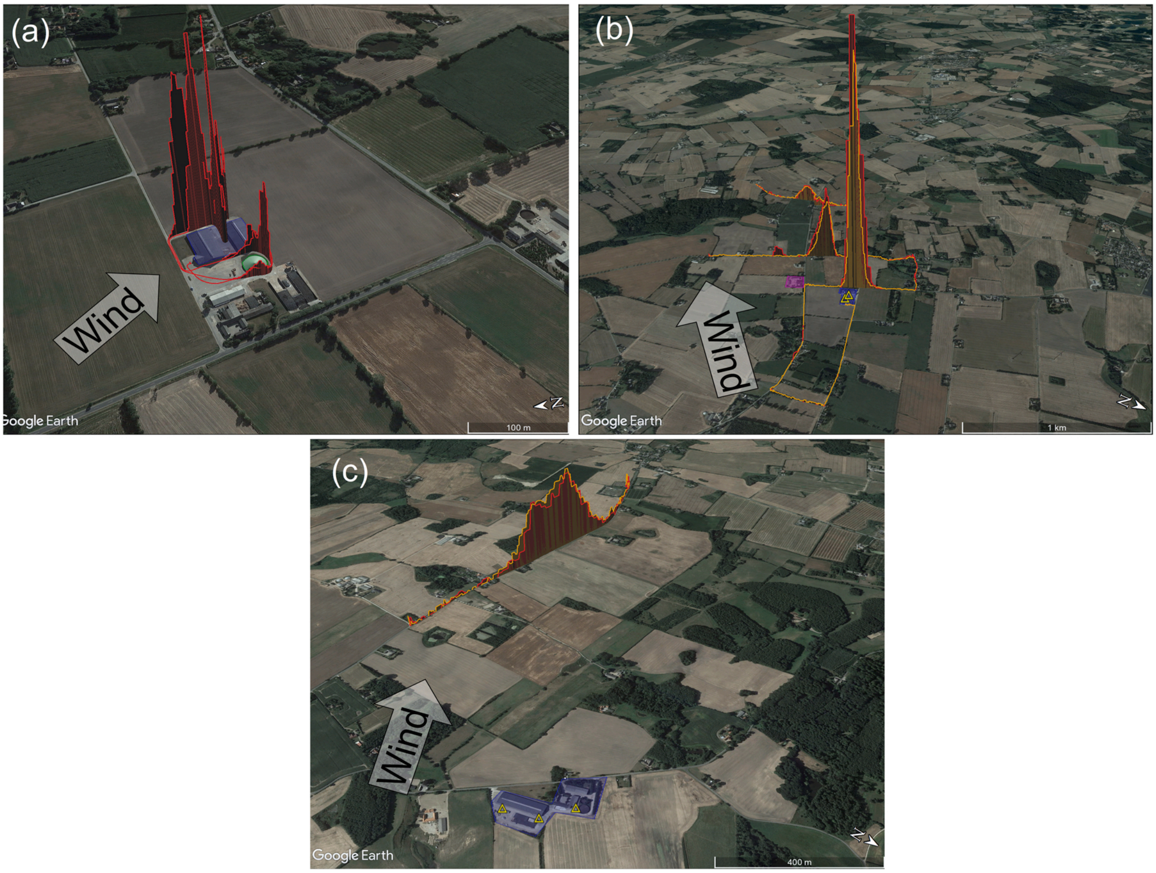

Fig. 2. (a) Example of on-site screening performed at farm C2, showing methane (red) concentrations (above background). The blue area indicates the location of the animal housings and the green area the location of the manure tank. (b) Example of off-site screening and plumes at different distances away from the farm (C2) (blue area) (160 m, 600 m and 1400 m). Two tracer gas bottles (yellow triangles) were positioned close to the animal barn, and the wind was blowing from the east-north-eastern direction. For the second plume (600 m), the methane (red) peak concentration was 108 ppb above background and 11 ppb for acetylene (yellow), while for the third plume the values were 30 ppb and 3.4 ppb, respectively. The small methane emission plume on the left of the target farm's plume came from a small horse farm, indicated by the purple area, which was clearly distinguishable from the farm's emissions, due to the lack of tracer gas. (c) Example of a plume transect at farm C9. Three gas bottles were positioned close to the animal barn and manure tanks, the wind blew in the north-easterly direction and the methane peak (red) was 17 ppb above background, with 4 ppb for acetylene (yellow). (For interpretation of the references to colour in this figure, the reader is referred to the web version of this article.)

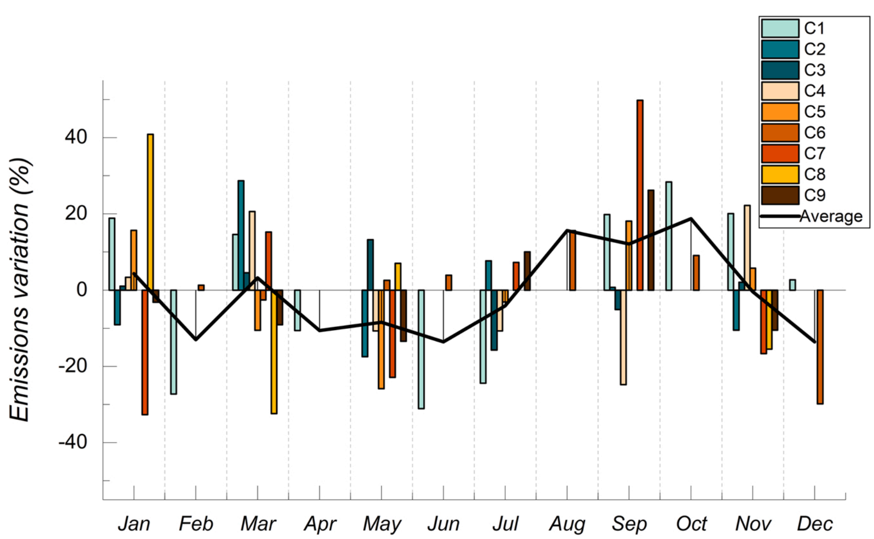

Fig. 3. Methane emission variations during the year. For each farm the variation is the measured emission in a specific month minus the mean annual emission of the farm and divided by the mean annual emission of the farm. The black line represents average variations for each month. Note that in some months, only one or two measurements were available.

constant in most of the farms, since animal numbers or feeding patterns did not vary much throughout the year. Therefore, monthly variations are most likely an effect of fluctuations in manure emissions, which in turn is expected due to changes in atmospheric temperature and the amount of manure stored during the year. In addition, most of the farms stored anaerobically digested (degassed) manure, so the expected contribution of this source was reduced, consequently causing small variations in the total farm emissions – as indicated by the results. The highest average emissions were seen in late summer/early autumn (August to October), which was expected, because at this time of year, there is a combination of higher temperatures and higher amounts of stored manure, thereby increasing emissions (Fig. 3) (Kariyapperuma et al., 2018). At some farms (C1, C2, C3, C4 and C7), slightly higher emissions were recorded in March, which was due to the high amount of manure stored at the time. The manure tanks are emptied in early spring (April/May), thus explaining the reduction in emissions at this point in time.

The maximum and minimum values observed were + 49% and − 32% of the mean annual emissions, respectively. They were found on farm C7, most likely because, during the first measured months (March to September), raw manure was being stored in on-site manure tanks before being sent for anaerobic digestion, following which the farm stored degassed manure. Farm C1 had a lower number of heifers in combination with its dairy cows producing less milk in spring due to pregnancy, thereby decreasing enteric emissions, which is in agreement with the observed data showing lower emissions in April and June in comparison to September and October (Fig. 3). C8 also had a few more suckling cattle in January than in March, possibly explaining the higher emissions in January. Some of the outliers can be explained; for example, C4 had lower emissions in September, in complete opposition the overall trend, because the manure tanks remained empty due to the manure constantly being applied to the fields from March to November.

Finally, other factors might explain some of the observed emission variation, such as time of the measurement in relation to feeding and general activity of the cattle, type of fodder, amount of manure accumulated under the housing, measurement uncertainty and others. Diurnal variation of methane emissions caused by periods of feeding has being observed in some studies (Ngwabie et al., 2011; VanderZaag et al., 2014) although, others have not observed such significant emission variation (Arndt et al., 2018; Bühler et al., 2021). At the farms investigated in this study, fodder was available for the animals during the whole day, therefore the animals would have alternate periods of feeding and resting, which would level out any emission variation to due feed intake. However, the data set did not allow for an in depth analysis of the influence of these factors on the measured emissions.

3.2. Methane emission factors

Converting the measured emission rates to EFs resulted in EFs ranging from 11 to 54 g LU^{-1} h^{-1}, with an average EF of 23 ± 9 g LU^{-1} h^{-1} and a median of 22 g LU^{-1} h^{-1} (Table 2 and Fig. 4). For dairy cows, normalising the measured emissions according to milk production resulted in EFs ranging from 21 to 67 g $L_{milk}{}^{-1}$, with an average EF of 39 g $L_{milk}{}^{-1}$ or 35 g $head^{-1}$ h^{-1} when normalising milk per head of cow (Table A1).

For comparison, Table 3 compiles methane EFs from dairy cows, including only studies where whole-farm methane emissions were measured. The values ranged from 7.1 to 60.2 g LU^{-1} h^{-1}, which is comparable to the values found in this paper (11–54 g LU^{-1} h^{-1}); however, a direct comparison must be made with caution, due to differences in management systems, seasons and measurement techniques. First of all, there are relatively few studies, and most of them were performed in the USA or Canada, which might not reflect Danish conditions in terms of either climatic conditions or manure management practices (Arndt et al., 2018; Bjorneberg et al., 2009; Leytem et al., 2011). An important difference in manure management between DK and North America dairy farms (especially in USA) is the use of open anaerobic lagoons by the latter, while in DK external manure is stored in concrete tanks. Only three European studies on whole-farm methane emissions were found, and each reported very different EFs, i.e. relatively low 11.2 – 15.0 g LU^{-1} h^{-1} in Austria (Amon et al., 2001) and 11 – 14 g LU^{-1} h^{-1} in Switzerland (Bühler et al., 2021) and relatively high 28.7 – 50.5 g LU^{-1} h^{-1} in Netherlands (Hensen et al., 2006) in comparison to the EFs in our study. In addition, seasonal variations can play a role in emissions, and most of these studies did not systematically measure emissions across the whole year. Therefore, it is difficult to conclude whether the EFs found in our study were elevated or not when compared to the studies compiled in Table 3, due to the lack of comparability between them.

In the following sections different factors are discussed, which can explain some of the variations in EFs found across the farms investigated in this study (Fig. 4).

3.2.1. Housing type

Of the Jersey farms (C1, C2 and C3), farm C3 had an EF significantly higher than the other two Jersey farms ($p < 0.05$, Tables A6 and A7). Of the Holsteins dairy farms (C4, C5 and C6), C6 had a significantly higher EF than C5 and C4 ($p < 0.05$, Table A6), while the C4 and C5 farms were significantly similar ($p > 0.05$, Table A6). Farms C3 and C6 both used deep litter with two months of retention time as their main house management system (60% of the manure produced is deposited in deep litter and mixed with straw) (Table A1), which might explain the higher methane emissions (Fig. A1b in Appendix A). In the deep litter house management system, faeces, urine and straw are compressed into mats, thereby limiting oxygen diffusing into the material, and as a result anaerobic conditions and methane formation develop in the bottom and centre of the material, potentially leading to higher emissions than other housing systems (Nicks et al., 2003; Webb et al., 2012). Farms C5 and C7 also used deep litter, albeit to a lesser extent (between 13% and 30% of the manure is handled as deep litter). Additionally, C5 also applied a

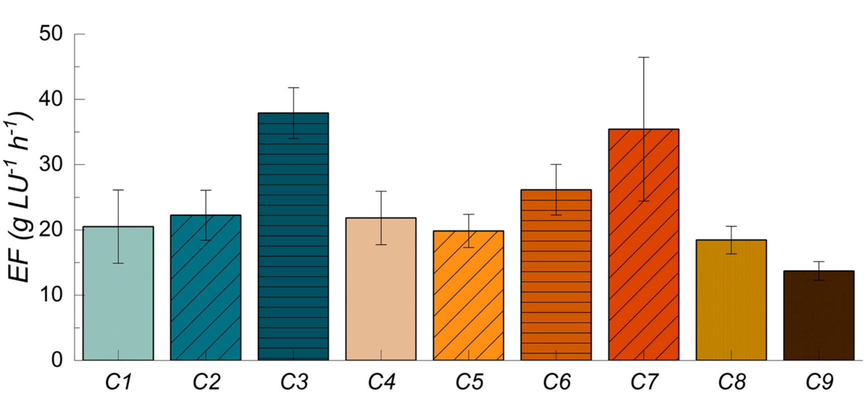

Fig. 4. Average yearly methane emission factors (EFs) (g LU^{-1} h^{-1}). Error bars represent the standard deviations of six or more measured EFs. C1- Organic dairy, Jersey, no manure treatment; C2 – Traditional dairy, Jersey, biogas; C3 – Traditional dairy, Jersey, deep litter and biogas; C4 – Organic dairy, Holstein, biogas, C5 – Traditional dairy, Holstein, deep litter (35%) and biogas; C6 – Traditional dairy, Holstein, deep litter and biogas; C7 – Traditional dairy, Red Danish cow, deep litter (50%) and biogas; C8 – Traditional Beef cattle, Limosine, deep litter and grazing; C9 – Traditional beef cattle, Holstein, deep litter (20%) and biogas.

Table 3
Overview of whole-farm methane emission factors (EFs) measured at dairy farms.

Ref	Country	Period	Farm management	Measurement technique	EFs (g LU^{-1} h^{-1})
Present study	Denmark	Yearly	Dairy and beef cows with manure tank	TDM	23.6
(Arndt et al., 2018)	USA-California	Summer	Dairy cows 1 (Jersey) - free stalls and anaerobic lagoon	Open-path spectrometer and inverse dispersion modelling, TDM and aircraft close-path	60.2
		Winter			28.5
		Summer	Dairy cows 2 (Jersey) - free stalls and anaerobic Lagoon		46.8
		Winter			18.9
(Leytem et al., 2011)	USA- Idaho	Spring, summer, winter and fall	Dairy cows CAFO - anaerobic lagoons	Open-path spectrometer and inverse dispersion modelling	57.9
(Bjorneberg et al., 2009)	USA- Idaho	Spring, summer, winter and fall	Dairy cows - anaerobic lagoons	Open-path spectrometer and inverse dispersion modelling	9.7
(McGinn and Beauchemin, 2012)	Canada	Fall	Dairy cows 1 - open lagoon	Open-path spectrometer and inverse dispersion modelling	7.5
			Dairy cows 2 - open lagoon		7.1
			Dairy cows 3 - open lagoon		8.1
(VanderZaag et al., 2014)	Canada	Spring	Dairy cows 1 - earthen storage	Open-path spectrometer and inverse dispersion modelling	7.3
		Fall			19.6
		Spring	Dairy cows 2 - earthen storage and concrete tank		10.4
		Fall			21.8
(Amon et al., 2001)	Austria	Yearly	Tied stall and solid manure (heap - aerobic conditions)	FTIR - flux conversions using exhaust air flow or open dynamic chambers	11.2
			Tied stall and solid manure (heap - anaerobic conditions)		15.0
(Hensen et al., 2006)	Netherlands	Spring and summer	Dairy cows - manure tanks - slurry based system	TDLAS - Gaussian plume method and fast box measurement Technique	28.7
			Dairy cows - manure tanks - straw based systems		50.5
(Bühler et al., 2021)	Switzerland	Fall (Sep-Oct)	Dairy cows - loose- holding, slurry pit	Open-path spectrometer and inverse dispersion modelling	14.2
		Fall (Nov-Dec)			11.2

comparatively short manure retention time (6 weeks), thus reducing emissions caused by deep litter accumulation (IPCC, 2019).

3.2.2. Animal breed

Emission factors for Jersey cow farms (C1 – C3) were 21 ± 6, 22 ± 4 and 38 ± 4 g LU^{-1} h^{-1} for farms C1, C2 and C3, respectively (Fig. 4). For the Holstein dairy cows (C4 – C6), the average EFs were 22 ± 4.1, 21 ± 2.7 and 26 ± 3.9 g LU^{-1} h^{-1}, for C4, C5 and C6, respectively, while for the Red Danish milk breed (RDM) farm C7 the averaged emission factor obtained was 35 ± 11 g LU^{-1} h^{-1}. Comparing the two groups of dairy farms (Jersey versus heavy species (Holstein and RDM)), EFs did not differ as a result of breed differences. The same was the case when emission rates were normalised by the number of cows instead of body weight (Table A1).

3.2.3. Production target

The largest difference in EFs was recorded between the dairy and beef farms (Fig. A1a). Emission factors for the C8 and C9 beef cattle farms were between 11 and 24 g LU^{-1} h^{-1} (Fig. 4) with an average EF of 16 ± 4.1 g LU^{-1} h^{-1}, which is approximately 38% lower than the average EF for dairy cows 26 ± 8.5 g LU^{-1} h^{-1} (Fig. 4). The higher EF for dairy cows is mainly caused by differences in enteric emissions, due to the higher feed intake (caused by milk production) – as described in the Danish guideline (Børsting et al., 2020). Dry matter intake is known to be correlated with enteric emissions (Hristov et al., 2018).

3.2.4. Other factors

Farms C1 and C2 had similar average EFs, even though farm emissions were significantly different according to the Wilcoxon test ($p < 0.05$, Table A6, Fig. 4). Farms C1 and C2 had rather different management systems; C1 is an organic farm where cows spend part of their time grazing, and they do not treat the manure but instead apply it to the fields more frequently. Farm C2 is a conventional farm and treats its manure at a centralised biogas plant. Stored digestate in the tanks is only removed in spring, therefore it is difficult to draw a conclusion from their comparison. C7 had the highest EF among the heavy race farms, two factors might have caused this elevated EF. First, 50% of the dairy cows were managed in deep litter with a long eating space and an extended retention time (4 months), and the second, there was a lack of liquid/slurry manure treatment (only implemented in September) (Fig. 4). This notion is also supported by the large variability in emissions seen on this farm, which was potentially caused by variations in manure emissions, since enteric emissions is expected to have been constant during the year as no changes in animal numbers occurred (Arndt et al., 2018; VanderZaag et al., 2014). Generally, for dairy cows, a significant difference between EFs was observed for farms using deep litter management and other treatments (Fig. A1b).

The two beef farms had similar average EFs in spite of different housing systems, with C8 having 18 ± 2.1 g LU^{-1} h^{-1} and C9 having 14 ± 1.4 g LU^{-1} h^{-1} ($p > 0.05$ for a t-test, but $p < 0.05$ for a Wilcoxon test, Tables A6 and A7). At farm C8, methane emissions were not measured during the summer months, because the cows grazed outside (24/7) from May to November. However, in November, emissions were measured for two groups of cows, namely those grazing in the field and those in a barn, resulting in an EF of 24 ± 6 g LU^{-1} h^{-1} for the first cohort, higher than second group in the barn at 18 ± 5 g LU^{-1} h^{-1}. These results are most likely due to the high feed intake in pasture conditions, during measurements or issues in the adopted normalization (calculation of livestock units), since the animals here were a mix of calves, heifers and suckling cows. Nevertheless, more data are required, in order to support a more substantive conclusion.

Housing type and production target was the two factors, which caused a larger impact on the EFs. Other factors like the use of anaerobic digestion for manure treatment did not show a large impact because among the dairy cows only one farm did not treat their manure and their management was not comparable with the other farms.

3.3. Comparison of measured methane emissions with international and national inventory estimates

The measured emissions were compared to methane emissions predictions made by IPCC models and the Danish national model. Both IPCC models showed a similar average underestimation of emissions (−35% for the 2019 refinement, and −33% for the IPCC 2006 model (Fig. 5),

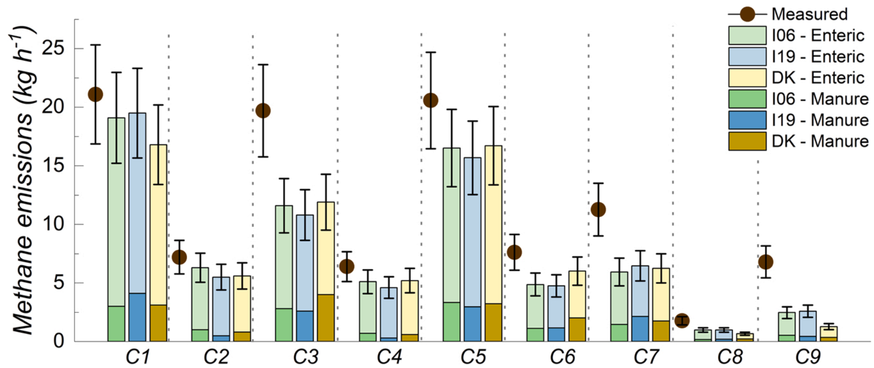

Fig. 5. Comparison between inventories and measured methane emission rates. The bars represent the emission estimated by the models, where the light colours correspond to enteric emissions and the dark colour shows manure emissions. The brown dot shows measured emissions. The error bar for the models corresponds to their respective uncertainties (± 20%), and for the measured emissions it corresponds to method uncertainty (± 20%) based on Fredenslund et al. (2019).

while the national Danish inventory resulted in the highest underestimation (−37%). Although the measured annual averaged emissions were higher than estimated by the inventory models for all farms (Fig. 5), the differences were within uncertainty limits when considering the models and measurements' uncertainty (as indicated by the error bars in Fig. 5). Exceptions were C3, C7, C8 and C9, for which none of the models managed to estimate emissions within the uncertainty limit. C3 and C7 utilised a deep litter house with high retention times (> 1 month). This type of management resulted in the largest differences between the measured and modelled emissions. Similar observations were noted at farm C6, which also used deep litter (Fig. 5). For this type of house management (with deep litter), the Danish model considers both the manure produced and the straw used for the beds in the VS estimation (Table A4), resulting in a higher manure methane emission than the IPCC models, although it is still lower than the measured emissions for C3 and C7 (Fig. 5). Fig. 6 shows the difference between international and national VS estimations, whereby the farms using deep litter as part of their dairy cow management (C3, C5, C6 and C7) all have higher VSs in the Danish model, in comparison to the IPCC models.

Considering the beef farms (C8 and C9), the national inventory performed worse (higher underestimation in comparison to measured emissions) than the IPCC models (Fig. 5). IPCC models estimate enteric emissions based on the weight of and energy used by the animals, whereas the Danish national guidelines use predefined feed intake according to the breed and the animal's life stage. As a result, the IPCC models calculated a significantly higher gross energy intake of 146 MJ head^{-1} day^{-1} in comparison to the Danish model, resulting in a value of 63 MJ head^{-1} day^{-1} (Fig. 6 farms C8 and C9), which might suggest the need to revise the Danish model's feed intake values used for bulls for slaughtering. The low gross energy used in the Danish models resulted in lower enteric emissions for this type of animal in this model (Table A5) and consequently in lower emission estimations. However, in comparison, the IPCC models also underestimated the emissions on these farms (C8 and C9), which might point to a lack of knowledge on emissions from beef cattle production, since it is unclear whether the source of error is enteric or manure emissions estimations. For C8, deep litter with a high retention time might have played a role in increasing model underestimation, as observed in the dairy cows' inventory comparison.

The differences between the 2006 and 2019 IPCC models were, on average, small, because the models are very similar in structure and to a large extent use analogous equations and approaches to estimate the variables, and in some cases they even use the same input parameters (such as for the net energy calculations) (IPCC, 2019, 2006). This is especially the case for modelling enteric fermentation emissions, which accounted for most of the estimated emissions (77% in average) (Fig. 5). Therefore, the differences between the two IPCC models (2006 and 2019 refinement) are mostly caused by differences in the modelling of emissions from manure management. For the anaerobic digestion of manure, IPCC 2019 uses a lower methane conversion factor (MCF) (3.5%) than IPCC 2006 (7.5%, based on the national model), resulting in a lower emission estimation by the 2019 methodology (farms C2, C3, C4, C5, C7 and C9). For on-site storage of liquid slurry (as was the case for farms C1 and C7), MCF values for IPCC 2019 were higher (14% and 22% for C1 and C7, respectively) in comparison to the MCF values used in IPCC 2006 (10% and 17% for C1 and C7, respectively), which made the manure emissions slightly higher in the IPCC 2019 predictions for those farms. For the Danish inventory, the annual MCF factors were estimated according to typical management conditions in the country, for cattle manure without (12.5%) and with biogas treatment (7.5%), while the MCF value for deep litter (17%) was adopted from the IPCC 2006 model.

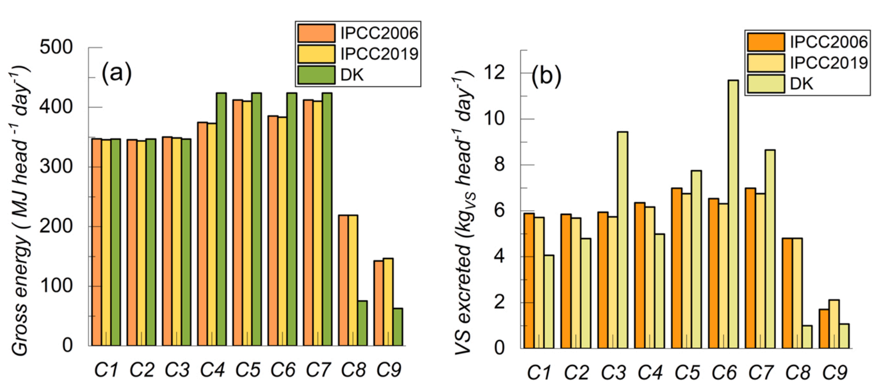

Fig. 6. Parameters used in the EF model calculations, estimated according to each model's methodology (for more information, please refer to Fig. 2. or Appendix A). (a) Gross energy intake (MJ head^{-1} day^{-1}) for dairy cows (C1 to C7) and bulls (C8 and C9). (b) Volatile solids excreted (kg$_{VS}$ head^{-1} day^{-1}) for dairy cows (C1 to C7) and bulls (C8 and C9).

It is difficult to assess the impact of the MCF on emissions calculations in the Danish model in comparison to the IPCC models, because other parameters also play an important role, as discussed previously for VS.

A European study comparing top-down (tower measurements and inverse dispersion modelling) and bottom-up approaches (UNFCC/IPCC approaches) generated similar results to ours, with emissions being lower when using bottom-up inventories in comparison to top-down measurement approaches, albeit they were still within the uncertainty limits set for the modelled and measured emissions (Bergamaschi et al., 2015). In addition, a Danish study estimated methane emissions from manure stored under animal housing by calculating methane emission rates produced by incubating the collected manure at ambient temperatures (Petersen et al., 2016). They found that only the contribution made by manure emissions from animal housing was close to the total modelled manure emissions (accounting housing and external storage sources), which might indicate underestimations of total manure emissions by the national inventory (Petersen et al., 2016).

4. Conclusion

Annual whole-farm methane emissions were measured at nine cattle farms in Denmark, using the tracer gas dispersion method. Of the nine farms, seven were dairy and two beef cattle, and they were representative of common Danish breeds, housing systems and manure management practices. The seasonality of the emissions was addressed by measuring emissions every second month throughout a whole year. Methane emissions varied from 0.7 to 28 kg h^{-1}, while normalised measured emission factors (EFs) ranged between 14 and 54 g LU^{-1} h^{-1} for dairy and 11–24 g LU^{-1} h^{-1} for beef.

On average, the EF for dairy cows was 26 g LU^{-1} h^{-1} and for beef cattle 16 g LU^{-1} h^{-1}, the latter being approximately 38% lower than for dairy cow farms. Methane emissions tended to be higher in late summer/autumn (August to October), but annual variations in measured methane emissions were in general relatively low, varying between − 16% and + 13% of the annual mean emission for all farms. Among the dairy farms, housing systems using deep litter with high retention times seemed to result in higher emissions in comparison to farms using slatted or drained floors. Measurements of more farms are necessary to strengthen the conclusion that higher emissions are caused by deep litter house management and the mitigation of emissions using anaerobic digestion, which was not possible to evaluate herein.

A comparison of the measured emissions with modelled emissions showed an underestimation by all models: − 35%, − 33% and − 37% for IPCC 2019 and 2006 and the Danish national inventory, respectively. The underestimation fell within uncertainty limits for the modelled and measured emissions for most of the farms while for the beef farms this difference was large. The national model largely underestimated the measured emissions therefore a revision of national values in terms of feed intake for bulls for slaughter might be needed. Additionally, in order to improve model estimations of dairy cow methane emissions, the focus should fall on the estimation of manure emissions, with particular emphasis on deep litter management.

Declaration of Competing Interest

The authors declare that they have no known competing financial interests or personal relationships that could have appeared to influence the work reported in this paper.

Acknowledgements

This work was funded in part by the Kvægafgiftsfoden: Måling af udledning af metan fra kvægbrug (27-2020), Denmark, and SEGES, Denmark. The authors wish to thank the farmers for their willingness to participate in the study and their assistance in collecting information from their facilities.

Appendix A. Supporting information

Supplementary data associated with this article can be found in the online version at doi:10.1016/j.agee.2022.107885.

References

Amon, A., Kryvoruchko, V., Amon, T., Zechmeister-Boltenstern, S., 2006. Methane, nitrous oxide and ammonia emissions during storage and after application of dairy cattle slurry and influence of slurry treatment. Agro Food Ind. Hi. Tech. 28, 2700–2704. https://doi.org/10.1016/j.agee.2005.08.030.

Amon, B., Amon, T., Boxberger, J., Alt, C., 2001. Emissions of NH3, N2O and CH4 from dairy cows housed in a farmyard manure tying stall (housing, manure storage, manure spreading). Nutr. Cycl. Agroecosyst. 60, 103–113. https://doi.org/10.1023/A:1012649028772.

Arndt, C., Leytem, A.B., Hristov, A.N., Zavala-Araiza, D., Cativiela, J.P., Conley, S., Daube, C., Faloona, I., Herndon, S.C., 2018. Short-term methane emissions from 2 dairy farms in California estimated by different measurement techniques and US Environmental Protection Agency inventory methodology: a case study. J. Dairy Sci. 101, 11461–11479. https://doi.org/10.3168/jds.2017-13881.

Baldé, H., VanderZaag, A.C., Burtt, S.D., Wagner-Riddle, C., Crolla, A., Desjardins, R.L., MacDonald, D.J., 2016. Methane emissions from digestate at an agricultural biogas plant. Bioresour. Technol. 216, 914–922. https://doi.org/10.1016/j.biortech.2016.06.031.

Bergamaschi, P., Corazza, M., Karstens, U., Athanassiadou, M., Thompson, R.L., Pison, I., Manning, A.J., Bousquet, P., Segers, A., Vermeulen, A.T., Janssens-Maenhout, G., Schmidt, M., Ramonet, M., Meinhardt, F., Aalto, T., Haszpra, L., Moncrieff, J., Popa, M.E., Lowry, D., Steinbacher, M., Jordan, A., O'Doherty, S., Piacentino, S., Dlugokencky, E., 2015. Top-down estimates of European CH4 and N2O emissions based on four different inverse models. Atmos. Chem. Phys. 15, 715–736. https://doi.org/10.5194/acp-15-715-2015.

Bjorneberg, D.L., Leytem, A.B., Westermann, D.T., Griffiths, P.R., Shao, L., Pollard, M.J., 2009. Measurement of atmospheric ammonia, methane, and nitrous oxide at a concentrated dairy production facility in southern Idaho using open-path FTIR spctrometry. Trans. Am. Soc. Agric. Biol. Eng. 52, 1749–1756. https://doi.org/10.13031/2013.29137.

Börjesson, G., Samuelsson, J., Chanton, J., Adolfsson, R., Galle, B., Svensson, B.H., 2009. A national landfill methane budget for Sweden based on field measurements, and an evaluation of IPCC models. Tellus Ser. B Chem. Phys. Meteorol. 61 B, 424–435. https://doi.org/10.1111/j.1600-0889.2008.00409.x.

Børsting, C.F., Hellwing, A.L.F., Lund, P., 2020. Normative Figures 2020. DCA - Danish Centre for Food and Agriculture, Aarhus University accessed 3.15.21. http://anis.au.dk/forskning/sektioner/husdyrernaering-og-fysi-ologi/normtal/.

Bühler, M., Häni, C., Ammann, C., Mohn, J., Neftel, A., Schrade, S., Zähner, M., Zeyer, K., Brönnimann, S., Kupper, T., 2021. Assessment of the inverse dispersion method for the determination of methane emissions from a dairy housing. Agric. . Meteor. 307 https://doi.org/10.1016/j.agrformet.2021.108501.

Danish agriculture & Food Council, 2020a. Statistics 2019 - Beef. URL ⟨https://agricultureandfood.dk/prices-and-statistics/annual-statistics⟩ (accessed 3.14.21).

Danish agriculture & Food Council, 2020b. Statistics 2019 - Dairy. URL ⟨https://agricultureandfood.dk/prices-and-statistics/annual-statistics⟩ (accessed 3.14.21).

Danish Agriculture & Food Council, 2018. Danish Dairy Industry [WWW Document]. Danish Agric. Food Counc, accessed 3.14.21. http://www.agricultureandfood.dk/danish-agriculture-and-food/danish-dairy-industry.

Daube, C., Conley, S., Faloona, I.C., Arndt, C., Yacovitch, T.I., Roscioli, J.R., Herndon, S. C., 2019. Using the tracer flux ratio method with flight measurements to estimate dairy farm CH4 emissions in central California. Atmos. Meas. Tech. 12, 2085–2095. https://doi.org/10.5194/amt-12-2085-2019.

Delre, A., Mønster, J., Scheutz, C., 2017. Greenhouse gas emission quantification from wastewater treatment plants, using a tracer gas dispersion method. Sci. Total Environ. 605–606, 258–268. https://doi.org/10.1016/j.scitotenv.2017.06.177.

Forster, P., Storelvmo, T., Armour, K., Collins, W., Dufresne, J.L., Frame, D., Lunt, D.J., Mauritsen, T., Palmer, M.D., Watanabe, M., Wild, M., Zhang, H., 2021. The Earth's Energy Budget, Climate Feedbacks, and Climate Sensitivity. In: Masson-Delmotte, V., Zhai, P., Pirani, A., Connors, S.L., Péan, C., Berger, S., Caud, N., Chen, Y., Goldfarb, L., Gomis, M.I., Huang, M., Leitzell, K., Lonnoy, E., Matthews, J.B.R., Maycock, T.K., Waterfield, T., Yelekçi, O., Yu, R., Zhou, B. (Eds.), Climate Change 2021: the physical science basis. contribution of working group i to the sixth assessment report of the intergovernmental panel on climate change. Cambridge University Press.

Fredenslund, A.M., Rees-White, T.C., Beaven, R.P., Delre, A., Finlayson, A., Helmore, J., Allen, G., Scheutz, C., 2019. Validation and error assessment of the mobile tracer gas dispersion method for measurement of fugitive emissions from area sources. Waste Manag 83, 68–78. https://doi.org/10.1016/j.wasman.2018.10.036.

Galle, B.O., Samuelsson, J., Svensson, B.H., Borjesson, G., 2001. Measurements of methane emissions from landfills using a time correlation tracer method based on FTIR absorption spectroscopy. Environ. Sci. Technol. 35, 21–25. https://doi.org/10.1021/es0011008.

Grainger, C., Clarke, T., McGinn, S.M., Auldist, M.J., Beauchemin, K.A., Hannah, M.C., Waghorn, G.C., Clark, H., Eckard, R.J., 2007. Methane emissions from dairy cows measured using the sulfur hexafluoride (SF6) tracer and chamber techniques. J. Dairy Sci. 90, 2755–2766. https://doi.org/10.3168/jds.2006-697.

Hammond, K.J., Humphries, D.J., Crompton, L.A., Green, C., Reynolds, C.K., 2015. Methane emissions from cattle: estimates from short-term measurements using a

GreenFeed system compared with measurements obtained using respiration chambers or sulphur hexafluoride tracer. Anim. Feed Sci. Technol. 203, 41–52. https://doi.org/10.1016/j.anifeedsci.2015.02.008.

Hensen, A., Groot, T.T., Van Den Bulk, W.C.M., Vermeulen, A.T., Olesen, J.E., Schelde, K., 2006. Dairy farm CH4 and N2O emissions, from one square metre to the full farm scale. Agric. Ecosyst. Environ. 112, 146–152. https://doi.org/10.1016/j.agee.2005.08.014.

Hristov, A.N., Kebreab, E., Niu, M., Oh, J., Bannink, A., Bayat, A.R., Boland, T.M., Brito, A.F., Casper, D.P., Crompton, L.A., Dijkstra, J., Eugène, M., Garnsworthy, P.C., Haque, N., Hellwing, A.L.F., Huhtanen, P., Kreuzer, M., Kuhla, B., Lund, P., Madsen, J., Martin, C., Moate, P.J., Muetzel, S., Muñoz, C., Peiren, N., Powell, J.M., Reynolds, C.K., Schwarm, A., Shingfield, K.J., Storlien, T.M., Weisbjerg, M.R., Yáñez-Ruiz, D.R., Yu, Z., 2018. Symposium review: Uncertainties in enteric methane inventories, measurement techniques, and prediction models. J. Dairy Sci. 6655–6674. https://doi.org/10.3168/jds.2017-13536.

IPCC, 2019. 2019 Refinement to the 2006 IPCC Guidlines for National Greenhouse Gas Inventories. Vol. 4 Agric. For. other L. use 4, 209. URL ⟨https://www.ipcc-nggip.iges.or.jp/public/2019rf/index.html⟩ (accessed 3.14.21).

IPCC, 2013. Climate change 2013: the physical science basis. Contribution of Working Group I to the Fifth assessment Report of the Intergovernmental Panel on Climate Change. Cambridge University Press,, Cambridge, United Kingdom and New York, NY, USA. https://doi.org/10.1017/CBO9781107415324.

IPCC, 2006. IPCC Guidelines for National Greenhouse Gas Inventories, Agriculture, forestry and other land use, Prepared by the National Greenhouse Gas Inventories Programme. CIGES,, Japan. Accessed 3.14.21. http://www.ipcc-nggip.iges.or.jp/public/2006gl/index.html.

Johansson, D.J.A., Persson, U.M., Azar, C., 2008. Uncertainty and learning: implications for the trade-off between short-lived and long-lived greenhouse gases. Clim. Change 88, 293–308. https://doi.org/10.1007/s10584-007-9381-x.

Kaharabata, S.K., Schuepp, P.H., 1998. Methane emissions from aboveground open manure slurry tanks oxygen demand z 218. Glob. Biogeochem. Cycles 12 (3), 545–554. https://doi.org/10.1029/98GB01866.

Kariyapperuma, K.A., Johannesson, G., Maldaner, L., VanderZaag, A., Gordon, R., Wagner-Riddle, C., 2018. Year-round methane emissions from liquid dairy manure in a cold climate reveal hysteretic pattern. Agric. . Meteorol. 258, 56–65. https://doi.org/10.1016/j.agrformet.2017.12.185.

Kupper, T., Häni, C., Neftel, A., Kincaid, C., Bühler, M., Amon, B., VanderZaag, A., 2020. Ammonia and greenhouse gas emissions from slurry storage - a review. Agric. Ecosyst. Environ. 300 https://doi.org/10.1016/j.agee.2020.106963.

Leytem, A.B., Dungan, R.S., Bjorneberg, D.L., Koehn, A.C., 2011. Emissions of Ammonia, methane, carbon dioxide, and nitrous oxide from dairy cattle housing and manure management systems. J. Environ. Qual. 40, 1383. https://doi.org/10.2134/jeq2009.0515.

McGinn, S.M., Beauchemin, K.A., 2012. Dairy farm methane emissions using a dispersion model. J. Environ. Qual. 41, 73. https://doi.org/10.2134/jeq2011.0266.

Mønster, J., Samuelsson, J., Kjeldsen, P., Rella, C., Scheutz, C., 2014. Quantifying methane emission from fugitive sources by combining tracer release and downwind measurements - A sensitivity analysis based on multiple field surveys. Waste Manag 34, 1416–1428. https://doi.org/10.1016/j.wasman.2014.03.025.

Mønster, J., Samuelsson, J., Kjeldsen, P., Scheutz, C., 2015. Quantification of methane emissions from 15 Danish landfills using the mobile tracer dispersion method. Waste Manag. 35, 177–186. https://doi.org/10.1016/j.wasman.2014.09.006.

Ngwabie, N.M., Jeppsson, K.H., Gustafsson, G., Nimmermark, S., 2011. Effects of animal activity and air temperature on methane and ammonia emissions from a naturally ventilated building for dairy cows. Atmos. Environ. 45, 6760–6768. https://doi.org/10.1016/j.atmosenv.2011.08.027.

Nicks, B., Laitat, M., Vandenheede, M., Désiron, A., Verhaeghe, C., Canart, B., 2003. Emissions of ammonis, nitrous oxide, methane, carbon dioxide and water vapor in the raising of weaned pigs on straw-based and sawdust-based deep litters. Anim. Res. 299–308. https://doi.org/10.1051/animres.

Nielsen, O.-K., Plejdrup, M.S., Winther, M., Nielsen, M., Gyldenkærne, S., Mikkelsen, M. H., Albrektsen, R., Thomsen, M., Hjelgaard, K., Fauser, P., Bruun, H.G., Johanssen, V., Nord-Larsen, T., Vesterdal, L., Stupak, I., Scott-Bentsen, N., Rasmussen, E., Petersen, S.B., Olsen, T.M., Hansen, M.G., 2021. Denmark's national inventory report 2021. Emission Inventories 1990–2019 - submitted for publication under the United Nations Framework Convention on Climate Change and the Kyoto Protocol. URL ⟨http://dce2.au.dk/pub/SR437.pdf⟩ (accessed 3.14.21).

NOAA, 2021. NOAA/GML. ⟨https://www.esrl.noaa.gov/gmd/ccgg/trends_ch4/⟩ (Accessed 3.14.21).

Owen, J.J., Silver, W.L., 2015. Greenhouse gas emissions from dairy manure management: a review of field-based studies. Glob. Chang. Biol. 21, 550–565. https://doi.org/10.1111/gcb.12687.

Petersen, S.O., Olsen, A.B., Elsgaard, L., Triolo, J.M., Sommer, S.G., 2016. Estimation of methane emissions from slurry pits below pig and cattle confinements. PLoS One 11, 1–16. https://doi.org/10.1371/journal.pone.0160968.

Roscioli, J.R., Yacovitch, T.I., Floerchinger, C., Mitchell, A.L., Tkacik, D.S., Subramanian, R., Martinez, D.M., Vaughn, T.L., Williams, L., Zimmerle, D., Robinson, A.L., Herndon, S.C., Marchese, A.J., 2015. Measurements of methane emissions from natural gas gathering facilities and processing plants: measurement results. Atmos. Meas. Tech. 8, 2017–2035. https://doi.org/10.5194/amt-8-2017-2015.

Samuelsson, J., Delre, A., Tumlin, S., Hadi, S., Offerle, B., Scheutz, C., 2018. Optical technologies applied alongside on-site and remote approaches for climate gas emission quantification at a wastewater treatment plant. Water Res. 131, 299–309. https://doi.org/10.1016/j.watres.2017.12.018.

Scheutz, C., Fredenslund, A.M., 2019. Total methane emission rates and losses from 23 biogas plants. Waste Manag. 97, 38–46. https://doi.org/10.1016/j.wasman.2019.07.029.

Scheutz, C., Kjeldsen, P., 2019. Guidelines for landfill gas emission monitoring using the tracer gas dispersion method. Waste Manag. 85, 351–360. https://doi.org/10.1016/j.wasman.2018.12.048.

Scheutz, C., Samuelsson, J., Fredenslund, A.M., Kjeldsen, P., 2011. Quantification of multiple methane emission sources at landfills using a double tracer technique. Waste Manag. 31, 1009–1017. https://doi.org/10.1016/j.wasman.2011.01.015.

SEGES, 2021. Årsstatistik 2020 - Dansk kødkvæg 1–12. URL ⟨http://www.danskkoedkvaeg.dk/media/3541/aarsstatistik-2020.pdf⟩ (accessed 3.14.21).

Sorg, D., Difford, G.F., Mühlbach, S., Kuhla, B., Swalve, H.H., Lassen, J., Strabel, T., Pszczola, M., 2018. Comparison of a laser methane detector with the GreenFeed and two breath analysers for on-farm measurements of methane emissions from dairy cows. Comput. Electron. Agric. 153, 285–294. https://doi.org/10.1016/j.compag.2018.08.024.

VanderZaag, A.C., Flesch, T.K., Desjardins, R.L., Baldé, H., Wright, T., 2014. Measuring methane emissions from two dairy farms: seasonal and manure-management effects. Agric. . Meteorol. 194, 259–267. https://doi.org/10.1016/j.agrformet.2014.02.003.

Wagner-Riddle, C., Park, K.H., Thurtell, G.W., 2006. A micrometeorological mass balance approach for greenhouse gas flux measurements from stored animal manure. Agric. . Meteorol. 136, 175–187. https://doi.org/10.1016/j.agrformet.2004.11.014.

Webb, J., Sommer, S.G., Kupper, T., Groenestein, K., Hutchings, N.J., Eurich-Menden, B., Rodhe, L., Misselbrook, T.H., Amon, B., 2012. Emissions of ammonia, nitrous oxide and methane during the management of solids manures. Agroecol. Strateg. Clim. Change Sustain. Agric. Rev. Volume 8. ed.

Wolf, J., Asrar, G.R., West, T.O., 2017. Revised methane emissions factors and spatially distributed annual carbon fluxes for global livestock. Carbon Bal. Manag. https://doi.org/10.1186/s13021-017-0084-y.

II

Methane emissions from five Danish pig farms: Mitigation strategies and inventory estimated emissions.

Vechi, N.T., Jensen, N.S., & Scheutz, C.

Journal of Environmental Management, 317, 115319

https:// doi.org/10.1016/j.jenvman.2022.115319

Journal of Environmental Management 317 (2022) 115319

Contents lists available at ScienceDirect

Journal of Environmental Management

journal homepage: www.elsevier.com/locate/jenvman

Methane emissions from five Danish pig farms: Mitigation strategies and inventory estimated emissions

Nathalia T. Vechi *, Nina S. Jensen, Charlotte Scheutz

Department of Environmental Engineering, Technical University of Denmark, Denmark

ARTICLE INFO

Keywords:
Pig farms
Tracer gas dispersion method
Manure management
Acidification
Biogas

ABSTRACT

This study investigated whole-farm methane emissions from five Danish pig farms with different manure management practices and compared measured emission rates to international and national greenhouse gas inventory emission models. Methane emissions were quantified by using the tracer gas dispersion method. Farms were measured between five and eight times throughout a whole year. One of the farms housed sows and weaners (P1) and the others focused on fattening pigs (P2–P5). The farms had different manure treatment practices including biogasification (P3), acidification (P4–P5) and no manure treatment (liquid slurry) (P1–P2). Quantified methane emissions ranged from 0.2 to 20 kg/h and the highest rates were seen at the farms with fattening pigs and with no manure treatment (P2), while the lowest emissions were detected at farms with manure acidification (P4 and P5). Average methane emission factors (EFs), normalised based on livestock units, were 14 ± 6, 18 ± 9, 8 ± 7, 2 ± 1 and 1 ± 1 g/LU/h, for P1, P2, P3, P4 and P5, respectively. Emissions from fattening pig farms with biogasification (P3) and acidification (P4–P5) facilities were 55% and 91–93% lower, respectively, than from farm with no manure treatment (P2). Inventory models underestimated farm-measured methane emissions on average by 51%, across all models and farms, with the Danish model performing the worst (underestimation of 64%). A revision of model parameters related to manure emissions, such as the estimation of volatile solids excreted and methane conversion factor parameters, could improve model output, although more data needs to be collected to strengthen the conclusions. As one of the first studies assessing whole-pig farm emissions, the results showed the potential of the applied measuring method to identify mitigation strategy efficiencies and highlighted the necessity to investigate inventory model accuracy.

1. Introduction

Denmark is one of the world's leading pig exporters, shipping approximately 90% of the country's production to China as well as other European countries (ITC, 2020; Danish Agriculture and Food Council, 2021). The pig industry is thus of great importance to the Danish economy, with a population of 12.3 million pigs across all life stages counted in 2019 (Danish Agriculture and Food Council, 2021; Nielsen et al., 2021). Due to the large number of animals, methane emissions from pig production make up about 13% of the agricultural sector's total greenhouse gas (GHG) emissions – a sector which itself contributes 25% of Denmark's total GHG emissions (Nielsen et al., 2021).

The majority of methane emissions from pig farms originate from manure storage, where methane is produced via the anaerobic degradation of slurry retained in animal housing and in outdoor storage tanks. In contrast, enteric methane emissions are rather low for pigs, because they have a simple monogastric digestive system. Therefore, methane emissions in a typical pig farm are often spatially distributed between animal housing and outdoor manure storage tanks. In Denmark, manure is temporarily stored in slurry pits under animal housing, and emissions vary according to the amount of manure stored and in-house temperature. Methane emissions from outdoor manure tanks depend on weather conditions, such as temperature, relative humidity, wind speed and rainfall, in addition to the adopted manure management and the treatment strategy (Philippe and Nicks, 2015).

In Denmark, 82% of pig manure is stored in liquid slurry form, without any treatment, and spread directly on agricultural land – often in early spring, with a smaller proportion in summer or fall (Nielsen et al., 2021). In 2019, about 14% of the generated pig manure was used in biogas production in Denmark, and for most of these biogas plants, the manure is collected at the farm and after treatment, the digested manure is returned and stored on-site, at the farm, until it is spread on

* Corresponding author.
E-mail address: navei@env.dtu.dk (N.T. Vechi).

https://doi.org/10.1016/j.jenvman.2022.115319
Received 4 November 2021; Received in revised form 12 May 2022; Accepted 13 May 2022
Available online 26 May 2022

agricultural land. Only few farms have their own on-site biogas plant (Nielsen et al., 2021). The anaerobic digestion of manure in biogas plants can reduce emissions from manure storage, while the biomethane produced offsets the use of fossil fuels (Petersen et al., 2013). Based on modelling, Sommer et al. (2004) reported a 90% reduction in methane emissions from digested manure storage in comparison to the storage of raw manure, while real-scale farm measurements found a reduction of 85% (Maldaner et al., 2018). The frequent removal of manure from housing units has also been discussed as an efficient mitigation strategy (Amon et al., 2007). Moreover, manure acidification is a technique used to reduce ammonia emissions; however, it has also shown potential to reduce methane emissions by 17–90%, depending on the acid used (Fangueiro et al., 2015).

Current research on methane emissions from pig livestock production has focused on emissions from either animal housing or outdoor manure storage (Husted, 1994; Philippe et al., 2007). The method most commonly used to estimate methane emissions from closed pig houses involves measuring gas concentrations at ventilation exit points and combining these with flow rates at these outlets (Hassouna et al., 2020). Emissions from manure tanks are often measured by using flux chambers, which are popular due to their simplicity (Kupper et al., 2020). However, the placement of a chamber can significantly influence the surface methane flux, due to the unavoidable disturbance of the manure surface, and the method has poor spatial representation, as measurements (due to practical restrictions) are often performed close to the tank wall. Methods such as dispersion modelling or micrometeorological techniques are other approaches used to estimate fugitive methane emissions primarily from manure tanks (Husted, 1994; Park and Wagner-Riddle, 2010). These techniques use methane concentrations measured at a distance away from the source, and therefore they do not interfere with the emission source. However, atmospheric models and meteorological data are needed to infer methane emissions, thus adding uncertainty to the results. To the authors' best knowledge, there is a lack of studies on whole-farm methane emissions assessment from pig farms, especially using measurement techniques to quantify fugitive emissions. Moreover, the data produced in such studies could help to validate and improve inventory models, which in turn could be used to calculate national and global methane emissions from pig production. Inventory models used to estimate annual methane emissions from livestock often require information about animal housing and manure management practices. A comparison between methane emissions estimated using international and national accounting methods and methane emissions measured at operational pig farms is not commonly made. For pigs, most of the current studies reported in the literature compare either housing manure emissions (Petersen et al., 2016) or outdoor manure storage (Rodhe et al., 2012).

The aim of this study is to quantify whole-site methane emissions from pig farms with different manure management strategies. Additionally, it investigates the performance of inventory models in predicting pig farm emissions in northern European conditions. The study contributes to the knowledge on methane emission factors (EFs) from pig livestock production. The novelty of the study lies in the use of the tracer gas dispersion measurement technique for whole-farm methane emission quantification at pig farms with different manure management practice and a comparison of total farm emissions with inventory estimations.

2. Materials and methods

2.1. Investigated sites

Five pig farms were investigated (P1–P5). One pig farm (P1) focused on pig breeding, thus its population was made up of gestating and farrowing sows (230 kg on average), piglets (1–7 kg) and weaners (8–32 kg) and a smaller amount of fattening pigs and gilts (32–110 kg). The other four farms (P2–P5) produced fattening pigs (32–110 kg), and thus their populations were fattening pigs and a few weaners (for P3). About 14% of the total number of farms in Denmark house only sows and weaners, while 42% focus on producing fattening pigs and other farms have a mix of different life stages (Danish Agriculture and Food Council, 2020). Measured methane emissions were normalised to one livestock unit (LU) equalling 500 kg of body weight. At farms P1–P3, the numbers of LUs were almost constant during the year. At farms P4 and P5, the weight of the animals varied over the year (e.g. at certain periods, more animals with a high body weight were housed and vice-versa), and thus also the farms' LU varied between measurement campaigns. Information on the numbers of animals and house management was collected in interviews with the farmers.

At farm P1, gestating sows were housed in a loose holding were 40% of the area had a slatted floor and 60% had deep litter, while farrowing sows were kept in individual housings with a partly slatted floor, and weaners had dual-climate housing (partly slatted floor together with an adjustable cover, where the temperature was optimal for the weaners). At P2–P5, the pigs had either partly slatted and partly drained floors or partly slatted and partly solid floors, corresponding to 49% and 10% of typical farm management in Denmark, respectively. At all farms, the manure was managed as liquid slurry, and only the breeding farm (P1) had a small amount of deep litter. Farms P1 and P2 did not use any strategy to mitigate methane emissions from manure storage. In contrast, farm P3, on a weekly basis, would send raw manure to a biogas plant and in return receive digested manure, co-digested with other animal manure and industrial organic biomass. About 14% of manure from pigs in Denmark was treated in biogas plants in 2019 (Nielsen et al., 2021). Farms P4 and P5 added sulfuric acid to the raw manure, lowering its pH to 5.5. The acid was added to the manure by mixing in an external tank and stored under the floor of animal housing, and a daily proportion of the manure would be sent to an outdoor storage tank, leaving about 25 cm of manure in the house storage area. In Denmark, 20% of manure is treated with acidification, mainly in the outdoor storage tank or during field application (Foged et al., 2017; Jensen et al., 2018). For all the farms, the manure, after removed from the house, was stored in external storage tanks, which were fully emptied in spring (March–April), and partially emptied in autumn. Additionally, farms P2, P3, P4 and P5 had a plastic tent cover on their manure tank, while P1 had a natural crust and some addition of straw on the top the tank. The tank tent cover is not gas tight and mainly serves to preserve storage capacity and reduce dilution of the stored manure due to rainfall.

2.2. The tracer gas dispersion method

The tracer gas dispersion method has been used previously to quantify emissions from landfills (Mønster et al., 2015), wastewater treatment plants (Delre et al., 2017), biogas plants (Scheutz and Fredenslund, 2019) and, more recently, dairy farms (Arndt et al., 2018; Daube et al., 2019; Vechi et al., 2022). The method considers that two gases with a long atmospheric life-time will disperse similarly in the atmosphere (Galle et al., 2001; Scheutz et al., 2011; Roscioli et al., 2015; Mønster et al., 2015), therefore assuming that a tracer gas with a known release rate (Q_{tr}) (kg/h) can be used to simulate target source emissions (E_{tg}) (kg/h). The target emission is calculated by using the ratio between the known tracer gas flux and the concentration ratio between the target (C_{tg}) (ppb) and the tracer gas (C_{tr}) (ppb), minus their background concentration ($C_{tg,bg}$ and $C_{tr,bg}$) (ppb), which should be measured downwind of the source at a suitable distance, thereby allowing for the proper mixing of the gases (Eq. (1)). Acetylene (C_2H_2) was chosen as the tracer gas, which was released from gas cylinders at controlled flowrates set by calibrated flowmeters to ensure a stable flow. Cylinders were weighed before and after release to calculate tracer gas flow rates.

$$E_{tg} = Q_{tr}\frac{\int_{x1}^{x2}\left(C_{tg} - C_{tg,bg}\right)dx}{\int_{x1}^{x2}\left(C_{tr} - C_{tr,bg}\right)dx}\cdot\frac{MW_{tg}}{MW_{tr}} \tag{1}$$

where MW_{tg} (g/mol) and MW_{tr} (g/mol) are molar weights of the methane and tracer gas, and x(m) is the transect distance. According to best practice, the ratio between the target and tracer gas was calculated by integrating the whole plume transect to minimise gas misplacement errors (Mønster et al., 2014; Fredenslund et al., 2019). A transect was considered invalid and discarded when there was: (1) poor visual correlation between methane and the tracer gas concentrations, (2) a signal-to-noise ratio lower than three and (3) incomplete plume traverses. Measurements were conducted following best practice as described by Scheutz and Kjeldsen (2019) and consisted of on-site screening to assess primary emissions sources for optimal tracer gas bottle positioning and source simulation. Thereafter followed a screening of the farm's surroundings to identify possible interfering methane sources and to determine useful measurement roads. Finally, tracer gas was released, and a minimum of 10 plume transects (preferably more) were performed to reduce measurement random uncertainties (Fredenslund et al., 2019), which usually takes around one to 3 h, according to the weather and road conditions.

A mobile analytical platform, fitted with a fast-response cavity ring-down spectroscopy analyser from Picarro Inc., was used in the measurements. On the car's roof (~2 m), atmospheric air was sampled with the help of an auxiliary pump, which directed the flow to the analytical instrument. Most of the measurements were done using a methane and acetylene analyser (G2203, Picarro Inc., CA, response time 2 s, precision (3σ) of 2.14 and 0.34 ppb for methane and acetylene). When not available, a combination of an acetylene analyser (S/N JADS 2001, Picarro Inc., CA, response ~3 s, precision (3σ) of 2.5 ppb) and a methane analyser (G1301, Picarro Inc., CA, with a response time ~4secs, precision (3σ) of 3.4 ppb) was used instead. Additionally, the location of the analytic platform was continuously recorded via a global positioning system (GPS).

2.3. Methane emission measurement campaigns

In general, whole-farm emissions (including house and manure tank emissions) were measured at each farm every second month over a year, totalling six measurements. Exceptions were farm P1, which had two extra measurements, while farm P5 had a total of five measurements, due to limited road availability and requirement of specific wind direction. For all farms, the measurement period was on average 60–120 min, and most transects were performed 1 km away from the source. With the exception of one quantification (at farm P5), the numbers of plume transects were always 10 or more (in average 20 transects per campaign) (Table 2). Meteorological information was obtained by a Kestrel weather meter positioned 1.5 m high. Considering the equal monthly distribution of the measurements, annual emission averages were calculated using simple averaging. The tracer gas bottles were positioned according to the farm's main methane sources, identified from methane screening performed on-site the farm and in close vicinity to the farm. Between one and three bottles were distributed on the farm to provide a good correlation between tracer and target gases, mostly close to the manure tanks and the animals' house.

2.4. Estimation of methane emissions, using IPCC and Danish inventory models

The Intergovernmental Panel on Climate Change (IPCC) has developed guidelines for countries to estimate their GHG emissions, which includes methane emissions from pig livestock production (IPCC, 2006). Recently, the 2006 guidelines (I06) were refined and a few changes made, in order to update default values as a result of more recent research (I19) (IPCC, 2019). Moreover, Denmark adopted models (DK) from these guidelines to calculate its emissions, adding some improvements and considering country-specific conditions (Nielsen et al., 2021). In this study, we estimated the inventory emissions for farms P1–P3 (Table 3). The only parameters that were farm-specific for this modelling were the number and type of animals, choice of manure management (e.g. biogas, liquid slurry), floor type of the animal housing and frequency of manure removal from outdoor tanks. At the time of writing this study, acidification treatment had not been adopted as a methane mitigation strategy by the inventories, and as a result, emissions from farms P4 and P5 could not be modelled.

For the IPCC estimates, enteric emissions from pigs were calculated at the Tier 1 level, using a single default methane EF (1.5 kg/head/year) multiplied by the numbers of pigs (IPCC, 2006, 2019). The Danish model uses the Tier 2 level, because pig livestock production contributes significantly to the agricultural sector's GHG emissions and as a result should be estimated using more detailed information (Nielsen et al.,

Table 1
Management characteristics of the studied farms.

Farm	Number of animals			Livestock units[a]	Housing	Manure management
	Sows	Fattening pig	Weaner			
P1	625	69	3973–4200	452–461[b]	*Farrowing sows* - individual housing, partly slatted floor *Gestational sows* - loose holding, deep litter, slatted floor *Weaners* - two climate housing *Fattening pigs* - partly slatted floor (25–49% solid floor)	*Slurry storage* Natural or straw cover; Removal of housing manure - monthly
P2		4200–5000		584–695[b]	Partly slatted and drained floor	*Slurry storage* Plastic tent cover Removal of housing manure - monthly
P3		2400–3400	500–800	365–492[b]	Partly slatted floor (50–75% solid floor)	*Biogasification* Plastic tent cover Removal of housing manure – monthly (complete) or weekly (partially)
P4		6945–8304	400	767–1352[c]	Partly slatted and drained floor	*Acidification* Plastic tent cover Partial removal of housing manure - daily
P5		6025–7796		984–1486[c]	Partly slatted and drained floor	*Acidification* Plastic tent cover Partial removal of housing manure - daily

[a] For all farms, one livestock unit (LU) equalled 500 kg of body weight.
[b] Sows 230 kg; fattening pigs 70 kg; weaners 19.5 kg (Based on farmers' information).
[c] LU was calculated based on the weight ranges provided by the farmer (30–60 kg; 60–90 kg; 90–120 kg).

Table 2
Quantitative measurement information. Details on the weather, time of day and dates are shown in the table, together with the resulting emission rates and factors.

Farm	Date (dd-mm-yy)	Time interval (hh:mm)	Wind speed (m/s) and direction	Tempe-rature (°C)[b]	Measuring distance (km)[c]	Number of transects	Methane emissions ± STD (kg/h)	Emission factors ± STD (g/LU/h)
P1	08-03-19	18:15–20:30	10, W	5	1.4	19	4.7 ± 0.5	11.8 ± 1.3
	28-06-19	00:15–01:05	2, WSW	16	1.4	22	4.1 ± 0.4	10.3 ± 1.0
	04-09-19	23:00–00:00	1.5, WSW	15	1.4	31	10.0 ± 1.0	25.6 ± 2.6
	14-11-19	22:00–23:00	2, ESE	5	1.5	14	9.0 ± 1.5	22.7 ± 3.8
	22-01-20	17:00–19:00	4.5, W	6	1.4	18	4.8 ± 0.8	12.1 ± 2.0
	29-04-20	10:30–12:30	6, ESE	9	1.5	11	2.4 ± 0.5	6.0 ± 1.3
	24-07-20	15:30–17:10	3, W	20	1.5	29	6.8 ± 0.5	17.1 ± 1.3
	02-10-20	12:30–14:30	3, ESE	16	1.4	17	6.3 ± 0.3	15.8 ± 0.7
P2	11-11-19	17:00–19:00	3, SE	4	1.2	18	20.0 ± 3.3	28.8 ± 4.8
	28-01-20	09:30–11:00	2, SSE	8	1.2	16	15.3 ± 2.9	23.4 ± 4.4
	02-03-20	16:20–18:20	2, S	8	1.2	21	7.5 ± 1.6	12.8 ± 2.7
	01-05-20	19:00–20:00	3.5, S	10	1.2	23	4.7 ± 0.3	8.1 ± 0.5
	14-07-20	18:15–20:00	2, S	15	1.2	23	20.0 ± 2.1	30.0 ± 3.1
	14-09-20	17:00–18:10	1, S	19	1.2	18	10.4 ± 1.0	15.6 ± 1.5
P3	22-11-19[a]	06:45–09:30	4, SE	8.5	0.8 (20) 1.3 (10)	30	6.7 ± 1.3	18.4 ± 3.6
	23-01-20	18:00–20:00	2, WSW	3	0.9	11	2.9 ± 0.9	7.9 ± 2.8
	02-03-20	20:00–21:30	2, ESE	6	0.7 (14) 1.6 (7)	21	1.3 ± 0.3	3.1 ± 0.7
	04-06-20	21:00–22:40	4.5, ESE	12	1.6	20	4.1 ± 0.6	8.3 ± 1.2
	14-07-20	16:45–18:00	2, SSW	16	1.2	20	3.7 ± 0.5	8.5 ± 1.2
	14-09-20	20:00–21:00	1, E	15	0.7 (15) 1.6 (3)	18	1.8 ± 0.3	4.4 ± 0.7
P4	04-09-19	20:00–22:00	4, SW	15	1.0	29	2.2 ± 0.4	1.8 ± 0.3
	14-01-20	16:30–18:30	2.5, SSW	7	1.0	14	1.0 ± 0.2	0.7 ± 0.2
	09-03-20	18:30–20:00	1.5, WSW	7	1.0	21	1.1 ± 0.2	1.0 ± 0.2
	04-05-20	19:45–20:45	1.5, WNW	10	1.0	21	0.6 ± 0.1	0.7 ± 0.1
	10-07-20	18:00–19:00	2.5, WSW	12	1.0	26	2.7 ± 0.6	3.5 ± 0.8
	03-11-20	17:00–18:40	1.5, SW	9	1.0	22	1.1 ± 0.2	1.2 ± 0.2
P5	11-09-19	20:00–22:00	4.5, W	15	1.8	18	2.3 ± 0.5	2.0 ± 0.4
	05-02-20	16:30–19:00	4.5, W	5	1.8	8	1.6 ± 0.4	1.2 ± 0.3
	27-03-20	20:30–21:40	7, NNE	6	0.3	10	0.2 ± 0.1	0.2 ± 0.1
	12-07-20	18:15–19:15	3, W	13	1.8	30	1.4 ± 0.2	1.2 ± 0.2
	03-11-20	19:00–20:30	3, W	11	1.8	16	1.5 ± 0.1	1.0 ± 0.1

[a] Emissions measured during the removal of raw manure from temporary storage and the discharge of digested manure into the storage tanks.
[b] Averaged and rounded air temperature measured by the weather station.
[c] The numbers in parentheses indicate the number of transects performed at the respective distances

Table 3
Methane conversion factors (MCFs) and estimated annual excreted volatile solids (VS) in manure for each farm by IPCC methodology (I06 and I19) and Danish guidelines (DK). VS is specific according to the animal life stage, while MCF is specific to the applied manure system (MS) and corresponds to the annual comparison.

Farm	Farm specific information		Model input parameter used				
	Pig life stage	Type of manure systems and proportion (%)	Volatile solids (kg VS/head/year)		MCF (%)		
			I06/I19	DK	I06	I19	DK
P1	Gestating sows	Deep litter (60%)	397	308	17.0	21.0	14.7
		Liquid slurry (40%)			10.0[b]	29.0	13.4
	Fattening pigs	Liquid slurry (100%)	160	116	10.0[b]	29.0	13.4
	Weaners	Liquid slurry (100%)	61	43			
P2	Fattening pigs	Liquid slurry (100%)	160	116	17.0	30.0	13.4
P3	Fattening pigs	Biogas (100%)	132[a]	96	10.3	3.6	10.3
	Weaners	Biogas (100%)	61	38			

[a] The VS values for P3 are lower, because the pig's growing cycle is greater than P2 or P1.
[b] P1 farm had a crust formed on top of the manure tank, but this was not the case for P2.

2021). For Tier 2, EFs for enteric emissions were estimated for each life stage (e.g. sows, weaners and fattening pigs), using standard values for feed units, gross energy per feed unit and associated methane conversion factors (Børsting et al., 2020). This resulted in EFs of 2.8, 1.7 and 0.6 kg/head/year for sows, fattening pigs and weaners, respectively. For comparison of average annual emissions, enteric emissions in this study were calculated by taking the annual average number of animals at the farm (Section 3.3), whereas for comparison of monthly emissions the number of animals present at the farm at the time when the individual measurement was carried out was used (Section 3.4).

Methane emissions from pig manure storage were calculated at the Tier 2 level, using Eq. (2) for all models. Some of the important parameters considered in this equation are volatile solids excreted (VS) (kg_{VS}/head/day) by the animals, at different life stages, and the methane conversation factor (MCF) (%), varying according to manure handling (e.g. liquid slurry or biogas). IPCC guidelines and Danish national guidelines assume a maximum methane-producing capacity (B_0) of 0.45 m^3_{CH4}/kg_{VS}. And finally, the management system (MS), which is the percentage of the specific type of manure handling (liquid slurry, biogas and deep litter) applied at the farm (Table 3) (Eq. (2)), is considered.

$$EF = (VS \cdot 365).\left(B_0 \cdot 0.67 \cdot \sum \frac{MCF}{100} \cdot MS\right) \tag{2}$$

The national and the international models, however, take different approaches for estimating volatile solids (VS) in excreted manure. The estimation of excreted VS in excreted manure by IPCC is based on gross energy, resulting in a value for each life stage, whereas the Danish model estimates VS based on manure excreted, using standard values for each life stage and housing system (Børsting et al., 2020) (Table 3). The methodology used by the national model typically leads to a lower amount of VS than the IPCC estimated value, which is mainly explained by the high feed efficiency of Danish pigs (Nielsen et al., 2021).

The methane conversation factor (MCF) is temperature-dependent and varies according to manure handling (e.g. solid, liquid slurry or biogas treatment). The IPCC 2006 defines MCF values for the manure management technologies for different climates (e.g. temperate, tropical) around the globe. However, it does not differentiate between pig and cattle manure, although it considers the effect of a natural crust on top of the manure (Table 3, for P1), which is different from the Danish national model. The well-known Van't Hoff-Arrhenius equation is used to include the temperature dependency on the VS degradation rate (Mangino et al., 2001), which is used in all three models. The IPCC 2006 guidelines adjust the MCF factor by considering the national average annual temperature. The IPCC 2019 refinement has instead improved the MCF estimation of liquid slurry manure by adding a sub-model considering the manure storage time and monthly variations in temperature, which is different from the previous 2006 version (Table 3, applicable for farms P1 and P2). A factor f, for the VS degradation rate, can be calculated for each month, which can then be used to estimate monthly MCFs.

The Danish methodology includes a similar assessment to the IPCC 2019, in that monthly temperature variations and outdoor storage time for typical farm management policies are considered (Table 3) (Eq. (3)). The differences between inventories lie in the consideration of housing and outdoor storage as two separate entities by the Danish model, while, when choosing liquid slurry management with the IPCC model, the assumption is that manure emissions only come from outdoor manure tanks. For the Danish model, since the annual average temperature inside a housing unit is rather constant and higher (18.6 °C) than the average outdoor storage temperature (11.2 °C), this leads to an assumption that 72% of the manure producing methane emissions comes from manure storage system under the housing floor (Nielsen et al., 2021). Additionally, VS content stored in the outdoor tanks, i.e. excreta minus the VS degraded during storage in the housing, is further divided into degradable (VS_d) and non-degradable portions (VS_{nd}), whereby the latter has a degradation rate 100 times slower than the former (Sommer et al., 2004) (Eq. (3)). The percentages of VS_d and VS_{nd} used in our calculation were the ones reported in the Danish inventory, being 51% and 49%, respectively. Additionally, the temperature of the building is considered constant throughout the year, while outdoor storage temperature varies according to atmospheric temperature (T). Manure emissions from the house storage were calculated following the approach reported on the Danish inventory, considering a manure retention time of approximately 18 days and the EF for house methane emissions (563 g_{CH4}/kg_{VS}/year). Although farm P1 and P2 applied a retention time of around 30 days, we followed the national guidelines, which use an average retention time of 18 days. Methane emissions from manure outdoor storage tanks are calculated using Eq. (3), where F(t) is the methane production rate (kg_{CH4}/h), and the Arrhenius equation parameters, such as ln(A) (kg_{CH4}/kg_{VS}/h) and Ea (J/mol), are based on Elsgaard et al. (2016), Maldaner et al. (2018) and Petersen et al. (2016). R is the gas constant 8.3 (J/(K.mol)) and T_{manure} is the manure temperature in Kelvin.

$$F(t) = (VS_d + 0.01 VS_{nd}) \cdot e^{\left(lnA - Ea \cdot \left(\frac{1}{R \cdot T_{manure}}\right)\right)} \tag{3}$$

The manure temperature in outdoor storages is calculated based on air temperatures, T_{air} with following parameters $T_{manure} = T_{air} \cdot 0.5011 + 5.1886$ (Nielsen et al., 2021). Finally, the Danish model assumes that only 25% of the carbon degraded in the VS is lost as methane, whereas the remaining part is degraded aerobically and lost to air as carbon dioxide (Nielsen et al., 2021), therefore, only 25% of the degraded VS was assumed to be converted to methane and lost as emissions to air, according to the Danish inventory methodology. The Danish inventory applies the model (Eq. (3)) according to Danish practices, resulting in a single MCF value used to estimate annual emissions (Table 3). The MCF is calculated by considering methane emissions (from Eq. (3)) divided by the VS available, which is then further divided by the B_0 (methane maximum potential) and methane gas density. Another MCF value is estimated, using similar modelling, for the farms that treat their manure with biogasification, considering a reduction of 23% in total methane emissions (Table 3).

For estimation of annual methane emissions from manure storage, information on the annual average number of animals and life stage (section 3.3) were used for all three models. Estimated annual average methane emissions including both enteric and manure emissions were compared to whole-farm measured annual average emissions. Annual average emissions were calculated based on the six measurement campaigns distributed throughout a full year. In addition, for two of the farms (P1 and P2), emissions were estimated for specific months using the IPCC 2019 and Danish National inventory and compared to emissions measured during these months. In this case, information from the specific month, such as monthly-specific MCF and animal numbers were used.

3. Results and discussions

3.1. Whole-farm methane emissions rates

Whole-farm methane emissions from five pig farms were successfully quantified through 31 quantitative measurements. The measured emission rates ranged from 0.2 to 20.0 kg/h, combining emissions from animal housing and outdoor manure storage. P2 had the largest emissions, ranging from 4.7 to 20 kg/h, while P4 and P5 had the lowest, ranging from only 0.2–2.3 kg/h. In general, emissions did not vary much during the measurement period, apart from the first campaign performed at the P3 farm. In this campaign, raw manure was being removed from the temporary storage tank, and its discharge caused a peak in methane emissions, observed in three or four transects for which the methane/tracer gas ratio increased, corresponding to emissions four times higher (26.5 kg/h) than the whole measurement period quantification (6.7 kg/h). These single high emission events were not included in the average emissions for this campaign. An example of the obtained plume measurements and on-site screening is shown in Fig. 1.

The mean monthly emission variation (around the average annual emission), considering all farms and measurements, was −33% to +40%, with maximum and minimum variations of 97% and −63% (Fig. 2). Emissions tended to be lower in the first half of the year (spring and early summer) and higher during the second half of the year (late summer and autumn). Temperature is a factor well-known to affect manure methane emissions. The temperature inside the housing unit should be rather stable during the year, according to other research, averaging 18.6 °C (14.8–22.3 °C) (Petersen et al., 2016), with a small increase during the warmer months. Outdoor manure storage temperature, however, is affected more by ambient temperature, and previous studies in Danish conditions have shown an average manure temperature of 11.2 °C, varying from 4 °C to 18 °C during the year, with the higher temperature recorded in July and the lower one in the winter months (Husted, 1994). In addition to temperature, the amount of manure stored in the tanks influences the magnitude of emissions, which explains the lower emissions in spring and early summer, because the tanks are emptied in spring. In addition, some farms partially remove manure from the tanks in autumn. For farms P2 and P3, their September measurements were made after this partial manure removal, which explains the lower emissions observed (Fig. 2).

It is relevant to mention that shorter-term temporal emissions dynamics were not investigated in this study. However, the authors believe that shorter-term emission dynamics are expected to be limited and only have a minor effect on the presented results. For pig farms, methane emissions from manure are much higher than enteric emissions. For the studied farms, enteric emissions are expected to be near to constant throughout the year since the farms keep approximately the same number of animals at same weight throughout the year. Any emission variability is therefore expected primarily to be due to variations in factors influencing manure storage. Monthly emission variations were

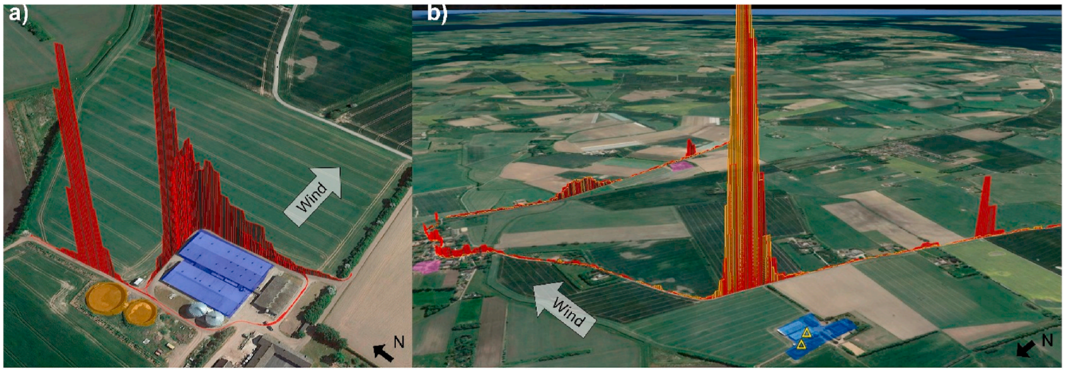

Fig. 1. (a) On-site screening at P1 farm; methane concentrations above background are represented in red. Orange marked areas correspond to outdoor manure storage, and blue denotes animal housing. (b) Off-site screening of the area surrounding farm P1, where the blue marked area corresponds to the target source and the yellow triangular markers indicate tracer gas positions. Measured plumes can be seen at two distances: the plume closer to the farm (400 m) has a peak above background levels of 205 ppb for methane and 23 ppb for acetylene. The plume further away (1400 m) has peaks of 15 ppb for methane and 1.7 ppb for acetylene. (For interpretation of the references to colour in this figure legend, the reader is referred to the Web version of this article.)

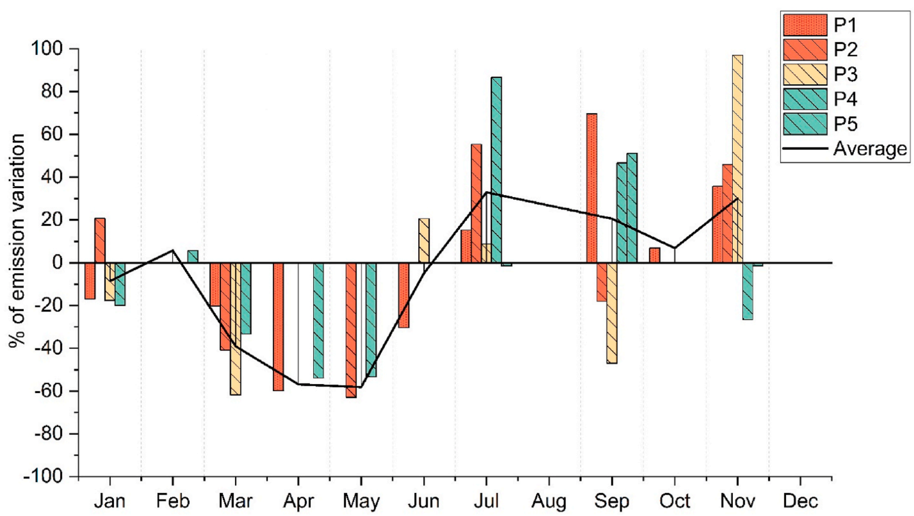

Fig. 2. Variations in measured methane emissions at the five pig farms. The percentages correspond to relative emissions in the respective month in relation to the annual average of each farm, represented by the bars. The solid line indicates the average percentage of all farms in the respective month. Note that some months have only one measurement or none at all.

covered by measuring six times evenly distributed during the year, covering all seasons as well as periods with high and low amounts of stored manure. Day-to-day variations are expected to have minor impact on emissions due to the temperate climate conditions in the region (average daily temperature around 15–16° in summer and just above freezing in winter) and the management practices adopted (near constant number of animals at specific ages and constant temperature in housing) (Haeussermann et al., 2006). Diurnal variations in methane emissions from pig houses have been reported to be small (about 10%). For manure tanks higher emissions have been observed in warmer months, peaking at day-time (around midday, or early morning) (Baldé et al., 2016; Blanes-Vidal et al., 2008; Maldaner et al., 2018). However, most of the measurements in this study were made in late evening (after sunset), especially in warmer months and therefor emissions measured during summer are not biased.

3.2. Whole-farm methane emission factors

Average whole-farm methane EFs for the five farms ranged between 1.2 ± 0.6 and 18.1 ± 8.7, g/LU/h (Fig. 3), with the highest seen for farms with no manure treatment, and the lowest from farms with manure acidification. Farms with no manure treatment (P1–P2) had an

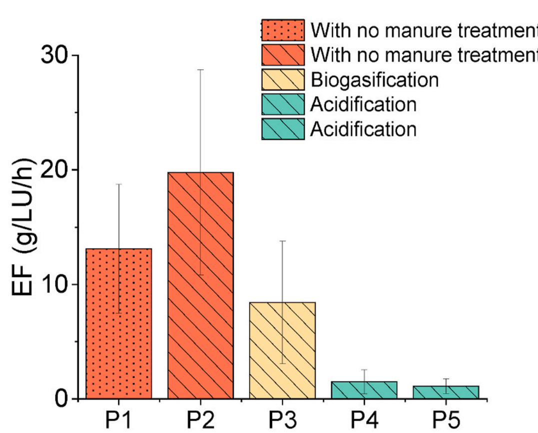

Fig. 3. Pig farm methane emission factors (EFs) based on whole-farm emission measurements. Bars correspond to the average EF across all measurement campaigns, and the error bars represent the standard deviation from the EF.

average EF of 15.8 ± 7.5 g/LU/h, whereas those with biogasification (P3) and acidification (P4–P5) had average EFs of 8.4 ± 5.4 g/LU/h and 1.3 ± 0.9 g/LU/h, respectively (Fig. 3). Methane EFs normalised by the number of fattening pigs averaged 2.7 ± 1.2, 1.3 ± 0.8, 0.2 ± 0.1 and 0.2 ± 0.1 g/head/h for P2, P3, P4 and P5, respectively. The lower and upper 95% confidence interval are 8.4–17.8, 10.4–28.4, 2.8–14.1, 0.4–2.6 and 0.3–1.9 for P1, P2, P3, P4 and P5, respectively. Considering only farms with fattening pigs (P2–P5), EFs from the biogasification farm (P3) were 55% lower in comparison to the farm with no manure treatment (P2). This decrease is higher than stated in the Danish inventory guidelines, which suggests a reduction of 23% in methane manure emissions when manure is treated by biogasification (Nielsen et al., 2021). A study on anaerobic manure treatment, focusing on emissions from the outdoor storage of cattle manure, found an 85% decrease in methane emissions (Maldaner et al., 2018). On a whole-farm level, emission reduction would likely be lower, because emissions from manure stored in animal housing are not affected. Furthermore, a fair comparison with the literature is difficult, because very few data are available on farms with and without anaerobic digestion manure treatment; consequently, further studies should be carried out to determine a reliable emission reduction factor.

Farms with manure acidification had EFs of 91% (P4) and 93% (P5) lower than the farm with no manure treatment (P2). Previous studies looking at emission reduction via acidification mainly focused on outdoor storage tanks. Sommer et al. (2017), for instance, found a 68% emission reduction, whereas Sokolov et al. (2019) recorded 87–89% in this regard and Kupper et al. (2020) a 61–96% reduction. A further analysis of the methane conversion factor estimated an MCF decrease from 16% for raw manure to about 2% for acidified manure (Sokolov et al., 2019). Finally, Petersen et al. (2012) noted emission reductions of 67–87% based on laboratory-scale test. The reason for the higher decline in our study might possibly be due to the frequent removal of manure from animal housing (daily removal, Table 1) compared to the non-management scenario (P2 – monthly removal, Table 1). The frequent removal of manure from the pit under the housing has also been discussed as an emissions reduction strategy (Sommer et al., 2009). Methane emissions (annual average 1.5 kg/h) from farms P4 and P5 were comparable to the modelled enteric emissions (according to the Danish model 1.5 kg/h, and IPCC 1.3 kg/h) supporting that methane emissions from stored manure at these farms were minor.

To the authors' knowledge, no other studies have measured whole-farm direct methane emissions from pig farms, or integrated emissions from both housing and outdoor manure storage. Instead, studies have focused on methane emissions from pig houses with different floor types and management practices, but they did not consider outdoor manure storage, and vice-versa. With regards to animal housing emissions, an average methane EF, obtained from a combination of other studies (n = 38, including two review papers covering European, North American and Asian studies) was 5.3 ± 5.4 g/LU/h, with EFs ranging from 0.4 to 24.3 g/LU/h (Philippe et al., 2007; Blanes-Vidal et al., 2008; Ni et al., 2008; Philippe and Nicks, 2015; Rzeźnik and Mielcarek, 2016). The large array of EF values is due to differences in house management, temperature, fodder or even the measurement methods used in the studies. According to a review study, there was no significant difference in methane EFs between gestating sows and fattening pig, normalised by livestock unit (Philippe and Nicks, 2015), which is different from the results found in the present study.

Furthermore, a few studies have examined methane emissions from real-scale pig manure tanks (Husted, 1994; Kaharabata and Schuepp, 1998; Park et al., 2006; Loyon et al., 2007; Flesch et al., 2013), for which the average (n = 7) methane EF factor was 4.3 ± 2.8 g/LU/h (ranging from 2.0 to 9.6 g/LU/h). The methane EFs range, however, was less broad than for housing emissions.

Adding the EFs for housing and manure storage, an average whole-farm methane emission of 9.6 ± 6.1 g/LU/h is obtained, which is comparable to the EFs obtained from farms P1–P3 with no manure treatment or with biogasification (Fig. 3).

3.3. Comparison of measured and modelled annual methane emissions

All three tested models underestimated methane emissions when compared to measured methane emission rates (Fig. 4), and only the results of the IPCC 2019 model for the P1 farm were within measured and modelled uncertainties. On average, the modelled emissions were −51%, −36% and −64% lower than the emissions measured for the IPCC 2006 (I06), IPCC 2019 (I19) and Danish models (DK), respectively (Fig. 4). Methane emissions from farms P4 and P5 were not modelled, because none of the inventories had methane conversion factors for manure acidification (cf. section 2.4). The prediction of enteric methane emissions was comparable between models (Fig. 4) and made up about 20% of the total modelled emissions for farms with no manure treatment (P1 and P2) and, 38% for the farm using biogasification (P3). The largest difference between the models was most likely a result of underestimating methane emissions from manure management, where the variables excreted VS and the MCF played an important role (Table 3). The I19 model calculated the highest manure methane emissions (P1 and P2, no manure treatment), even though for farm P2 the figure was still significantly lower than the measured rates (Fig. 4). The higher emissions for P1 and P2 when using I19 in comparison to I06 and DK were due to the higher MCF values used in I19 (Table 3). The revised version (I19) considers monthly temperature variations and the frequency of manure removal of outdoor storage, which is different to the IPCC 2006 model. In addition, the older IPCC model (I06) accounts for emissions reductions due to the presence of crust on the manure's surface, which was the case for P1 but not for P2; therefore, for P1, the MCF value was even lower in the I06 model for liquid slurry management (Table 3, 10% for P1 and 17% for P2). The lower emissions estimated using the national model (DK) in comparison to the international alternatives (I19 and I06) might be due to the lower VS and MCF values used by the national model (DK), when compared to I19 (Table 3). The Danish guidelines calculate VS based on the amount of manure excreted and on the housing system, instead of on gross energy (as done by the IPCC guidelines), thereby resulting in a lower VS value for the national

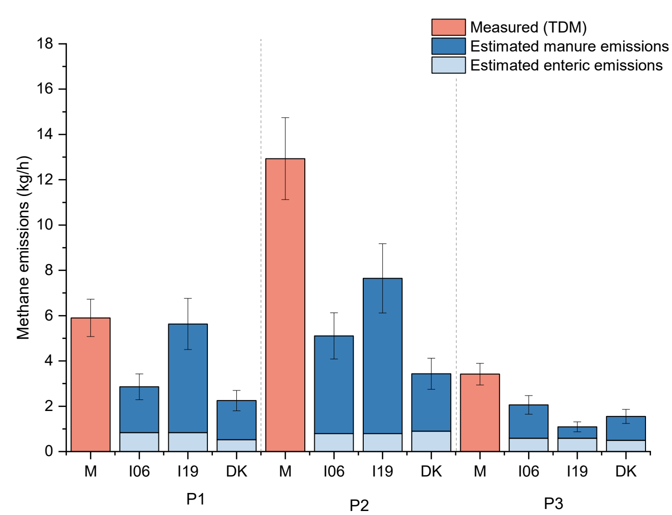

Fig. 4. Comparison between measured methane emissions (pink bars) and emissions estimated using GHG inventory guidelines (blue bars). Light blue represents enteric methane contributions, and dark blue represents the manure contribution. I06 stands for IPCC guidelines 2006, I19 for IPCC guideline refinement 2019 and DK for the Danish guidelines. The error bars correspond to the uncertainty of the modelled (±20% across all models) and measured emissions (±20%, uncertainty of the measurement technique (Fredenslund et al., 2019)). (For interpretation of the references to colour in this figure legend, the reader is referred to the Web version of this article.)

model (IPCC, 2006; Nielsen et al., 2021). Additionally, the MCF factor calculated by the national guide takes different views on manure methane emissions inside animal housing and in outdoor manure storage tanks. The main differences include the assumption of an annual constant housing temperature and that 100% of the loaded VS in the house is easily degradable. Conversely, for outdoor storage, temperature varies according to atmospheric conditions, and only half of the loaded VS is easily degradable (Nielsen et al., 2021). These assumptions lead to a lower MCF value than in the IPCC guidelines (Table 3) and reflect emission estimations made by the international models and the national model.

For farm P3, which treats manure by biogasification, I19 estimated the lowest emissions out of all models, because it uses a lower MCF value, as it only considers emissions from outdoor storage tanks, thereby ignoring regular housing and the temporary storage of raw manure. The IPCC 2006 model uses national MCF values, and so it is similar to the national estimation. Additionally, in the Danish model the MCF was calculated for degassed pig slurry, however, the sludge stored at P3 came from a biogas plant that co-digested manure with other types of feedstock.

Further conclusions on the models' underestimations need to be supported by a larger range of measured farm emissions and ideally by the segregation of emissions from housing units and storage tanks. The study highlights that methane emissions from manure might be the main reason for the models' inaccuracy, rather than enteric emissions, since the contribution of the former is more significant, and many factors affect it, as well as the models approach in handling the different variables. According to our results, assumptions regarding the influence of temperature variations on manure emissions (from house pits and outdoor storage units) and the amount of VS available in the models, might need some revision, however, a larger data set would be necessary to confirm the assumptions.

3.4. Comparison of measured and modelled monthly methane emissions

Fig. 5 compares monthly methane emissions for farms P1 and P2 estimated with the IPCC 2019 and Danish inventory with measured emissions. The models considered variations in numbers of animals and life stage, atmospheric temperature and the amount of manure stored in the tanks when the measurement was carried out. For both models, enteric methane emissions were relatively constant throughout the year, and thus any variations in emissions were primarily due to manure management. The IPCC's 2019 model captured seasonal emission variability the best, showing a trend similar to the measured emissions at both farms. The correlation between the modelled and measured emission values, however, was best for the P1 farm, resulting in an R^2 of 0.66, while for P2 it was 0.23. Interestingly, for both farms, the model underestimated emissions in November, we speculate that this might be because the models lack a lag time for the period when the temperature starts decreasing and the methanogenic activity is still high.

For the Danish model (Fig. 5), however, emissions were close to constant throughout the year, presumably because manure emissions primarily came from animal housing (72%), which has constant metrics throughout the year (amounts of manure and temperature). Additionally, the IPCC 2019 model assumed that the amount of VS easily available for methane production in the outdoor storage tank, which is the

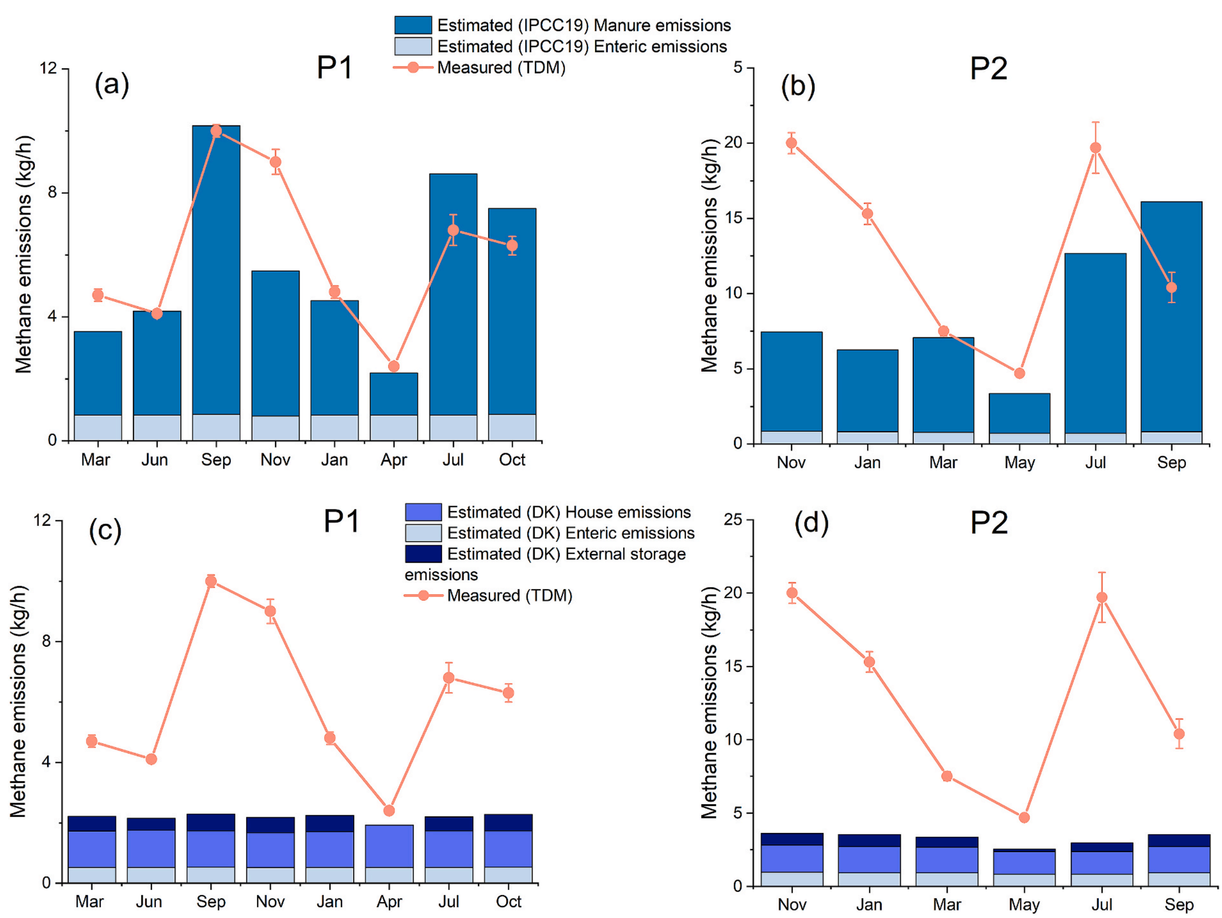

Fig. 5. Comparison of measured and monthly modelled emissions using the IPCC 2019 model (a, b) and the Danish model (c, d) for farms P1 and P2. For P1, house emissions also included emissions from deep litter. The bars represent the modelled emissions, while the line + symbol plot represents the measured emissions (average ± standard deviation). For the I19 model, the estimated monthly emissions largely vary year round, in contrast to the Danish models.

source exposed to yearly emissions variations, is 100% of the excreted VS, while for the DK model is only 51% of the VS coming from the house (approximately 40% of excreted VS). Furthermore, the Danish model assumes that only 25% of the carbon in the VS stored in the outdoor tank is converted anaerobically to methane, whereas the remaining part is instead degraded aerobically and emitted as carbon dioxide. Although the IPCC 2019 performed better, the assumption that all the excreted VS is stored in atmospheric temperature conditions does not agree with typical management systems in Denmark. Additionally, in the Danish model, average farm information is used as default, however, adding more specific farm data, e.g. VS contents, manure retention time and volume of manure stored in house and outdoor storage, and manure temperature, could improve the model performance. More studies on emission variations in manure stored in pits under animal housing and outdoors need to be carried out, in order to pinpoint the source of underestimation.

4. Conclusion

Whole-farm methane emissions were measured at five pig farms in Denmark (P1–P5) and quantified using the tracer gas dispersion method and covered methane emissions from animal housing and outdoor manure storage tanks. One of the farms treated their manure in a biogas plant (P3) and two used acidification treatment (P4 and P5). Methane emission rates ranged from 0.2 to 20 kg/h across all farms, the sampling was discrete, comprising six measurements distributed over a year, each with 1–3 h sampling coverage. In addition, methane emissions varied throughout the year, with emissions lower in spring and higher in autumn. Methane emission factors (EF) for the farms were 14 ± 6, 18 ± 9, 8 ± 7, 2 ± 1 and 1 ± 1 g/LU/h, for P1, P2, P3, P4 and P5, respectively. The different manure management practices adopted by the farms were reflected in the EFs, with a methane emission 55% lower on the farm with manure biogasification (P3) compared to the farm with no manure treatment (P2) while for the farms with manure acidification (P4–P5) the emissions were 91–93% lower compared to P2. Because of the limited number of measured farms, a larger data set is needed for further investigation of the impact of these mitigation technologies.

Moreover, a comparison of measured methane emissions and modelled emissions, using international and national guidelines, revealed a large underestimation of 51% across all models and all farms (P1–P3). The Danish inventory model performed worse than the international models, averaging an underestimation of 64%. The IPCC 2019 model captured seasonal emission variability the best, highlighting a similar trend in emissions to the measured emissions, whereas the Danish inventory model provided almost constant emission rates throughout the year. The results indicate that methane conversion factors and volatile solids for calculating emissions from manure management might need revision across all models, based on the farms we measured. However, due to the limited number of farms included in this study, more data should be collected, with attention paid to specific parameters such as volatile solids (amount, composition and degradability), storage temperature (inside house and outdoor), storage times, etc. Since large seasonal emission variations were recorded, future studies should focus on understanding the dynamics of manure emissions during storage in both manure pits under animal housing and in outdoor storage tanks and its temporal variations. This study demonstrated that methane emitted from Danish pig farms might be underestimated and that mitigation strategies, including manure biogasification and acidification, are not well-integrated in current models. Assuming that the results from the three studied farms are representative of all Danish pig farms, anthropogenic methane emissions in Denmark might be about 17% higher than current estimates. Accurate emission measurement methods are therefore required to quantify true emission rates, to document mitigation actions and to validate emission inventories, thereby closing the gap between modelled emissions and true emissions.

Author statement

Nathalia T. Vechi: Conceptualization, Methodology, Investigation, Formal analysis, Writing – original draft. **Nina S. Jensen:** Investigation, Writing – review & editing. **Charlotte Scheutz:** Conceptualization, Methodology, Writing – review & editing, Supervision, Project administration and funding acquisition.

Declaration of competing interest

The authors declare that they have no known competing financial interests or personal relationships that could have appeared to influence the work reported in this paper.

Acknowledgements

The project was internally funded by DTU. We would like to acknowledge Michael Holm, team leader at Landbrug & foedevarer SEGES, for providing the farms' contacts and for many fruitful discussions. Additionally, we thank the farmers for their willingness to participate and provide information on farm management.

References

Amon, B., Kryvoruchko, V., Fröhlich, M., Amon, T., Pöllinger, A., Mösenbacher, I., Hausleitner, A., 2007. Ammonia and greenhouse gas emissions from a straw flow system for fattening pigs: housing and manure storage. Livest. Sci. 112, 199–207. https://doi.org/10.1016/j.livsci.2007.09.003.

Arndt, C., Leytem, A.B., Hristov, A.N., Zavala-Araiza, D., Cativiela, J.P., Conley, S., Daube, C., Faloona, I., Herndon, S.C., 2018. Short-term methane emissions from 2 dairy farms in California estimated by different measurement techniques and US Environmental Protection Agency inventory methodology: a case study. J. Dairy Sci. 101, 11461–11479. https://doi.org/10.3168/jds.2017-13881.

Baldé, H., VanderZaag, A.C., Burtt, S., Evans, L., Wagner-Riddle, C., Desjardins, R.L., MacDonald, J.D., 2016. Measured versus modeled methane emissions from separated liquid dairy manure show large model underestimates. Agric. Ecosyst. Environ. 230, 261–270. https://doi.org/10.1016/j.agee.2016.06.016.

Blanes-Vidal, V., Hansen, M.N., Pedersen, S., Rom, H.B., 2008. Emissions of ammonia, methane and nitrous oxide from pig houses and slurry: effects of rooting material, animal activity and ventilation flow. Agric. Ecosyst. Environ. 124, 237–244. https://doi.org/10.1016/j.agee.2007.10.002.

Børsting, C.F., Hellwing, A.L.F., Lund, P., 2020. Normative Figures 2020. DCA - Danish Centre for Food and Agriculture. Aarhus University (accessed 3.15.21). http://anis.au.dk/forskning/sektioner/husdyrernaering-og-fysi-ologi/normtal/.

Danish Agriculture & Food Council, 2020. Statistics - Pig Meat. Copenhagen (accessed 6.1.21). https://agricultureandfood.dk/prices-and-statistics/annual-statistics.

Danish Agriculture and Food Council, 2021. Danish Pig Meat Industry (accessed 6.1.21). http://www.agricultureandfood.dk/.

Daube, C., Conley, S., Faloona, I.C., Arndt, C., Yacovitch, T.I., Roscioli, J.R., Herndon, S. C., 2019. Using the tracer flux ratio method with flight measurements to estimate dairy farm CH4 emissions in central California. Atmos. Meas. Tech. 12, 2085–2095. https://doi.org/10.5194/amt-12-2085-2019.

Delre, A., Mønster, J., Scheutz, C., 2017. Greenhouse gas emission quantification from wastewater treatment plants, using a tracer gas dispersion method. Sci. Total Environ. 605–606, 258–268. https://doi.org/10.1016/j.scitotenv.2017.06.177.

Elsgaard, L., Olsen, A.B., Petersen, S.O., 2016. Temperature response of methane production in liquid manures and co-digestates. Sci. Total Environ. 539, 78–84. https://doi.org/10.1016/j.scitotenv.2015.07.145.

Fangueiro, D., Hjorth, M., Gioelli, F., 2015. Acidification of animal slurry– a review. J. Environ. Manag. https://doi.org/10.1016/j.jenvman.2014.10.001.

Flesch, T.K., Vergé, X.P.C., Desjardins, R.L., Worth, D., 2013. Methane emissions from a swine manure tank in western Canada. Can. J. Anim. Sci. 93, 159–169. https://doi.org/10.4141/cjas2012-072.

Foged, H.L., Lyngvig, H.S., Toft, M., Jacobsen, B.H., 2017. Scenarie for Forsuring Af Halvdelen Af Gyllen I Danmark, pp. 1–39 (accessed 6.1.21). https://mim.dk/media/218212/scenarie_for_forsuring_af_halvdelen_ af_gyllen_i_danmark.pdf.

Fredenslund, A.M., Rees-White, T.C., Beaven, R.P., Delre, A., Finlayson, A., Helmore, J., Allen, G., Scheutz, C., 2019. Validation and error assessment of the mobile tracer gas dispersion method for measurement of fugitive emissions from area sources. Waste Manag. 83, 68–78. https://doi.org/10.1016/j.wasman.2018.10.036.

Galle, B., Samuelsson, J., Svensson, B., Borjesson, G., 2001. Measurements of methane emissions from landfills using a time correlation tracer method based on FTIR absorption spectroscopy. Environ. Sci. Technol. 35 (1), 21–25. https://doi.org/10.1021/es0011008.

Haeussermann, A., Hartung, E., Gallmann, E., Jungbluth, T., 2006. Influence of season, ventilation strategy, and slurry removal on methane emissions from pig houses. In: Agriculture, Ecosystems and Environment, pp. 115–121. https://doi.org/10.1016/j.agee.2005.08.011.

Hassouna, M., Calvet, S., Gates, R.S., Hayes, E., Schrade, S., 2020. Measurement of gaseous emissions from animal housing. In: Holden, N.M., Wolfe, M.L., Ogejo, J.A., Cummins, E.J. (Eds.), Introduction to Biosystems Engineering. American society of Agriculture and Biological Engineers - ASABE. https://doi.org/10.21061/introbiosystemsengineering/gaseous_emissions.

Husted, S., 1994. Seasonal variation in methane emission from stored slurry and solid manures. J. Environ. Qual. 23, 585–592. https://doi.org/10.2134/jeq1994.00472425002300030026x.

IPCC, 2019. 2019 Refinement to the 2006 IPCC Guidlines for National Greenhouse Gas Inventories, vol. 4. Agriculture, forestry and other land use (accessed 3.14.21). https://www.ipcc-nggip.iges.or.jp/public/2019rf/index.html.

IPCC, 2006. IPCC Guidelines for National Greenhouse Gas Inventories, Agriculture, Forestry and Other Land Use, Prepared by the National Greenhouse Gas Inventories Programme. CIGES, Japan (accessed 3.14.21). http://www.ipcc-nggip.iges.or.jp/public/2006gl/index.html.

ITC, 2020. Trade Map - List of Exporters for the Selected Product (All Products) [WWW Document]. Int. Trade Cent (accessed 5.31.21). https://www.trademap.org/Country_SelProduct.aspx?nvpm=1%7C%7C%7C%7C%7C0203%7C%7C%7C4%7C1%7C1%7C2%7C1%7C1%7C2%7C1%7C1%7C1.

Jensen, J., Krogh, P.H., Sørensen, P., Petersen, S.O., 2018. Potentielle miljøeffekter ved anvendelse af forsuret gylle på landbrugsjord, Videnskabelig rapport fra DCE (accessed 6.1.21). http://dce2.au.dk/pub/SR257.pdf.

Kaharabata, S.K., Schuepp, P.H., 1998. Methane emissions from aboveground open manure slurry tanks oxygen demand z 218. Global Biogeochem. Cycles 12, 545–554.

Kupper, T., Häni, C., Neftel, A., Kincaid, C., Bühler, M., Amon, B., VanderZaag, A., 2020. Ammonia and greenhouse gas emissions from slurry storage - a review. Agric. Ecosyst. Environ. 300 https://doi.org/10.1016/j.agee.2020.106963.

Loyon, L., Guiziou, F., Beline, F., Peu, P., 2007. Gaseous Emissions (NH3, N2O, CH4 and CO2) from the aerobic treatment of piggery slurry-Comparison with a conventional storage system. Biosyst. Eng. 97, 472–480. https://doi.org/10.1016/j.biosystemseng.2007.03.030.

Maldaner, L., Wagner-Riddle, C., VanderZaag, A.C., Gordon, R., Duke, C., 2018. Methane emissions from storage of digestate at a dairy manure biogas facility. Agric. For. Meteorol. 258, 96–107. https://doi.org/10.1016/j.agrformet.2017.12.184.

Mangino, J., Bartram, D., Brazy, A., 2001. Development of a methane conversion factor to estimate emissions from animal waste lagoons. In: US EPA's 17th Annual Emission Inventory Conference. Atlanta, Georgia.

Mønster, J., Samuelsson, J., Kjeldsen, P., Rella, C., Scheutz, C., 2014. Quantifying methane emission from fugitive sources by combining tracer release and downwind measurements - a sensitivity analysis based on multiple field surveys. Waste Manag. 34, 1416–1428. https://doi.org/10.1016/j.wasman.2014.03.025.

Mønster, J., Samuelsson, J., Kjeldsen, P., Scheutz, C., 2015. Quantification of methane emissions from 15 Danish landfills using the mobile tracer dispersion method. Waste Manag. 35, 177–186. https://doi.org/10.1016/j.wasman.2014.09.006.

Ni, J.-Q., Heber, A.J., Lim, T.T., Tao, P.C., Schmidt, A.M., 2008. Methane and carbon dioxide emission from two pig finishing barns. J. Environ. Qual. 37, 2001. https://doi.org/10.2134/jeq2007.0386.

Nielsen, O.-K., Plejdrup, M.S., Winther, M., Nielsen, M., Gyldenkærne, S., Mikkelsen, M.H., Albrektsen, R., Thomsen, M., Hjelgaard, K., Fauser, P., Bruun, H.G., Johanssen, V., Nord-Larsen, T., Vesterdal, L., Stupak, I., Scott-Bentsen, N., Rasmussen, E., Petersen, S.B., Olsen, T.M., Hansen, M.G., 2021. Denmark's National Inventory Report 2021. Emission Inventories 1990-2019 - Submitted under the United Nations Framework Convention on Climate Change and the Kyoto Protocol.

Park, K.H., Thompson, A.G., Marinier, M., Clark, K., Wagner-Riddle, C., 2006. Greenhouse gas emissions from stored liquid swine manure in a cold climate. Atmos. Environ. 40, 618–627. https://doi.org/10.1016/j.atmosenv.2005.09.075.

Park, K.H., Wagner-Riddle, C., 2010. Methane emission patterns from stored liquid swine manure. AJAS (Asian-Australas. J. Anim. Sci.) 23, 1229–1235. https://doi.org/10.5713/ajas.2010.90536.

Petersen, S.O., Andersen, A.J., Eriksen, J., 2012. Effects of cattle slurry acidification on ammonia and methane evolution during storage. J. Environ. Qual. 41, 88–94. https://doi.org/10.2134/jeq2011.0184.

Petersen, S.O., Blanchard, M., Chadwick, D., Del Prado, A., Edouard, N., Mosquera, J., Sommer, S.G., 2013. Manure management for greenhouse gas mitigation. Animal 7, 266–282. https://doi.org/10.1017/S1751731113000736.

Petersen, S.O., Olsen, A.B., Elsgaard, L., Triolo, J.M., Sommer, S.G., 2016. Estimation of methane emissions from slurry pits below pig and cattle confinements. PLoS One 11, 1–16. https://doi.org/10.1371/journal.pone.0160968.

Philippe, F.X., Laitat, M., Canart, B., Vandenheede, M., Nicks, B., 2007. Comparison of ammonia and greenhouse gas emissions during the fattening of pigs, kept either on fully slatted floor or on deep litter. Livest. Sci. 111, 144–152. https://doi.org/10.1016/j.livsci.2006.12.012.

Philippe, F.X., Nicks, B., 2015. Review on greenhouse gas emissions from pig houses: production of carbon dioxide, methane and nitrous oxide by animals and manure. Agric. Ecosyst. Environ. 199, 10–25. https://doi.org/10.1016/j.agee.2014.08.015.

Rodhe, L.K.K., Abubaker, J., Ascue, J., Pell, M., 2012. Greenhouse Gas Emissions from Pig Slurry during Storage and after Field Application in Northern European Conditions Intergovernmental Panel on Climate Change 3. https://doi.org/10.1016/j.biosystemseng.2012.09.010.

Roscioli, J.R., Yacovitch, T.I., Floerchinger, C., Mitchell, A.L., Tkacik, D.S., Subramanian, R., Martinez, D.M., Vaughn, T.L., Williams, L., Zimmerle, D., Robinson, A.L., Herndon, S.C., Marchese, A.J., 2015. Measurements of methane emissions from natural gas gathering facilities and processing plants: measurement methods. Atmos. Meas. Tech. 8, 2017–2035. https://doi.org/10.5194/amt-8-2017-2015.

Rzeźnik, W., Mielcarek, P., 2016. Greenhouse gases and ammonia emission factors from livestock buildings for pigs and dairy cows. Pol. J. Environ. Stud. 25, 1813–1821. https://doi.org/10.15244/pjoes/62489.

Scheutz, C., Fredenslund, A.M., 2019. Total methane emission rates and losses from 23 biogas plants. Waste Manag. 97, 38–46. https://doi.org/10.1016/j.wasman.2019.07.029.

Scheutz, C., Kjeldsen, P., 2019. Guidelines for landfill gas emission monitoring using the tracer gas dispersion method. Waste Manag. 85, 351–360. https://doi.org/10.1016/j.wasman.2018.12.048.

Scheutz, C., Samuelsson, J., Fredenslund, A.M., Kjeldsen, P., 2011. Quantification of multiple methane emission sources at landfills using a double tracer technique. Waste Manag. 31, 1009–1017. https://doi.org/10.1016/j.wasman.2011.01.015.

Sokolov, V., VanderZaag, A., Habtewold, J., Dunfield, K., Wagner-Riddle, C., Venkiteswaran, J.J., Gordon, R., 2019. Greenhouse gas mitigation through dairy manure acidification. J. Environ. Qual. 48, 1435–1443. https://doi.org/10.2134/jeq2018.10.0355.

Sommer, S.G., Clough, T.J., Balaine, N., Hafner, S.D., Cameron, K.C., 2017. Transformation of organic matter and the emissions of methane and ammonia during storage of liquid manure as affected by acidification. J. Environ. Qual. 46, 514. https://doi.org/10.2134/jeq2016.10.0409.

Sommer, S.G., Olesen, J., Petersen, S.O., Weisbjerg, M., Valli, L., Rodhe, L., Béline, F., 2009. Region-specific assessment of greenhouse gas mitigation with different manure management strategies in four agroecological zones. Global Change Biol. 15, 2825–2837. https://doi.org/10.1111/j.1365-2486.2009.01888.x.

Sommer, S.G., Petersen, S.O., Møller, H.B., 2004. Algorithms for calculating methane and nitrous oxide emissions from manure management. Nutrient Cycl. Agroecosyst. 69, 143–154. https://doi.org/10.1023/B:FRES.0000029678.25083.fa.

Vechi, N.T., Mellqvist, J., Scheutz, C., 2022. Quantification of methane emissions from cattle farms, using the tracer gas dispersion method. Agric. Ecosyst. Environ. 330, 107885. https://doi.org/10.1016/j.agee.2022.107885.

III

Measurements of methane emissions from manure tanks using a stationary tracer gas dispersion.

Vechi, N.T., & Scheutz, C.

Submitted to Biosystems Engineering

Measurements of methane emissions from manure tanks, using a stationary tracer gas dispersion method

Nathalia T. Vechi, Charlotte Scheutz

[1]Department of Environmental and Resource Engineering, Technical University of Denmark, Denmark

Correspondence to: Nathalia T. Vechi (navei@dtu.dk)

Abstract

Methods to measure fugitive methane emissions from farm-scale manure outdoor tanks are needed to improve understanding of these emissions. Tracer gas dispersion methods have rarely been used for measuring gaseous emissions from manure tanks likely due to limitations in terms of farm layout, road availability, and complex setup for tracer gas release. To offer more flexibility to the mobile tracer dispersion method (TDM), this paper tested a stationary sampling approach while keeping the TDM method assumptions. Unlike the mobile TDM, which consists of driving across the plume measuring downwind concentrations, the stationary method uses fixed sampling points downwind the source to sample concentrations, independently of road availability. The aim of this study was to develop, validate and apply the new approach for methane emission quantification of manure storages.

Controlled gas release experiments validated the method, and the stationary TDM had an average and standard deviation of 95 ± 12% methane recovery rate, while the mobile TDM achieved a 107 ± 5% recovery rate. Moreover, the stationary TDM was applied to measure methane emissions from dairy manure tanks. Over more than a year of measurements using the stationary TDM, methane emissions average and the standard deviation was 2.19 ± 0.66 kg h^{-1} or, normalized by volume of manure, 0.58 ± 0.17 g m^{-3} h^{-1}. Atmospheric and manure temperatures correlated well (R^2= 0.72, R^2=0.85, respectively) with methane emissions from the tank. In conclusion, the stationary method was shown to be an alternative method to facilitate measurements when the mobile TDM is not applicable.

Graphical abstract

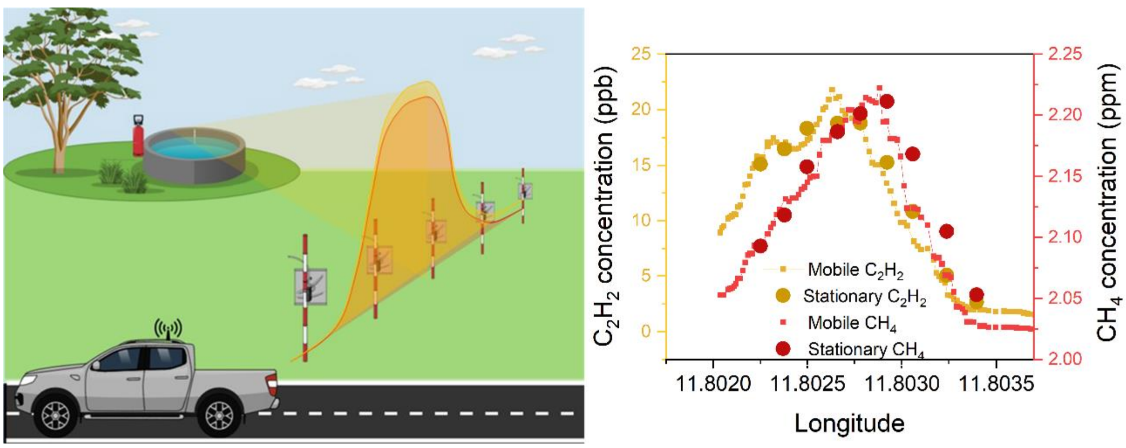

1. Introduction

Agriculture is a significant source of greenhouse gas (GHG) emissions, contributing 12.4% of emissions globally, whilst manure emissions from livestock production account for 2.4% of the total (Climate Watch, 2022). In Denmark, these numbers are even higher, with agriculture producing 25% of total GHG emissions and animal manure corresponding to 4.2% of the total (Nielsen et al., 2021). Pig and dairy cattle liquid manure, which has dry matter content lower than 12% (Christensen & Sommer, 2013), is partly degraded by anaerobic digestion during storage, producing methane. In northern European and North American farm systems, the manure is temporarily stored under the animal house and later removed to outdoor concrete tanks, where it remains until application on agricultural land. Improvements in monitoring and modelling these emission sources allow countries to estimate their GHG emissions budgets better and find efficient mitigation strategies.

The study of manure methane emission can be done on smaller scales (lab or pilot scale) or in farm-scale storage tanks, with measurement complexity scaling in line with the storage size. Additionally, manure methane emissions are dynamic and vary around the year according to temperature and the amount of manure stored. A recent review study found that 46% of gaseous emissions studies have been done at farm-scale manure storage facilities, most often using surface flux chambers (31%) and micrometeorological methods (63%) to quantify emissions (Kupper et al., 2020). The surface flux chamber method (Husted, 1994; Loyon, Guiziou, Picard, & Saint-Cast, 2016) is well-known and relatively straightforward in its application. However, it is an intrusive method in that surface emissions might be affected by the placement of the chamber and lacks spatial and temporal resolution. As for micrometeorological techniques, backward Lagrangian stochastic modelling (bLS) (Baldé, VanderZaag, Burtt, Gordon, & Desjardins, 2016; Flesch, Vergé, Desjardins, & Worth, 2013) and mass balance (MMB) (Maldaner, Wagner-Riddle, VanderZaag, Gordon, & Duke, 2018; Wagner-Riddle, Park, & Thurtell, 2006) have been frequently used. As a challenge, micrometeorological methods require modelling of atmospheric conditions, thus adding some uncertainty to the measurements.

Tracer gas techniques have been used in only 2% of farm-scale measurement campaigns (Kupper et al., 2020), with sulphur hexafluoride (SF_6) as a tracer gas. In the first study, Kaharabata and Schuepp (1998) used a grid array placed over the centre of the storage tank surface for the tracer release (SF_6). Concentrations were sampled one metre downwind and half a metre above the tank's edge and measured by gas chromatography (CH_4) and a tuneable diode laser tracer gas analyser (SF_6). In a second study by Sneath et al. (2006), the tracer was released around the edge of the storage tank. Furthermore, concentrations were sampled 30 metres upwind and downwind from the tank, at a single point, with a custom-made setup using a GC spectrometer. More recently, with the development of high-precision and fast-response instruments, the called tracer gas dispersion method (TDM or mobile TDM) has been developed further and applied to quantify sources such as whole dairy and pig farms by coupling the instruments to mobile platforms as vehicles (Arndt et al., 2018; Vechi, Jensen, & Scheutz, 2022; Vechi, Mellqvist, & Scheutz, 2022) and aircraft (Daube et al., 2018). In contrast with the previous studies, tracer gas was released close to the source directly from gas cylinders without a fixed release setup. Concentrations were measured downwind at greater distances from the target source (500 to 2000 metres) by driving across the whole concentration plume, minimising errors caused by tracer positioning (Mønster, Samuelsson, Kjeldsen, Rella, & Scheutz, 2014; Taylor, Chow, Delkash, & Imhoff, 2016). Additionally, SF_6 should not be used as tracer gas because it is a potent GHG and due to its heavy molecular weight, which hinders gas dispersion, alternatively acetylene (C_2H_2) or nitrous oxide (N_2O) are now commonly used.

The TDM is a non-intrusive method with high accuracy, which does not depend on wind modelling and has a rather easy setup, making it advantageous for emissions quantification. However, the application of the TDM method for quantifying emissions from manure storage tanks will be hindered at many farms by road availability, wind conditions, high animal housing densities and farm layout. Therefore, a complementary stationary sampling approach to the mobile TDM can make the method more flexible, as it allows for air concentration sampling in surrounding fields, where driving is not possible. The novelty of this study is the sampling strategy differentiating from the previous studies because it applies the best practices of the mobile TDM. In addition, the tracer gas is released using a simple system, to allow for mobility and faster setup, and C_2H_2 is used as tracer gas instead.

This study aims to develop, validate and apply a stationary mobile tracer dispersion method for quantifying methane emissions from manure storage tanks. We validate the method with controlled release tests and apply it by measuring methane emissions from a manure tank for a whole year. Additionally, we develop quality parameters and guidelines for the method's best practices. Employing a large portfolio of methods to quantify accurate emissions from agricultural sources is essential to cover the methods' limitations and align them with emissions source dynamics.

2. Materials and methods

2.1 Mobile tracer gas dispersion method

In the TDM, a tracer gas is released at a known rate (Q_{tr}) (kg h^{-1}) close to the target source to simulate the target source emissions (E_{tg}) (kg h^{-1}). The target and tracer gas should have a long atmospheric lifetime, because they will then disperse in a similar manner (Mønster et al., 2014). C_2H_2 and N_2O were used as tracer gases in this study based on the instruments available and on the source characteristics (Delre, Mønster, Samuelsson, Fredenslund, & Scheutz, 2018).They were released from calibrated flowmeters, thereby guaranteeing flow stability. Additionally, the tracer gas release rate was assured by weighing the gas cylinders. Methane and C_2H_2 concentrations were measured by a fast-response cavity ring-down spectrometer (CRDS) (G2203, Picarro Inc., CA, response time 2 sec), with a precision (3σ) of 0.34 and 2.14 ppb for C_2H_2 and methane, fitted to a mobile platform. N_2O concentrations were measured using another CRDS instrument (S/N JADS 2001, Picarro Inc., CA, response ~3 secs) with a precision (3σ) of 47 ppb. The air was sampled approximately two metres height, on the top of a car, and directed to the analytical instrument via an auxiliary pump, additionally, global positioning (GPS) was recorded. Gas concentration measurements were performed downwind from the source, crossing the full plume at approximately 200 metres' distance to the source (Fig. 1). The ratio between the known tracer gas (C_{tr}) (ppb) and target gas (C_{tg}) (ppb), minus their background concentration ($C_{tg,bg}$ and $C_{tr,bg}$), was calculated by integrating the whole plume transect. The emission was estimated using Eq.1, where MW_{tg} (g mol^{-1}) and MW_{tr} (g mol^{-1}) are molar weights of the methane and tracer gas, respectively, and l (metre) is the distance across the transect.

$$E_{tg} = Q_{tr} \frac{\int_{l1}^{l2}(C_{tg} - C_{tg,bg})dl}{\int_{l1}^{l2}(C_{tr} - C_{tr,bg})dl} \cdot \frac{MW_{tg}}{MW_{tr}} \quad (1)$$

Fredenslund et al. (2019) described five different methods for calculating the target-to-tracer gas ratio and found that integrating the area under the plume concentration transect (Equation (1)) is the best approach when using a mobile TDM. The method can be applied to different target gases, but in our study, only methane emissions were investigated.

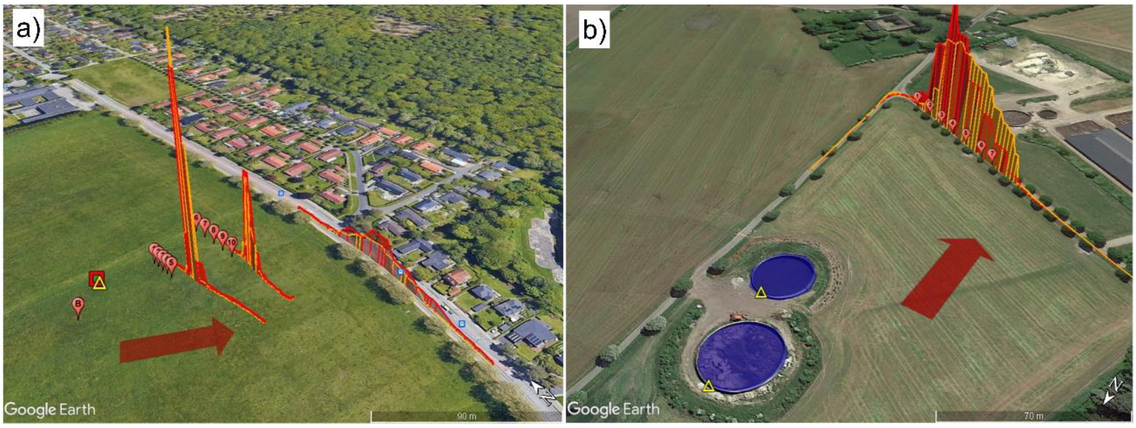

Fig. 1: a) Overview of the controlled release test (Test #3 25/02), b) Overview of air concentration measurements performed downwind two manure tanks (Blue shaped area) (31/08). The red square indicates the CH_4 release and yellow triangle the C_2H_2, the balloons indicated the bags sampling points. The red plumes show the CH_4 concentrations while the yellow show the C_2H_2 concentrations, which were measured at three different distance on the controlled release test. The red arrow shows the wind direction. Map source: Google Earth ©

2.2 Stationary tracer gas dispersion method

When applying the stationary version of the TDM, concentrations are measured in air samples collected at fixed sampling points positioned downwind from the source, instead of measuring the concentrations by crossing the plume with a mobile platform (Fig. 1). Air sampling was done with peristaltic or SKC pocket pumps, which pumped air at 50 - 150 ml min^{-1} into gastight bags of 9 – 12 l. Bags were made of heat seal aluminium foil material, commonly used for food storage. The number of sampling points varied from five to ten in a measurement campaign, which is a measurement activity lasting 4 to 6 hours. Similarly to the mobile tracer method, gas concentrations in the gas bags were analysed using CRDS Picarro instruments. Samples were collected over a certain period (30 min to 1 hour), following which gas concentrations in the bags were measured. Usually, the sampling was repeated two to four times, which is referred to as "repetitions". When necessary, the sampling points were repositioned and the air sampling repeated. Additionally, background concentrations were measured by either sampling air upwind from the manure tanks (~20 m), using gas bags, or by driving outside the emission plume and further calculating the average concentration of the sampled air.

Similar to the analysis described in Fredenslund et al. (2019) and Mønster et al. (2014), we tested different approaches to calculate the target-to-tracer gas ratio from the sampling points. This exercise was done in order to establish the best approach to estimate the ratio, mainly because – differently from the mobile TDM – the whole plume is often not completely covered by sampling points. The first approach (1), called "Area", follows the same approach as the mobile TDM strategy, using equation (1), which integrates the area under the concentration plume transect. The second approach (2), called "Point average", uses equation (2) to infer the ratio in each sampling bag, and the final emission rate is calculated as an average of these.

$$E_{tg} = Q_{tr} \frac{C_{tg} - C_{tg,bg}}{C_{tr} - C_{tr,bg}} \cdot \frac{MW_{tg}}{MW_{tr}} \qquad (2)$$

In the third approach (3), "Point correlation", the sampling points were correlated using a linear fit (Equation 3), where the calculated slope was used as the target-to-tracer ratio, which was then multiplied by the tracer release rate (Q_{tr}) to obtain E_{tg}.

$$C_{tg} = C_{tr} \cdot Ratio_{tg:tr} + C_{bg,tg} \qquad (3)$$

Another approach (4), named "Gaussian", used the Gaussian plume model to infer the plume, based on the sampling points as described in Mønster et al. (2014). This method fitted the Gaussian model curve to the measured methane plume concentrations using the bags (Equation 4). The Gaussian model uses parameters related to atmospheric stability, wind conditions and measurement distance, and it is based on a dispersion model; therefore, no tracer gas information was used herein. The Gaussian model inputs assumed neutral conditions for most of the campaigns (Class D), with exception of campaign #5, which was slightly unstable (Class C), regarding the topography, it was considered an urban area.

$$C_{tg}(x,y,z) = \frac{E_{tg}}{2\pi U \sigma_y \sigma_z} exp^{\frac{-y^2}{2\sigma_y(x)^2}} \left(exp^{\frac{-(z-H)^2}{2\sigma_z(x)^2}} + exp^{\frac{-(z+H)^2}{2\sigma_z(x)^2}} \right) \qquad (4)$$

Finally, the last approach (5), called "Gaussian tracer", combines Gaussian plume modelling and knowledge of the tracer gas in order to estimate emissions. The method uses modelling (Equation 4) not only for the methane concentrations, but also for the tracer gas. Further, it calculates the area under both gas emissions' modelled dispersion curves. Thereafter, emissions are estimated similarly using equation 1, combining the area of both modelled emissions and the known tracer release rate.

2.2.1 Quality requirements

Stationary TDM best practices were established to minimise quantification errors when measuring methane emissions from manure tanks similar to executed in previous studies (Scheutz & Kjeldsen, 2019). Additionally, quality parameters were identified to score the quality of the data collected, interpret data usefulness and determine issues with tracer gas misplacement, sideways of the emission source, as this is the main cause of potential errors in the TDM.

The quality parameters considered were: (1) the tracer and target gas correlation coefficient (R^2), (2) plume coverage and (3) plume representation; in other words, whether concentrations were measured in the plume peak or only in the plume tails. The correlation coefficient (R^2) between tracer and target gas concentration indicates whether the tracer and target gases are similarly dispersed (Fig. 2a). According to Foster-Wittig et al. (2015) and Roscioli et al. (2015), who applied the mobile TDM, R^2 should be higher than 0.8 and 0.75, respectively. When using the stationary TDM, only a few points are measured, thus making the parameter more sensitive to random distribution; therefore, the accepted R^2 was lowered to 0.5. Other studies have shown that a sideways misplacement of the tracer gas release does not influence emission rate quantification, so even with a low R^2, accuracy might be achieved – as long as the whole plume is covered (Mønster et al., 2014; Matacchiera et al., 2018; Taylor et al., 2016). For this reason, plume coverage (2) was another parameter used in the quality assessment. It was obtained by fitting a Gaussian curve to the measured tracer gas concentration points (Fig. 2b). Furthermore, it was calculated how much the measured points represent the full modelled plume (area of the covered points, grey area on Fig 2b divided by the area of the entire estimated plume). The parameter was considered fulfilled when plume coverage was higher than 50%. Finally, the last factor used in the quality assessment was the presence of the plume peak concentration in the measured points. Based on Gaussian modelling (Fig. 2c), it was evaluated that when the sampled points were positioned in the centre of the plume, it reflected a better representation of the target-to-tracer gas ratio, although gases are sideways misallocated, in comparison to when points are positioned in the plume tail (0.75 to 1.25, from one peak to another, yellow square). A scoring system was used to classify the quality of each measurement repetition, summing one point each time one of the three requirements was fulfilled, resulting in a maximum of three points.

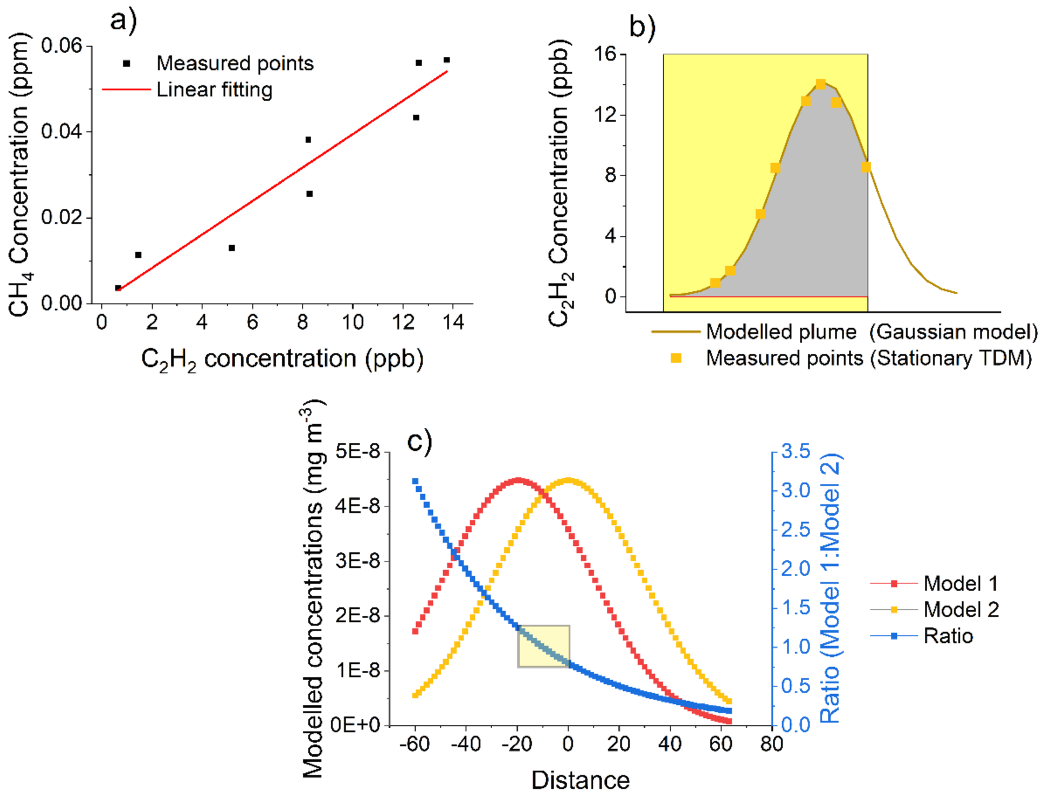

Fig. 2: Quality parameters. a) Correlation coefficient between target-to-tracer ratio relative concentrations (C_{bag} - $C_{background}$) measured in each stationary sampling point (R^2 0.92). b) Plume coverage, obtained by fitting the concentrations to a Gaussian model, and estimating the percentage of plume coverage. c) Plume representation; the relevance of this parameter is demonstrated by modelling Gaussian plumes with equal emissions but a side-way tracer misplacement of 20 metres (yellow and red squares), and the ratio between each point (blue squares). Data from graphs a, and b correspond to measurements from April 2021.

2.3 Description of the measurement campaigns

2.3.1 Controlled release test

Table 1 summarises conditions during the five controlled release test campaigns (#1-5). The release tests were carried out in an open grass field (480 m x 420 m), and air samples were collected (at ~ 1m height) at five different locations across the plume and at two different distances downwind from the release point, namely ~40 m and ~80 m (stationary method). Simultaneously, the analytical mobile platform measured air concentrations (at a 2 m height) by traversing the plume next to the sampling points on multiple occasions (nine to 28 transects per test) (mobile method) (Fig. 1a). The sampling lasted from one to one and half hours. In two of the campaigns (#3 and #4), plume transects, using the mobile platform, were also done at a third distance (~120 m) (Fig. 1a). The acetylene release rate varied from 0.26 to 0.76 kg h^{-1}, while the methane release rate was between 0.61 and 1.21 kg h^{-1}.

For emission quantification using the mobile TDM approach, the target-to-tracer gas ratio was estimated by using plume integration (Equation 1), whereas for the stationary TDM, five approaches were tested to calculate the target-to-tracer ratio, as explained in section 2.2. To assess the methods' performance, the methane recovery rate was used, which calculates the percentage of the measured methane divided by the true release rate, corresponding to method accuracy.

Table 1: Summary of the five controlled release test campaigns

Test	Atmospheric temperature (°C)	Wind speed (m s^{-1}), wind direction	Stationary method		Mobile method		
			Distance 1 (~40 m)	**Distance 2 (~80 m)**	**Distance 1 (~45 m)**	**Distance 2 (~85 m)**	**Distance 3 (~120 m)**
			Number of sampling points	*Number of sampling points*	*Number of transects*	*Number of transects*	*Number of transects*
#1	10	8-9, WNW	3	3	24	23	
#2	3	2-3, NE	5	4	23	20	
#3	6	3-4, W	5	5	28	33	5
#4	10	6-8, W	3	1	9	20	14
#5	25	4-6, SE	5	4	10	7	

2.3.2 Manure tank methane measurements

Methane emissions were quantified at two manure storage tanks at a cattle farm located in Denmark. They were measured as one source, due to their proximity (Fig. 1b), and methane was selected as the target gas. The tanks were surrounded by grass fields, and roads suitable for the measurements were available with northerly winds only; simultaneous measurements using the mobile and stationary approach were made in these conditions (Fig. 1b). The location of the tanks allowed for the use of most wind directions with the stationary method, except for the southerly wind, due to the interference of methane emissions from the animal barns. Manure volume and temperature were measured in most of the campaigns (Table 2). Air sampling was similar to that described above, with the difference that the sampling event was only 30 min, in order to avoid misplacement of the sampling points due to changes in wind direction. Each of the manure measurement campaigns included two to four air sampling repetitions, which took place over two or more hours. Distance from the sampling points to the tank varied from 100 to 200 metres according to the wind direction (Table 2). The number of air sampling points varied due to pump availability. The tracer gas was released from two gas cylinders, each placed on the upwind edge of the storage tanks (Fig. 1b).

In addition to quantifying methane emissions from the manure tank, a comparison between quantifications made using the stationary and mobile methods was done. In total, 17 measurement campaigns were carried out, nine of which included both the stationary and the mobile measuring approach (Table 2). Simultaneously with air sampling (~ 30 minutes from five to 10 sampling points), the mobile platform was driven across the plume, performing on average six to eight plume transects during ~20 min. The first tank had a storage capacity of 5000 m^3 and a depth of 5.2 meters, whereas the smaller tank had a capacity of 3500 m^3 and a depth of 5.7 meters. Both tanks were partially above the ground.

Table 2: Overview of the manure tank measurement campaigns. "S" corresponds to the stationary method and "M" to the mobile method. Total capacity of the tanks is 5000 m^3 for one of them, and 3500 m^3 for the other. The measurement distance varied with the wind direction. For a westerly wind direction, the measuring distance was ~ 160 meters, for northerly winds the distance was ~ 180 meters and for easterly winds it was ~ 110 meters.

Date	Time of the day	Method	Atmospheric temperature (°C)	Capacity of tank occupied (%)[a]	Manure temperature (°C)	N° of sampling points	N° of repetitions	Wind speed ($m\ s^{-1}$), wind direction.
11-04-2019	13:00 to 15:00	S, M	10	-	-	5	2	4, NE
28-06-2019	03:00 to 07:00	S, M	14	-	-	5	3	3, W
20-09-2019	16:00 to 20:00	S, M	14	-	-	5	4	6, WNW
04-03-2020	10:30 to 15:00	S	6	85	-	5	4	3, W
20-05-2020	12:00 to 15:00	S	15	39	-	5	3	2.5, W
23-06-2020	11:30 to 15:30	S, M	20	24	-	7	4	3, W
13-07-2020	12:30 to 16:00	S	18	24	-	8	3	3, W
31-08-2020	15:00 to 19:30	S, M	19	38	-	7	3	1.5, NW
02-10-2020	09:00 to 12:00	S	15	48	-	6	3	2.5, E
05-11-2020	12:00 to 15:00	S	11	61	-	8	3	5.5, WNW
02-12-2020	14:30 to 17:00	S	5	65	11	8	3	4, ESE
10-12-2020	10:00 to 14:00	S	3	77	10	10	4	4, ESE
03-01-2021	11:30 to 15:30	S, M	3	89	9	9	3	5, ENE
17-02-2021	14:00 to 16:30	S, M	2	90	6	10	3	3, NW

18-03-2021	12:30 to 16:00	S, M	7	36	7	9	2	3, N
15-04-2021	17:00 to 19:30	S, M	9	36	8	8	3	6, N
19-05-2021	13:00 to 17:00	S	13	34	13	10	3	8, W

[a]For the combination of both tanks

2.3.3 Evaluation of errors caused by tracer gas misplacement

To evaluate the possibility of tracer gas release misplacement error caused by the gas cylinder position, methane emission measurements were taken with the tracer gas positioned first upwind and then downwind of the manure tank, using C_2H_2 as a tracer gas. In this case, the mobile TDM was used, and the measurements were taken at approximately 190 metres away from the tanks.

Moreover, the dual release of N_2O and C_2H_2 was performed, whereby N_2O was released from the centre of the tank (SI, Figure S2) while C_2H_2 was released on the upwind edge of the tank. Plume concentration measurements at three different distances to the tanks were made 35, 92 and 162 metres away from the centre of the tanks (SI, Figure S3). At the closest distance, traverses were done with the mobile platform, while the stationary method was used to measure the other two distances. Each traverse using the stationary method had five sampling points, which resulted in two repetitions with quality data.

3. Results and discussions

3.1 Method development and validation

3.1.1 Mobile tracer dispersion method – controlled release

Fig. 3 shows the methane recovery rate from the five controlled gas release tests (#1-5), with TDM performed at two or three different distances (40, 80 and 120 m) away from where the methane and C_2H_2 were released. For the mobile TDM controlled release experiments, the average methane recovery rate varied between 92 and 115% at the shortest measuring distance (T1 ~ 40 metres), showing slightly better results in comparison to the greater distances (T2-3 ~80-120 metres) (Fig. 3). All measurement transects distances showed recovery rates within the uncertainty of the TDM, which for more complex emission sources have been previously assessed as being lower than ±15-20% (Fredenslund et al., 2018; Mønster et al., 2014). The best performance was obtained for the short measuring distance (T1 ~ 40 metres), where the error of the average recovery rate (3%) was within the controlled gas release uncertainty (±5%).

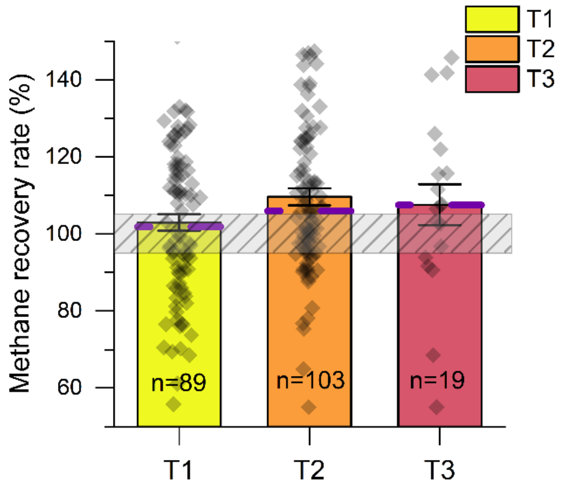

Fig. 3: Methane recovery rates from five controlled release tests based on mobile TDM measurements performed at three distances, namely T1 ~45 metre, T2 ~80 metres and T3 ~120 metres. The bars show the average value, the dashed line the median value and the error bar the standard error. Black diamonds represent each measured transect for all controlled releases. The grey area corresponds to release rate uncertainty (±5%).

3.1.2 Stationary tracer dispersion method – controlled release

For the stationary TDM, four of the five approaches ("Area" (Equation 1), Point average" (Equation 2), "Point correlation" (Equation 3), and "Gaussian tracer") employed to obtain the tracer-to-target gas ratio produced similar results, considering the average recovery (90-95%) and the median recovery (90-98%) (Fig. 4). The "Area" method had the best median recovery (98%) and the second-best average recovery (94%), so it was chosen for further quantifications using the stationary TDM (Fig. 4). This method is less sensitive to poor plume mixing, while "Point correlation" and "Point average" are similar to the "Area" method when the source simulation is correct (Mønster et al., 2014). Moreover, as tracer and target gases were released from the same point in the controlled release experiments, problems with source simulation and improper plume mixing would be less likely to occur. For the "Point correlation" estimation, all sample correlation coefficients (R^2) were higher than 0.83, with the lowest being obtained in test #4. The stationary methods ("Area" (Equation 1), Point average" (Equation 2), "Point correlation" (Equation 3)) generated recovery rates comparable to the mobile TDM (median and average recovery rates of 109%, including all data and disregarding differences in measurement distances) when considering method uncertainty.

The "Gaussian" model method, however, performed the worst among the tested methods (average 170% and median 127%) (Fig. 4), especially in one of the campaigns, which had a higher emission estimation (methane recovery of ~350%, test #2), albeit all of the other campaigns were also above the controlled release rate. This method is very sensitive to the parameters used for atmospheric class stability (unstable, neutral and stable) and the type of topography (open country and urban), which may explain the weaker performance. On the other hand, when the Gaussian model used tracer information ("Gaussian tracer"), accuracy increased when compared to the model by itself, with an average of 93% and a median of 97%, thus demonstrating how accuracy increases in line with the use of a tracer gas.

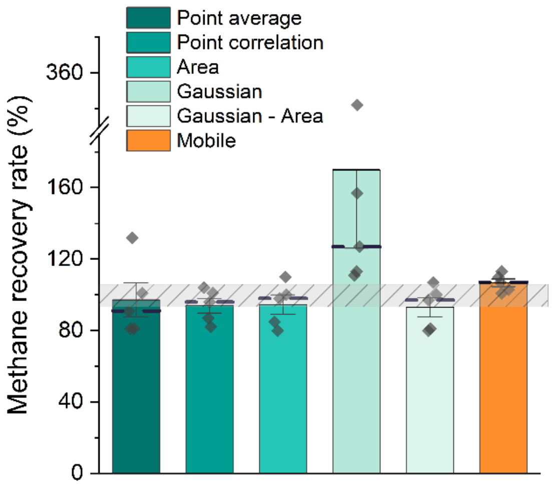

Fig. 4: Methane recovery rates for the five controlled release tests based on stationary TDM measurements and using six different approaches for obtaining the target-to-tracer ratio. The bars show the average value, the dashed line the median value and the error bar the standard error. Black diamonds represent each controlled release test. The grey area corresponds to release rate uncertainty (±5%).

3.1.3 Number of sampling points – controlled release

Quantification using a stationary TDM requires that a number of sampling points are positioned across the plume. A large quantity of sampling points would provide a good description of the plume; however, the method would also be more labour-intensive for operators, as it would require more pumps, additional time and, consequently be more expensive. The optimal number of sampling points provides quality data and eliminates unnecessary costs. The influence of the number of plume sampling points on the recovery rate was examined by using results from the controlled release tests (Fig. 5a). The methane recovery rate was calculated by randomising the order of the sampled points and increasing the number of samples from one to eight. The CH_4 recovery rate (%) for all controlled release tests was lower than 120% and higher than 80%, and it did not significantly change with an increase in the number of bags, especially after the fourth sampling point. With the exemption of controlled release test #2, most of the other campaigns showed changes in variability when considering four samples; thereafter, variability decreased. In controlled release test #2, there was significant variability between the eight samples, although the reason for this anomaly is unclear. Therefore, based on the results from the controlled release test, a minimum number of five bags is acceptable for decreasing variability among the sampling points, whilst error, however, is less affected by the number of samples.

The sampling location within the plume is another crucial parameter when the tracer and emission source are not as well aligned – differently from the controlled release test. An analysis was done to identify the effect of sampling positioning within the plume, using data from the manure tank quantification. We compared emissions calculated using ratios from single bags, with the emissions quantified by mobile TDM, assuming that the latter of the two options was the most accurate emission estimation. Furthermore, we classified the bags according to their position relative to the plume peak (in the tail, 25%, 50% or 75% away from the peak). In Fig. 5b, we observed that when the bags' measured concentrations were 25 or 50% away from peak concentrations, they tended to overestimate the emissions. In comparison, when placed at 75% of the peak or at the peak, emissions were ± 10% of emissions quantified using the mobile method. As illustrated in Fig. 5b, when the bags are on the tails, with concentrations below 50% of the plume peak, the error is most likely to be significantly independent of the number of bags. On the other hand, when the bags are above 50% of the peak, the error tends to be lower.

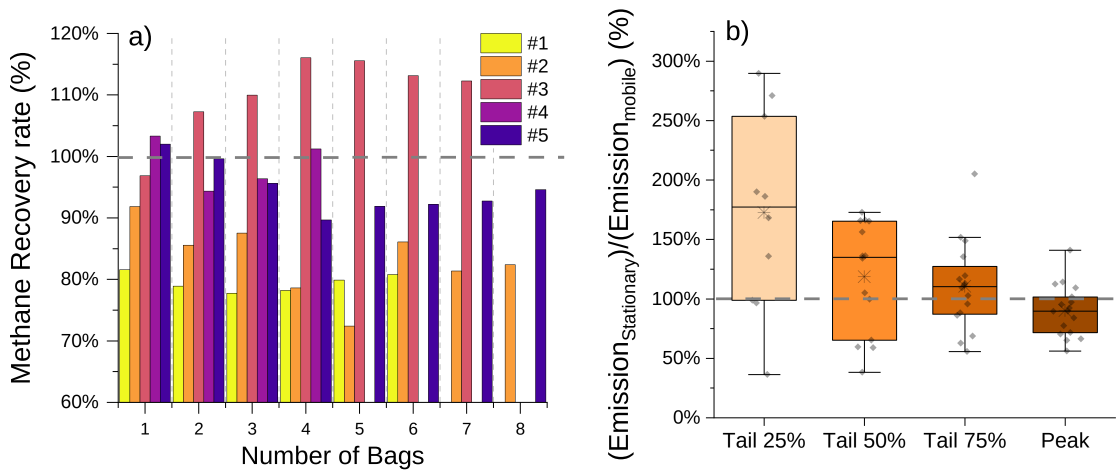

Fig. 5: (a) Methane recovery rate (%) average according to the number of stationary sampling points in each controlled release test. (b) Comparison between emissions quantified using

stationary sampling points and mobile TDM according to the position of the sampling point within the plume. Close to the plumes' peaks, the ratio is close to the true, which is one.

3.2 Manure tank measurements – method application

3.2.1 Comparison of the mobile and stationary tracer dispersion method

In nine of the campaigns, quantification using both stationary and mobile methods was possible (Table 2); a comparison between these quantifications is shown in Fig. 6. One of the campaigns was excluded based on the quality assessment (Section 3.2.3 and SI Table S1). The correlation between the quantifications was $R^2 = 0.93$, while the slope was close to 1 (0.92) (Fig. 6), indicating how similar the mobile and stationary methods results are, and that the stationary method demonstrated good performance when compared to the mobile method.

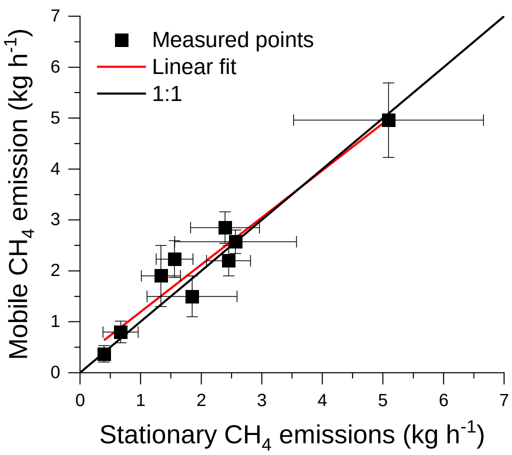

Fig. 6: Correlation plot of the manure tank emissions rates quantified using the mobile and stationary method. Error bars represent the standard deviation of each quantification. The red line shows the correlation between both methods, and the black line represents a one-to-one correlation.

3.2.2 Tracer gas misplacement – manure tank emissions

The position of the tracer gas release point is an important variable in the tracer gas method (TDM), as misplacement of the tracer release can lead to under- or overestimate emissions if the tracer is placed upwind or downwind of the emission source, respectively (Delre, Mønster, Samuelsson, Fredenslund, & Scheutz, 2018; Mønster et al., 2014). Proper tracer gas release positioning might be challenging when quantifying emissions from manure storage tanks, due to the large tank size and inaccessible surface area of the tank. However, the effect of tracer misallocation will decrease in line with an increase in measurement distance (Mønster et al., 2014; Taylor et al., 2016).

Two tests were performed to access the potential effect of tracer misallocation on emission quantification. The first test was done by releasing the tracer gas on the upwind edge of the tank (~ 15 metres to the centre of the tanks) and secondly on the downwind edge of the tank (~ 15 metres to the centre of the tank). Emissions were measured at ~190 metres away from the tanks. Placing the tracer release bottle on the upwind edge resulted in average emissions of 1.95 ± 0.39 kg h^{-1}, while placing it downwind resulted in 1.62 ± 0.25 kg h^{-1} (Fig. 7a). Overestimation is expected when the tracer is positioned upwind from the source, and vice versa for downwind, and a similar pattern was observed in our results. However, by applying a Wilcoxon test, the difference between the two datasets was insignificant (hypothesis: $p<0.05$ if the distance is significant, result: $p=0.089$). In conclusion, most likely, the overestimation potentially produced by placing the tracer upwind from the tank was minimised due to the greater measurement distance.

In the second test, a dual tracer release was used. A C_2H_2 bottle was positioned on the upwind edge of the manure tank, and N_2O was released from the middle of the tank. Concentration measurements were taken at three distances, namely 35, 90 and 160 metres away from the centre of the tank (SI, Figure S3). Tracer misallocation, which is the distance from the N_2O tracer release position to the measurement transect, divided by the distance of the C_2H_2 release position to the transect, was 43, 24, and 7%, respectively. Methane emissions quantified using C_2H_2 and N_2O at each different transect are represented in Fig. 7b. C_2H_2 estimated higher emissions than N_2O, which was also expected due to the longer distance for C_2H_2 to travel in comparison to N_2O, thereby resulting in more plume dilution. This was especially the case in the two nearest transects (shortest measuring distance), while the difference was smaller for the third and furthest transect. According to a Wilcoxon test, the difference between the quantifications using C_2H_2 and N_2O was only significant on the first transect (hypothesis $p<0.05$; $p=0.01$) but not relevant on the second or third transects ($p= 0.123$ and $p= 0.796$, respectively). Looking at a Gaussian model for this scenario, considering the model characteristics as “open country” and Class D of stability (neutral), expected overestimation was +79%, +45% and +8%, while what was measured was +33%, +26% and -5% for T1, T2 and T3, respectively.

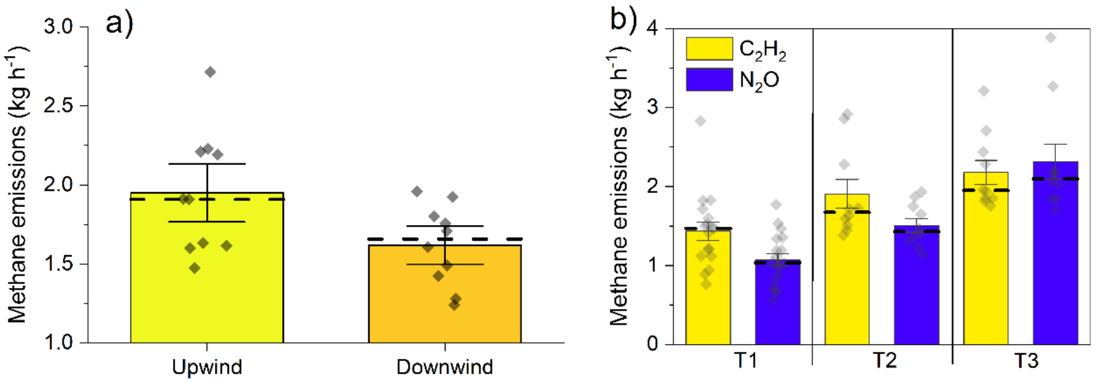

Fig. 7: Tracer gas misplacement evaluation using two different tracers (C_2H_2 and N_2O) released from two different positions. (a) Methane emissions determined using the tracer positioned on the upwind edge of the tank using acetylene (C_2H_2) as tracer or in the centre of the tank using nitrous oxide instead as a tracer (N_2O). (b) Test on misplacing the tracer release upwind and downwind from the tanks. The bar indicates the average and error bars the standard error, the dashed line shows the median of the values and the diamond shapes point to the individual plumes or points measured.

3.2.3 Quality assessment

A quality assessment of the data obtained from measurements carried out at the manure tanks was performed according to section 2.2.1 (SI, Table SI1), where for each sampling repetition a score was given. Only one repetition did not sum any points, 22% summed one point and 41% and 35% amounted to two and three points, respectively. We considered that "one-point" data was worst in terms of quality; therefore, it was not included when calculating annual manure methane emissions, which means that 24% of the total data was excluded. The difference between the annual emissions calculated using all the data (2.25 kg h^{-1}) and the data passed on the score test (2.19 kg h^{-1}) was 3%.

3.3 Annual manure methane emissions and dynamics

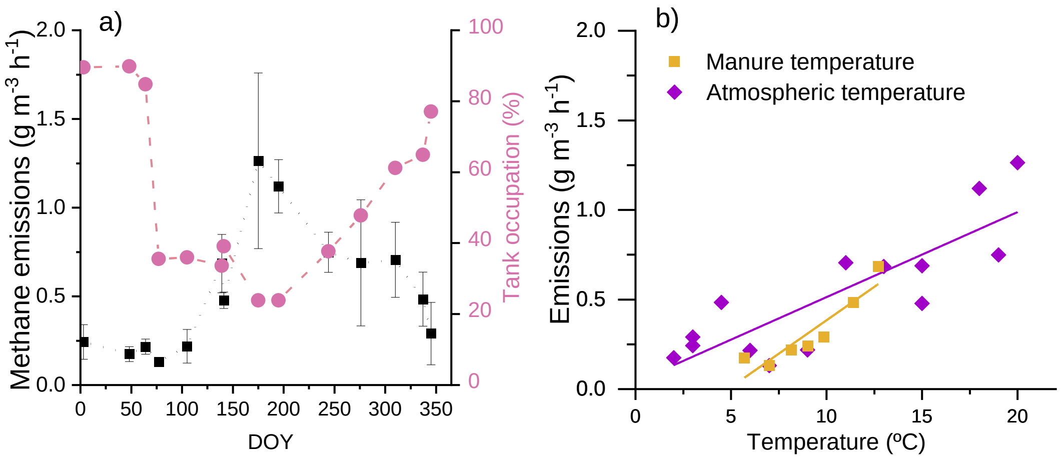

Fig. 8: (a) Manure tank methane emissions (average and standard deviations), quantified using the stationary tracer dispersion method. The black squares show emissions in g m^{-3} h^{-1}, while the pink circles represent the percentage of manure occupation in the tank. (b) Correlation between measured methane emissions (g m^{-3} h^{-1}) and temperature, where the purple diamonds and dark purple line correspond to atmospheric temperature, and orange squares and the dark orange line correspond to manure temperature.

Annual average manure tank emissions measured using the stationary TDM and standard deviation were 2.19 ± 0.66 kg h^{-1}, or 0.58 ± 0.15 g m^{-3} h^{-1} normalized by volume of manure stored and calculated as a weighted average according to the distribution of the measurements over the year (Fig. 8a). In comparison to the literature, the quantified emission is similar to the annual emission baseline for cattle manure stored in tanks (0.58 g m^{-3} h^{-1}) obtained by Kupper et al., (2020), which is estimated based on quantifications obtained from many other studies. Husted (1994) measured emissions from Danish cattle manure tanks, for which annual emissions averaged 0.34 g m^{-3} h^{-1}. Average emissions using the stationary approach were 2.19 ± 0.66 kg h^{-1}, while for the mobile TDM they were 1.99 ± 0.34 kg h^{-1}.

Manure emissions were the highest in summer, when the temperature was higher, although the amount of manure stored was low (Fig. 8a). Manure was removed from the tanks in the spring (March - April), and these tanks were kept relatively empty during summertime and until late autumn, when they started to be filled again (Fig. 8a). Emissions normalized by volume of manure stored, in g m^{-3} h^{-1}, correlated well with atmospheric temperature R^2= 0.72, and even more with manure temperature R^2=0.85 (Fig. 8b). The correlation between methane emissions and temperature was expected, because the microbiological community responsible for the anaerobic decomposition is temperature-dependent (Husted, 1994; Westermann, 1996).

In our study, diurnal dynamics of the emissions were not taken into consideration. The stationary method was used for discrete measurements, which corresponded to 30-min intervals, and repeated two to four times at each measurement campaign. However, under stable wind conditions, the method can be applied for a longer period without becoming labour-intensive, because there will be less need for repositioning the sampling points, and sampling can be done over a longer period. This might be relevant, since diurnal variation is expected at some times of the year, especially in summer and autumn (Maldaner et al., 2018). Considering that most of our measurements were done in the early afternoon, it is possible this could have caused a positive methane quantification bias during months when there is diurnal variation, because high emissions are expected around midday due to surface heating (Wood, Gordon, & Wagner-Riddle, 2013). Total methane emissions from the farm, including housing and the two manure tanks, were quantified in a few of the campaigns, when the weather and operational conditions allowed. In the spring, when the tanks were emptied and the manure temperature was low, emissions from the manure tanks corresponded to only 5% of the whole farm rate (Fig. 9). During the rest of the year, this contribution varied from 9% to 20%, reaching its highest point in autumn. According to IPCC modelled data, specific for this farm data, the contribution of manure to whole-farm emissions is approximately 20% (Vechi, Mellqvist, et. al., 2022).

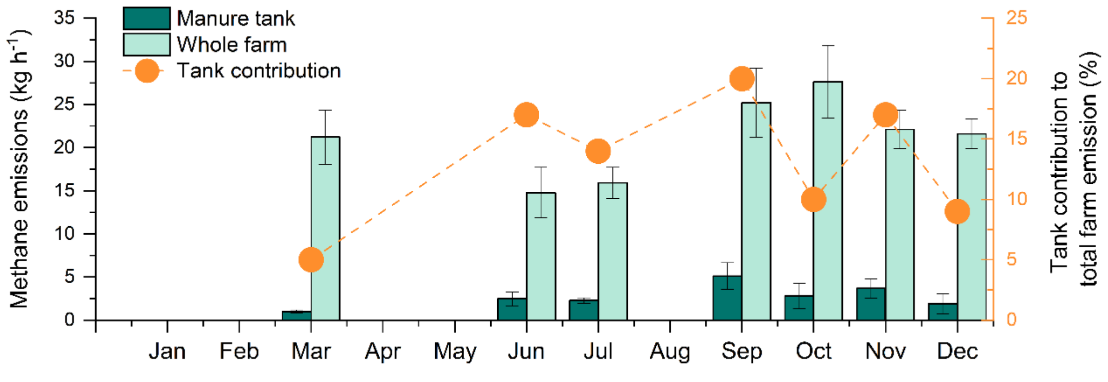

Fig. 9: (a) Monthly methane emissions (average and standard deviations) of whole-farm emissions (light green) and the manure tanks (dark green). Whole-farm emissions were quantified using the mobile TDM, while for the manure tanks the stationary TDM was used. Orange points correspond to the percentage of whole-farm emissions emitted by the studied manure tanks.

4. Employment of the stationary tracer dispersion method and best practices

The mobile TDM has proven to be an accurate method for quantifying emissions from large heterogeneous sources such as landfills, wastewater treatment plants and biogas plants (Scheutz et al., 2011; Mønster et al., 2015; Delre et al., 2017; Scheutz and Fredenslund, 2019). The method has been validated in several controlled release and comparison tests, and its uncertainty has been assessed to be within 15-20% (e.g. Mønster et al., 2014; Delre et al., 2018; Fredenslund et al., 2019; Feitz et al., 2018) when applied following best practice (Scheutz & Kjeldsen, 2019). In this study, the mobile TDM was applied to a smaller area source (20-30 m wide), and where plume measurements were performed at a closer distance (100-200 m downwind) in comparison to many of the referenced studies, where the source can span over several hectares and plume measurements are often performed 2-3 km downwind. This study showed that mobile TDM performed well on a smaller scale such as a manure tank, and controlled release tests showed recovery rates close to 100%. We also demonstrated that the stationary TDM could be applied for discrete measurements of methane emissions from manure tanks. However, the mobile method is preferable because it does not require the installation of a sampling setup in the field and consequently is less labour-intensive; nevertheless, when a mobile platform is used, the method is limited by road availability and weather conditions (wind direction and atmospheric stability). This can especially be the case for manure tanks, which are often located relatively close to farms and interfered by emissions from animal housing, or in agricultural fields with limited road accessibility. For this reason, using stationary sampling points provides more flexibility to the measurement method, and in this study monthly measurements could be obtained without having to depend on the "right" wind conditions, although the sampling needed to be carried out with more care.

The number of sampling points and their position in the plume are important factors. As discussed in section 3.1.3, a minimum of five sampling points decreased emission estimation variability; however, more sampling points are likely to cover a more significant part of the plume and its peak, thus increasing accuracy. Therefore, a minimum of seven bags generally produced better quality results (a data quality score of 3 in 40% of the repetitions) than fewer bags (a score of 3 in 26%). The position of the bags within the plume is another critical aspect, being one of the quality parameters, because, in the case of misallocation between the emission from the source and the tracer release, the error in quantification is smaller when samples are taken around the plume peak than from its tails. In the case of two nearby sources, it is also crucial to cover the plume peak to ensure that both sources are considered. In the validation experiment executed by Feitz et al. (2018), a similar approach to the stationary TDM was tested in order to measure emissions, with the difference being that sampling was done in canisters instead of bags. The method did not function well, and the lower amount of sampling points was pointed out as an issue affecting uncertainty. Additionally, canister analysis was done mostly by using an FTIR instrument in the field, which had lower precision than the CRDS.

A sampling time of 30 min was adopted in our study, and even though other sampling times were not investigated, we believe that 15 to 30 min is ideal because wind direction is likely to change during longer time intervals, hence making it more viable to sample outside the plume or on the fringes thereof. Instead of longer sampling times, we suggest repeating sampling two to four times. This offers the ability to adjust the position of the sampling locations in between sampling events. For continuous measurements, the setup can be improved by optimising the sampling procedure with automatic sampling, such as in the example described in the experiment by Finn et al. (2010).

The setup time for tracer gas release can be decreased when compared to other studies, because it does not require a fixed setup in which a grid of gas release points is necessary (Kaharabata & Schuepp, 1998; Sneath et al., 2006). This can be supported by measuring at greater distances as this reduces the effect of misallocation of the tracer release (Mønster et al., 2014; Taylor et al., 2016). We adopted typical distances of 100 to 200 metres (three to six times the manure tank's diameter), and the dual tracer gas experiment showed that at distances of 100 m upwards, in neutral conditions, the effect of tracer gas misplacement was low, although the difference between centred and the misplaced releases was smaller at 160 metres. The concentration measurements at a greater distance are viable due to high-precision instruments such as the CRDS. In addition, we analysed the bags in the field, after each sampling exercise, which allowed for sampling repositioning. This is not mandatory, and the bags can indeed be taken for analysis away from the field, but in-situ analysis improves the quality of the data and reduces the risk of invalid field campaigns. The challenge in measuring the combined emissions from two tanks is related to the tracer release rate, which should be proportional to each tank's emissions. A proportional release rate is needed because stationary sampling most likely will not cover the whole plume, and the same tracer gas release rates from different emissions will produce different ratios across the plume, which can be misinterpreted as poor-quality measurements. In this case, covering a larger part of the plume (minimum 50%) as well as the plume peak is essential; otherwise, emissions from only one tank might be quantified.

Finally, to obtain high-quality data when using the stationary TDM, best practice should be followed. A quality assessment of the measured data can be performed when conditions are not ideal to support reliable data. In these cases, the measured data should be filtered according to three quality scores (described in section 2.2.1), namely (1) correlation coefficient $R^2 > 50\%$, (2) plume coverage > 0.50 and (3) plume peak representation. An example of the quality assessment for the data used in this paper is provided in the SI (Table S1). Data receiving a lower score (one point) is deduced as being low quality and might be excluded. Excluding this data, did not affect the results of our measurements (difference between annual average emissions was 6%).

4.1 Guidelines for best practice using the stationary tracer gas dispersion method

Based on the results described above, and in the guideline for the mobile tracer gas dispersion method (Scheutz & Kjeldsen, 2019), best practice for quantifying methane emissions from manure tanks using the stationary TDM is described in the following section.

Interfering sources. Initially, a desktop analysis is performed, using imagery tools and Google Earth, to investigate possible interfering methane sources, identify the most suitable wind conditions and set the measuring distance for emission quantification. On the measurement day, a methane screening of the surrounding area is done to exclude methane sources that could otherwise interfere with measuring emissions from the specific manure tank. For this task, a mobile analytical platform with high precision instrumentation is recommended. In cases where several tanks are located too close to each other, they can be measured as a single source instead, because they will result in a combined plume, making it difficult to distinguish sources. Planning the measurements also involves understanding emission dynamics.

Tracer gas release. The tracer gas should ideally be released from the centre of the manure tank, which can be done with the help of an extended tube (SI, Fig.S1). Alternatively, the tracer gas bottles can be placed upwind or downwind of the tank, as long as a certain distance is considered for positioning the sampling points (three to five times the tank's diameter). The tracer gas release should be constant throughout the measurements and controlled using high-precision flow controllers. In order to control the amount of tracer gas released, the weight loss of the gas bottles should be recorded using a high-precision scale. In the case of two tanks, the proportionality of the tracer gas released from each tank can be assessed by screening concentrations close to – or even above the surface of – the tanks.

Plume sampling. A minimum five stationary sample points is needed, but more are preferred in order to ensure good plume coverage, including the plume peak. Sampling points should be marked downwind of the source, whilst air samples can be collected in bags or, alternatively, containers (Duan, Scheutz, & Kjeldsen, 2021). After starting the tracer gas release, air samples are collected over a period of 30 minutes. Ideally, the collected samples are analysed in the field before proceeding with the next sampling repetition. If recorded target and tracer gas concentrations are not correlated, the sampling locations should be adjusted. At least two repetitions should be repeated, ideally three.

Data processing. The calculation of methane emissions should be done by following the "Area" approach. This method uses the area under both the measured target and tracer gas plumes to estimate the ratio between the gases. After that, methane emissions are obtained by using the ratio and tracer release information. To evaluate data quality, the data quality scoring analysis should be performed as described in section 2.2.1, namely (1) correlation coefficient (R^2), (2) plume coverage and (3) plume peak representation. Any score of 1 or lower indicates low-quality data that may be excluded from the dataset.

5. Conclusion

Methane emissions from manure storage tanks contribute to the greenhouse gas emission budget, and they can be mitigated by strategies such as anaerobic digestion and biogas production, acidification and other options. Nonetheless, it is important to verify mitigation efficiencies and understand emission dynamics. Measurements of real-scale manure tanks are somewhat challenging, so it is essential to have validated emission quantification methods that can be used either on their own or in combination, in order to overcome different measurement challenges and limitations.

This study investigates a variant of the well-known tracer gas dispersion method (TDM), by adopting some of the principles of the improved mobile TDM but using a stationary sampling approach, which brings more flexibility to the method. The stationary TDM was validated by using controlled methane release tests, which demonstrated the accuracy of both the mobile and stationary TDM, with the methane recovery rate varying on average from 94 to 97% for the stationary method and 107% for the mobile approach. The stationary method was further developed by determining the minimum number of stationary sampling points and the effect of the tracer gas release position, and further developed a best practice measurement guideline.

Finally, the stationary method was applied for quantifying methane emissions from manure tanks, and a comparison between the mobile and stationary approach was approximately 96%. Annual methane emissions from the manure tanks averaged at 0.58 g m^{-3} h^{-1}, which is in line with literature estimations for dairy cattle manure. It was also possible to observe the temperature dependency of the emissions.

The study concludes that the stationary TDM is useful for quantifying methane emissions from manure tanks and can be used to complement the original mobile TDM. The stationary method also offers greater flexibility in terms of less dependency on road availability and weather conditions; however, labour intensity is higher, and measurements need to be carried out with care by following best practice.

Acknowledgements
We would like to thank Zhenhan Duan and Vincent Maklawe Essonanawe Edjabou from the Department of Environmental Engineering at DTU for their assistance with the five controlled release tests. This work was funded in part by the Kvægafgiftsfoden.

References

Arndt, C., Leytem, A. B., Hristov, A. N., Zavala-Araiza, D., Cativiela, J. P., Conley, S., … Herndon, S. C. (2018). Short-term methane emissions from 2 dairy farms in California estimated by different measurement techniques and US Environmental Protection Agency inventory methodology: A case study. *Journal of Dairy Science*, *101*(12), 11461–11479. https://doi.org/10.3168/jds.2017-13881

Baldé, H., VanderZaag, A. C., Burtt, S. D., Gordon, R. J., & Desjardins, R. L.

(2016). Does fall removal of the dairy manure sludge in a storage tank reduce subsequent methane emissions? *Journal of Environment Quality*, *45*(6), 2038. https://doi.org/10.2134/jeq2016.03.0083

Baldé, H., VanderZaag, A. C., Burtt, S. D., Wagner-Riddle, C., Evans, L., Gordon, R., … MacDonald, J. D. (2018). Ammonia emissions from liquid manure storages are affected by anaerobic digestion and solid-liquid separation. *Agricultural and Forest Meteorology*, *258*(February), 80–88. https://doi.org/10.1016/j.agrformet.2018.01.036

Climate Watch Historical GHG Emissions. (n.d.). World Resources Institute. Retrieved from https://www.climatewatchdata.org/sectors/agriculture#drivers-of-emissions

Christensen, M. L., & Sommer, S. G. (2013). Manure characterisation and inorganic chemistry. *Animal Manure: Recycling, Treatment, and Management; Jensen, LS, Christensen, ML, Sommer, SG, Schmidt, T., Eds*, 41-65.

Daube, C., Conley, S., Faloona, I. C., Arndt, C., Yacovitch, T. I., Roscioli, J. R., & Herndon, S. C. (2018). Using the tracer flux ratio method with flight measurements to estimate dairy farm CH4 emissions in central California, (November), 1–20. https://doi.org/10.5194/amt-2018-356

Delre, A., Mønster, J., Samuelsson, J., Fredenslund, A. M., & Scheutz, C. (2018). Emission quantification using the tracer gas dispersion method: The influence of instrument, tracer gas species and source simulation. *Science of the Total Environment*, *634*, 59–66. https://doi.org/10.1016/j.scitotenv.2018.03.289

Duan, Z., Scheutz, C., & Kjeldsen, P. (2021). Trace gas emissions from municipal solid waste landfills: A review. *Waste Management*, *119*, 39–62. https://doi.org/10.1016/j.wasman.2020.09.015

Feitz, A., Schroder, I., Phillips, F., Coates, T., Neghandhi, K., Day, S., … Griffith, D. (2018). The Ginninderra CH4 and CO2 release experiment: An evaluation of gas detection and quantification techniques. *International Journal of Greenhouse Gas Control*, *70*(March), 202–224. https://doi.org/10.1016/j.ijggc.2017.11.018

Finn, D., Clawson, K. L., Carter, R. G., Rich, J. D., Eckman, R. M., Perry, S. G., … Heist, D. K. (2010). Tracer studies to characterize the effects of roadside noise barriers on near-road pollutant dispersion under varying atmospheric stability conditions q. *Atmospheric Environment*, *44*(2), 204–214. https://doi.org/10.1016/j.atmosenv.2009.10.012

Flesch, T. K., Vergé, X. P. C., Desjardins, R. L., & Worth, D. (2013). Methane emissions from a swine manure tank in western Canada. *Canadian Journal of Animal Science*, *93*(1), 159–169. https://doi.org/10.4141/cjas2012-072

Foster-Wittig, T. A., Thoma, E. D., & Albertson, J. D. (2015). Estimation of point source fugitive emission rates from a single sensor time series: A conditionally-sampled Gaussian plume reconstruction. *Atmospheric Environment*, *115*, 101–109. https://doi.org/10.1016/j.atmosenv.2015.05.042

Fox, T. A., Barchyn, T. E., Risk, D., Ravikumar, A. P., & Hugenholtz, C. H. (2019). Erratum: A review of close-range and screening technologies for mitigating fugitive methane emissions in upstream oil and gas (Environmental Research Letters (2019) 14 (053002) DOI: 10.1088/1748-9326/ab0cc3). *Environmental Research Letters*, *14*(6). https://doi.org/10.1088/1748-9326/ab20f1

Fredenslund, A. M., Rees-White, T. C., Beaven, R. P., Delre, A., Finlayson, A., Helmore, J., … Scheutz, C. (2019). Validation and error assessment of the mobile tracer gas dispersion method for measurement of fugitive emissions from area sources. *Waste Management*, *83*, 68–78. https://doi.org/10.1016/j.wasman.2018.10.036

Fredenslund, Anders M, Hinge, J., Holmgren, M. A., Rasmussen, S. G., & Scheutz, C. (2018). Bioresource Technology On-site and ground-based remote sensing measurements of methane emissions from four biogas plants : A comparison study. *Bioresource Technology*, *270*(August), 88–95. https://doi.org/10.1016/j.biortech.2018.08.080

Husted, S. (1994). Seasonal Variation in Methane Emission from Stored Slurry and Solid Manures. *Journal of Environmental Quality*, *23*(3), 585–592. https://doi.org/10.2134/jeq1994.00472425002300030026x

Kaharabata, S. K., & Schuepp, P. H. (1998). Methane emissions from aboveground open manure slurry tanks oxygen demand z 218. *Global Biogeochemical Cycles*, *12*(3), 545–554.

Kupper, T., Häni, C., Neftel, A., Kincaid, C., Bühler, M., Amon, B., & VanderZaag, A. (2020). Ammonia and greenhouse gas emissions from slurry storage - A review. *Agriculture, Ecosystems and Environment*, *300*(April). https://doi.org/10.1016/j.agee.2020.106963

Loyon, L., Guiziou, F., Picard, S., & Saint-Cast, P. (2016). Farm-Scale Applicability of Three Covers (Peat, Polystyrene Balls and Synthetic Sheet Roof) to Reduce Ammonia Emissions from Pig Slurry Storage. *Agricultural*

Sciences, *07*(06), 396–406. https://doi.org/10.4236/as.2016.76041

Maldaner, L., Wagner-Riddle, C., VanderZaag, A. C., Gordon, R., & Duke, C. (2018). Methane emissions from storage of digestate at a dairy manure biogas facility. *Agricultural and Forest Meteorology*, *258*(June 2017), 96–107. https://doi.org/10.1016/j.agrformet.2017.12.184

Matacchiera, F., Manes, C., Beaven, R. P., Rees-white, T. C., Boano, F., Mønster, J., & Scheutz, C. (2018). AERMOD as a Gaussian dispersion model for planning tracer gas dispersion tests for landfill methane emission quantification. *Waste Management*. https://doi.org/10.1016/j.wasman.2018.02.007

Mønster, J., Samuelsson, J., Kjeldsen, P., Rella, C., & Scheutz, C. (2014). Quantifying methane emission from fugitive sources by combining tracer release and downwind measurements - A sensitivity analysis based on multiple field surveys. *Waste Management*, *34*(8), 1416–1428. https://doi.org/10.1016/j.wasman.2014.03.025

Mønster, Jacob, Kjeldsen, P., & Scheutz, C. (2019). Methodologies for measuring fugitive methane emissions from landfills – A review. *Waste Management*, *87*, 835–859. https://doi.org/10.1016/j.wasman.2018.12.047

Nielsen, O.-K., Plejdrup, M. S., Winther, M., Nielsen, M., Gyldenkærne, S., Mikkelsen, M. H., … Hansen, M. G. (2021). *Denmark's national inventory report 2021. Emission Inventories 1990-2019 - Submitted under the United Nations Framework Convention on Climate Change and the Kyoto Protocol*. Retrieved from http://dce2.au.dk/pub/SR189.pdf

Roscioli, J. R., Yacovitch, T. I., Floerchinger, C., Mitchell, A. L., Tkacik, D. S., Subramanian, R., … Marchese, A. J. (2015). Measurements of methane emissions from natural gas gathering facilities and processing plants: Measurement methods. *Atmospheric Measurement Techniques*, *8*(5), 2017–2035. https://doi.org/10.5194/amt-8-2017-2015

Scheutz, C., & Kjeldsen, P. (2019). Guidelines for landfill gas emission monitoring using the tracer gas dispersion method. *Waste Management*, *85*, 351–360. https://doi.org/10.1016/j.wasman.2018.12.048

Sneath, R. W., Beline, F., Hilhorst, M. A., & Peu, P. (2006). Monitoring GHG from manure stores on organic and conventional dairy farms. *Agriculture, Ecosystems and Environment*, *112*(2–3), 122–128. https://doi.org/10.1016/j.agee.2005.08.020

Taylor, D. M., Chow, F. K., Delkash, M., & Imhoff, P. T. (2016). Numerical simulations to asses the tracer dilution method for measurement of landfil methane emissions. *Waste Management*.

Tedeschi, L. O., Abdalla, A. L., Álvarez, C., Anuga, S. W., Arango, J., Beauchemin, K. A., … Kebreab, E. (2022). Quantification of methane emitted by ruminants: A review of methods. *Journal of Animal Science*, (June), 1–22. https://doi.org/10.1093/jas/skac197

Vechi, N. T., Jensen, N. S., & Scheutz, C. (2022). Methane emissions from five Danish pig farms: Mitigation strategies and inventory estimated emissions. *Journal of Environmental Management*, *317*(May), 115319. https://doi.org/10.1016/j.jenvman.2022.115319

Vechi, N. T., Mellqvist, J., & Scheutz, C. (2022). Quantification of methane emissions from cattle farms, using the tracer gas dispersion method. *Agriculture, Ecosystems and Environment*, *330*(February), 107885. https://doi.org/10.1016/j.agee.2022.107885

Wagner-Riddle, C., Park, K. H., & Thurtell, G. W. (2006). A micrometeorological mass balance approach for greenhouse gas flux measurements from stored animal manure. *Agricultural and Forest Meteorology*, *136*(3–4), 175–187. https://doi.org/10.1016/j.agrformet.2004.11.014

Westermann, P. (1996). Temperature regulation of anaerobic degradation of organic matter. *World Journal of Microbiology and Biotechnology*, *12*(5), 497–503. https://doi.org/10.1007/BF00419463

Supplementary Material

Measurements methane emissions from manure tanks using a stationary tracer gas dispersion method

Nathalia T. Vechi[1,], Charlotte Scheutz[1]

[1]Department of Environmental and Resource Engineering, Technical University of Denmark, Denmark

Fig. S1. Air concentration measurements performed downwind two manure tanks using a mobile analytical platform. The read plume represents the methane (CH_4) plume and the yellow the tracer gas (C_2H_2) plume. The icons show the location of stationary samplings in the plume. Map source: Google Earth ©

Fig. S2. Tracer gas released from the middle of the manure tank. The tube is attached to a bottle, which floats on the manure surface.

Fig. S3. Dual tracer gas release experiment. Purple line represents measurement transect 1, the green markers transect 2 and the red, transect 3. The yellow triangles represent the location of the C_2H_2 release, and the blue the N_2O release. Map source: Google Earth ©

Table S1. Quality assessment of measured data using the stationary tracer dispersion method for quantification of manure tank emissions. The data marked in red corresponds to score 1 data, which was rejected, the green marked data corresponds to score 2 and 3. In total, 18 measurement campaigns were carried out consisting of in total 54 plume sampling repetitions each of 30 minutes.

Campaign-Sampling	R^2	Plume representation	Plume coverage	Score		R^2	Plume representation	Plume coverage	Score
#1-B1	37%	Yes	32%	1	#12-B1	89%	No	49%	1
#1-B2	94%	no	16%	1	#12-B2	22%	Yes	50%	2
#2-B1	67%	yes	88%	3	#12-B3	43%	Yes	68%	2
#2-B2	21%	yes	50%	2	#12-B4	2%	No	66%	1
#2-B3	1%	yes	51%	2	#13-B1	22%	Yes	56%	2
#3-B1	24%	Yes	69%	2	#13-B2	59%	Yes	61%	3
#3-B2	76%	yes	10%	2	#13-B3	62%	Yes	66%	3
#3-B3	97%	no	51%	2	#14-B1	83%	Yes	25%	2
#3-B4	63%	yes	65%	3	#14-B2	69%	Yes	16%	2
#4-B1	0%	yes	20%	1	#14-B3	97%	Yes	64%	3
#4-B2	94%	yes	69%	3	#15-B1	90%	Yes	84%	3
#4-B3	70%	yes	37%	2	#15-B2	67%	Yes	78%	3
#4-B4	0%	Yes	10%	1	#16-B1	93%	No	25%	1
#5-B1	76%	Yes	90%	3	#16-B2	91%	Yes	87%	3
#5-B2	74%	yes	98%	3	#16-B3	97%	no	21%	1
#5-B3	91%	no	10%	1	#17-B1	67%	no	50%	2
#6-B1	90%	Yes	84%	3	#17-B2	1%	Yes	50%	2
#6-B2	37%	Yes	68%	2	#18-B1	50%	Yes	69%	3
#6-B3	88%	yes	71%	3	#18-B2	6%	Yes	50%	2
#6-B4	94%	yes	84%	3					
#7-B1	2%	yes	46%	1					
#7-B2	44%	Yes	95%	2					
#7-B3	92%	Yes	95%	3					
#8-B1	94%	Yes	54%	3					
#8-B2	93%	Yes	32%	2					
#8-B3	92%	No	50%	2					
#9-B1	2%	Yes	60%	2					
#9-B2	36%	Yes	56%	2					
#9-B3	21%	Yes	76%	2					
#10-B1	87%	Yes	90%	3					
#10-B2	80%	Yes	38%	2					
#10-B3	31%	Yes	10%	1					
#11-B1	68%	Yes	52%	3					
#11-B2	100%	No	10%	1					
#11-B3	1%	No	28%	0					

IV

Methane emission rates averaged over a year from ten farm-scale manure storage tanks.

Vechi, N.T., Falk, J.M., Fredenslund, A.M., Edjabou, M.E., & Scheutz, C.

Submitted to Journal of Environmental Management

Methane emission rates averaged over a year from ten farm-scale manure storage tanks

Nathalia T. Vechi[1], Julie M. Falk[1], Anders M. Fredenslund[1], Maklawe E. Edjabou[1], Charlotte Scheutz[1].

[1]Department of Environmental and Resource Engineering, Technical University of Denmark, Kgs. Lyngby, Denmark.

Correspondence to: Nathalia T. Vechi (navei@dtu.dk)

Abstract

Methane (CH_4) emissions from animal manure stored in outdoor tanks are difficult to predict because of several influential factors. In this study, the tracer gas dispersion method (TDM) was used to quantify CH_4 emissions from ten manure storage tanks, along with the collection of supporting information, in order to further identify emission drivers. The dataset included two tanks storing dairy cattle manure, six holding pig manure and two with digestate from manure-based biogas plants. CH_4 emissions from the tanks were measured six to 14 times, covering a whole year. Emissions varied from 0.02 to 14.30 kg/h, or when normalised by the volume of manure stored, they varied from 0.05 to 11 g/m^3/h. Annual average CH_4 emission rates varied greatly between the tanks, ranging from 0.20 to 2.75 g/m^3/h. The averaged manure temperature for all tanks varied from 10.6 to 16.4 °C, which was higher than reported in a previous Danish study. Volatile solids (VS) concentration was higher for cattle manure (3.1 and 4.4%) than pig manure (1.0 to 3.6%). CH_4 emissions were positively correlated with manure temperature, whereas this was not the case for VS manure content. Annual average CH_4 emissions normalised to manure volume were higher for pig than for cattle manure (a factor of 2.5), which was greater than digested manure emissions (a factor of 1.2). For the pig manure storage tanks, CH_4 emissions were higher for covered tanks than for not-covered tanks (by a factor of 2.3). In this study, manure storage tanks showed a large disparity in emissions, driven not only by physical factors, but also by farm management practices.

Graphical abstract

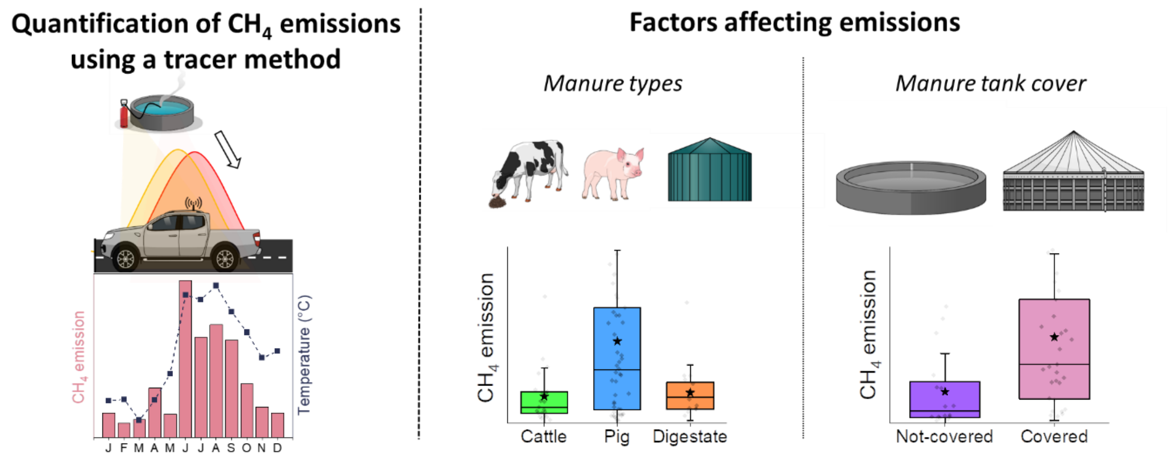

1. Introduction

The recently released sixth International Panel for Climate Change (IPCC) assessment report highlighted the importance of reducing methane (CH_4) emissions in order to lower peak warming caused by greenhouse gases (GHG) accumulation over the coming years. Ultimately, CH_4 contributes to 30% of global warming and has a relatively short lifetime in the atmosphere; therefore, the impacts resulting from its reduction can be seen sooner than for carbon dioxide (CO_2) mitigation (IPCC, 2022).

Agriculture is a significant source of CH_4 emissions, and about 4.7% of total anthropogenic CH_4 discharges come from manure degradation (FAO, 2022; United Nations Environment Programme and Climate and Clean Air Coalition, 2021). Liquid manure, or slurry, which is manure with a lower dry matter content (<12%) (Sommer et al., 2013), can be stored in anaerobic lagoons or concrete tanks. In many farms in northern Europe and North America, slurry is stored in concrete tanks, holding the material until it is ready for application on crop fields. Many factors can affect CH_4 production and emissions, for instance volatile solids (Maldaner et al., 2018), total ammonia nitrogen (Dalby et al., 2021), temperature (Husted, 1994), wind speed (Leytem et al., 2017), type of storage (Kupper et al., 2020) and manure removal efficiency when emptying the storage tank (Baldé et al., 2016b). These factors influence the manure's microbiological composition and activity, thereby affecting CH_4 production and emissions.

Moreover, to estimate annual CH_4 emissions from manure storage, the IPCC inventory schemes have adopted simple models to account for annual emissions (IPCC, 2019), but when used in short-term studies, they show limitations in terms of capturing these emissions (Baldé et al., 2016a; Baral et al., 2018; Vechi et al., 2022a). To support model improvements, emission rates representing farm-scale manure storage tanks must also be acquired. Kupper et al. (2020) comprehensively analysed a number of studies investigating gaseous emissions from manure tanks, highlighting the necessity of manure tank measurements, on the farm scale, using non-intrusive methods, covering different seasons of the year and collecting supporting data related to farm operations and manure characteristics (Kupper et al., 2020). Additionally, they pointed out the need to investigate experimental biases, since the methods applied in the studies had different limitations, which might partially explain the variability of emission rates (Kupper et al., 2020).

Manure-based biogas is considered climate-neutral, as it substitutes the use of fossil fuels. Additionally, the storage of digested manure is considered to reduce

CH_4 emissions in comparison to storing raw manure (IPCC, 2019; Nielsen et al., 2021). CH_4 emissions from the full-scale storage of digested manure, however, have only been the focus of a few studies (Baldé et al., 2016c; Maldaner et al., 2018; Rodhe et al., 2015). At many farms (24% pig and 10% dairy) in Denmark, manure storage tanks are covered with a fixed PVC tent to mitigate NH_3 emissions (Data from 2018) (Mikkelsen and Albrektsen, 2020), which is a well-documented NH_3 emission reduction strategy. However, it is unclear how these tent covers affect CH_4 generation and emissions.

The tracer gas dispersion method (TDM) has been used to measure CH_4 emissions across entire farms (Arndt et al., 2018; Vechi et al., 2022a, 2022b). It is a non-intrusive method and is well documented in the literature and recognised by its precision. This study used the TDM to quantify discrete emissions from ten manure tanks over a whole year in Danish management conditions. The aim was twofold: first, to obtain and compare CH_4 emission rates from manure tanks with different management systems using the TDM, and second, to investigate factors driving CH_4 emissions during manure storage at the studied tanks. The novelty lies in quantifying several farm-scale manure tanks, using the same data collection and emission measuring methodology, including tanks storing pig and cattle raw and digested manure. Additionally, the effect of the storage tank cover on CH_4 emissions from manure has been limited in the literature.

2. Methods

2.1. Site description

CH_4 emission rates were quantified at ten outdoor storage tanks, an overview of which can be found in Table 1. The ten manure tanks stored manure with different characteristics: two tanks stored dairy cattle manure (CN1, CN2), six contained pig manure (PN1, PN2, PC1, PC2, PC2, PC4) and, finally, two stored digestate from centralised biogas plants (DC1, DN1) primarily fed with livestock manure (Table 1).

Regarding the two tanks receiving cattle manure, they were both located at organic dairy farms, meaning that from mid-April to the end of October, milk cows were grassing for six hours during the day. CN2 was the farm’s primary storage tank, while CN1 was a secondary tank that stored manure when the primary tank was full. The amount of stored manure was low during the summer because cows were grazed for part of the day, and the collected manure was also more frequently applied to the fields. Furthermore, manure levels increased towards autumn and reached total capacity in winter.

Regarding the tanks storing pig manure, one of them was located at a breeding farm (PN1, sows and piglets), while the others were located at growing farms (piglets and fattening pigs). Two farms removed manure from the animal barn every week (PN2, PC2). The manure was first transferred to a small temporary tank and later to the larger tank PC2, while in the site PN2 manure was sent directly to tank. Moreover, PC3 removed manure from the animals' barn every week during summer because water was used to cool the barn, resulting in more rapid filling of the manure storage unit under the house's floor, thereby meaning more frequent emptying during this season. During the rest of the year, manure was removed every second week. For PN1, PC1 and PC4, manure was removed from the animals' barns once a month.

In Denmark, many centralised biogas plants operate in agreement with farmers by collecting raw manure from farms and providing a similar amount of digestate back to the farm to be deposited in outdoor storage tanks. This was the case for tanks DC1 and DN1. Tank DC1 held digestate from a biogas plant with a high retention time (approximately 90 days). Feedstock for the biogas plant consisted of a mix of pig, cattle and chicken manure, deep litter, beets and straw. The second biogas tank (DN1) stored digestate from a biogas plant with a short retention time (34 days). The feedstock used in this biogas plant was animal manure (pig and dairy), industrial waste and energy crops.

Of the ten tanks, five had a tent cover (PC1, PC2, PC3, PC4 and DC1). In our study, "covers" refer to fixed tent structures made of PVC with service hatches to mix and remove manure. The tent structure is fixed to the wall of the concrete tank by elastic straps, and it is not gas tight. Tank covers are a requirement for manure storage tanks in Denmark to reduce ammonia (NH_3) emissions, which can be fulfilled by either a fixed tent cover or a natural crust (Ministeriet for Fødevarer Landbrug og Fiskeri, 2021). Of the tanks without a cover (CN1, CN2, PN1, PN2, DN1), some occasionally had a natural crust.

Half of the farms had two manure tanks positioned very close to each other (Table 1), so discriminating between their emissions was not feasible. In these cases, the two tanks were measured as one, and supporting information (manure temperature, volume, and VS) was taken from both tanks. The sizes of the tanks also varied, with the smallest having a storage capacity of only 800 m^3 and the largest 7200 m^3.

Table 1: Farms characteristics

Tank[a]	Manure type	Cover	Animal (number)	Tank storage capacity (volume m^3)	Tanks surface area (m^2)
CN1	Cattle	No	Dairy cows (220)	T1 (1300)	315
CN2	Cattle	No	Dairy cows (700)	T1 (5000) T2 (3500)	834
PN1	Pig	No	Sows (710) and piglets (4000)	T1 (1640) T2 (3000)	560
PN2	Pig	No	Fattening pigs (1500)	T1 (2200) T2 (2200)	490
PC1	Pig	Yes	Fattening pigs (2500)	T1 (4400)	804
PC2	Pig	Yes	Fattening pigs (5000)	T1 (5500)	960
PC3	Pig	Yes	Fattening pigs (1800) and piglets (1125)	T1 (4300)	855
PC4	Pig	Yes	Fattening pigs (2300) and piglets (1300)	T1 (5000)	615
DC1	Digestate – high HRT	Yes	NA	T1 (7200) T2 (3000)	860
DN1	Digestate – low HRT	No	NA	T1 (800) T2 (3100)	465

[a] The tanks' names were giving as follows: C for cattle, P for pigs and D for digestate as the first letter. Further, N was given to not-covered tanks and C to covered tanks. The number follows the number of tanks with the same manure type and cover. In general, pig farms added manure to their storage tank every month, with the exception of PN2 and PC2, which removed manure from the animal barn every week. Additionally, PC3 removed manure from the house weekly during the summer months and every second week for the rest of the year.

2.2. Tracer gas dispersion method (TDM)

The TDM was used to measure CH_4 emissions from the storage tanks. The method uses a tracer gas with a known release rate (Q_{tr}) to simulate target source emissions (E_{tg}) and quantifies discrete emissions during the short tracer release period (1 – 3 hours). The tracer gas should have a long life in the atmosphere and therefore disperse in a similar way to the measured gas. Ground plume concentrations of tracer and target gases are measured downwind from the source at the furthest measurable distance, in order to allow for a proper mixture between gases (Galle et al., 2001; Scheutz et al., 2011). The known tracer release rate is combined with the target-to-tracer ratio to estimate target emissions, as shown in Eq. 1.

$$E_{tg} = Q_{tr} \cdot \frac{\int_{x1}^{x2} (C_{tg} - C_{tg,bg})dx}{\int_{x1}^{x2} (C_{tr} - C_{tr,bg})dx} \cdot \frac{MW_{tg}}{MW_{tr}} \quad (1)$$

where C_{tg} and C_{tr} are the target and tracer gas concentrations in ppb, respectively. $C_{tg,bg}$ and $C_{tr,bg}$ are the background concentrations of the respective gases. Furthermore, x indicates the distance across the plume, and MW (g/mol) is the molar weight of the correspondent gases.

In this study, acetylene (C_2H_2) was used as the tracer gas, released by calibrated flowmeters to ensure a constant flow rate. In addition, cylinders were weighted before and after release, to confirm the release rates from flowmeter readings. The tracer gas was released directly either from bottles located next to the tanks or from the middle of the tank, using an extended tube connected to a floating material placed on the surface of the manure inside the tank. Gas concentrations were measure by a high precision instrument using the principle of cavity ring-down spectroscopy (CRDS) from Picarro Inc. (California, USA). The main instrument was the G2203 model, which measures both C_2H_2 and CH_4 (precision (3σ) of 2.14 and 0.34 ppb for CH_4 and C_2H_2). For a few campaigns where the G2203 was not available, two instruments were combined, namely a G1301 measuring CH_4 (precision (3σ) of 2.5 ppb) and a custom-made CRDS instrument measuring C_2H_2 (precision (3σ) of 3.4 ppb).

The TDM was applied in three approaches. In the first approach (1), the instruments were placed in a car and driven across the plume to measure concentrations. The tracer-to-target ratio was calculated by integrating the entire measured plume (Eq. 1) (Fredenslund et al., 2019) – identified as "M" in Table 2 (Supplementary Information (SI), Fig. S1). When driving across the plume was not feasible, two stationary approaches were used instead (Fredenslund et al., 2010; Scheutz and Kjeldsen, 2019). In the second (2), a single-point stationary TDM measured concentrations at a fixed position without driving across the plume (Fredenslund et al., 2010). This approach was used when the measurement road was not long enough to cross the whole plume. The ratio was calculated using a scatter plot of tracer versus target gas concentrations. In Table 2, the method corresponds to "S". Finally, in the third approach, (3) another stationary TDM approach was used, when roads were unavailable, in the form of gas sampling bags positioned in a field covering the CH_4 plume from the tank. Five to ten points were sampled within the plume, and the ratio was calculated as the integrated area of the measured plume. Sampling took an average of 30 minutes and was repeated two to four times. This method corresponds to "B" in Table 2.

Table 2: Information on manure tank measurements

Tanks	Number of measurements	Method[a]	Number of VS samples	Measurement period	Average of days in between measurements
CN1	7	M,S	3	Oct/20 to Sep/21	52 (4 - 93)
CN2	14	M,B	3	Mar/20 to May/21	26 (2 - 49)
PN1	8	M	3	Oct/20 to Oct/21	46(2 - 77)
PN2	8	M,S	2	Feb/21 to Nov/22	46 (11 – 81)
PC1	8	M	2	Jul/21 to Jul/22	46 (16 – 69)
PC2	7	M	2	May/21 to Jul/22	52 (6 – 142)
PC3	12	M,S	3	Feb/21 to Dec/22	30 (4 – 89)
PC4	6	M	0	Feb/21 to Jun/22	60 (4 – 118)
DC1	8	M	3	Oct/20 to Oct/21	46 (9 - 84)
DN1	8	M, S	3	Nov/20 to Oct/21	46 (16 - 83)

[a] M – Mobile TDM, the plume concentration was measured by driving across the plume, S – Stationary single-point TDM, whereby plume concentrations were measured at a single point over ~30 min by parking the instrumented vehicle downwind in the middle of the plume. B – Stationary bag TDM, where plume concentrations were measured by placing sampling bags (5 to 10 bags) across the plume. This approach was used when roads were not available.

2.3. Measurement campaigns

A minimum of six measurement campaigns were executed to obtain annual average emission rates. They were performed as equidistant as possible according to the measurement possibilities, covering every season (SI, Table S1). Most of the tanks were measured more than six times, and two were measured more than ten times. Data sampling lasted from 30 min to 4 hours, and they were done mostly during daytime. An emission measurement sampling simulation was performed using data from CN2 and PC3, i.e., the tanks with the largest number of measurements (SI, Fig. S2). When equidistant, six samples already produced an error smaller than ±10% on annual average emission rates (SI, Fig. S3).

Emission quantifications were performed across different calendar years. Five tanks were measured between 2020 and 2021, whilst the others ranged from 2021 to 2022. Table 2 shows the minimum, maximum and average days in between measurements for each studied site. The tanks with a large gap between measurements were PC2 and PC4, with no measurements for more than 110 days (~ 4 months). At these two sites, measurements were resumed before planned, due to changes to the management.

2.4. Characterisation of manure and storage tanks

Emission quantification was supported by collecting additional information such as manure temperature, manure volume and dry matter (DM) and volatile solids (VS) content. Manure temperature was measured using a temperature probe inserted approximately one metre deep into the manure. However, when a lower volume of manure was stored, the probe was inserted at a minimum of 20 cm. Manure temperature information was recorded during most campaigns, except for tank CN2, for which the temperature was not measured during summer. Atmospheric temperature was considered as the daily average of the three days' prior measurements, and the temperature values used were obtained from nearby Danish Meteorological Institute (DMI) stations. The volume of stored manure was determined by measuring the manure depth for each campaign.

Manure samples were taken on three occasions from six tanks (CN1, CN2, PN1, PC3, DC1, DN1) and twice from four tanks (PC1, PC2, and PN2); no samples were taken from PC4. The manure was collected using a custom-made device, namely a pipe with a diameter of 10 cm and 4 metres in height, which therefore collected a column of manure, thus avoiding sampling bias due to manure stratification. The bottom of the device was locked by a rubber stopper pulled by a string (Bernstad et al., 2013). For tanks without a cover, sampling was performed at five points around the tank. For covered tanks, sampling was done twice at three service hatches, i.e. a total of six samples. The collected manure was mixed into a composite sample. A 500 mL sub-sample was collected while stirring the composite sample and stored in a plastic bottle, which was then frozen until analysis. Samples were analysed for DM and VS. DM was obtained by drying approximately 10g of the manure, in triplicate, in a 105 ºC oven for 24 hours. Furthermore, the dried samples were combusted in a 550 ºC oven and weighed in order to calculate the VS.

2.5. Evaluation of diurnal variation – continuous setup

Annual emission variability was captured by measuring emissions several times over a whole year, thereby distributing the measurements over the seasons. However, CH_4 emissions might vary throughout the day. Significant diurnal variations have been observed in summer and autumn by Maldaner et al. (2018) and VanderZaag et al. (2014), while Baldé et al. (2016c) reported fewer significant deviations. As these studies were carried out in open tanks, an extra experiment – in tank PC3– was devised for the present study to verify diurnal variations in covered tanks. For this experiment, the tent cover was made even more airtight than one would ordinarily find in typically covered tanks, and a ventilation pump (Grundfos MGE 037, H50) was installed for suction with a pump rate of 100 m^3/h (pumping maintains a slight negative pressure (0-10 Pa) inside the headspace to minimise gas leaks from around the tent cover, in which case most of the CH_4 is pumped out). Although the quantification did not reflect total emissions from the tank, because less than 100 % of the gas produced was extracted by the pump, emission patterns should still be equivalent for the hourly variation comparison. Additionally, the flow rate was measured using a Proline Prosonic B200 (Endress + Hauser), which also measures gas temperature in the gas stream out. CH_4 concentration was measured using an IR Biogas5000 (Geotech, Warwickshire, UK). Furthermore, emissions were estimated by combining information on the CH_4 concentrations and the pump flow. Data was filtered to remove any days where the cover was opened to remove manure, or where an instrument was unavailable; therefore, the analyses only included 103 days of the year, namely 21 in winter, 26 in spring, 11 in summer and 45 in autumn.

2.6. Data analysis

Annual average emission rates (E_{annual}) were calculated by weighing emission rates according to the number of days between measurements (Eq. 2).

$$E_{annual} = \sum_{i=1}^{n} w_i \, . \, x_i , \quad w_i = \frac{(DOY_{(n-1)} - DOY_n)}{365} \tag{2}$$

where w_i is the weight of the emissions interval, DOY is the day of the year and x_i is measured emissions normalised by the volume of manure (g/m^3/h). The data was assembled over one calendar year, because no management changes at the farms were observed during the measurement campaign.

To evaluate the effect of different emission drivers, data analysis was carried out using the statistical programming software R (R Core Team, 2022). Covariance analysis was chosen for the investigation because the response variable was continuous (emission rates) while the explanatory variables were both continuous (e.g. manure temperature) and categorical (e.g. manure type) (Crawley, 2005). We investigated the effect of manure temperature (°C), wind speed (m/s), tank-filled capacity (%), VS (tons), tank cover (yes/no) and manure type (cattle, pig or digested) on CH_4 emissions. Assumptions underlying the covariance analysis were tested. Additionally, a permutation test was used to confirm the significance of the factor "cover," due to the presence of many outliers; this type of test evaluates significant differences between two datasets, and it is less sensitive to outliers (Hayes, 1996). In addition, the same test was used to evaluate manure temperature differences in the covered and not-covered tanks.

3. Results and discussions

3.1. Manure characteristics and environmental factors

The annual average manure temperature was 13.8 ± 2.2 ºC (Table 3, all tanks except CN2 and PC4), which was about 4.4 ºC higher than the atmospheric temperature. The average annual manure temperatures of cattle, pig and digested manure were 13.3 ºC, 12.8 ± 1.7 ºC and 16.4 ± 0.1 ºC, respectively. In general, average manure temperatures were higher than those found in other Danish and Swedish studies; for example, Husted (1994) measured the mean annual manure temperature for Danish pig and cattle manure storage tanks (not covered) at 11.2 ºC, whilst a Swedish study found temperature averages of 7.9 and 8.2 ºC for pig manure in pilot-scale storage tanks (Rodhe et al., 2012), 8.9 and 10.4 ºC for cattle manure and 11.1 and 13.5 ºC for digested manure in farm-scale tanks (Rodhe et al., 2015). According to Danish GHG inventory reporting, the annual average manure temperature should be approximately 10 ºC, which sits at the lower end of the measured manure temperatures in our study.

Table 3: Manure characteristics and manure volume parameters. Average corresponds to the weighted annual average.

Tank	Manure temperature (ºC)	Atmospheric temperature (ºC)[a]	DM (%)	VS (%)	Manure volume (m^3)
CN1	13.3 (7.4 – 23.4)	8.4 (-3.9 – 18.4)	4.2 (3.6 – 5.2)	3.1 (2.6 – 4.0)	540 (170 – 1300)
CN2	10.3 (6 – 13)[b]	8.8 (0.2 – 17.0)	8.6 (6.9 – 9.2)	4.4 (4.0 – 4.7)	4520 (2030 – 7630)
PN1	14.1 (8.9 – 19.4)	8.4 (-2 – 18.6)	1.8 (1.6 – 2.0)	1.1 (0.9 – 1.3)	2460 (1050 – 3950)
PN2	10.6 (1.9 – 19.9)	9.4 (-3 – 21.5)	4.7 (2.9 – 4.9)	3.5 (1.9 – 3.6)	1380 (550 – 2150)
PC1	14.4 (8 – 21.4)	9.4 (1.3 – 21.3)	4.2 (3.7 – 5.2)	3.0 (2.6 – 3.7)	2840 (1500 – 4010)
PC2	11.3 (5.8 – 16.4)	10.2 (4.5 – 21.3)	5.6 (4.0 – 8.4)	3.4 (2.4 – 5.3)	2720 (800 – 5500)
PC3	13.5 (5.4 – 20.7)	9.5 (-3.8 – 21.4)	2.1 (1.7 – 2.2)	1.2 (1 – 1.3)	2850 (600 – 4290)
PC4	14.7 (2.4 – 20.7)[b]	7.3 (-2.6 – 15.3)	-	-	1530 (200 – 3050)

DC1	16.4 (9.4 – 34.2)	8.3 (-3.0 – 15.9)	3.6 (3.5 – 4.0)	1.9 (1.8 – 2.3)	5280 (2580 – 9690)
DN1	16.7 (14 – 22.8)	11.3 (6.2 – 17.8)	4.4 (4.0 – 5.2)	3.0 (2.7 – 3.6)	2050 (1150 – 3820)
Avg ± Std dev.	13.8 ± 2.2[c]	9.4 ± 1.0	4.4 ± 2.0	2.7 ± 1.1	2620 ± 1420

[a] Annual temperatures in 2020 were around 9.5-10.3, and in 2021 they were 8.4 – 9.3. [b] For CN2, manure temperatures were not measured in summer; therefore, the average temperature is biased toward the lower end. For PC4, it was possible to measure temperatures only half of the time, due to low manure volume; therefore, it does not reflect an annual average. [c] CN2 and PC4 were not included in the average calculation.

Differences in temperature between tanks relate to farm management practices, as exemplified by storage tank PC2. After removal from the animal barn, the manure was first stored in a temporary tank (outdoor, not covered, 1350 m^3, 17.9 ± 2.9 ºC), before being transferred to the primary manure storage tank (Table 3). This management practice most likely decreased the temperature of the manure transferred to the primary tank.

Digested manure (DC1 and DN1) average temperatures (~ 16.4 and 16.7 ºC) were considerably higher than the average of the other tanks (~ 10.6 – 14.4 ºC) (Table 3). These higher temperatures were the result of the digestate being discharged in a warm state. The higher average temperatures found in digested manure, in comparison to raw manure, are in agreement with another study (Maldaner et al., 2018). The reason for the higher annual temperature in our study when compared to other studies in a similar climate (Danish or Swedish conditions) is unclear, but it might indicate greater microbial activity.

Average annual dry matter (DM) and volatile solids (VS) contents were 4.4% and 2.7%, respectively (Table 3). Average VS content was higher for cattle manure (3.7%) than for pig manure (2.4%), which is comparable to a Danish study stating 1.2% for pig slurry and 4.7% for cattle (Husted, 1994). DM content followed VS content, whereby the latter was 63% of the DM content on average. Our numbers for VS follow, to some extent, the values reported in a review study (Kupper et al., 2020), i.e. an average of 48 g/L for cattle and 37 g/L for pigs, while our numbers were 38.7 and 25.7 g/L, respectively. For the digestate, the plant with a higher retention time (DC1) had lower VS content than the one with a low retention time; however, these values are not comparable to each other or to other raw manure tanks because the substrate used in the biogas plants had different compositions and did not consist of raw pig or cattle manure only.

3.2. Temporal CH_4 emission variations

3.2.1. Seasonal CH_4 emission variations

CH_4 emissions from manure tanks varied significantly throughout the year and were connected to the volume of manure stored and its temperature (SI, Fig. S4). Fig. 1 displays the monthly values for tank stored manure, temperature, CH_4 emission rates in kg/h and emissions normalised by the amount of manure stored in g/m^3/h for all the tanks. On average, the tanks were full at the start of the year, and during spring, they were emptied and the manure was applied to field crops, which is a common practice in Denmark (Fig. 1a). Thereafter, the tanks were slowly filled and reached almost maximum storage capacity at the end of year. At some farms, manure was also removed during summer and autumn. The seasonal trend in manure temperature was somewhat in line with atmospheric temperature (Fig. 1b, grey solid line and black dashed line, respectively), being lower at the beginning and at the end of the year and higher in summer in comparison to atmospheric temperature. In April and May, the temperature of the manure was close to the atmospheric temperature because the volume of stored manure was low. Manure temperature peaked in June and remained elevated until October; thereafter, it slowly decreased again.

CH_4 emission rates varied from 0.01 to 14.3±8.8 kg/h, with lower emissions noted at the beginning of the year, whilst they were higher in summer and autumn, peaking in August (Fig. 1c). Temperature and manure storage period influenced CH_4 emission patterns, in that they caused a hysteresis loop in tank emissions, i.e. when emissions were higher in a cooler period (September, October and November) than in a warmer period (March, April and May) (Cárdenas et al., 2021; Kariyapperuma et al., 2018). A similar emission pattern was observed when normalising emission rates by the volume of stored manure (Fig. 1d). Normalised emissions varied from 0.01 to 11 ± 6.4 g/m^3/h, with emissions peaking in August. The difference between CH_4 emission rates and normalised emission rates is most noteworthy in summer emissions (June and July), where they are closer to August emissions than the rates in kg/h (Fig. 1d). The volume of manure stored in summer is low; however, the temperature is high, thus producing more CH_4. Therefore, when taking into consideration the volume of stored manure, normalised rates are high during the whole summer period (June to September). These seasonal trends confirm an older Danish study, which also identified the highest CH_4 emissions in summer, peaking in August, for both cattle and pig manure (Husted, 1994). In contrast, emissions and manure temperatures were higher in our study. An exception to the general seasonal emission trend was PC3, which had high normalised emissions even in winter (1.2 g/m^3/h) whereas other tanks had normalised emissions close to zero (<0.2 g/m^3/h).

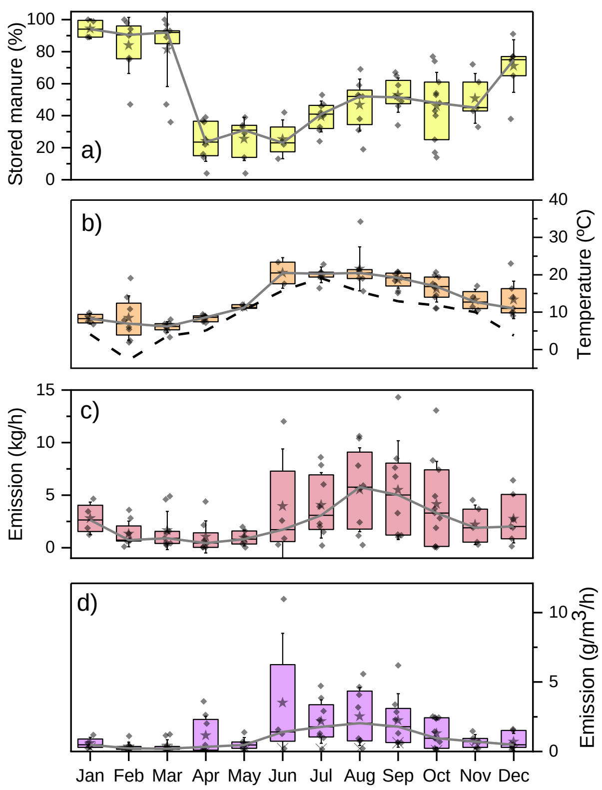

Figure 1: Box plot of monthly values measured in all tanks for: (a) Stored manure given in % of the tank capacity (b) manure temperature (black dashed line corresponds to average atmospheric temperature), (c) CH_4 emissions in kg/h and (d) CH_4 emissions normalised to stored manure volume in g/m^3/h. The grey continuous line shows the median values for the corresponding factors, while the box shows the 75% and 25% distribution intervals. Error bars indicate the standard deviation, and lastly the star symbols indicate mean values. The grey dots are the measured points.

3.2.2. Diurnal CH_4 emission variations

Fig. 3 shows hourly CH_4 emissions normalised to the daily average emissions and grouped by season for tank PC3. No significant diurnal emission pattern for the four seasons was observed. Daily CH_4 emission variations were less than ±20%, which is approximately the method's level of uncertainty (Fredenslund et al., 2019). Other studies have shown daytime emissions about two times higher than nighttime emissions – most likely due to surface heating, which leads to CH_4

bubble bursting (e.g. Maldaner et al., 2018). These studies were carried out on uncovered tanks, and it is likely that the tent cover, on tank PC3, prevented direct surface heating and thereby emission variations, albeit this needs to be explored further. In March only, emissions averaged by month showed a clear diurnal variation up to 30% (SI, Fig. S5, S6, S7 and S8), and these correlated well with the temperature measured at the tank's headspace.

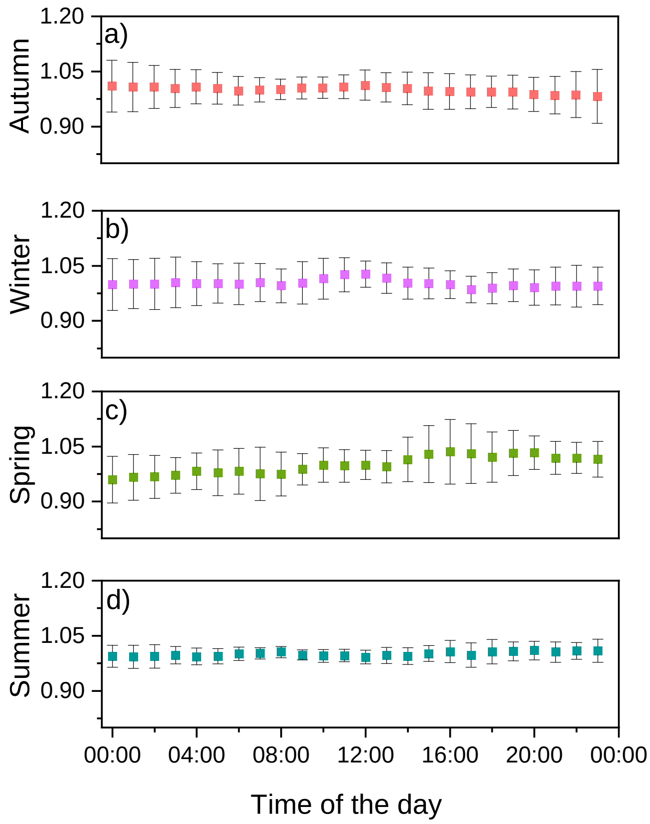

Figure 2: (a) Diurnal pattern divided into different seasons: (a) autumn, (b) winter, (c) spring and (d) summer.

3.3. Annual average manure tank CH_4 emissions

The highest annual average CH_4 emission rates, normalised by the volume of stored manure, were seen for pig manure (1.56 ± 0.93 g/m^3/h) followed by cattle manure (0.63 ± 0.09 g/m^3/h) and then digested manure (0.50 ± 0.02 g/m^3/h) (Fig. 3). Normalising emissions to the VS content of the stored manure resulted in average values of 81.6 ± 85.4 g/tonVS/h, 16.7 ± 6.5 g/tonVS/h and 20.3 ± 5.2 g/tonVS/h for pig, cattle and digestate slurries, respectively (Fig. 3).

Among the pig manure tanks, PN2 had significantly lower emissions than the others (Fig 3), and it was also lower than the cattle manure tanks. Additionally, it had the lowest average temperature and was the only tank that did not have any seasonal variation patterns (SI, Fig. S4) (Table 3). Moreover, manure was removed from the animal barn every week, which would be expected to increase emissions from the tank, due to the frequent discharge of warm and relatively fresh manure. The product used to clean the animal barn should have no effect on emissions. Only one of the two manure storage tanks was used throughout most of the year, and because the other tank remained empty for a long time before filling again, methanogenic activity could have reduced and therefore affected CH_4 production. Nonetheless, more investigation is still needed to explain the unusually low emissions from PN2, such as an analysis of manure microbiological composition and biological CH_4 potential.

Furthermore, while most of the covered pig manure storage units had high emission rates, PC2 had the lowest rates among the covered tanks – most likely due to the storage of manure in a temporary tank prior to transfer to the studied tank, which affected manure temperature and, consequently, emissions. A similar practice was applied at the two cattle manure tanks (CN1 and CN2).

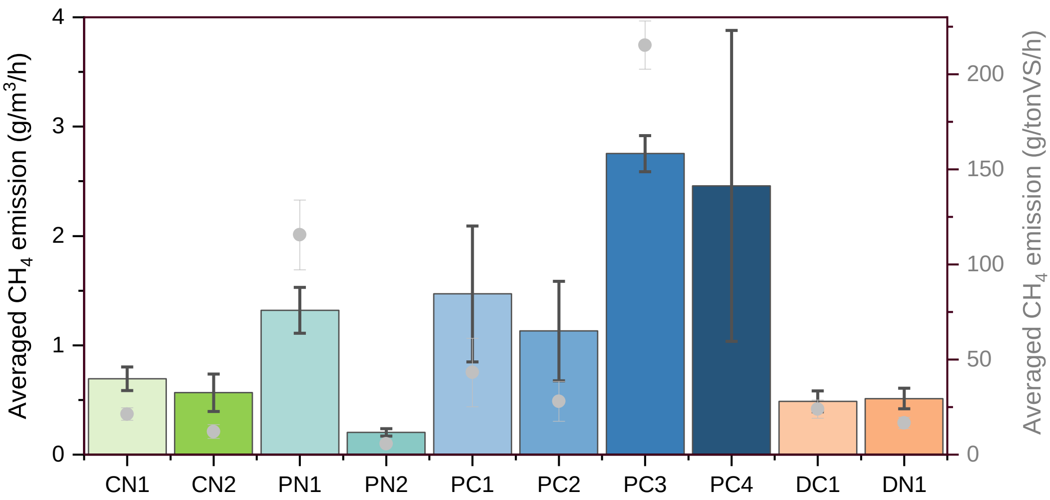

Figure 3: Average annual emission rates for each measured manure tank. The bar plot and the left y-axis show emissions in g/m^3/h, while the right y-axis and the scatter plot in grey show emissions in g/tonVS/h.

A recent review paper summarising CH_4 emissions from manure storage tanks reported in the literature found average CH_4 emissions, weighted according to the measurement period, of 0.58 g/m^3/h for cattle and 0.68 g/m^3/h for pig manure (Kupper et al., 2020). Our average emission rates from dairy cattle manure (Fig. 4) were close to the average value found by Kupper et al. (2020). For pigs, however, our emissions were more towards the high end identified by other studies with consistent seasonal measurements. The study with the highest emissions (Loyon et al., 2007) did not run a measurement campaign for all seasons. The effect of the tank tent cover could explain higher emissions than other studies with no cover, which will be discussed in section 3.4. Additionally, it is relevant to highlight that temperature is a well-known factor affecting CH_4 emissions, and that the relationship is exponential; therefore, the higher the temperature, the greater the impact on the emissions, especially above 15 °C (Sommer et al., 2007). This fact might partly explain why our emissions were higher than established in the literature, since our average manure temperatures were higher than in other studies (Husted, 1994). Finally, for tanks storing digested manure, emission rates were quite close to other studies.

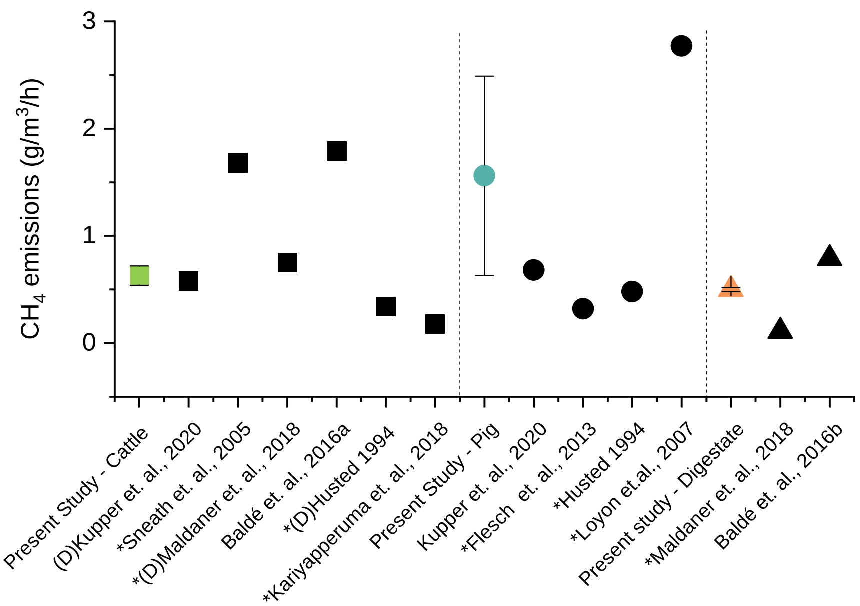

Figure 4: Comparison between measured emissions (g/m^3/h) in the present study and other studies found on the literature. The error bars correspond to the standard deviation of the emissions from the different tanks. The coloured points correspond to emissions from this study, while the black points are taken from the literature. Squares represent cattle manure emissions, circles pig manure emissions and triangles digestate emissions. Studies with a "*" in front of their names represent emission factors that were used in the study by Kupper et al. (2020) to calculate average CH_4 emissions. The letter "D" represent emissions corresponding to dairy raw manure, found in papers measuring more than one type of manure (e.g. dairy and digestate).

CH_4 emission rates normalised by VS content did not follow a similar pattern to the rates normalised by manure volume. Very few farm-scale studies report emission rates on a VS basis. Different from other studies, Maldaner et al. (2018) found an annual average CH_4 emission rate of 8.68 g/tonVS/h for raw dairy manure and 2.97 g/tonVS/h for digested manure, while Baldé et al. (2016c) measured 11.25 g/tonVS/h, also for digested manure. In comparison, our emission rates on a VS basis were higher than the literature for cattle and digested manure. For pigs, no comparable studies were found. Tanks PN1 and PC3 stored manure with a relatively low VS content (~1.2%), while their emissions were relatively high; emissions were especially high for PC3.

3.4. Factors driving CH_4 emissions

A statistical analysis showed that the measured CH_4 emissions were significantly influenced by manure type, manure temperature and tank cover (SI Table S2). Different than expected, amount of VS stored was not a significant variable. Digested manure had the lowest emissions, followed by dairy cattle and pig manure (Figure 5). Moreover, normalised annual CH_4 emission rates in g/m^3/h were higher for pig manure than for dairy cattle and digested manure (Figure 4). Many studies (Husted, 1994; Kupper et al., 2020) have observed higher emissions from pig slurry than from cattle storage tanks. CH_4 emissions are expected to be higher for pig than cattle manure, because the volatile solids in the former are more degradable by methanogens than in the latter (Husted, 1994; Petersen et al., 2016). The result also indicates that emissions from the digestate were lower than raw manure, which has also been observed by Maldaner et al. (2018). In comparison to emissions from raw pig manure, digested manure emissions were 68% lower, while they were 21% lower compared to dairy cattle manure. However, our knowledge about the fractions of pig and dairy manure in biogas plant feedstock is limited for a further comparison.

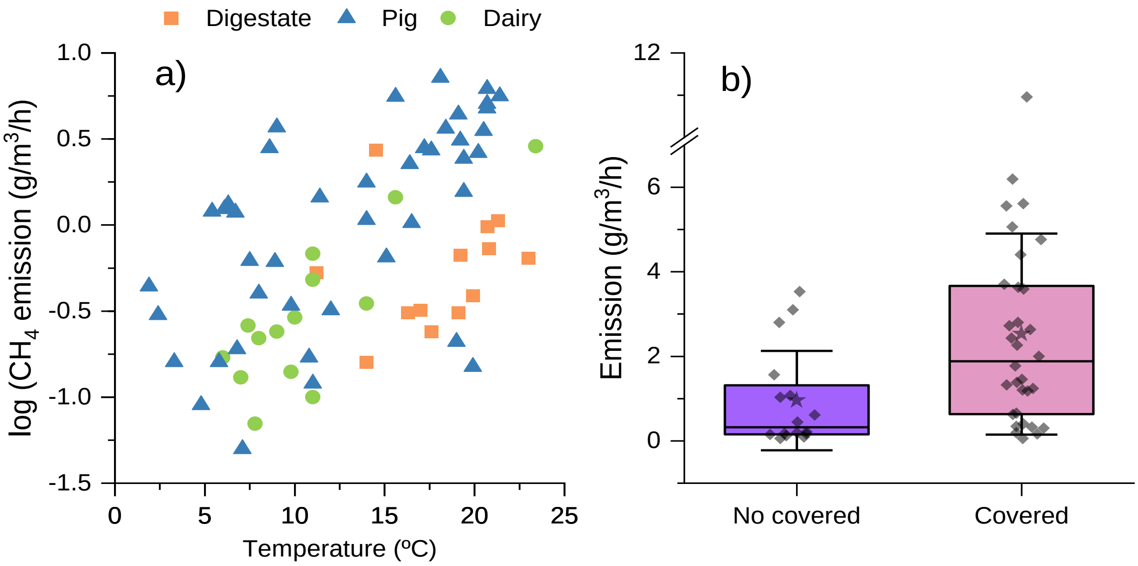

Figure 5: Correlation between different emission drivers. (a) Correlation of the emissions logarithm versus manure temperature for the three different manure types, namely cattle, pig and digested manure. (b) The graph indicates the effect of the cover on the tanks' emissions. Data only for pig manure, to eliminate the manure type effect.

In addition to manure type, the manure storage cover significantly affects emissions, since covered tanks have higher CH_4 emissions in comparison to uncovered pig manure tanks (SI Table S2). This conclusion was confirmed by a permutation test (p-value <0.05) revealing significant differences between the datasets (Fig. 5). This factor might be associated with a higher manure temperature in covered tanks, because the cover better conserves heat, whereas this is not the case for uncovered tanks (Im et al., 2022). Higher manure temperature will consequently lead to more CH_4 emissions (Im et al., 2022). However, the manure temperatures for covered and uncovered tanks were not significantly different in our dataset. A limitation of our temperature measurements is that they were not continuous and instead occurred in different years and at various times of the year. Therefore, instead of looking for differences in absolute manure temperature, it is better to analyse the offset between manure temperature and atmospheric temperature, as it will indicate how much warmer the manure was compared to the external temperature, thus assuming that covered tanks would have a higher offset. By analysing the whole dataset, the covered tanks' offset temperature was slightly higher than for the uncovered tanks, albeit the difference was not significant according to the permutation test (p>0.05) (Fig. 6). Therefore, continuous data on CH_4 emissions and manure temperature is needed to confirm this hypothesis. Moreover, the presence of a natural crust could also play a role because it is only formed on uncovered tanks. Some studies have pointed to a reduction in emissions caused by CH_4 oxidation in the natural crust (Husted, 1994), although a homogeneous crust was not always present for the uncovered tanks, which could have allowed CH_4 to slip through any cracks. To our knowledge, the impact of this type of PVC tent cover on CH_4 emissions is not mentioned in the literature. However, a larger dataset is necessary to gain a better estimate of this impact because, in our study, only two tanks were not covered, while four were covered.

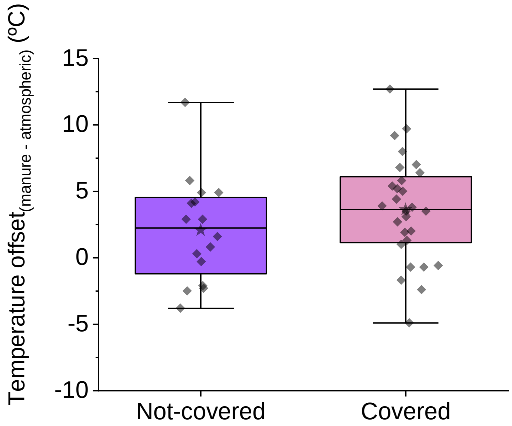

Fig. 6: Temperature offset on covered and uncovered tanks.

4. Conclusion

Methane (CH_4) emissions from ten manure tanks were quantified using the tracer gas dispersion method over a full year. The studied tanks stored dairy cattle, pig and digested manure, and half of them had a tent cover. Measurements were taken a minimum of six times a year, but on average more than eight measurements were applied to most tanks. In addition, data was collected in relation to manure temperature, manure volume, atmospheric conditions and volatile solid manure content. The average manure temperature (raw manure 13 ºC, digested manure 16 ºC) was higher than reported in the literature.

The highest annual average CH_4 emissions were seen for pig manure storage tanks (1.56 ± 0.93 g/m^3/h) followed by cattle manure tanks (0.63 ± 0.09 g/m^3/h) and digested manure tanks (0.50 ± 0.02 g/m^3/h). CH_4 emissions tended to be higher during summer and autumn due the combination of more manure being stored in the tanks and relatively high atmospheric temperatures at these times of the year.

CH_4 emissions tended to be higher from covered tanks; however, more studies should be done to explain if temperature is the reason for such a result. Finally, the variability of the quantified annual emissions reveals the complexity of emission dynamics, with several factors contributing to these variations. Delving into the tank's microbiology could complement and help understand emission variability.

Acknowledgements
This work was funded in part by the Danish Energy Agency (Project – Measurement of methane emissions from biogas plants), the Danish Agricultural Agency (GUPD – Biomet project) and the Danish Environmental Protection Agency (Intermet project). Additionally, the authors wish to thank the farmers for their willingness to participate in the study.

References

Arndt, C., Leytem, A.B., Hristov, A.N., Zavala-Araiza, D., Cativiela, J.P., Conley, S., Daube, C., Faloona, I., Herndon, S.C., 2018. Short-term methane emissions from 2 dairy farms in California estimated by different measurement techniques and US Environmental Protection Agency inventory methodology: A case study. J. Dairy Sci. 101, 11461–11479. https://doi.org/10.3168/jds.2017-13881

Baldé, H., VanderZaag, A.C., Burtt, S., Evans, L., Wagner-Riddle, C., Desjardins, R.L., MacDonald, J.D., 2016a. Measured versus modeled methane emissions from separated liquid dairy manure show large model underestimates. Agric. Ecosyst. Environ. 230, 261–270. https://doi.org/10.1016/j.agee.2016.06.016

Baldé, H., VanderZaag, A.C., Burtt, S.D., Gordon, R.J., Desjardins, R.L., 2016b. Does fall removal of the dairy manure sludge in a storage tank reduce subsequent methane emissions? J. Environ. Qual. 45, 2038. https://doi.org/10.2134/jeq2016.03.0083

Baldé, H., VanderZaag, A.C., Burtt, S.D., Wagner-Riddle, C., Crolla, A., Desjardins, R.L., MacDonald, D.J., 2016c. Methane emissions from digestate at an agricultural biogas plant. Bioresour. Technol. 216, 914–922. https://doi.org/10.1016/j.biortech.2016.06.031

Baral, K.R., Jégo, G., Amon, B., Bol, R., Chantigny, M.H., 2018. Greenhouse gas emissions during storage of manure and digestates : Key role of methane for prediction and mitigation. Agric. Syst. 166, 26–35. https://doi.org/10.1016/j.agsy.2018.07.009

Bernstad, A., Davidsson, å, Tsai, J., Persson, E., Bissmont, M., la Cour Jansen, J., 2013. Tank-connected food waste disposer systems - Current status and potential improvements. Waste Manag. 33, 193–203. https://doi.org/10.1016/j.wasman.2012.09.022

Cárdenas, A., Ammon, C., Schumacher, B., Stinner, W., Herrmann, C., Schneider, M., Weinrich, S., Fischer, P., Amon, T., Amon, B., 2021. Methane emissions from the storage of liquid dairy manure: Influences of season, temperature and storage duration. Waste Manag. 121, 393–402. https://doi.org/10.1016/j.wasman.2020.12.026

Dalby, F.R., Hafner, S.D., Petersen, S.O., VanderZaag, A.C., Habtewold, J., Dunfield, K., Chantigny, M.H., Sommer, S.G., 2021. Understanding methane emission from stored animal manure: A review to guide model development. J. Environ. Qual. 50, 817–835. https://doi.org/10.1002/jeq2.20252

FAO, 2022. GLEAM v3 Dashborad. [WWW Document]. Shiny Apps.

Fredenslund, A.M., Rees-White, T.C., Beaven, R.P., Delre, A., Finlayson, A., Helmore, J., Allen, G., Scheutz, C., 2019. Validation and error assessment of the mobile tracer gas dispersion method for measurement of fugitive emissions from area sources. Waste Manag. 83, 68–78. https://doi.org/10.1016/j.wasman.2018.10.036

Fredenslund, A.M., Scheutz, C., Kjeldsen, P., 2010. Tracer method to measure landfill gas emissions from leachate collection systems. Waste Manag. 30, 2146–2152. https://doi.org/10.1016/j.wasman.2010.03.013

Galle, B.O., Samuelsson, J., Svensson, B.H., Borjesson, G., 2001. Measurements of methane emissions from landfills using a time correlation tracer method based on FTIR absorption spectroscopy. Environ. Sci. Technol. 35, 21–25. https://doi.org/10.1021/es0011008

Husted, S., 1994. Seasonal Variation in Methane Emission from Stored Slurry and Solid Manures. J. Environ. Qual. 23, 585–592. https://doi.org/10.2134/jeq1994.00472425002300030026x

Im, S., Mostafa, A., Lim, K.H., Kim, I., Kim, D.H., 2022. Automatic temperature rise in the manure storage tank increases methane emissions: Worth to cool down! Sci. Total Environ. 823, 153533. https://doi.org/10.1016/j.scitotenv.2022.153533

IPCC, 2022. Climate Change 2020: Impact, Adaptation, and Vulnerability, Contributi. ed. United Kingdom and New York, NY, USA.

IPCC, 2019. 2019 Refinement to the 2006 IPCC Guidlines for National Greenhouse Gas Inventories, Volume 4: Agriculture, forestry and other land use.

Kariyapperuma, K.A., Johannesson, G., Maldaner, L., VanderZaag, A., Gordon, R., Wagner-Riddle, C., 2018. Year-round methane emissions from liquid dairy manure in a cold climate reveal hysteretic pattern. Agric. For. Meteorol. 258, 56–65. https://doi.org/10.1016/j.agrformet.2017.12.185

Kupper, T., Häni, C., Neftel, A., Kincaid, C., Bühler, M., Amon, B., VanderZaag, A., 2020. Ammonia and greenhouse gas emissions from slurry storage - A review. Agric. Ecosyst. Environ. 300. https://doi.org/10.1016/j.agee.2020.106963

Leytem, A.B., Bjorneberg, D.L., Koehn, A.C., Moraes, L.E., Kebreab, E., Dungan, R.S., 2017. Methane emissions from dairy lagoons in the western United States. J. Dairy Sci. 100, 6785–6803. https://doi.org/10.3168/jds.2017-12777

Loyon, L., Guiziou, F., Beline, F., Peu, P., 2007. Gaseous Emissions (NH3, N2O, CH4 and CO2) from the aerobic treatment of piggery slurry-Comparison with a conventional storage system. Biosyst. Eng. 97, 472–480. https://doi.org/10.1016/j.biosystemseng.2007.03.030

Maldaner, L., Wagner-Riddle, C., VanderZaag, A.C., Gordon, R., Duke, C., 2018. Methane emissions from storage of digestate at a dairy manure biogas facility. Agric. For. Meteorol. 258, 96–107. https://doi.org/10.1016/j.agrformet.2017.12.184

Mikkelsen, M.H., Albrektsen, R., 2020. Forbedring af datagrundlaget for opgørelse af ammoniakemissionen fra landbruget.

Ministeriet for Fødevarer Landbrug og Fiskeri, 2021. Bekendtgørelse om miljøregulering af dyrehold og om opbevaring og anvendelse af gødning.

Nielsen, O.-K., Plejdrup, M.S., Winther, M., Nielsen, M., Gyldenkærne, S., Mikkelsen, M.H., Albrektsen, R., Thomsen, M., Hjelgaard, K., Fauser, P., Bruun, H.G., Johanssen, V., Nord-Larsen, T., Vesterdal, L., Stupak, I., Scott-Bentsen, N., Rasmussen, E., Petersen, S.B., Olsen, T.M., Hansen, M.G., 2021. Denmark’s national inventory report 2021. Emission Inventories 1990-2019 - Submitted under the United Nations Framework Convention on Climate Change and the Kyoto Protocol.

Petersen, S.O., Olsen, A.B., Elsgaard, L., Triolo, J.M., Sommer, S.G., 2016. Estimation of methane emissions from slurry pits below pig and cattle confinements. PLoS One 11, 1–16. https://doi.org/10.1371/journal.pone.0160968

Rodhe, L.K.K., Abubaker, J., Ascue, J., Pell, M., Nordberg, åke, 2012. Greenhouse gas emissions from pig slurry during storage and after field application in northern European conditions. Biosyst. Eng. 113, 379–394. https://doi.org/10.1016/j.biosystemseng.2012.09.010

Rodhe, L.K.K., Ascue, J., Willén, A., Persson, B.V., Nordberg, Å., 2015. Greenhouse gas emissions from storage and field application of anaerobically digested and non-digested cattle slurry. Agric. Ecosyst. Environ. 199, 358–368. https://doi.org/10.1016/j.agee.2014.10.004

Scheutz, C., Kjeldsen, P., 2019. Guidelines for landfill gas emission monitoring using the tracer gas dispersion method. Waste Manag. 85, 351–360. https://doi.org/10.1016/j.wasman.2018.12.048

Scheutz, C., Samuelsson, J., Fredenslund, A.M., Kjeldsen, P., 2011. Quantification of multiple methane emission sources at landfills using a double tracer technique. Waste Manag. 31, 1009–1017. https://doi.org/10.1016/j.wasman.2011.01.015

Sommer, S.G., Christensen, M.L., Schmidt, T., Jensen, L.S., 2013. Animal manure recycling: Treatment and management. John Wiley & Sons.

Sommer, S.G., Petersen, S.O., Sørensen, P., Poulsen, H.D., Møller, H.B., 2007. Methane and carbon dioxide emissions and nitrogen turnover during liquid manure storage. Nutr. Cycl. Agroecosystems 78, 27–36. https://doi.org/10.1007/s10705-006-9072-4

United Nations Environment Programme and Climate and Clean Air Coalition, 2021. Global methane assessment: Benefits and costs of mitigating methane emissions. Nairobi.

VanderZaag, A.C., Flesch, T.K., Desjardins, R.L., Baldé, H., Wright, T., 2014. Measuring methane emissions from two dairy farms: Seasonal and manure-management effects. Agric. For. Meteorol. 194, 259–267. https://doi.org/10.1016/j.agrformet.2014.02.003

Vechi, N.T., Jensen, N.S., Scheutz, C., 2022a. Methane emissions from five Danish pig farms: Mitigation strategies and inventory estimated emissions. J. Environ. Manage. 317, 115319. https://doi.org/10.1016/j.jenvman.2022.115319

Vechi, N.T., Mellqvist, J., Scheutz, C., 2022b. Quantification of methane emissions from cattle farms, using the tracer gas dispersion method. Agric. Ecosyst. Environ. 330, 107885. https://doi.org/10.1016/j.agee.2022.107885

Supplementary material

Methane emission rates averaged over a year from ten farm-scale manure storage tanks

Nathalia T. Vechi[1], Julie M. Falk[1], Anders M. Fredenslund[1], Maklawe E. Edjabou[1], Charlotte Scheutz[1].

[1]Department of Environmental and Resource Engineering, Technical University of Denmark, Kgs. Lyngby, Denmark.

Figure S1: Example of measured plumes using the mobile TDM. Blue shadowed areas show the measured tanks, the yellow triangles the position of the tracer gases, and the arrow illustrate the wind direction. Red and yellow plumes are the concentrations of CH_4 and C_2H_2, respectively. In the top-left figure, the two tanks were isolated, while in all the other figures, contributions of CH_4 from the animal house can be seen in the plume. Map source: Google Earth ©

Table S1: Overview about the manure tanks measurements and supplementary information about the tank

Tank	Date	Measurement time	Wind speed (m/s)	Wind direction	Atmospheric temperature (°C)	Manure temperature (°C)	Tank volume (m^3)	TS (%)	VS (%)	Emission (kg/h)	Std. Dev. (kg/h)	Emission ($g/m^3/h$)	Std. Dev. ($g/m^3/h$)
CN1	03-10-2020	1540	9	W	15	14	141	4.0	2.9	0.1	0.0	0.4	0.1
	27-10-2020	1300	6	SSE	11	11	104	4.0	2.9	0.0	0.0	0.1	0.0
	25-12-2020	1135	5	NNW	2	10	885	4.0	2.9	0.1	0.0	0.1	0.0
	09-02-2021	1223	6	NE	-4	8	1218	4.0	2.9	0.1	0.0	0.1	0.0
	16-04-2021	1720	7	N	5	7	126	3.6	2.6	0.0	0.0	0.3	0.1
	29-06-2021	1000	2	NNW	18	23	94	3.6	2.6	0.3	0.0	2.9	0.4
	30-09-2021	1450	8	SW	12	16	692	5.2	4.0	1.0	0.2	1.5	0.2
CN2	04-03-2020	1030	3	W	5	-	7207	9.2	4.7	1.6	0.3	0.2	0.0
	20-05-2020	1200	3	W	11	-	3324	9.2	4.7	1.6	0.2	0.5	0.0
	23-06-2020	1130	3	W	17	-	2031	9.2	4.7	2.6	1.0	1.3	0.5
	13-07-2020	1230	3	W	14	-	2031	9.2	4.7	2.3	0.3	1.1	0.2
	31-08-2020	1500	2	NW	16	-	3201	9.1	4.4	2.4	0.4	0.8	0.1
	02-10-2020	900	3	E	15	-	4063	9.1	4.4	2.8	1.4	0.7	0.4
	05-11-2020	1200	6	WNW	10	-	5202	9.1	4.4	3.7	1.1	0.7	0.2
	02-12-2020	1430	4	ESE	3	11	5515	9.1	4.4	2.7	0.8	0.5	0.2
	10-12-2020	1000	4	ESE	4	10	6550	6.9	4.0	1.9	1.2	0.3	0.2
	03-01-2021	1130	5	ENE	2	9	7608	6.9	4.0	1.9	0.7	0.2	0.1
	17-02-2021	1400	3	NW	0	6	7635	6.9	4.0	1.3	0.3	0.2	0.0
	18-03-2021	1230	3	N	3	7	3024	6.9	4.0	0.4	0.1	0.1	0.0
	15-04-2021	1700	6	N	5	8	3059	9.2	4.7	0.7	0.3	0.2	0.1
	19-05-2021	1300	8	W	11	11	2856	9.2	4.7	2.0	0.5	0.7	0.2
PN1	08-10-2020	1300	3	SW	13	17	3194	2.1	1.3	3.3	0.5	1.0	0.2
	25-11-2020	1345	5	SSW	7	14	1760	2.1	1.3	1.9	0.3	1.1	0.2
	09-02-2021	1700	4	NE	-2	11	3954	2.1	1.3	0.7	0.2	0.2	0.0
	15-04-2021	1150	5	NE	5	9	790	1.6	0.9	0.5	0.1	0.6	0.1
	01-07-2021	1030	3	NE	19	19	1278	1.6	0.9	2.0	0.3	1.6	0.3
	28-08-2021	1515	6	N	15	21	2208	2.0	1.2	7.8	1.2	3.5	0.5
	21-09-2021	920	3	S	12	19	2738	2.0	1.2	8.5	1.3	3.1	0.5
	07-10-2021	1010	2	SE	13	17	1747	2.0	1.2	4.9	0.8	2.8	0.5
PN2	04-02-2021	1320	3	ENE	-3	2	1677	4.9	3.6	0.7	-	0.4	0.0
	15-03-2021	1850	4	SW	4	3	2015	4.9	3.6	0.3	0.1	0.2	0.0
	21-04-2021	1820	8	N	9	7	543	4.9	3.6	0.0	0.0	0.1	0.0
	13-07-2021	1710	5	ESE	20	20	1162	4.9	3.6	0.2	-	0.2	0.0
	04-03-2022	1050	3	ESE	2	5	2138	4.9	3.6	0.2	0.1	0.1	0.1
	15-08-2022	700	6	E	22	19	1157	4.9	3.6	0.2	0.1	0.2	0.1
	21-10-2022	1600	3	ENE	15	11	882	4.9	3.6	0.1	0.1	0.1	0.1

	15-11-2022	1400	3	ESE	13	11	1454	4.9	3.6	0.3	0.1	0.2	0.1
	05-07-2021	1145	2	S	17	-	1671	5.2	3.7	6.0	2.8	3.6	1.7
	05-08-2021	1920	4	ESE	15	21	1888	5.2	3.7	10.6	2.8	5.6	1.5
	26-09-2021	1300	2	SE	14	20	2572	5.2	3.7	6.8	3.6	2.6	1.4
PC1	04-12-2021	1800	4	SE	1	14	3617	3.7	2.6	6.4	2.7	1.8	0.8
	23-01-2022	1300	4	NW	5	10	3537	3.7	2.6	1.2	0.4	0.3	0.1
	20-03-2022	1230	8	ESE	5	8	3537	3.7	2.6	1.4	0.3	0.4	0.1
	18-05-2022	1400	3	SE	14	12	1101	3.7	2.6	0.4	0.1	0.3	0.1
	20-07-2022	1400	4	S	21	21	1648	5.2	3.7	7.9	3.1	4.8	1.9
	27-05-2021	1430	3	NNE	10	-	800	8.4	5.3	1.1	0.3	1.4	0.4
	05-08-2021	1100	4	SE	15	16	1061	8.4	5.3	5.9	4.1	5.6	3.9
	09-09-2021	1215	4	SE	17	15	1894	4.1	2.4	1.2	0.7	0.7	0.4
PC2	29-01-2022	1400	13	SW	6	8	5500	4.1	2.4	3.4	0.7	0.6	0.1
	20-03-2022	1700	9	SE	5	6	5500	4.1	2.4	0.9	0.4	0.2	0.1
	26-03-2022	1500	4	NW	8	7	2567	4.1	2.4	0.5	0.4	0.2	0.2
	20-07-2022	1900	4	S	21	16	1721	8.4	5.3	3.9	1.6	2.3	0.9
	10-02-2021	1020	5	ENE	-4	5	2985	2.0	1.3	3.6	0.4	1.2	0.1
	15-03-2021	1550	4	SW	3	6	3698	2.0	1.3	4.6	0.2	1.2	0.1
	19-03-2021	1100	4	NE	2	6	3698	2.0	1.3	4.9	0.3	1.3	0.1
	03-04-2021	1250	3	NNW	5	9	1559	2.0	1.3	4.4	0.2	2.8	0.1
	16-04-2021	1050	5	NNE	5	9	578	2.0	1.3	2.1	0.3	3.7	0.5
PC3	14-07-2021	1430	4	ENE	21	21	1701	2.0	1.3	8.6	-	5.1	0.0
	27-08-2021	1350	9	NE	15	19	2361	2.0	1.2	10.4	1.1	4.4	0.5
	01-10-2021	830	4	SSE	12	18	3047	2.2	1.3	8.3	2.1	2.7	0.7
	29-11-2021	1200	5	NE	2	11	3119	2.2	1.3	4.5	0.2	1.5	0.1
	31-01-2022	1320	2	SW	4	7	3948	2.2	1.3	4.6	0.2	1.2	0.1
	23-09-2022	1000	3	S	11	18	2093	2.2	1.3	7.6	1.2	3.6	0.6
	20-12-2022	1300	5	S	7	9	3168	1.7	1.0	5.1	0.8	1.6	0.2
	16-02-2021	1010	4	SSE	-3	2	2340	-	-	0.7	0.3	0.3	0.1
	21-04-2021	1200	9	NNW	9	-	200	-	-	0.4	0.2	2.0	1.0
PC4	28-05-2021	1230	3	NNW	10	-	200	-	-	0.0	0.0	0.1	0.0
	01-06-2022		4	WNW	10	-	1095	-	-	12.0	7.0	11.0	6.4
	01-09-2021	1420	3	WNW	15	21	2310	-	-	14.3	8.8	6.2	3.8
	21-10-2021		6	WNW	11	19	3040	-	-	7.4	4.0	2.4	1.3
	10-10-2020	1200	3	SSW	9	20	9509	3.5	1.8	3.7	0.6	0.4	0.1
	18-12-2020	1600	6	SSW	6	23	3122	3.5	1.8	2.0	0.3	0.6	0.1
	03-02-2021	1545	7	ENE	-3	19	8930	3.5	1.8	2.8	0.4	0.3	0.1
DC1	28-04-2021	1240	4	SSW	5	9	3052	3.5	1.8	0.0	0.0	0.0	0.0
	25-06-2021	1130	5	SW	15	18	3578	3.5	1.8	0.9	0.6	0.2	0.2
	06-08-2021	1440	5	SE	16	34	6378	4.0	2.3	5.6	1.0	0.9	0.2
	05-09-2021	1810	3	SE	14	21	4501	4.0	2.3	3.3	0.5	0.7	0.1

	20-10-2021	1000	6	SW	11	15	4782	4.0	2.3	13.0	2.0	2.7	0.4
DN1	04-11-2020	1400	7	WSW	11	17	1611	4.3	2.8	0.5	0.1	0.3	0.1
	21-12-2020	1100	5	SW	6	16	2781	4.3	2.8	0.9	0.1	0.3	0.1
	24-02-2021	1400	8	SW	9	14	3673	4.3	2.8	0.6	0.1	0.2	0.0
	18-05-2021	1000	3	E	10	11	995	4.0	2.7	0.5	0.1	0.5	0.1
	07-07-2021	1050	3	SW	18	23	1393	4.0	2.7	1.5	0.3	1.1	0.2
	07-08-2021	1240	5	SSW	17	21	1066	5.2	3.6	1.1	0.2	1.1	0.2
	21-09-2021	1430	3	SSW	11	19	1752	5.2	3.6	1.2	0.2	0.7	0.1
	07-10-2021	1100	3	SSW	11	21	1916	5.2	3.6	1.9	0.7	1.0	0.4

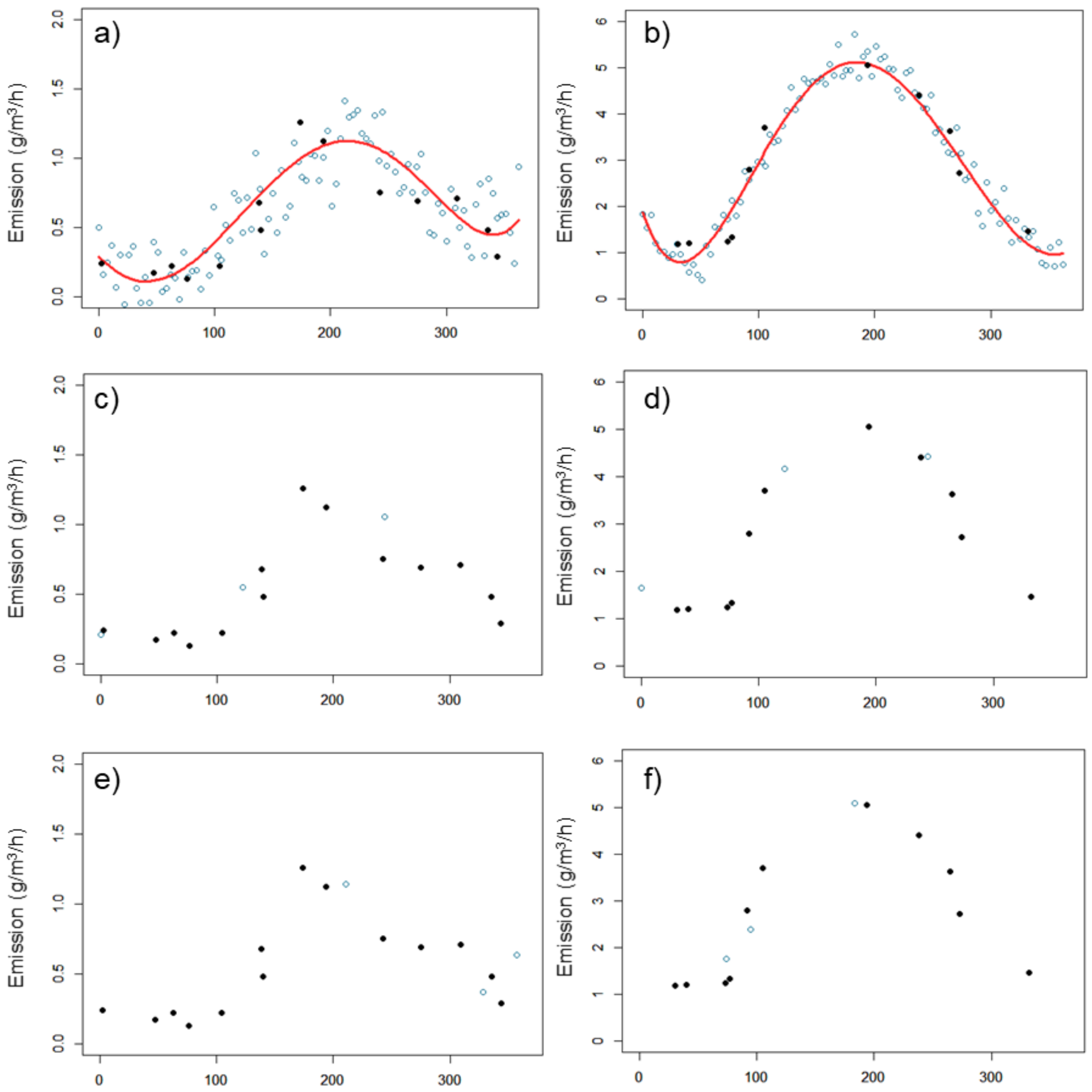

Figure S2: Analysis on the number of measurements analysis. The “a”, “c” and “e” corresponds to CN2 data and “b”, “d”, and “f” are the PC3 data. The “a” and “b” are the modelled emissions (open circles) based on the measured points (closed circles). The “c” and “d” figures are examples of measured and modelled emissions in case of only three equidistant measurements. The “e” and “f” are n-sample at random intervals.

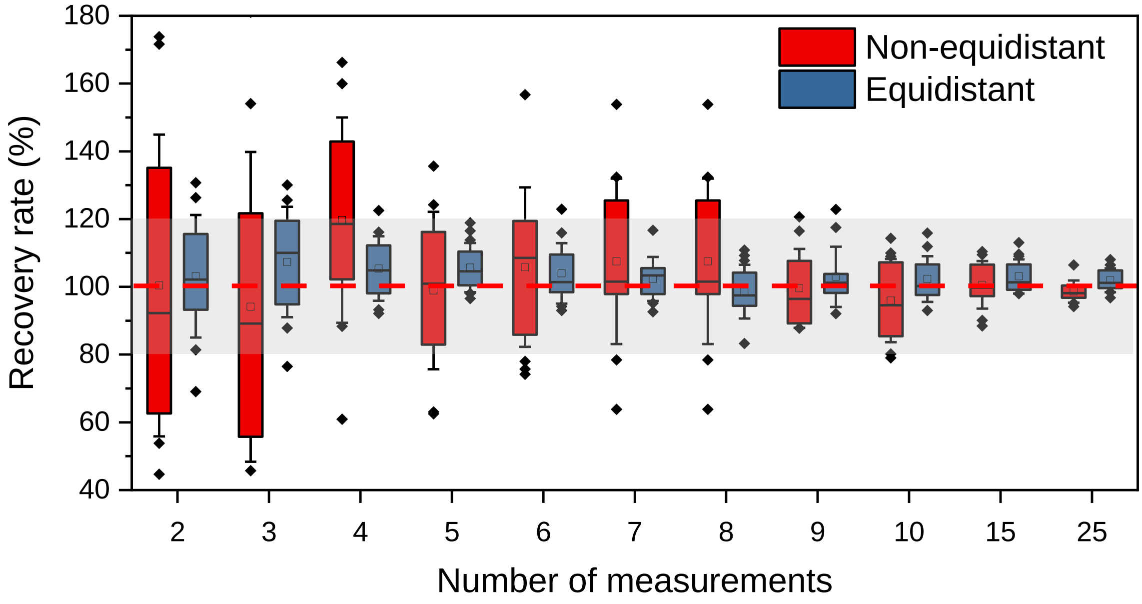

Figure S3: Analysis on the number of measurements analysis - Recovery rate (%) ($Rate_{n\text{-}sampling}/Rate_{100\text{-}sampling}$). Simulated sampling using different number of samples, for either equidistant or non-equidistant points.

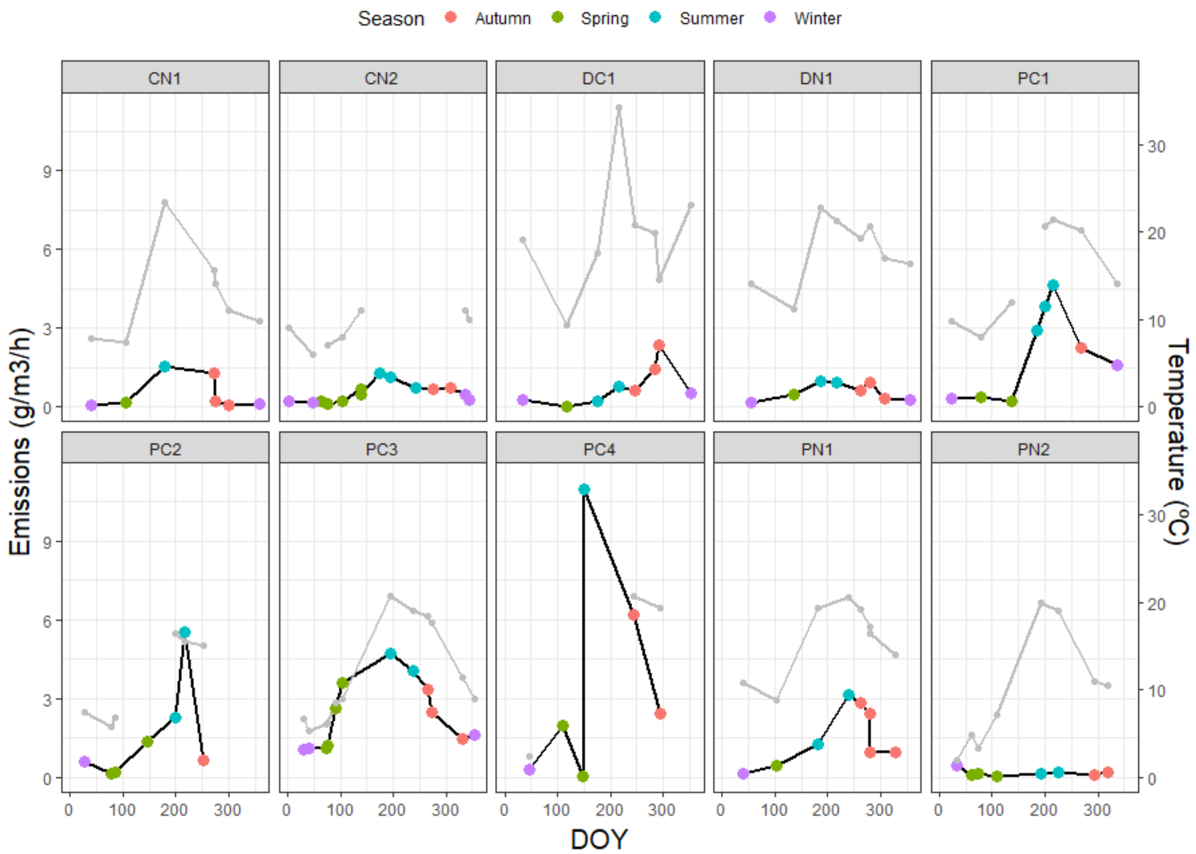

Figure S4: CH_4 Emissions in $g/m^3/h$ (left-axis) and manure temperature (right-axis) for each tank over the year.

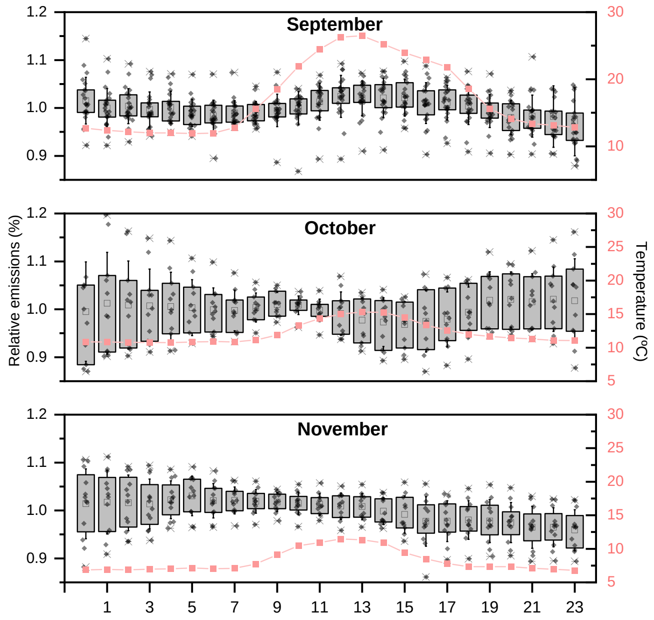

Figure S5: Autumn - Relative emissions (left-axis) binned to day time (Emissions$_{hh:mm}$/Emissions$_{daily\text{-}avg}$) and the average temperature in the tank's headspace (right-axis).

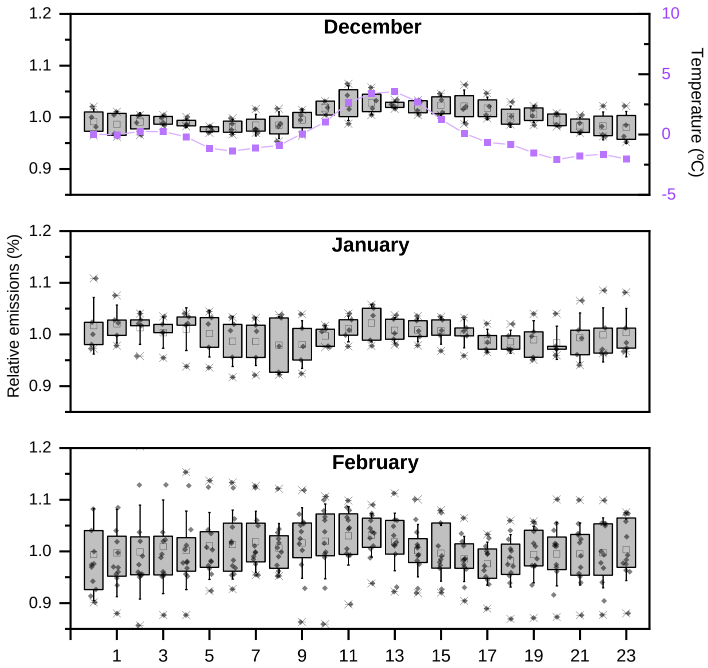

Figure S6: Winter - Relative emissions (left-axis) binned to day time (Emissions$_{hh:mm}$/Emissions$_{daily\text{-}avg}$) and the average temperature in the tank's headspace (right-axis). The temperature sensor was not working on January and February.

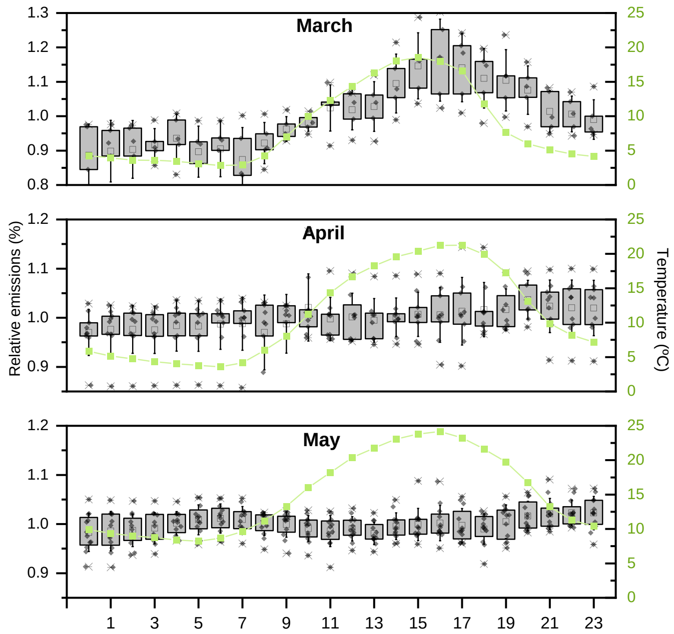

Figure S7: Spring - Relative emissions (left-axis) binned to day time ($Emissions_{hh:mm}/Emissions_{daily\text{-}avg}$) and the average temperature in the tank's headspace (right-axis).

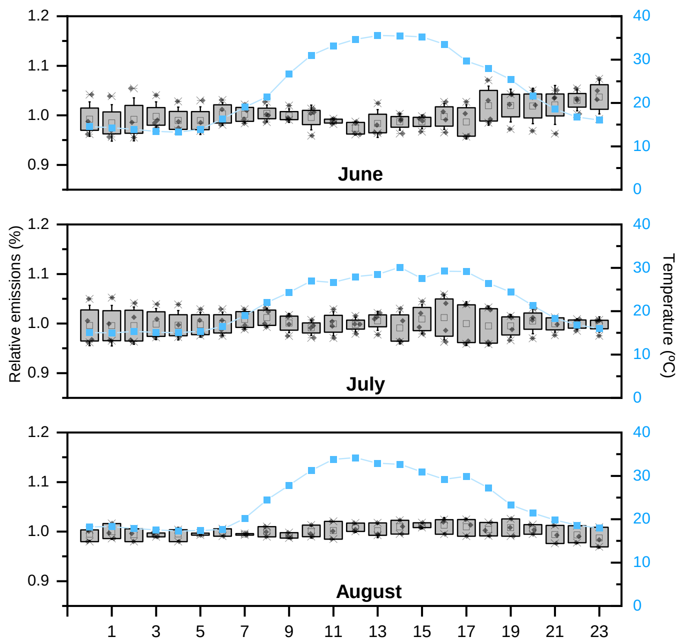

Figure S8: Summer - Relative emissions (left-axis) binned to day time ($Emissions_{hh:mm}/Emissions_{daily\text{-}avg}$) and the average temperature in the tank's headspace (right-axis).

Table S2: Model – analysis of covariance. R^2 of the manure type model was 0.45, while for the pig manure tank cover effect, R^2 was 0.56.

Model	Parameter	Coefficient	Standard errors	P-value	Confidence interval	
Full model[a]	Intercept	-1.45	0.19		-1.83	-1.07
	Temperature	0.06	0.01	< 0.001	0.04	0.08
	Manure type	0.19 (Cattle) 0.66 (Pigs)	0.17 (Cattle) 0.13 (Pigs)	<0.001	-0.14 0.39	0.52 0.92
Only covered tank[b]	Intercept	-1.03	0.16		-1.36	-0.71
	Temperature	0.05	0.01	<0.001	0.03	0.07
	Cover	0.50	0.12	<0.001	0.25	0.75

[a] The factor cover was also significant in the first model, but because we wanted to evaluate the effect of the cover only and not the type of manure, it was removed. Full model: log10(Emis_gm3h) ~ Temp_Manure + Manure_type. [b] log10(Emis_gm3h) ~ Temp_Manure + Cover.

V

Ammonia and methane emissions from dairy concentrated animal feeding operations in California, using mobile optical remote sensing.

Vechi, N.T., Mellqvist, J., Samuelsson, J., Offerle, B., & Scheutz, C.

Atmospheric Environment, *293*,119448

https://doi.org/10.1016/j.atmosenv.2022.119448

Atmospheric Environment 293 (2023) 119448

Contents lists available at ScienceDirect

Atmospheric Environment

journal homepage: www.elsevier.com/locate/atmosenv

Ammonia and methane emissions from dairy concentrated animal feeding operations in California, using mobile optical remote sensing

N.T. Vechi [a,b,*], J. Mellqvist [a], J. Samuelsson [c], B. Offerle [c], C. Scheutz [b]

[a] *Department of Space, Earth and Environment, Chalmers University of Technology, Göteborg, Sweden*
[b] *Department of Environmental and Resource Engineering, Technical University of Denmark, 2800 Kgs, Lyngby, Denmark*
[c] *FluxSense AB, SE-41296, Göteborg, Sweden*

HIGHLIGHTS

- NH_3 and CH_4 emissions were quantified using direct and indirect flux methods.
- NH_3 and CH_4 emission factors averaged 9.1 g_{NH3}/LU/h and 40.1 g_{CH4}/LU/h.
- Day-time NH_3 emission factors were 28% higher than estimated by NEI 2014.
- Quantified CH_4 emission factors were 60% higher than the CARB inventory.

ARTICLE INFO

Keywords:
CAFO
SOF
Dairy
Emission inventory
Emission factor

ABSTRACT

Dairy concentrated animal feeding operations (CAFOs) are significant sources of methane (CH_4) and ammonia (NH_3) emissions in the San Joaquin Valley, California. Optical techniques, namely, remote sensing by Solar Occultation Flux (SOF) and Mobile extractive FTIR (MeFTIR), were used to measure NH_3 air column and ground air concentrations of NH_3 and CH_4, respectively. Campaigns were performed in May and October 2019 and covered 14 dairies located near Bakersfield and Tulare, California. NH_3 and CH_4 emission rates from single CAFOs averaged 101.9 ± 40.6 kg_{NH3}/h and 437.7 ± 202.0 kg_{CH4}/h, respectively, corresponding to emission factors (EFs) per livestock unit of 9.1 ± 2.7 g_{NH3}/LU/h and 40.1 ± 17.8 g_{CH4}/LU/h.

The NH_3 emissions had a median standard uncertainty of 17% and an expanded uncertainty (95% Confidence Interval (CI)) of 37%; meanwhile, CH_4 emissions estimates had greater uncertainty, median of 25% and 53% (in the 95% CI). Decreasing NH_3 to CH_4 ratios and NH_3 EFs from early afternoon (13:00) to early night (19:00) indicated a diurnal emission pattern with lower ammonia emissions during the night. On average, measured NH_3 emissions were 28% higher when compared to daytime emission rates reported in the National Emissions Inventory (NEI) and modeled according to diurnal variation. Measured CH_4 emissions were 60% higher than the rates reported in the California Air Resources Board (CARB) inventory. However, comparison with airborne measurements showed similar emission rates. This study demonstrates new air measurement methods, which can be used to quantify emissions over large areas with high spatial resolution and in a relatively short time period. These techniques bridge the gap between satellites and individual CAFOs measurements.

1. Introduction

The quantification and monitoring of ammonia (NH_3) and methane (CH_4) emission sources are crucial to effectively plan and implement air quality and climate change policies. CH_4 is a potent greenhouses gas and has a global warming potential of 27 over a 100-year span (IPCC, 2021). NH_3 is a critical precursor of fine particulate matter ($PM_{2.5}$), which has implications for human health and climate change (Lelieveld et al., 2015). In addition, atmospheric NH_3 can be transported to downwind ecosystems leading to eutrophication and loss of biodiversity (Harris et al., 2016). Livestock operations are large emission sources of both NH_3 and CH_4, and in California, the agricultural sector contributes 8% of total GHG emissions and approximately 57% of the state's anthropogenic CH_4 emissions (CARB, 2019a). For NH_3, livestock operations are

* Corresponding author. Department of Space, Earth and Environment, Chalmers University of Technology, Göteborg, Sweden.
E-mail address: navei@dtu.dk (N.T. Vechi).

https://doi.org/10.1016/j.atmosenv.2022.119448
Received 24 June 2022; Received in revised form 20 October 2022; Accepted 24 October 2022
Available online 29 October 2022

responsible for 56% of total emissions in California (U.S. Environmental protection Agency, 2018). These numbers are a reflection of the state's number one ranking, as the largest milk producer in the USA, with production concentrated in the San Joaquin Valley (SJV) (Monson et al., 2017; USDA, 2021). However, these estimates have large uncertainties, and better understanding of NH_3 and CH_4 emissions from livestock operations can facilitate policymaking for achieving California's air quality and climate goals. Concentrated animal feeding operations (CAFOs) are defined as operations where animals are confined for a certain amount of time and where vegetation is not sustained, additionally, they should meet the requirement of more than 700 milk cows (US-EPA, 2012).

NH_3 emissions from livestock originate from the mixture of animal urine and feces, and they are highly variable and depend on a number of factors such as temperature, pH, wind speed, manure composition, and manure management (Hristov et al., 2011). Shortly, nitrogen molecules in the manure are converted to NH_3, which stays in equilibrium with its ionized form ammonium (NH_4^+). In favorable conditions NH_3 is transported to the manure surface by diffusion and further volatilized from the manure surface by convection (Hristov et al., 2011). NH_3 lifetime in the atmosphere varies from hours to a few days according to atmosphere composition. In Palm Springs (California) for example, the load of oxidants reduced NH_3 life time to four to six hours (Leifer et al., 2017). Part of the NH_3 emitted reacts neutralizing acid species as H_2SO_4 and HNO_3 forming $PM_{2.5}$, during the San Joaquin Valley (SJV) episodes of high particulate concentrations occuring specially in the winter (Lonsdale et al., 2017). Moreover, the NH_3 left is deposited on soil and water surfaces. Miller et al. (2015) measured a ~30% decrease in the ratio of NH_3:CH_4 within a few kilometers of a dairy facility in the SJV and attributed the difference to NH_3 deposition. Overall the modeling and understanding of NH_3 dynamics is a complex task having to account for all the mechanism mentioned above (Lonsdale et al., 2017; Zhu et al., 2015b). On the other hand, CH_4 emissions from dairy operations come from both manure management and enteric fermentation, with emissions from the latter depending mainly on animal age, feed intake, and body weight (Hristov et al., 2018), while emissions from manure are affected by temperature and management practices (Rennie et al., 2018). Furthermore, emissions might have a diurnal trend associated with wind speed, temperature, and cattle activity (Leytem et al., 2011). Although many studies (Leytem et al., 2011; Sun et al., 2015) show a clear diurnal pattern for NH_3, the same is not true for CH_4, which provide contradictory results (Arndt et al., 2018; Bjorneberg et al., 2009; Golston et al., 2020).

Direct emissions quantification offers information that can be used to improve inventories, evaluate emission dynamics, and determine the efficiency of different mitigation strategies. Several studies in North America show that inventories have lower emissions estimations than measurements of both NH_3 (Lonsdale et al., 2017; Nowak et al., 2012) and CH_4 (Hristov et al., 2017; Miller et al., 2013; Owen and Silver, 2015), while others reveal good agreement (Arndt et al., 2018; Golston et al., 2020).

The solar occultation flux (SOF) technique has been used to measure industrial emissions for about 20 years, with most studies focusing on VOCs (alkanes and alkenes) (Johansson et al., 2014; Mellqvist et al., 2010) and industrial NH_3 (Mellqvist et al., 2007). NH_3 measurements of dairy and beef farms using the SOF technique have been carried out by Kille et al. (2017) in Colorado. Mass fluxes can be obtained by combining wind information and the path-integrated concentrations retrieved from the gas columns of solar spectra collected by the SOF instrument on a moving measurement platform. The technique can be used to study emissions from single-point sources to larger areas (radius ~ 50 km), and it can therefore help to fill gaps between point concentration measurements and satellite remote sensing.

In this study, SOF together with local wind profile measurements were used to measure NH_3 emissions from CAFOs. In addition, CH_4 measurements were carried out via an emission ratio approach, combining direct NH_3 flux measurement by SOF with plume NH_3 to CH_4 concentration ratios. The aim of this study was threefold. First CH_4 and NH_3 emissions were investigated from several individual dairy CAFOs located at the SJV. These facilities were selected according to measurements possibilities with respect to wind direction and drivable roads and due to their large size. Results were then evaluated by comparing them with the inventory estimates and other reports in the literature. Lastly, the causes of variability in the NH_3 emission factors obtained were identified and discussed.

2. Methodology

2.1. CAFOs and measurement campaigns

The study focused on emissions from dairy concentrated animal feeding operations (CAFOs) in the SJV, California. The first campaign took place in May 2019 and consisted of 11 measurement days, while the second took place in October 2019, lasting five days. In May, CAFOs were measured in Kern (near Bakersfield) and Tulare Counties, whereas in October, only the facilities in Kern County were revisited.

In the application of the SOF method for industrial measurements (European standard 2022, EN 17628:2022) there are quality criteria for the measurements to be valid. In this study we have used a subset of these, given that animal operations are less complex than industries, including that at least four plume transects need to be carried out on a single day and that the wind speed is higher than 1.5 m/s. In total, emissions from 14 individual dairy CAFOs passed the quality control requirements. Table 1 provides an overview of the facilities measured, including information on numbers of animals as well as manure management (Fig. 1c). Emission factors (EFs) were calculated by normalizing the measured emission rates by livestock units (LU) based on animal body weight, with one LU equaling 500 kg (Ngwabie et al., 2011). Although emission measurements were also successful at two facilities in Madera County in May, they were excluded from the EFs and inventory analysis since the numbers of animals were unavailable for them, but a comparison of their emissions rates with other studies is shown in section 4.3.2. All the CAFOs stored the manure in anaerobic

Table 1
CAFOs characteristics. The CAFOs are named according to their geographic location (Fig. 1c), whereby the first letter corresponds to the cardinal direction (North, South, West, East) and the second letter to the nearby city (Bakersfield (Kern County) or Tulare).

CAFOs	Mature cows[a]	Heifers and bulls	Calves	Livestock unit[b]	Covered lagoon and gas collection
SB2	7380	13414	2880	21626	No
SB3	6450	6280	1300	14184	Yes
SB4	4000	2358	0	7361	No
SB5	8115	2100	0	12749	No
NB1	5250	3620	0	10056	No
NB2	6640	1925	0	10592	No
WT1	11350	8870	0	14883	Yes
WT3	12100	0	925	12618	No
WT4	9980	2060	0	15241	No
WT5	3075	3600	0	7111	Yes
WT6	4820	4620	0	10308	No
WT7	2770	2135	0	5503	Yes
ET1	1375	1000	0	2678	No
ET8	10900	5000	0	12368	Yes

[a] Accounting both milking and dry cows.
[b] One LU = 500 kg of body weight. Holstein dairy cow = 1.36 LU, Jersey dairy cow = 0.91 LU, Holstein heifer = 0.81 LU, Jersey heifer = 0.5, Holstein calf = 0.23 LU, Jersey calf = 0.18 LU. Body weight based on U.S. Environmental Protection Agency (2013) for Holstein, by The Pennsylvania State University (2017) for heifers and calves, and American Jersey Cattle Association (2015) for mature Jersey. The numbers of mature cows, heifers, and calves at the individual farms were obtained from San Joaquin Valley Air Pollution Control District (San Joaquin Valley Air Pollution Control District, Personal Communication, 2019) and based on data from the last inspection between 2018 and 2019.

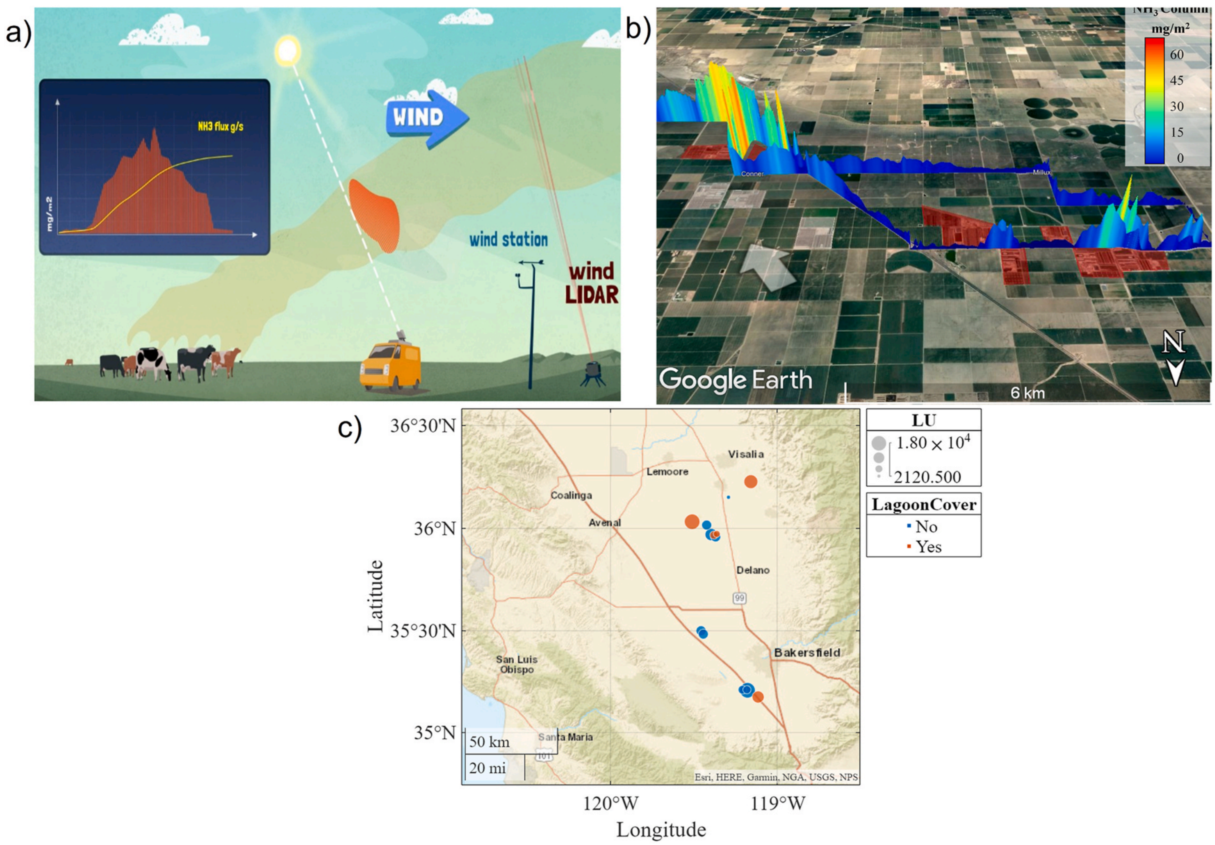

Fig. 1. (a) The principle behind the solar occultation flux (SOF) method, which was used to measure NH_3 fluxes. The car drives across the plume, measuring enhanced NH_3 concentration air columns, while the wind LIDAR is positioned close to the source and measures wind speed from 10 to 300 m high. (b) Example of SOF columns measured downwind at six facilities (red areas). The white arrow indicates the wind direction, the white shadowed areas are other farms were not measured Map source: Google Earth. (c) CAFOs location in the San Joaquin Valley, California. The size of the bubbles are proportional to the dairy size (number of animals) and the color is related to the presence of a covered lagoon (digester). (For interpretation of the references to color in this figure legend, the reader is referred to the Web version of this article.)

lagoons, and five of them had a covered lagoon, which worked as a digester, for gas collection and utilization for generation of electricity and conversion to compressed natural gas (CNG). There was some uncertainty, though, whether they were actually operational.

2.2. *Measuring principles and instrumentations*

CH_4 and NH_3 emissions were measured using a mobile laboratory equipped with several optical systems (Mellqvist et al., 2017). Two measurement systems were used, i.e., the solar occultation flux method (SOF), consisting of a solar tracker connected to a Fourier transform infrared spectrometer (FTIR), and a mobile extractive Fourier transform infrared (MeFTIR), consisting of an FTIR spectrometer coupled to a multireflection gas cell (Table 2). A GPS recorded the car's position while driving. Meteorological measurements were performed with (1) a sonic instrument (AIRMAR) located on the roof of the vehicle and (2) a light detection and ranging instrument (LIDAR, Zephyr) with a measurement range of 10–300 m in height and positioned close to the specific emission source (maximum distance of 5 km). The sonic sensor was only used for the operator's guidance during the measurements, while the LIDAR measurements were used for the emissions calculations (see section 2.3.3).

NH_3 columns (mg/m^2) were obtained using the solar SOF technique (Fig. 1a). In this method (Mellqvist et al., 2010), solar infrared spectra are recorded using a customized solar tracker, with mirrors reflecting the solar beam into an FTIR (Bruker IRCube), when crossing the plume concentration downwind of the emission source (Fig. S1, in Supplementary Information (SI)). The measurements do not provide the absolute atmospheric column but the differential one, relative to a reference point, usually taken outside of the plume, and a slant column of the target species is retrieved from each spectrum. The SOF retrieval uses customized analysis software (Fluxmeasure), which fits a set of spectra from the HITRAN2004 (Rothman et al., 2005) and PNNL (Sharpe et al., 2004) spectroscopic databases in a least-squares fitting procedure. The software has been tested (Kihlman, 2005) against other published codes (Griffith, 1996). The instrument incorporates a dual semi-conductor detector to increase the useable frequency range (InSb

Table 2
Summary of gas measurement techniques.

Method	Compound	Detection limit (3σ)[a]	Wind speed tolerance	Sampling time resolution	Measured quantity
SOF	NH_3	2.2 mg/m^2	1.5–12 m/s	4–5 s	Integrated vertical column mass (mg/m^2)
MeFTIR	CH_4 NH_3	30 ppbv 15 ppbv		9–10 s	Mass concentration at vehicle height (mg/m^3)

[a] The detection limit was calculated as the three times the standard deviation of constant concentration reading. These values are on the high end of the instrument limits because they were measured in field conditions, where air is not clean.

(1800–4000 cm^{-1})/MCT (700-1200 cm^{-1}). NH_3 is measured in the spectral region between 900 and 1000 cm^{-1} at a spectral resolution of 0.5 cm^{-1}, and the unique absorption features of this gas in the "fingerprint region" are advantageous in terms of specificity. More details on the instrument and validation experiments can be found in Johansson et al. (2014), Mellqvist et al. (2010), and Mellqvist et al. (2017).

CH_4 and NH_3 ground concentrations (mg/m^3) were measured using MeFTIR, in which infrared radiation from an internal glow is transmitted through an optical multi-pass measurement cell. The ambient air is pumped via an inlet placed at 2 m height through the cell at high flow (100 ml/min and cell pressure of 10 mbar below ambient pressure), to ensure that the gas volume in the cell is rapidly replaced ($t_{90} < 10$ s, gas exchange rate). The transmitted light is measured with an FTIR identical to that applied for SOF (Bruker IR Cube) (Figs. S1 and SI). Concentration retrieval of the gas species is carried out using the same spectroscopic software and databases as for SOF. NH_3 was retrieved in the same interval as in SOF (900–1000 cm^{-1}), while for CH_4 the interval used was in the C–H strength region (2760–3028 cm^{-1}). More details on the instruments and methods can be found in Samuelsson et al. (2018). The retrieval of NH_3 followed similar procedure as described for SOF while for CH_4 the retrieval was done by using the known published code, Multiple Atmospheric Layer Transmission (MALT) (Griffith, 1996).

In general, emissions were measured by driving downwind of the CAFO at a distance about hundred meters from its fenceline and this was close enough to avoid the influence of emissions from neighboring sources. Upwind measurements and the identification of external sources using GIS tools e.g., Google Earth, were used as a criterion to identify interfering emission sources (Fig. 1b). Because measurements were made by isolating the CAFOs in a box and checking upwind and downwind concentrations, interfering sources were most likely not affecting the quantification. In addition to diurnal measurements, ground concentration measurements were performed close to sunset or at night, when SOF measurements were no longer possible, this was to confirm potential variation in the NH_3:CH_4 ratio.

2.3. Emission rate calculations

2.3.1. Direct ammonia flux measurements

To obtain NH_3 emissions, the measured slant columns are first converted to vertical columns. These are subsequently integrated across the plume, corresponding to the accumulated mass across the plume (g/m). To obtain the gas flux (g/s), the accumulated mass (g/m) is multiplied by the average wind speed (m/s) of the plume (Eq. (1)). The latter applies when the plume is transected orthogonally; otherwise, the wind speed component orthogonal to the travel direction is utilized.

$$E_{NH3}\left(\frac{mg}{s}\right) = u_t\left(\frac{m}{s}\right)\int_{x1}^{x2} Column_{NH3}\left(\frac{mg}{m^2}\right) \bullet \cos(\theta) \bullet \sin(\alpha)dx(m) \tag{1}$$

where E_{NH3} is the NH_3 emission rate, u_t is the average wind speed at plume height, $column_{NH3}$ is the concentration retrieved from the solar spectrum, θ is the angle of the light path from zenith, α is the angle between the wind direction and driving direction, and x_1 and x_2 are the start- and endpoints of the plume transect, respectively. Note that because solar spectra are measured, the slant column densities will vary with latitude, season, and time of the day. The NH_3 emissions of each CAFO was calculated as the average emission of the performed transects on the respective facility.

2.3.2. Indirect CH_4 flux measurements

From MeFTIR, the ground concentrations for NH_3 and CH_4 are retrieved; hence, to quantify emissions, an indirect flux calculation approach is used. With this method, the measured concentration ratio between the two gases is combined with the gas flux measurements of one of these gases to derive the gas flux of the other one. Therefore, we combined the average NH_3:CH_4 ratio, with the average NH_3 flux obtained from SOF measurement (Eq. (1)), to find the average CAFO CH_4 emission (Eq. (2)).

$$E_{CH4} = \frac{1}{n}\sum_n E_{NH3}\left(\frac{kg}{h}\right) \Bigg/ \frac{1}{n}\sum_n \frac{\int_{x1}^{x2}(C_{NH3} - C_{BG-NH3})\left(\frac{\mu g}{m^3}\right)dx}{\int_{x1}^{x2}(C_{CH4} - C_{BG-CH4})\left(\frac{\mu g}{m^3}\right)dx} \tag{2}$$

Where E_{CH4} is the CH_4 emission rate, n is the number of transects and C is the concentration measured by MeFTIR. Additionally, the background concentrations ($C_{BG\text{-}NH3}$ or $C_{BG\text{-}CH4}$) were decreased from the concentrations measured when crossing the plume (C_{NH3} or C_{CH4}) Note that in this study, the SOF and MeFTIR measurements were not always carried out simultaneously, and Eq. (2) was therefore applied using average concentration ratio values and average flux values over the same time of day (from 09:00 to 17:30).

Ratio concentration measurements can be carried out with techniques other than MeFTIR, but the advantage of using the same spectroscopic approach for both column and concentration is that systematic spectroscopic errors are reduced, and there is consistency in which species are being measured. The indirect flux measurement approach relies on the assumption that the path-integrated concentration ratio of the two species is proportional to the ratio of the emissions. This means that the two species are dispersed in the same manner, requiring that they have the same release height and travel the same distance from the release point to the measurement point. NH_3 and CH_4 ground plumes were not always correlated, due to differences in the sources' location, which could lead to over- or underestimations (Delre et al., 2018; Miller et al., 2015). However, if the sources' distances to the actual road were very different in comparison to the measuring distance, the plumes were excluded, in order to avoid large under- and/or overestimations. Nevertheless, the spatial correlation was considered in the uncertainty analysis (Section 4.1).

2.3.3. Wind measurements

Local wind speed, along with its direction, is an integrated part of emission measurements (Eq. (1)), and associated uncertainties are directly propagated into the flux estimation. For the SOF method, the average wind speed of the emission plume should be used.

In this study, wind profiles close to the studied dairies were measured using wind LIDAR (LIght Detection and Ranging), i.e. a remote sensing technique, which measures wind speed by calculating the change in frequency due to the Doppler shift of the emitted laser wave (~1.5 μm) when reflected back on moving atmospheric aerosols (Locker and Woodward, 2010). The LIDAR used here (Campbell Scientific, LIDAR ZX 300) operates between 10 m and 300 m, and it is based on a continuous laser that transmits light in a 30° cone relative to zenith, combined with adaptive receiving optics that sequentially focuses on different atmospheric heights. In this study the wind speed was averaged in 5 min intervals over three height ranges, i.e. 10-50 m, 10–100 m, and 10–300 m. The accuracy of wind speed measurements is stated as 0.1 m/s, wind direction of 0.5°, and vertical precision at around 10 m. A field test comparing measurements done by cup anemometers on a 100 m wind tower to the Zephyr LIDAR showed a correlation between the two of 95% (3-week measurement period) (Smith et al., 2006).

As mentioned above, SOF measurements do not provide information on the height of the emission plume, which is of relevance when estimating average wind speed for the plume for Eq. (1). However, it is possible to estimate the plume height using vertical and horizontal wind speeds rates and distance from the measurement road to the source (Johansson, 2016). Based on previous studies in Texas (Johansson et al., 2014; Mellqvist et al., 2010) vertical dispersion rates of 0.5–1 m/s were used, which was obtained by wind soundings and aircraft measurements.

For most measurements, the wind intervals of 10–50 m and 10–100 m were found to be most appropriate for calculation of average plume wind speed, with just two exceptions. However, in reality there was only

12% difference between these two intervals since the wind variation is the strongest close to the ground and this was taken into account in the uncertainty analysis (Section 4.1).

The prevailing wind in southern San Joaquin Central Valley flows from the north/northwest direction during the day, and this was true for all measuring days in Bakersfield, when LIDAR measurements often resumed after the sunset, and the instrument was positioned at a maximum of 5 km downwind of the source. In Tulare, higher wind speeds and different directions were encountered (Fig. S2 in SI).

2.3.4. Techniques' advantages and challenges

NH_3 is a sticky gas that is easily being adsorbed on surfaces and this poses challenges for measurements using extractive techniques, and concentrations are thus easily underestimated. SOF, however, is a contact-free technique, which makes it more suitable to measure such types of gases. Other advantages of the technique lie in its capability to measure path integrated gas columns, mobility and real-time responsivity, thereby making it possible to measure multiple emission sources over a short time period. On the other hand, MeFTIR is a close-path instrument, where the adsorption of NH_3 in the cell and inlet might play a role. To minimize the adsorption on internal surfaces (Brodeur et al., 2009), which would cause a time delay in the measurements, the inlet tubing and the cell are heated to a minimum of 40 °C, thereby ensuring that NH_3 is not adsorbed inside the tubing or the measurement chamber.

Primarily, measurements of columns and ground concentrations were carried out simultaneously. However, sometimes this was not possible (25% of the time), due to very low concentrations at the ground level. SOF columns are only measured during daytime and sunny conditions (low cloud coverage), which generally is associated with strong vertical convection. However, it can be difficult to carry out ground concentration measurements during these conditions, where a better detection is often obtained after sunset.

2.4. Emission inventories

2.4.1. Ammonia emission rate comparison with the NEI 2014 inventory

The measured farm-scale NH_3 emission rates were compared to farm-specific daytime emission rates estimated by inventory models, in order to evaluate their performance (for more details, see Fig. S3 in SI).

NEI (2014v1) provides daily emission rates on county level (available at the inventory supporting information), which, for comparison, were converted to EFs averaged by month, resulting in values of 4.5 $g_{NH3}/head_{Milk\ cow}/h$ in May and 4.1 $g_{NH3}/head_{Milk\ cow}/h$ in October for both counties (Kern and Tulare) (Fig. S4b in SI). The calculation of EFs was solely based on the number of milk cows, while heifers, bulls, and calves housed in dairy CAFOs were not included, in order to follow the NEI 2014 methodology. The use of a more refined model was hampered by limited knowledge of the studied CAFOs.

Because NH_3 emissions vary over the day, this needed to be considered when comparing with the SOF daytime-measured emissions. Diurnal emission profiles from modelling by (Zhu et al., 2015a) were used in our study, these were calculated by the EPA (J. Bash, Personal communication, 2020) for the respective locations and measured months (May and October 2019) (Fig. S4a in SI). The calculations were based on weather information from the WRF model 4.1.1 (weather research and forecasting) and the calculated data was given as monthly hourly fraction of NH_3 emissions $N_{met(t)}$.

Zhu et al. (2015a) obtain the diurnal emission pattern of NH_3 from the two equations below. The hourly fraction $N_{met(t)}$ (%) (Fig. S3 in SI) is first obtained from Eq. (3). After that, the hourly NH_3 emission rates (E_h (kg/h)) (Fig. S4a in SI) are obtained from Eq. (4), where E_m (kg/h) is monthly total emissions from the NEI 2014 v1.

$$N_{met(t)} = \frac{H_{(t)}/R_{a(t)}}{\sum_{t=1}^{n}\left(\frac{H_{(t)}}{R_{a(t)}}\right)} \tag{3}$$

$$E_h(t) = E_m N_{met}(t) \tag{4}$$

Here $R_{a(t)}$ (m/s) is atmospheric resistance at a specific time t, and $H_{(t)}$ is Henry's equilibrium constant, which is where the temperature is incorporated. Each hourly fraction is then divided by the sum of fractions of the whole month.

Fig. S4a in SI shows the estimated hourly NH_3 emission rates (E_h (kg/h)) for one of the dairies (SB05) in May and October, compared to modeled emission rates without the consideration of diurnal variation.

2.4.2. CH_4 emission rate comparison with the CARB inventory

For CH_4, we compared the average measured emission rates at the farm scale with emission rates obtained by the modeled California Air Resources Board (CARB) inventory. In the US, both national (U.S. Environmental Protection Agency, 2013) and the statewide (CARB, 2019b) CH_4 emission rates are derived from the methodology suggested by the International Panel for Climate Change (IPCC) (IPCC, 2006). The CH_4 inventory data (EFs) used in this study is specified for the climate and management conditions in the studied region by using EFs provided by CARB (CARB, 2019b) (Fig. S5 in SI). These estimations are divided into enteric fermentation and manure management EFs for each animal class (e.g., dairy cows, replacement heifers, and calves). For enteric emissions, the EF is multiplied by the number of animals at each life stage. For manure management practices, the EFs from each type of management have a different weight, which is based on CAFOs practices across the whole state of California. In the CARB inventory the following distribution for the manure from the dairy cows was assumed: 60% anaerobic lagoons, 10% daily spread, 20% liquid slurry, and 9% solid storage. In contrast, for heifers, 88% of manure treatment is assumed to be in dry lots, 11% daily spread, 1% pasture, and 1% liquid slurry. This approach is used because knowledge on the specific manure handling of the studied CAFOs was limited. Similarly, a recent study calculating CH_4 manure emissions in SJV, estimate that the largest percentage of the dairy manure (58–70%) was handled in anaerobic lagoons (Marklein et al., 2021). For the CAFOs with an anaerobic digester, the EF for this management were used instead of the anaerobic lagoons EF.

The comparisons between measurements and inventories for NH_3 was done with respect to time of the day, in contrast to CH_4, which was done for the annual average, because we assumed negligible diurnal variations. To obtain annual averages from the campaign measurements, the average emission rates were scaled to the full year. It should be noted that some of the farms were measured during two seasons, i.e. May and October (SB3, SB4, SB5, NB1 and NB2), while others were only measured once in May.

3. Results

3.1. NH_3 and CH_4 emission rates and emission factors

Fig. 2 shows the measurement approach used in this study demonstrated at dairy SB5, consisting of two nearby facilities housing 10,227 animals (mature cows, heifers, and bulls) corresponding to 12,750 livestock units (the detailed measured transects at SB5 are in Table S1 in SI). The obtained NH_3 columns (Fig. 2a and b) and ground concentrations of NH_3 and CH_4 (Fig. 2c and d) are shown along a measurement transect downwind of the CAFO. This measurement was complemented by upwind measurements. In May, the average emission and standard deviation from eight transects were 113.5 ± 49.2 kg_{NH3}/h, measured on two different days from 12:00 to 18:00, at an average wind speed of 2.34 ± 0.68 m/s and an average temperature of 28.11 ± 1.45 °C (Table S1 in SI). The plume ground concentration measurements gave an average

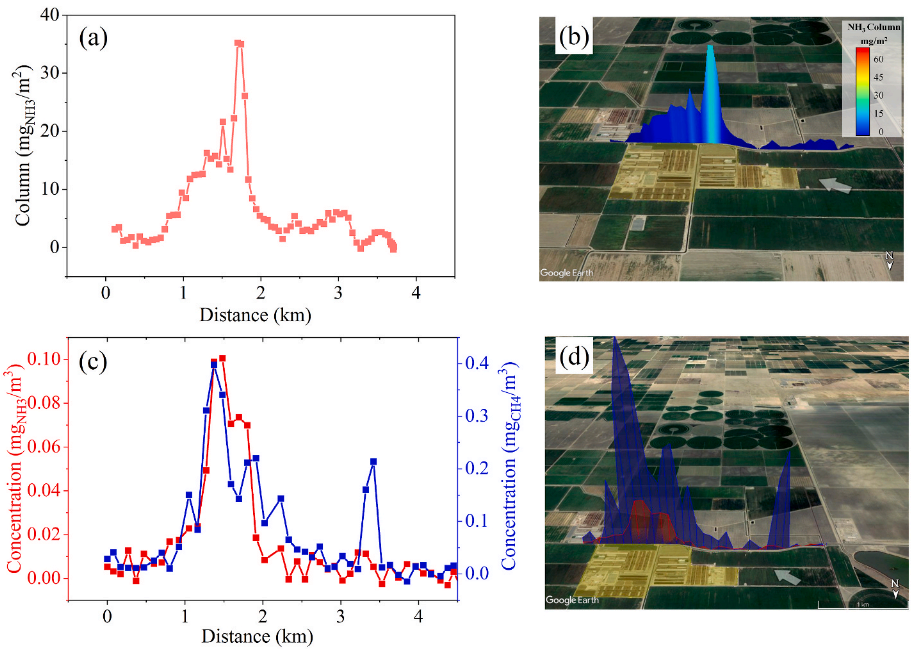

Fig. 2. Transects measured downwind of dairy SB05 on May 14th at 16:00. The measurements were obtained simultaneously, and the white arrow indicates wind direction. (a) NH_3 column. (b) Spatial location of the NH_3 column measurements. (c) Ground concentrations of NH_3 and CH_4. (d) Spatial location of NH_3 and CH_4 ground concentrations; the small CH_4 concentration plume on the far left side of the CAFO is likely due to emissions coming from a flooded area on the field. Map source: Google Earth.

NH_3:CH_4 ratio of 20.7 ± 8.9 g_{NH3}/g_{CH4}, resulting in an average CH_4 emission of 548 ± 137 kg_{CH4}/h. In October, NH_3 emission from SB05 averaged 130 ± 52 kg_{NH3}/h, and the NH_3:CH_4 ratio was 15 ± 9.1g_{NH3}/g_{CH4}, thereby giving a CH_4 emission of 873 ± 235 kg_{CH4}/h (Table S1 in SI).

Considering all CAFOs, average NH_3 emission rates varied between 31.9 kg_{NH3}/h and 191 kg_{NH3}/h (Tables S2 and SI), while average CH_4 emission rates varied between 155.3 kg_{CH4}/h and 873.6 kg_{CH4}/h (Tables S3 and SI). The highest NH_3 emissions were seen at WT4, which is one of the largest CAFOs, while for CH_4 the highest emission was seen at CAFO SB5 in the October campaign. The number of measurements per target facility was on average eight. The lowest emissions for both NH_3 and CH_4 were seen at ET1, which is the smallest dairy.

Fig. 3 shows the NH_3 and CH_4 EFs for the investigated 14 dairy CAFOs based on the measurements performed in May. EFs were obtained by normalizing the measured CAFOs emission rates by livestock unit. Around 40% of the dairies had an NH_3 EF higher than 10 $g_{NH3}/LU/h$ (Fig. S6a in SI), the EFs median value corresponded to 9.8 $g_{NH3}/LU/h$ and the 90th percentile of 12.1 $g_{NH3}/LU/h$ (Table S2 in SI). EFs obtained by normalizing to only the number of mature animals were on average 16.4 ± 5.7 $g_{NH3}/head_{Mature\ cow}/h$ or 18.9 ± 6.2 $g_{NH3}/head_{Milkcow}/h$. For CH_4, around 73% of the CAFOs had an EF below 50 $g_{CH4}/LU/h$ and an EFs median of 34 $g_{CH4}/LU/h$ (Fig. S6 in SI). For some of the dairies, such as NB2, the EF factors were rather high (Fig. 3b).

Comparison of the emissions measured in May and October for a subset of the CAFOs was done (Fig. 4). Average daytime temperatures during the individual measurements in each campaign were similar, i.e., 24 °C in May and 22 °C in October, respectively (Fig. S7 in SI). Average wind speeds during the individual measurement campaigns were higher in May (3.6 ± 1 m/s) than in October (2.8 ± 0.7 m/s). The results show that there was no difference in NH_3 emissions between the October and May campaigns (differences were within uncertainty levels), which could be expected from the fact that measurements were performed in seasons with similar average temperatures. The same is valid for the CH_4 measurements with the exception of CAFOs NB2 and SB4. One uncertainty that could not be accounted for was whether cattle numbers or CAFO management practices were the same during the two campaigns.

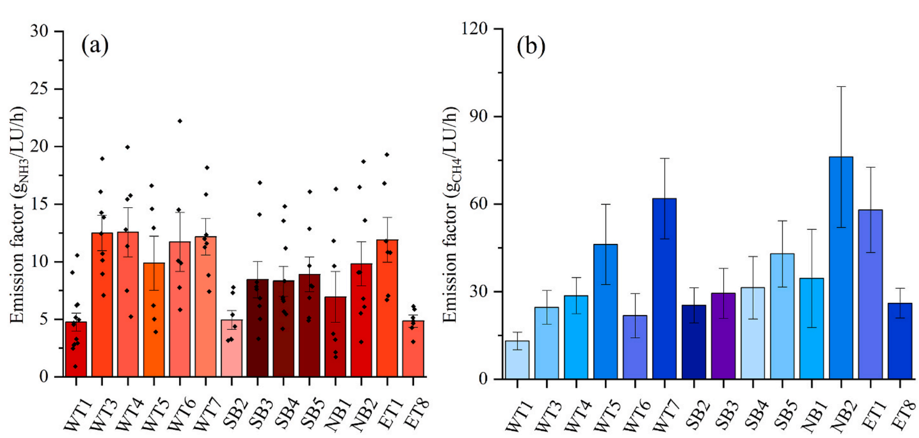

Fig. 3. (a) NH_3 emission factors (average and standard uncertainty (68% confidence limit)) and sampled transects (black dots). (b) CH_4 emission factors (average and standard uncertainty).

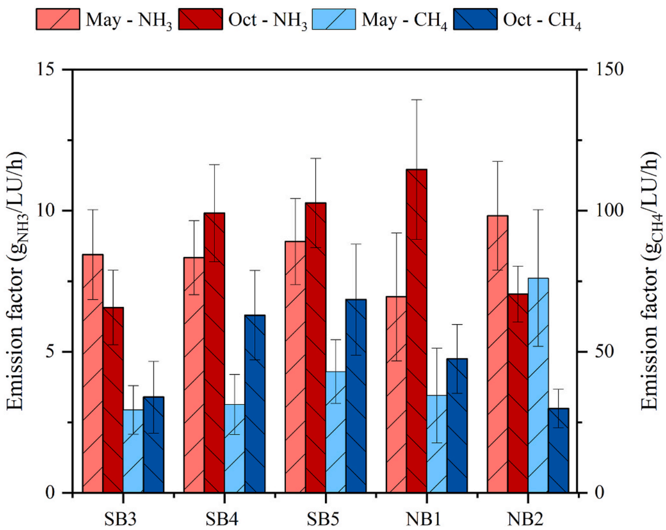

Fig. 4. EFs for five CAFOs during the October and May campaigns, and standard uncertainty.

4. Discussion

4.1. Measurement uncertainty

Errors in the SOF ammonia (NH_3) measurements were estimated per individual dairy (Table S4 in SI) following the GUM procedure (Joint Committee For Guides In Metrology, 2008), as illustrated in Table 3.

Uncertainty was dominated by the random error, directly estimated from the 1σ variability of the individual fluxes (or ratios) divided by the square root of the number of transects. In addition, systematic measurement errors, unchanged between measurements transects, were caused by the spectroscopic retrieval method, uncertainty in spectroscopic parameters, systematic inflow from upwind sources, and the assumed plume height. Here, the uncertainty related to the NH_3 cross-sections (Systematic error - strength of the cross-section) between 700 and 1200 cm^{-1} was obtained from Kleiner et al. (2003), which corresponds to 2% error. The retrieval error was obtained from the ratio between the standard deviation of the fitting residual, divided by square-root of the number of points, and the average NH_3 absorbance in 960–968 cm^{-1}. The wind speed error was obtained by the systematic discrepancy in the wind speed between the different heights intervals (0–50 m to 0–300 m). The last is a conservative estimate which, assumes that the plume height was estimated wrongly. The background error was estimated from any systematic differences in the upwind column values caused by the presence of interfering sources. The error was obtained by calculating the flux for the different baseline values, and comparing its average with the primarily estimate emission. Further, the average of the error from the different transects was used as the error value for the specific facility. Uncertainty was obtained by error propagation, taking the square root of the quadratic sum of the uncertainties as given in Table 3. The total estimated uncertainty for NH_3 median emission was 17% (range per facility of 11–32%) for 68% Confidence interval (CI) and 37% (range per facility of 23–76%) for 95% CI (Table 3 and Table S4 in SI).

The measurement error for CH_4 emissions includes uncertainty in both NH_3 emissions, as given above, and in estimating the NH_3-to-CH_4 ratio for the overall facility, since both are included when calculating the CH_4 emission. Uncertainty in the ratio is dominated by random uncertainty, estimated from the measured variability, although several systematic uncertainties are also important (Table 3 and Table S5 in SI). In particular, this includes the source misallocation error, which is caused by the fact that in some cases NH_3 and CH_4 are released at different distances away from the measurement position, and hence they are diluted differently. This error was assessed by Gaussian plume modeling (Fig. S8 in SI). Note that since the ratio is calculated from the integrated values across the measurement transect (Eq. (2)) it is mainly the difference in distance between source and measurement position along the wind that causes errors and not the sideways separation between the sources. Background error was similarly estimated for the concentration measurements of NH_3 and CH_4, while some of the systematic errors for NH_3 were cancelled out when doing the normalization between MeFTIR and SOF (Eq. (2)). The uncertainty on the CH_4 cross section was obtained from (Brown et al., 2003), while the reported error by MALT (Smith et al., 2011) was used as the CH_4 retrieval uncertainty. The median estimated uncertainty for CH_4 emissions was 25% (range per facility of 19–49%) for 68% CI and 53% (40–119%) for 95% CI (Table 3 and Table S5 in SI). Throughout the article, the authors adopted standard uncertainty (68% CI) in the data analysis, because it is more commonly used in scientific literature for this type of measurements (Johansson et al., 2014; Johnson et al., 2017).

Table 3
Measurement uncertainty for the direct and indirect flux calculations.

SOF/Direct Flux	
Systematic - Spectroscopic – strength of the cross-section NH_3	2 %[a]
Systematic - Spectroscopic - retrieval	4.4 %[a]
Systematic - Background errors (facility-specific)	1–14%
Systematic - Wind speed uncertainty in height	11–12%
Random - Measurement variability (facility-specific)	8–31%
Median standard uncertainty (68% confidence)	*17% (11–32%)*
Median expanded uncertainty (95% confidence)	*37% (23–76%)*
MeFTIR/Indirect flux	
Systematic - Spectroscopic – strength of the cross-section NH_3	0 %[a]
Systematic - Spectroscopic – strength of the cross-section CH_4	3%
Systematic - Spectroscopic – retrieval NH_3	0 %[a]
Systematic - Spectroscopic – retrieval CH_4	5.6%
Systematic - Sources mismatch (facility-specific)	5–41%
Systematic - SOF NH_3 uncertainty (facility-specific)	12–32%
Systematic - Background error – NH_3 (facility-specific)	1–10%
Systematic - Background error – CH_4 (facility-specific)	1–10%
Random - Ratios measurement variability (facility-specific)	5–36%
Median standard uncertainty (68% confidence)	*25% (19–49%)*
Median expanded uncertainty (95% confidence)	*53% (40–119%)*

[a] Some of the systematic spectroscopic errors for NH_3 will be cancelled out when doing the normalization (Eq. (2)) between SOF and MeFTIR.

4.2. Comparison of measured ammonia emission rates with other data

4.2.1. Measurement representativeness

NH_3 emissions from manure (feeding area, stall, or manure storage) are known to increase as a result of temperature, wind, and solar radiation (Hristov et al., 2011; Sun et al., 2015), consequently varying throughout different seasons (U.S. Environmental protection Agency, 2018). The measurements were carried out in May and October, and as can be seen in Fig. 4, the emissions are approximately the same during both periods and halfway between the modeled maximum and minimum emissions (Fig. S4b in SI). This is likely due to the fact that the average daily temperatures for both these months were close to the yearly average (May: 20 °C; Oct: 18.6 °C; Annual: 19.4 °C) (NOAA's National Weather Service, 2019). The diurnal model and the NEI inventory shows, that the NH_3 emissions should be 2% lower in October and 9% higher in May than the annual average, respectively (Fig. S4 in SI). Other variables as precipitation, humidity and solar radiation were not further evaluated, however, they should follow annual temperature trends, and therefore the measured months (October and May) would be close to the expected yearly average.

Studies that have measured NH_3 daily dynamics indicate that the difference between midday peak emissions and night-time lower emissions can vary by a factor of between two and five (Bjorneberg et al., 2009; Golston et al., 2020; Harper et al., 2009; Leytem et al., 2011; Sun et al., 2015). As the SOF technique uses the sun as a light source, NH_3 measurements were carried out during the daytime and in sunny conditions. The NH_3 emission factors measured in this study showed a diurnal behavior with peak emissions at around 14:00 (Fig. 5b). In order to evaluate the diurnal variation of the measured NH_3 emissions, they were compared to modeled diurnal emissions, which were calculated using the average emission factor from the NEI inventory and a model for diurnal variation (Zhu et al., 2015a) provided by the US EPA (J. Bash, personal communication, 2020) (see section 2.4)). The single measured transect and modeled NH_3 emissions were normalized to the average CAFOs emissions of each measured facility, thus obtaining the emission variations. The modeled diurnal behavior for the specific measurement times is shown in Fig. 5a and b, while the full measurement period is in Fig. S4 in SI. It is evident that the average of the normalized SOF data and the model data agree rather well. Fig. S4 in SI shows the average inventory EF (straight line) and the modeled daily emission variations for May and October (bell shaped curve). The impact of diurnal emission variations caused in inventory and measurements comparisons has previously been pointed out by Lonsdale et al. (2017), who noted that the CARB inventory would be overestimated by a factor of 2.4 when compared to a single measurement at 13:00 local time.

The obtained NH_3 to CH_4 ratios, were normalized with the average ratio of each individual dairy value (Fig. 5c and d). The diurnal behavior of the NH_3 to CH_4 emission ratios followed the same diurnal trend as the NH_3 emissions. A similar diurnal pattern has been observed also in other studies (Eilerman et al., 2016; Golston et al., 2020; Miller et al., 2015). Most of the diurnal variation in the ratios are probably caused by changes in NH_3 emissions rather than CH_4, since temperature and solar insolation have relatively small impact on the emission on the latter (Arndt et al., 2018; Bjorneberg et al., 2009; Golston et al., 2020; Leytem et al., 2011; Sun et al., 2015). On average, 71% of the daytime variation in the ratio can be explained by NH_3 variations in October, based on the comparison between measured ratios and quantified fluxes, and 83% for the May data (Fig. 5). Multi-variable linear regression analyses of the measurement data (ratios and emission rates) versus ambient parameters (Table S6 in SI) shows significant correlations only for the time of the day.

4.2.2. Comparison of measured ammonia emission rates with inventory and other literature

On average, the measured NH_3 emissions were 28% higher in comparison to inventory estimates accounting for diurnal variations, using the model provided by Zhu et al. (2015a) (Fig. 6). This was not the case for all individual facilities, for example CAFO WT6 (Fig. 6). Excluding daily emission variations in the inventory emission rates, the measured emissions would instead be 71% higher. Some of the differences between measured and estimated emissions for specific facilities might be related to uncertainties in the numbers of animals, which can vary between the inspection day for the San Joaquim Valley pollution control district and the measurement day.

A comparison of emission factors at dairy cattle farms obtained in various studies is shown in Table 4. The EFs in this study are at the high end, consistent with that the SOF data (Kille et al., 2017) corresponds to daytime values, as discussed above, and the same tendency can also be seen in other daytime studies. By assuming the modeled diurnal pattern described above (Zhu et al., 2015a), the measured EF factors were converted to daily averages corresponding to 3.0 g_{NH3}/h/LU/in May and to 4.2 g_{NH3}/h/LU in October, respectively; hence in better agreement with some of the other studies in Table 4. Additionally, according to recent studies, NH_3 emissions measured close to ground level might be underestimated due to NH_3 deposition or missampling of the concentrated part of the plume. The plume might be located lofted, which would not affect SOF measurements, since it measures whole air columns concentrations (Lassman et al., 2020), differently from ground measurements only. It is relevant to highlight that most of the farms were measured under similar wind speed conditions, except WT06 and WT04, measured at averaged higher wind speeds, which could partially explain the high emission factors observed compared to inventory estimates.

4.3. Comparison of the measured CH_4 emission rates with other data

The measured farm-scale CH_4 emissions were on average 60% higher than those modeled by inventories. For the five CAFOs that were measured both in May and October the average difference drops to 40%. The measured CH_4 emissions are associated with greater uncertainties than the NH_3 fluxes, and the variability between individual facilities

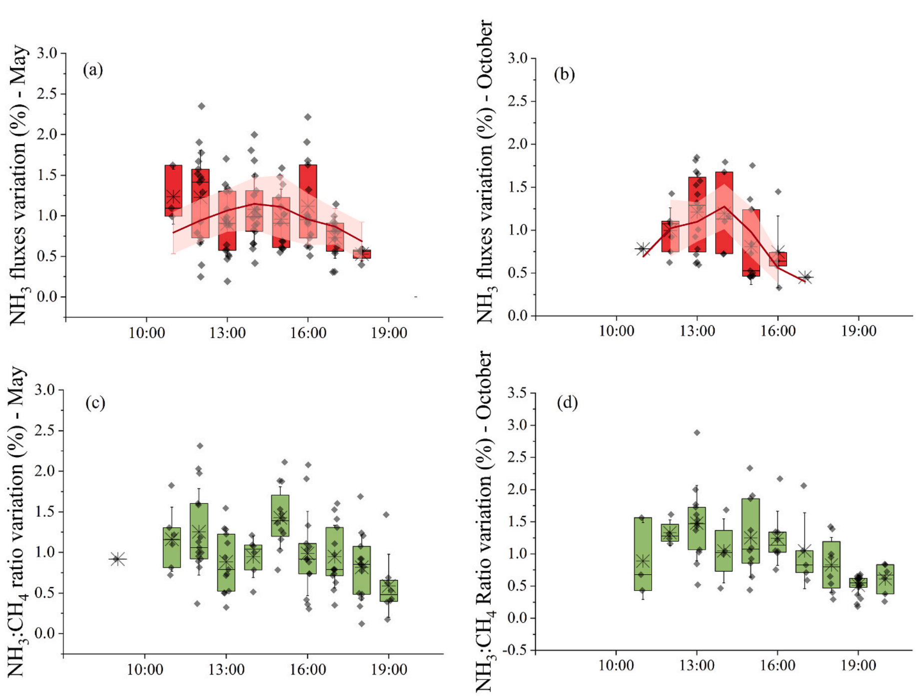

Fig. 5. Variation of NH_3 emissions (a, b) and NH_3:CH_4 ratios (c, d) versus time of the day for all CAFOs (time specific by average) and classified according to the measured period. Solid lines in Figures a and b correspond to the average of the modeled values from the same period as the measurements. In the box plot, the average is indicated by the star-shaped symbol. The diamond symbols correspond to each measured transect. The upper box represented the 75% percentile, while the lower corresponds to 25% percentile. The whiskers show the standard deviation.

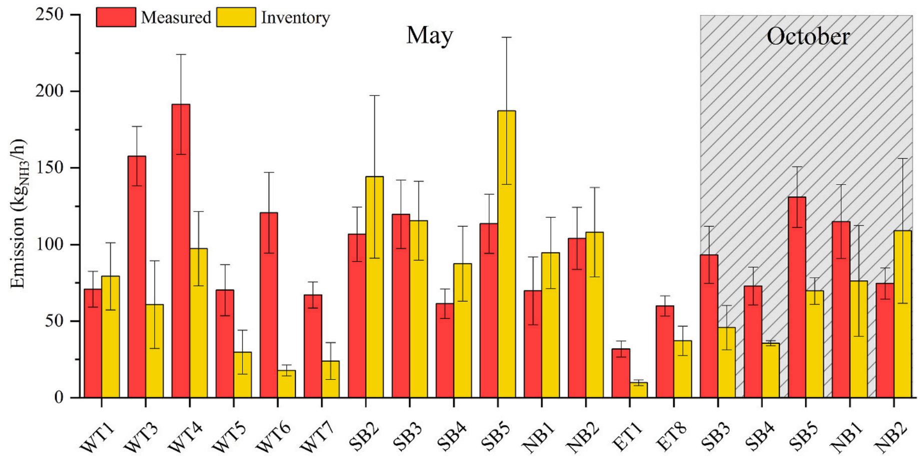

Fig. 6. Comparison of measured NH_3 emissions (average and standard uncertainty), and modeled day time emissions (average and standard deviation from hourly emissions), using NEI 2014 and (Zhu et al., 2015a)(average and standard deviation).

Table 4
Average emission factors at CAFOs for NH_3 and CH_4 with corresponding standard uncertainties. In addition, NH_3:CH_4 ratios from other studies are illustrated.

Farm	Period	Method/Instrument	NH_3 (g/h/LU) [k]	NH_3 (g/h/head)	CH_4 (g/h/LU)	CH_4 (g/h/head) [l]	NH_3:CH_4 g/g
Present study dairy, CAFO (California)	Spring and autumn (Day-time)	SOF and MeFTIR	9.0 ± 2.6	16.8 ± 5.5	40.1 ± 17.8	74.0 ± 32.8	21
Average farm NEI (NH_3) and CARB inventory (CH_4)[m]	Yearly	Inventory	6.7–6.8		30.7		
Dairy, CAFO (Colorado)[a]	August (Day-time)	SOF		11.4 ± 3.4			
Dairy, CAFO (Colorado)[b]	Summer, winter, spring, autumn	Cavity Ring spectroscopy					14–17
Dairy, CAFO (California)[c]	Winter (January)	Open-Path (WMS, Licor)					14 ± 3
Dairy farm (California)[d]	Winter and summer	Open path/Inverse dispersion modeling			26.0 ± 7.4 (Winter) 58.9 ± 10.5 (Summer)		
Dairy farm (Washington)[e]	Yearly model	DOAS, Tracer ratio flux		4.6			
Dairy CAFO (Idaho)[f]	Summer, winter, spring, autumn	Open-path FTIR/Inverse Dispersion modeling	8.1 1.2	10.4 1.7	17.1 5.3	22.9 8.3	12–90
Dairy CAFOs (California)[g]	Summer (June)	Airborne/surface (AMOG/MISTIR)		38		76	52
Dairy CAFO (Idaho)[h]	Whole year (Monthly)	Open-path/Inverse dispersion method	4.9	6.3	45.1	57.9	2–10
Dairy CAFO (Colorado)[i]	Summer	Tildas, Licor and others/ modeled emissions	5.3 ± 0.5		39.3 ± 3.9		40
Dairy farm(Canada)[j]	Spring and autumn	Open-path/inverse dispersion modeling				20.7 ± 1.2 8.8 ± 2.2	37

[a] Kille et al., 2017.
[b] Eilerman et al., 2016.
[c] Miller et al., 2015.
[d] Arndt et al., 2018.
[e] Rumburg et al., 2008.
[f] Bjorneberg et al., 2009.
[g] Leifer et al., 2018.
[h] Leytem et al., 2011.
[i] Golston et al., 2020.
[j] VanderZaag et al., 2014.
[k] Livestock unit (LU), 1 LU = 500 kg of body weight.
[l] head of dairy cows only.
[m] U.S. Environmental protection Agency, 2018, CARB, 2019b.

were relatively high (Fig. 7). The uncertainty is especially large for some CAFOs, e.g., NB1-May, a result of the combined SOF and ratios' large measurement variability.

The inventory values agree with the measurements in 9 out of 19 measurements when considering the 68% CI (Fig. 7).The measurements are at the high end of the values reported in other studies (Table 4). Recent studies have found a good correlation between measured CH_4 and inventory (Arndt et al., 2018; Golston et al., 2020).

Most (75%) of the measured NH_3:CH_4 ground concentration ratios (n = 205) were below 25 g_{NH3}/g_{CH4} (Fig. S6b in SI). Differences within CAFOs are likely a reflection of differences in management or measurement time. A few observed ratios were larger than 80 g_{NH3}/g_{CH4}, likely due to specific short-term activities, e.g., the mixing of solid manure piles, which could be observed from the CAFO fence line. The ratios obtained are comparable to results from recent studies carried out in the same area or at the same type of facility (Eilerman et al., 2016; Miller et al., 2015). There are differences when compared to some other studies (Bjorneberg et al., 2009; Kille et al., 2019; Leifer et al., 2018), but we believe this is mostly due to different seasons or manure management.

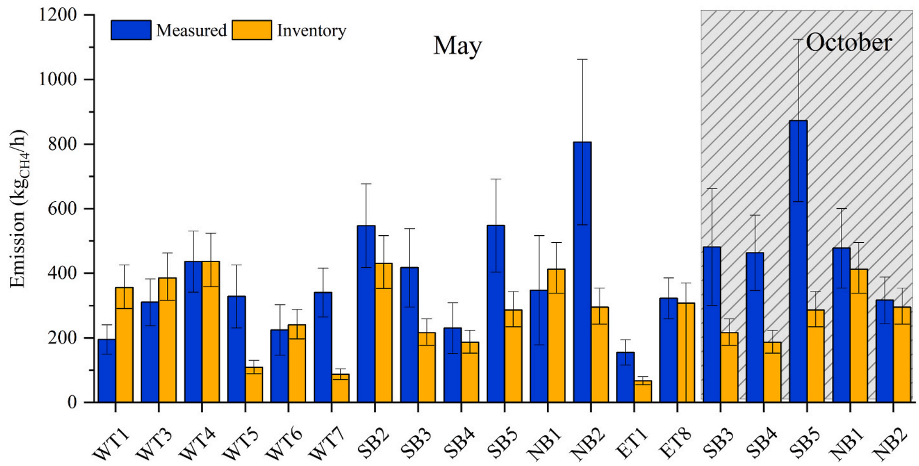

Fig. 7. Comparison of measured CH_4 emissions (average and standard uncertainty) and CARB inventory annual emissions (average and CI 95%) (U.S. Environmental Protection Agency, 2013).

4.3.1. Factors affecting CH_4 emissions

While NH_3 emissions are consistently reported to vary during the day, this is not the case for CH_4 emissions. Arndt et al. (2018) noted a small increase during rumination time, Leytem et al. (2011) found larger variations between day and night, Golston et al. (2020) and Sun et al. (2015) found an increase in emissions at the end of the day, while others did not observe any clear pattern at all (Bjorneberg et al., 2009). For CH_4 emissions, seasonal variations have also been reported (Bjorneberg et al., 2009; Leytem et al., 2011); however, since the campaign months of May and October have temperatures close to the annual average, our measurements should also be close to annual averaged emission values.

In this study, we lack detailed knowledge about manure management practices at the CAFOs that can influence CH_4 emissions, such as manure management, storage time, and animal feeding. However, a rough assessment of the manure practices at the individual facilities was done during the campaigns by studying maps and making visual observations, e.g., making it possible to identify farms with and without a manure lagoon cover, which enables the facility to collect the CH_4 produced in lagoons and use the gas as an energy source. In total, 5 of the measured CAFOs used this system. Noteworthy here is that these farms did not emit significantly less than those without a cover (Fig. 8). Uncertainties in terms of animal numbers or the measurements may have contributed to concealing any differences. An alternative explanation is that even though we did observe the presence of a lagoon cover, we lacked information regarding whether the system was actually operational. For example, observation of high CH_4 peaks persistently correlated to the digesters. Additionally, two of the farms had their systems recently built, thus raising doubts about whether or not they were already operational.

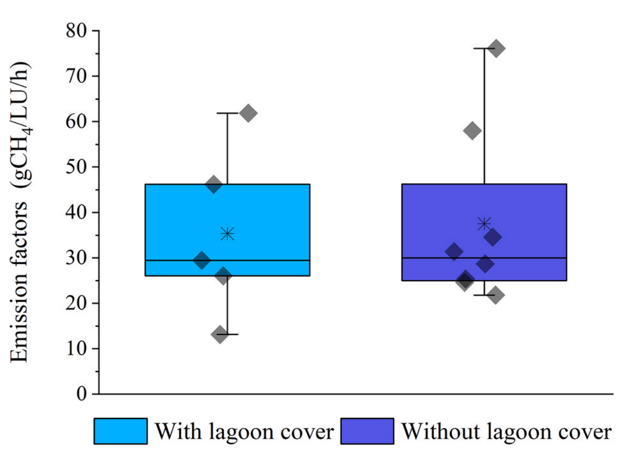

Fig. 8. Comparison of CH_4 emissions from CAFOs with and without a lagoon cover. The mean is represented by the square symbol, the median by the horizontal solid line, the lower part of the box shows the 25th percentile while the upper part is the 75th percentile.

4.3.2. Comparison of measured CH_4 emissions and previous measurements, using other techniques

Some of the farms in this study were previously measured for airborne CH_4 emissions by Scientific Aviation (Thompson et al., 2019), as illustrated in Fig. 9. The approach used by Scientific Aviation comprises a mass balance calculation, based on Gaussian law. The aircraft flies in circles around the facility, from the minimum safe height to above the plume height (Conley et al., 2017).

These measurements were carried out over four campaigns in 2018 and 2019, and the last one coincided in time with this study, as indicated in Fig. 9. For sites SB2 and SM1, measurements were done on the same day or within a few days. The error bars in the Scientific Aviation data correspond to measurement uncertainty. As evidence herein, the two datasets overlap reasonably well, given the measurement uncertainties, with the exception of ET8. Note that the latter airborne measurement

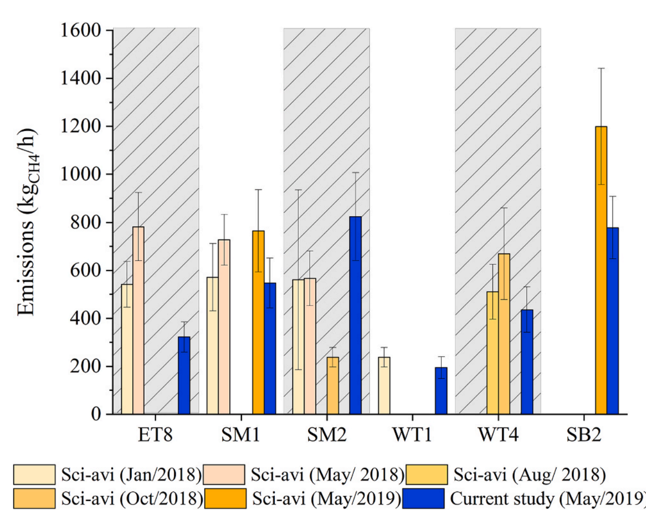

Fig. 9. Comparison of CH_4 emission rates measured by Scientific Aviation using a mass balance approach and SOF (present study) (average and standard uncertainty). The farms compared here are ET8, WT1, WT4, SB2, and two other from Madera County, which were not included in the inventory analysis. SB2 measurements were done on the same day.

was carried out one year before the present study. The advantage of the indirect flux technique over the airborne mass flux approach is its higher spatial resolution and, consequently, the ability to measure an individual facility more easily, although both approaches have a limitation relating to the measurement period, because they require specific weather conditions.

5. Conclusions

Several optical methods, i.e., solar occultation flux (SOF) and MeFTIR, were used to quantify ammonia (NH_3) and methane (CH_4) emissions, respectively, at dairy CAFOs in the San Joaquin Valley, California, United States. The measurement uncertainty of NH_3 flux by SOF for the measured CAFOs was estimated to a median value of 17% for 68% CI, and the largest error sources were measurement variability (random error) and wind speed uncertainty. When comparing daytime emissions of NH_3 measured by SOF with inventory data, the former yields 71% higher emission values than the latter, primarily driven by the fact that the emissions are affected by temperature and solar insolation. When taking diurnal variations in these environmental factors into account the difference is lowered to 28%. In addition, when comparing the daytime emission results from SOF to other studies in the literature, the former are at the high end, since most of the other studies include both day and night contributions.

The CH_4 emission measurements have larger uncertainties than the NH_3 measurements (25% for 68% CI, and 53% for 95% CI). The measured emissions are 60% higher than the CARB inventory, and the values are towards the high end when compared to other studies in the literature. An uncertainty in this study is in the lack of detailed knowledge about management practices in the measured facilities. From visual observations, it is estimated that 35% of the CAFOs had covered manure lagoons. However, this practice was not observed to abate the emissions. The obtained CH_4 emissions in this study correspond reasonably well with airborne measurements done using a mass balance approach at six of the studied CAFOs, indicating that our CH_4 results were consistent with other measurement approaches.

Complementary measurements during night periods or in different seasons could provide a better understanding of emissions dynamics. The methods described herein offer a suitable approach for monitoring emissions from CAFOs, as they can cover several facilities in a short time period, without being expensive or labor-intensive.

CRediT authorship contribution statement

N.T. Vechi: Conceptualization, Writing – original draft, Writing – review & editing, Data curation, Formal analysis, Investigation. **J. Mellqvist:** Conceptualization, Writing – review & editing, Methodology, Data curation, Funding acquisition, Supervision. **J. Samuelsson:** Methodology, Data curation, Project administration. **B. Offerle:** Methodology, Data curation, Formal analysis. **C. Scheutz:** Conceptualization, Formal analysis, Funding acquisition, Writing – review & editing, Supervision.

Declaration of competing interest

The authors declare that they have no known competing financial interests or personal relationships that could have appeared to influence the work reported in this paper.

Data availability

Data will be made available on request.

Acknowledgments

This data was collected under sponsorship from CARB, contract 17RD021 “Characterization of Air Toxics and GHG Emission Sources and their Impacts on Community-Scale Air Quality Levels in Disadvantaged Communities” by FluxSense Inc. We are especially thankful to Jesse Bash from the U.S. Environmental Protection Agency for providing us with the ammonia diurnal normalized profiles.

Appendix A. Supplementary data

Supplementary data to this article can be found online at https://doi.org/10.1016/j.atmosenv.2022.119448.

References

American Jersey Cattle Association, 2015. A Quality Heifer. Productive Life in the Industry.

Arndt, C., Leytem, A.B., Hristov, A.N., Zavala-Araiza, D., Cativiela, J.P., Conley, S., Daube, C., Faloona, I., Herndon, S.C., 2018. Short-term methane emissions from 2 dairy farms in California estimated by different measurement techniques and US Environmental Protection Agency inventory methodology: a case study. J. Dairy Sci. 101, 11461–11479. https://doi.org/10.3168/jds.2017-13881.

Bjorneberg, D.L., Leytem, a B., Westermann, D.T., Griffiths, P.R., Shao, L., Pollard, M.J., 2009. Measurement of atmospheric ammonia, methane, and nitrous oxide at a concentrated dairy production facility in southern Idaho using open-path FTIR spctrometry. Transcations Am. Soc. Agric. Biol. Eng. 52, 1749–1756. https://doi.org/10.13031/2013.29137.

Brodeur, J.J., Warland, J.S., Staebler, R.M., Wagner-Riddle, C., 2009. Technical note: laboratory evaluation of a tunable diode laser system for eddy covariance measurements of ammonia flux. Agric. For. Meteorol. 149, 385–391. https://doi.org/10.1016/j.agrformet.2008.08.009.

Brown, L.R., Benner, D.C., Champion, J.P., Devi, V.M., Fejard, L., Gamache, R.R., Gabard, T., Hilico, J.C., Lavorel, B., Loete, M., Mellau, G.C., Nikitin, A., Pine, A.S., Predoi-Cross, A., Rinsland, C.P., Robert, O., Sams, R.L., Smith, M.A.H., Tashkun, S. A., Tyuterev, V.G., 2003. Methane line parameters in HITRAN. J. Quant. Spectrosc. Radiat. Transf. 82, 219–238. https://doi.org/10.1016/S0022-4073(03)00155-9.

CARB, 2019a. CH4 [WWW Document]. URL. https://ww3.arb.ca.gov/cc/inventory/background/ch4.htm, 8.18.20.

CARB, 2019b. Greenhouse gas emissions inventory - query results [WWW Document]. Greenh. Gas Emiss. Invent. Summ. [2000 - 2017]. URL. https://www.arb.ca.gov/app/ghg/2000_2017/ghg_sector_data.php, 9.2.20.

Conley, S., Faloona, I., Mehrotra, S., Suard, M., Lenschow, D.H., Sweeney, C., Herndon, S., Schwietzke, S., Pétron, G., Pifer, J., Kort, E.A., Schnell, R., 2017. Application of Gauss's theorem to quantify localized surface emissions from airborne measurements of wind and trace gases. Atmos. Meas. Tech. 10, 3345–3358. https://doi.org/10.5194/amt-10-3345-2017.

Delre, A., Mønster, J., Samuelsson, J., Fredenslund, A.M., Scheutz, C., 2018. Emission quantification using the tracer gas dispersion method: the influence of instrument, tracer gas species and source simulation. Sci. Total Environ. 634, 59–66. https://doi.org/10.1016/j.scitotenv.2018.03.289.

Eilerman, S.J., Peischl, J., Neuman, J.A., Ryerson, T.B., Aikin, K.C., Holloway, M.W., Zondlo, M.A., Golston, L.M., Pan, D., Floerchinger, C., Herndon, S., 2016. Characterization of ammonia, methane, and nitrous oxide emissions from concentrated animal feeding operations in northeastern Colorado. Environ. Sci. Technol. 50, 10885–10893. https://doi.org/10.1021/acs.est.6b02851.

European standard, 2022. EN 17628:2022 [WWW Document]. URL. https://www.sis.se/api/docu ment/preview/80034943/.

Golston, L.M., Pan, D., Sun, K., Tao, L., Zondlo, M.A., Eilerman, S.J., Peischl, J., Neuman, J.A., Floerchinger, C., 2020. Variability of ammonia and methane emissions from animal feeding operations in northeastern Colorado. Environ. Sci. Technol. 54, 11015–11024. https://doi.org/10.1021/acs.est.0c00301.

Griffith, D.W.T., 1996. Synthetic calibration and quantitative analysis of gas-phase FT-IR spectra. Appl. Spectrosc. 50, 59–70. https://doi.org/10.1366/0003702963906627.

Harper, L.A., Flesch, T.K., Powell, J.M., Coblentz, W.K., Jokela, W.E., Martin, N.P., 2009. Ammonia emissions from dairy production in Wisconsin. J. Dairy Sci. 92, 2326–2337. https://doi.org/10.3168/jds.2008-1753.

Harris, T.D., Smith, V.H., Graham, J.L., Waa, D.B.V. de, Tedesco, L.P., Clercin, N., 2016. Combined effects of nitrogen to phosphorus and nitrate to ammonia ratios on cyanobacterial metabolite concentrations in eutrophic Midwestern USA reservoirs. Inl. Waters 6, 199–210. https://doi.org/10.5268/IW-6.2.938.

Hristov, A.N., Hanigan, M., Cole, A., Todd, R., McAllister, T.A., Ndegwa, P.M., Rotz, A., 2011. Review: ammonia emissions from dairy farms and beef feedlots. Can. J. Anim. Sci. 91, 1–35. https://doi.org/10.4141/CJAS10034.

Hristov, A.N., Harper, M., Meinen, R., Day, R., Lopes, J., Ott, T., Venkatesh, A., Randles, C.A., 2017. Discrepancies and uncertainties in bottom-up gridded inventories of livestock methane emissions for the contiguous United States. Environ. Sci. Technol. 51, 13668–13677. https://doi.org/10.1021/acs.est.7b03332.

Hristov, A.N., Kebreab, E., Niu, M., Oh, J., Bannink, A., Bayat, A.R., Boland, T.M., Brito, A.F., Casper, D.P., Crompton, L.A., Dijkstra, J., Eugène, M., Garnsworthy, P.C., Haque, N., Hellwing, A.L.F., Huhtanen, P., Kreuzer, M., Kuhla, B., Lund, P., Madsen, J., Martin, C., Moate, P.J., Muetzel, S., Muñoz, C., Peiren, N., Powell, J.M., Reynolds, C.K., Schwarm, A., Shingfield, K.J., Storlien, T.M., Weisbjerg, M.R., Yáñez-Ruiz, D.R., Yu, Z., 2018. Symposium review: uncertainties in enteric methane inventories, measurement techniques, and prediction models. J. Dairy Sci. 6655–6674. https://doi.org/10.3168/jds.2017-13536.

IPCC, 2006. IPCC Guidelines for National Greenhouse Gas Inventories, Agriculture, Forestry and Other Land Use, Prepared by the National Greenhouse Gas Inventories Programme. CIGES, Japan.

IPCC, 2021. Climate Change 2021: the Physical Science Basis.. Contribution of Working Group I to the Sixth Assessment Report of the Intergovernmental Panel on Climate Change. Cambridge University Press, Cambridge, United Kingdom and New York, NY, USA.

Johansson, J., 2016. Optical Remote Sensing of Industrial Gas Emission Fluxes. Chalmer University of Technology.

Johansson, J., Mellqvist, J., Samuelsson, J., Offerle, B., Lefer, B., Rappenglück, B., Flynn, J., Yarwood, G., 2014. Emission measurements of alkenes, alkanes, SO2 and NO2 from stationary sources in southeast Texas over a 5 year period using SOF and Mobile DOAS. J. Geophys. Res. 1–8. https://doi.org/10.1002/2013JD021350 (Received).

Johnson, M.R., Tyner, D.R., Conley, S., Schwietzke, S., Zavala-Araiza, D., 2017. Comparisons of airborne measurements and inventory estimates of methane emissions in the alberta upstream oil and gas sector. Environ. Sci. Technol. 51, 13008–13017. https://doi.org/10.1021/acs.est.7b03525.

Joint Committee For Guides In Metrology, 2008. Evaluation of measurement data - guide to the expression of uncertainty in measurement. Int. Organ. Stand. Geneva 50, 134. ISBN.

Kihlman, M., 2005. Application of Solar FTIR Spectroscoy for Quantingfying Gas Emissions. Chalmers University of Technology, Gothenburg, Sweden.

Kille, N., Baidar, S., Handley, P., Ortega, I., Sinreich, R., Cooper, O.R., Hase, F., Hannigan, J.W., Pfister, G., Volkamer, R., 2017. The CU mobile Solar Occultation Flux instrument: structure functions and emission rates of NH3, NO2 and C2H6. Atmos. Meas. Tech. 10, 373–392. https://doi.org/10.5194/amt-10-373-2017.

Kille, N., Chiu, R., Frey, M., Hase, F., Sha, M.K., Blumenstock, T., Hannigan, J.W., Orphal, J., Bon, D., Volkamer, R., 2019. Separation of methane emissions from agricultural and natural gas sources in the Colorado front range. Geophys. Res. Lett. 46, 3990–3998. https://doi.org/10.1029/2019GL082132.

Kleiner, I., Tarrago, G., Cottaz, C., Sagui, L., Brown, L.R., Poynter, R.L., Pickett, H.M., Chen, P., Pearson, J.C., Sams, R.L., Blake, G.A., Matsuura, S., Nemtchinov, V., Varanasi, P., Fusina, L., Di Lonardo, G., 2003. NH3 and PH3 line parameters: the 2000 HITRAN update and new results. J. Quant. Spectrosc. Radiat. Transf. 82, 293–312. https://doi.org/10.1016/S0022-4073(03)00159-6.

Lassman, W., Collett, J.L., Ham, J.M., Yalin, A.P., Shonkwiler, K.B., Pierce, J.R., 2020. Exploring new methods of estimating deposition using atmospheric concentration measurements: a modeling case study of ammonia downwind of a feedlot. Agric. For. Meteorol. 290 https://doi.org/10.1016/j.agrformet.2020.107989.

Leifer, I., Melton, C., Tratt, D.M., Buckland, K.N., Chang, C.S., Frash, J., Hall, J.L., Kuze, A., Leen, B., Clarisse, L., Lundquist, T., Van Damme, M., Vigil, S., Whitburn, S., Yurganov, L., 2018. Validation of mobile in situ measurements of dairy husbandry emissions by fusion of airborne/surface remote sensing with seasonal context from the Chino Dairy Complex. Environ. Pollut. 242, 2111–2134. https://doi.org/10.1016/j.envpol.2018.03.078.

Leifer, I., Melton, C., Tratt, D.M., Buckland, K.N., Clarisse, L., Coheur, P., Frash, J., Gupta, M., Johnson, P.D., Leen, J.B., Van Damme, M., Whitburn, S., Yurganov, L., 2017. Remote sensing and in situ measurements of methane and ammonia emissions from a megacity dairy complex: chino, CA. Environ. Pollut. 221, 37–51. https://doi.org/10.1016/j.envpol.2016.09.083.

Lelieveld, J., Evans, J.S., Fnais, M., Giannadaki, D., Pozzer, A., 2015. The contribution of outdoor air pollution sources to premature mortality on a global scale. Nature 525, 367–371. https://doi.org/10.1038/nature15371.

Leytem, A.B., Dungan, R.S., Bjorneberg, D.L., Koehn, A.C., 2011. Emissions of ammonia, methane, carbon dioxide, and nitrous oxide from dairy cattle housing and manure management systems. J. Environ. Qual. 40, 1383. https://doi.org/10.2134/jeq2009.0515.

Locker, I., Woodward, A., 2010. Introducing the New ZephIR 300. Wind. Int.

Lonsdale, C.R., Hegarty, J.D., Cady-pereira, K.E., Alvarado, M.J., Henze, D.K., Turner, M. D., Capps, S.L., Nowak, J.B., Neuman, J.A., Middlebrook, A.M., Bahreini, R., Murphy, J.G., Markovic, M.Z., Vandenboer, T.C., Russell, L.M., 2017. Modeling the diurnal variability of agricultural ammonia in Bakersfield. In: California , during the CalNex campaign, pp. 2721–2739. https://doi.org/10.5194/acp-17-2721-2017, 3.

Marklein, A.R., Meyer, D., Fischer, M.L., Jeong, S., Rafiq, T., Carr, M., Hopkins, F.M., 2021. Facility-scale inventory of dairy methane emissions in California: implications for mitigation. Earth Syst. Sci. Data 13, 1151–1166. https://doi.org/10.5194/essd-13-1151-2021.

Mellqvist, J., Samuelsson, J., Andersson, P., Brohede, S., Isoz, O., Ericsson, M., 2017. Using Solar Occultation Flux and Other Optical Remote Sensing Methods to Measure VOC Emissions from a Variety of Stationary Sources in the South Coast Air Basin.

Mellqvist, J., Samuelsson, J., Johansson, J., Rivera, C., Lefer, B., Alvarez, S., Jolly, J., 2010. Measurements of industrial emissions of alkenes in Texas using the solar occultation flux method. J. Geophys. Res. 115, D00F17. https://doi.org/10.1029/2008JD011682.

Mellqvist, J., Samuelsson, J., Rivera, C., 2007. HARC Project H-53 Measurements of industrial emissions of VOCs , NH 3 , NO 2 and SO 2 in Texas using the Solar Occultation Flux method and mobile. DOAS 2007, 1–69.

Miller, B.R., Dlugokencky, E.J., Eluszkiewicz, J., Fischer, M.L., Janssens-maenhout, G., 2013. Anthropogenic emissions of methane in the United States 110, 20018–20022. https://doi.org/10.1073/pnas.1314392110/-/DCSupplemental.www.pnas.org/cgi/doi/10.1073/pnas.1314392110.

Miller, D.J., Sun, K., Tao, L., Pan, D., Zondlo, M.A., Nowak, J.B., Liu, Z., Diskin, G., Sachse, G., Beyersdorf, A., Ferrare, R., Scarino, A.J., 2015. Ammonia and methane dairy emission plumes in the San Joaquin valley of California from individual feedlot to regional scales. J. Geophys. Res. 120, 9718–9738. https://doi.org/10.1002/2015JD023241.

Monson, J., Chigbu, C., Tang, L., Goss, S., 2017. California Dairy Statistics Annual: 2017 Data 18.

Ngwabie, N.M., Jeppsson, K.H., Gustafsson, G., Nimmermark, S., 2011. Effects of animal activity and air temperature on methane and ammonia emissions from a naturally ventilated building for dairy cows. Atmos. Environ. 45, 6760–6768. https://doi.org/10.1016/j.atmosenv.2011.08.027.

NOAA's National Weather Service, 2019. Bakersfield Climate [WWW Document].

Nowak, J.B., Neuman, J.A., Bahreini, R., Middlebrook, A.M., Holloway, J.S., McKeen, S. A., Parrish, D.D., Ryerson, T.B., Trainer, M., 2012. Ammonia sources in the California South Coast Air Basin and their impact on ammonium nitrate formation. Geophys. Res. Lett. 39, 6–11. https://doi.org/10.1029/2012GL051197.

Owen, J.J., Silver, W.L., 2015. Greenhouse gas emissions from dairy manure management: a review of field-based studies. Global Change Biol. 21, 550–565. https://doi.org/10.1111/gcb.12687.

Rennie, T.J., Gordon, R.J., Smith, W.N., VanderZaag, A.C., 2018. Liquid manure storage temperature is affected by storage design and management practices-A modelling assessment. Agric. Ecosyst. Environ. 260, 47–57. https://doi.org/10.1016/j.agee.2018.03.013.

Rothman, L.S., Jacquemart, D., Barbe, A., Benner, D.C., Birk, M., Brown, L.R., Carleer, M. R., Chackerian, C., Chance, K., Coudert, L.H., Dana, V., Devi, V.M., Flaud, J.M., Gamache, R.R., Goldman, A., Hartmann, J.M., Jucks, K.W., Maki, A.G., Mandin, J.Y., Massie, S.T., Orphal, J., Perrin, A., Rinsland, C.P., Smith, M.A.H., Tennyson, J., Tolchenov, R.N., Toth, R.A., Vander Auwera, J., Varanasi, P., Wagner, G., 2005. The HITRAN 2004 molecular spectroscopic database. J. Quant. Spectrosc. Radiat. Transf. 96, 139–204. https://doi.org/10.1016/j.jqsrt.2004.10.008.

Rumburg, B., Mount, G.H., Filipy, J., Lamb, B., Westberg, H., Yonge, D., Kincaid, R., Johnson, K., 2008. Measurement and modeling of atmospheric flux of ammonia from dairy milking cow housing. Atmos. Environ. 42, 3364–3379. https://doi.org/10.1016/j.atmosenv.2007.05.042.

Samuelsson, J., Delre, A., Tumlin, S., Hadi, S., Offerle, B., Scheutz, C., 2018. Optical technologies applied alongside on-site and remote approaches for climate gas emission quantification at a wastewater treatment plant. Water Res. 131, 299–309. https://doi.org/10.1016/j.watres.2017.12.018.

Sharpe, S.W., Johnson, T.J., Sams, R.L., Chu, P.M., Rhoderick, G.C., Johnson, P.A., 2004. Gas-phase databases for quantitative infrared spectroscopy. Appl. Spectrosc. 58, 1452–1461. https://doi.org/10.1366/0003702042641281.

Smith, D.A., Harris, M., Coffey, A.S., Park, T., 2006. Wind test site in høvsøre. Evaluation 87–93.

Smith, T.E.L., Wooster, M.J., Tattaris, M., Griffith, D.W.T., 2011. Absolute accuracy and sensitivity analysis of OP-FTIR retrievals of CO2, CH4 and CO over concentrations representative of "clean air" and "polluted plumes.". Atmos. Meas. Tech. 4, 97–116. https://doi.org/10.5194/amt-4-97-2011.

Sun, K., Tao, L., Miller, D.J., Zondlo, M.A., Shonkwiler, K.B., Nash, C., Ham, J.M., 2015. Open-path eddy covariance measurements of ammonia fluxes from a beef cattle feedlot. Agric. For. Meteorol. 213, 193–202. https://doi.org/10.1016/j.agrformet.2015.06.007.

The Pennsylvania State University, 2017. Growth charts for dairy heifers [WWW Document]. URL. https://extension.psu.edu/growth-charts-for-dairy-heifers, 6.16.21.

Thompson, C., Stockwell, C., Smith, M., Conley, S., 2019. Statewide Airborne Methane Emissions Measurement Survey - Final Summary Report 69.

U.S. Environmental protection Agency, 2018. National Emissions Inventory 2014. North Carolina.

U.S. Environmental Protection Agency, 2013. 2013 GHGI Annex.

US-EPA, 2012. Chapter 2 - AFOs and CAFOs. In: NPDES Permit Writers' Manual for CAFOs, pp. 1–16.

USDA, 2021. Usda ers - dairy data [WWW Document]. URL. https://www.ers.usda.gov/data-products/dairy-data/, 4.4.21.

VanderZaag, A.C., Flesch, T.K., Desjardins, R.L., Baldé, H., Wright, T., 2014. Measuring methane emissions from two dairy farms: seasonal and manure-management effects. Agric. For. Meteorol. 194, 259–267. https://doi.org/10.1016/j.agrformet.2014.02.003.

Zhu, L., Henze, D., Bash, J., Jeong, G.R., Cady-Pereira, K., Shephard, M., Luo, M., Paulot, F., Capps, S., 2015a. Global evaluation of ammonia bidirectional exchange and livestock diurnal variation schemes. Atmos. Chem. Phys. 15, 12823–12843. https://doi.org/10.5194/acp-15-12823-2015.

Zhu, L., Henze, D.K., Bash, J.O., Cady-Pereira, K.E., Shephard, M.W., Luo, M., Capps, S. L., 2015b. Sources and impacts of atmospheric NH3: current understanding and frontiers for modeling, measurements, and remote sensing in North America. Curr. Pollut. Rep. 1, 95–116. https://doi.org/10.1007/s40726-015-0010-4.

VI

An uncertainty methodology for solar occultation flux measurements of ammonia gaseous fluxes from agriculture

Mellqvist, J., Vechi, N.T., Scheutz, C., Durif, M., Gautier, F., Johansson, J., Samuelsson, J., Offerle, B., & Brohede, S.

Manuscript

An uncertainty methodology for Solar Occultation Flux measurements: ammonia emissions from agriculture

Johan Mellqvist[1], Nathalia T. Vechi[1,2], Charlotte Scheutz[2], Marc Durif[4], Francois Gautier[4], John Johansson[3], Jerker Samuelsson[3,] Brian Offerle[3] and Samuel Brohede[3]

[1]Department of Space, Earth and Environment, Chalmers University of Technology, Göteborg, Sweden
[2]Department of Environmental Engineering, Technical University of Denmark, Lyngby, Denmark
[3]Fluxsense AB, Göteborg, Sweden
[4]INERIS, Verneuil-en-Halatte, France

Correspondence to: Johan Mellqvist (johan.mellqvist@chalmers.se)

Abstract

Ammonia (NH_3) emissions can negatively impact ecosystems and human health; thus, they should be monitored and mitigated. NH_3 concentration measurements are troublesome, particularly due to the gas molecule's reactive nature. The solar occultation flux (SOF) is an open-path passive method in which NH_3 slant columns are retrieved from the solar spectrum, avoiding gas adsorptions in the instrument. Moreover, measurements of horizontal and vertical wind speeds and estimation of plume height is necessary to obtain accurate NH_3 gas fluxes. A novel methodology to access the uncertainties in the NH_3 emissions measurements using SOF is presented, where systematic and random errors are considered. The paper aims to introduce an uncertainty calculation methodology and demonstrate the use of the SOF method for quantifying NH_3 emissions from livestock production. First, a validation experiment was performed, and the measurement errors varied from -31 % to +14 % on average, while the calculated expanded uncertainty was from ±12 to ±17 %. Secondly, the method was used to quantify emissions rates from farms of different sizes. The error related to wind measurement was calculated according to the wind measurement setup, being either anemometers at one or two heights or the use of a wind LIDAR. The uncertainty of emission quantifications in each case study varied from ±21 to ±37 %, dominated mainly by wind and random uncertainties. SOF was able to quantify small (~1 kg h^{-1}) and large (~100 kg h^{-1}) emission sources, even in areas with high farm densities. The SOF is suitable for measuring NH_3 emissions from livestock production and has an expanded uncertainty lower than 40 %, which can be further improved following the best practices for the method's application.

1. Introduction

Agriculture is the primary source of ammonia (NH_3) emissions accounting for around 85% of total emissions (EDGAR database, 2023), which has increased since pre-industrial times due to the growing food demand (Galloway et al., 2003). Within the different agricultural sources, livestock production can release NH_3 during animal urine and faeces decomposition. NH_3 is a precursor of atmospheric fine particulate matter ($PM_{2.5}$), eutrophication, and an indirect greenhouse gas (GHG). $PM_{2.5}$ is associated with lung diseases, and NH_3 forms approximately 30 and 50 % of $PM_{2.5}$ in the US and Europe, respectively (Wyer et al., 2022). The atmospheric lifetime of NH_3 ranges from hours to days because it can either react in the atmosphere forming $PM_{2.5}$, or be retained in the ground due to dry or wet deposition. The complex emissions and depositions mechanisms of NH_3 hinder the understanding of these emissions and associated dynamics (Hristov et al., 2011) and highlight the need to monitor emissions and atmospheric concentrations (Wyer et al., 2022). Knowledge gaps still need to be filled regarding NH_3 emissions dynamics, which is reflect in the large discrepancy between modelled NH_3 and measured emissions (Lonsdale et al., 2017). A recent study on NH_3 emission hotspots using satellite data indicated that two-thirds of the high emissions sources are underestimated by at least an order of magnitude (Van Damme et al., 2018).

Consequently, NH_3 has gained attention over the last decades, increasing the development of instruments and models used to study its emission sources. Many monitoring stations worldwide still use old techniques to obtain NH_3 concentrations, such as wet-chemistry, which samples in the order of days and weeks (Twigg et al., 2022). Moreover, with improvements in infrared lasers, spectroscopy based instruments emerged, such as FTIR (Fourier Transform infrared spectrometer), cavity ring-down spectrometer (CSDR), and quantum cascade laser absorption spectrometer (QCLAS) (Twigg et al., 2022). NH_3 is challenging to quantify due to its strong reactivity, which makes the gas molecule adhere to surfaces, requiring that close-path instruments and inlets are coated or heated to decrease the response delay (Zhu et al., 2015b). A study using 13 instruments highlighted the importance of its setup, inlet design, and operation (flow rate and filter status), as these factors can affect measurements performance (Twigg et al., 2022).

For measurements instruments attached to a mobile (Eilerman et al., 2016; Golston et al., 2020; Miller et al., 2015), stationary (Sun et al., 2015a), or airborne platform (Guo et al., 2021; Miller et al., 2015; Sun et al., 2015b). Mobile platforms can resolve local scales greatly (Golston et al., 2020), even though they are limited by road availability. Furthermore, Lassman et al. (2020) found that a surface-based platform can underestimate NH_3 emissions by a factor of 1.5 because concentrations near the surface might be depleted due to the gas deposition. In recent years, satellite column retrievals complemented the information on NH_3 emissions on large scales. These platforms have extensive spatial coverage; however, as disadvantages, they have high emissions uncertainties and poor spatial and temporal resolution.

Solar occultation flux (SOF) is a method used for years in the quantification of alkenes, VOCs, and industrial NH_3 (Johansson et al., 2014; Mellqvist et al., 2007, 2010) and has been recently used to measured agricultural NH_3 emission sources (Kille et al., 2017, Vechi et al., 2023). The SOF technique measures spatially distributed slant columns (g/m^2), which can be converted to emission rates using information about the wind. It can be complementary to in-situ and satellite measurements, bridging both techniques (Guo et al., 2021). The uncertainty of this technique has been discussed before for both alkanes (Johansson et al., 2013), alkenes (Mellqvist et al., 2010), and NH_3 (Kille et al., 2017). Here, the aim is to deepen the error analysis with a comprehensive measurement uncertainty methodology and comparison to validation experiments. Furthermore, we illustrate the use of the technique in three different case studies investigating NH_3 emissions from agricultural sources. In addition, a description of plume height estimations obtained from the ground and column NH_3 concentration measurements is included. This study's results are also valuable when using SOF for other species and in other applications.

2. Instrument, flux quantification and measurement campaigns

2.1. SOF instrument and columns retrieval.

The SOF operation consists of recording solar infrared absorption spectra while driving through the gas plume (Fig. 1d and e). The spectra is captured by a solar tracker, containing several mirrors that transmit the solar light to the spectrometer, following the light as the car moves, thus there is a need for sunny or low cloud coverage conditions. Further, an FTIR instrument, Bruker IR cube, with a resolution of 0.5 cm^{-1} wavenumbers, and a dual detector InSb (Indium Antimonide, 2.5 – 5.5 µm) /MCT (Mercury cadmium telluride 9-14 µm) was used to detect the spectra. The detection limit for NH_3 columns by the SOF instrument calculated as 3σ is 2.2 mg m^{-2} at a sampling rate of five seconds.

Alkanes are retrieved in the "C-H stretch band" at approximately 3.3 µm, while alkenes, propene, and NH_3 are found in the "fingerprint region" at around 10 µm. The specificity of NH_3 is strong because this species' absorption at the fingerprint region is unique, with sharp absorption features, well separated from other species (Fig. 1c). During the measurements campaigns, the NH_3 retrieval was done either in a broad (900 – 1000 cm^{-1}) or a narrow spectral window (940 - 970 cm^{-1}). The broader window results in a more stable atmospheric background retrieval, however, at a slightly lower noise. The obtained column values correspond to the relative abundance compared to a reference spectrum recorded outside the plume (Fig. 1a). The best practice is to choose a location with a low target gas concentration as a reference. Additionally, a posterior re-evaluation can be performed with a new reference spectrum in the case of a noisy measurement. A retrieval of absolute columns is also possible, however, the signal-noise then becomes lower. The challenge of the spectral retrieval is the long atmospheric path length of the solar spectra, which is affected by the strong absorptions of H_2O and CO_2 in the atmosphere; therefore, other interfering species are considered. The retrieval is done by fitting a calibration spectrum from HITRAN (Rothman et al., 2005) infrared database to simulate the absorption spectra for atmospheric background, using nonlinear multivariate analysis, and calibrated according to pressure and temperature (Fig. 1b). A custom Software executes the retrieval (Kihlman, 2005), the fitting procedure is described in more detail in Mellqvist et al. (2010).

Each SOF measured transect should ideally be in one instant because then the wind and turbulence are "frozen". However, in practice, transects are performed over a few minutes, depending on the distance to the source, the size of the plume and the road characteristics, adding measurement uncertainties.

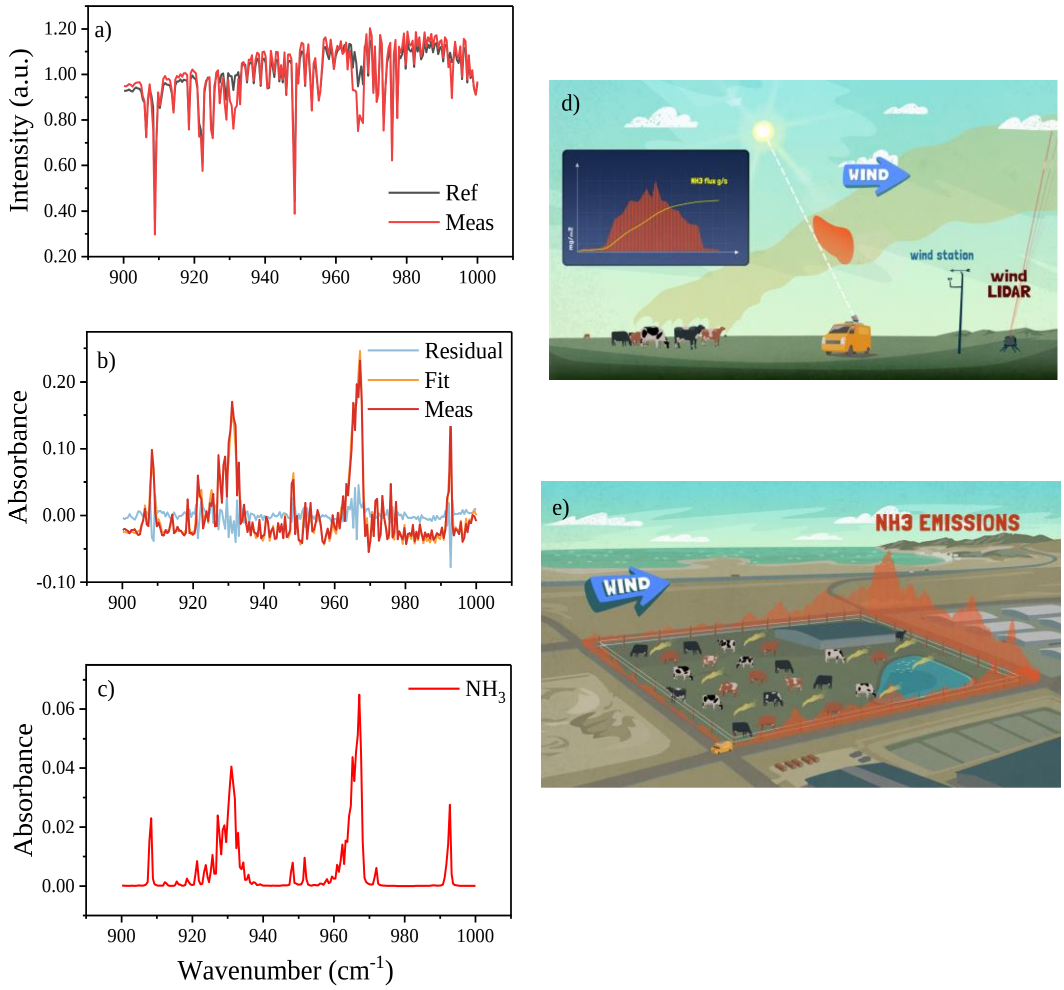

Fig. 1: a) Example of spectra measured in the plume and the reference spectra. b) Measured and fitted absorbance spectra and the calculated residual spectra. c) The NH_3 calibration absorbance used to model the fitted spectra (approx. 40 mg m^{-3}). d) Example of solar spectral measurements when crossing the target plume. e) Example of a box measurement around a target farm.

2.2. Emission quantification

2.2.1. Emission Calculation

The gas flux is obtained first by integrating the measured column concentrations across the plume and hence the integrated mass of the target gas species can be obtained (Eq. 1). Furthermore, to calculate the flux, the integrated mass is multiplied by the wind speed parameter, u_t (m s^{-1}) Eq. (1).

$$E_{NH3}(mg\ s^{-1}) = u_t(m\ s^{-1}) \int_P\ Column_{NH3_l}(mg\ m^{-2}) \cdot \cos(\theta_l) \cdot \sin(\alpha_l)\, dl(m) \qquad (1)$$

where, p is the transect path across the plume, l corresponds to the travel distance, α is the angle between the wind and driving direction. The slant angle of the Sun is compensated by multiplying the concentration with the cosine factor of the solar zenith angle θ.

2.2.2. Determination of the wind speed parameter

The wind is a crucial part of the SOF emission quantification (Eq. 1). SOF retrieves vertically integrated concentration; for this reason, the wind parameter (u_t, Eq. 1) should correspond to the plume speed. However, wind speed measurements are not straightforward; as usual, the wind is disturbed close to the ground and increases with the height above the surface. Therefore, an approximation of the plume speed, to be used u_t, is the averaged integrated wind profile (IWP_{avg}, Eq. 2) from the ground to the plume height (Fig. 2b). An assumption applied here is that the plume is vertically well mixed, meaning similar concentration from ground to plume height, which is usually the case during sunny conditions. Additionally, in very unstable atmospheric conditions, the wind speed gradient is smoothed out by convection (Fig. 2a).

The IWP_{avg} is obtained using Eq. 2, where H is the plume height (Section 2.2.3), and u_z is the horizontal wind speed (m/s) measured at the different heights (z).

$$IWP_{avg} = \frac{\int_0^H u_z \cdot dz}{H} \tag{2}$$

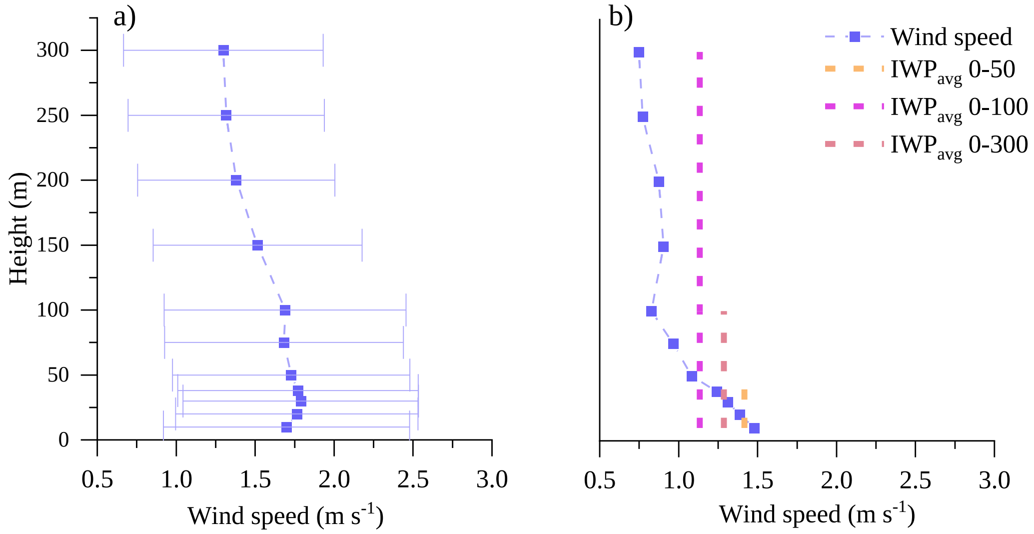

Fig. 2: a) Averaged wind profile measured for 1 hours using LIDAR, the error bars correspond to standard deviation. b) Typical wind profiles (five minutes average) during case study 3 (C3), additionally we show the integrated wind profile (IWP_{avg}) at three different height intervals (0-50, 0-100, 0-300 m).

2.2.3 Plume height (H_P)

A novel approach of estimating the plume height (H_p) was demonstrated using data from case study 3 (C3). This was done by calculating the ratio between the vertical column (mg/m^2) and the ground concentration (mg/m^3) of NH_3 (Eq. 3). This method relies again in the assumption that the plume is well mixed in height (Fig. 3, Case I). However, in reality, the plume might not disperse homogenously (Fig. 3 Case II or III), which brings uncertainty to the estimation, therefore, this is considered as an approximate assessment of H_p. For instance, when the plume is aloft (Fig. Case II), this methodology produces an unrealistically large plume height.
The vertical column of the NH_3 column (mg m^{-2}) was obtained by SOF, while a mobile extractive FTIR (MeFTIR) was used to measure ground NH_3 concentrations (mg m^{-3}). The latter instrument consists of an optical multi-path cell connected to a heated, temperature-controlled FTIR instrument (Galle et al., 2001; Vechi et al., 2023). In more detail, H_P is calculated by integrating the ground and column concentration while crossing the plume path x, where θ is the solar zenith angle (Eq. 3). This method is here called Vertical Column Ground Concentration ratio (VCGC). Further, the H_p is calculated from the median of multiple transects.

$$Hp = \cos(\theta)\ \frac{\int Column_{NH3}\ (x)dx(\frac{mg}{m^2})}{\int Concentration\ _{NH3}(x)dx(\frac{mg}{m^3})} \tag{3}$$

Alternatively, a rougher estimate of the H_P is obtained from a simpler calculation (Eq. 4), considering horizontal wind speed (u_z) at the available height, the distance from the emission source to the measurement road (P), and plume raise speed (σ_w) (m s^{-1}). Airborne measurements in Texas (Mellqvist et al., 2010) showed that the effective plume raised speed from industries in sunny conditions corresponded to 0.5 to 1 m s^{-1}, corresponding to approximately the typical standard deviation of the vertical wind (Tucker et al., 2009). Similar vertical wind data, i.e., ~0.5 m s^{-1}, were measured using a Light Detection and Ranging (LIDAR) instrument in C3. This method will be called Plume Transport Vertical Speed (PTVS).

$$H_p = \frac{P\ (m)}{u(m\ s^{-1})} w(m\ s^{-1}) \tag{4}$$

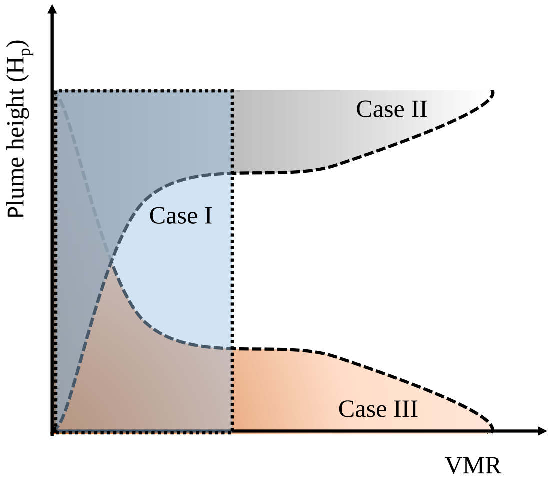

Fig. 3: An illustration of the assumptions used in plume height calculation. The y-axis represents the plume height while x-axis represents the volume mixing ratio (VMR). Case I: Ideal scenario, homogeneous distributions up to the H_P. Case II: The plume is aloft; therefore, no VMR will be measured, only columns. Case III: The plume is on the ground, and VMR values will be high.

2.3. Campaigns description

The SOF method was tested in a controlled release experiment and then demonstrated in three campaigns, measuring NH_3 emissions from livestock production. The campaigns took place in France, the US (California), and Denmark, countries with extensive agriculture production and significant differences in manure management and climate conditions. The campaigns were divided according to differences in wind measurements, the size of the target source, and the interference of nearby sources.

The wind measurements were made close to the source (~ 100 m), except for C3, in which a wind LIDAR was positioned at a maximum of five km from the source. Most campaigns used a 2D-sonic anemometer (WXT50, Vaisala) or a vane wind monitor (Model 05103, Young) mounted in a three and/or ten meters height mast. These 2-D wind sensors quantified the horizontal wind speed and direction.

SOF Validation - Controlled release test (Grignon, France)

A controlled release test was performed for three days at a site in Grignon (France) to test the accuracy of the SOF method in NH_3 emissions quantification. Four release episodes were carried out, and the release rates varied from 0.48 to 1.1 kg h^{-1}. Gas was released from two NH_3 cylinders (80 liters), a mass flow controller was used to secure constant flow, while a high precision scale was, a heater removed ice on the gas cylinder. Information on meteorological conditions such as temperature, relative humidity, precipitation, and wind speed are shown in the supplementary information (SI Fig. S1). The transect measurements were conducted downwind of the release at average distances of 150 - 300 m. The release rates were unknown to the SOF operators until the final results were submitted to ensure a proper “blind test” validation. The horizontal wind speed and direction were measured at three and ten meters height using a vane wind monitor and the sonic anemometer, respectively.

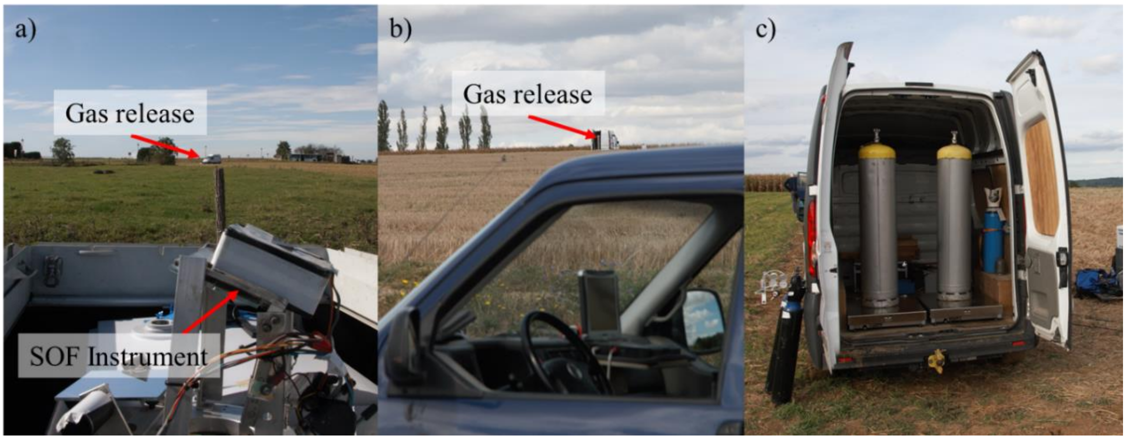

Fig. 4: NH_3 emission validation experiment in Grignon, France. a) Picture shows the gas release point and the distance to the SOF measurement while measuring (28-September). b) Similarly picture shows the release point and the distance to the measurement road, although SOF could not measure at these cloud conditions (22-September). c) Two gas cylinders with 80 liters were positioned on high-precision scales. A mass flow controller was used to ensure a steady flow.

Case study 1 (C1) - Pig and dairy farm (Denmark)

Case study 1 consisted of a two days measurement campaign at two small-scale animal farms in Denmark, which were well isolated from other interfering sources. NH_3 emissions were measured at a pig farm (C1a) and a cattle farm (C1b), and transects were performed at 250 and 900 m, respectively. The pig farm housed approximately 600 sows with piglets and weaners, while the cattle farm had approximately 700 dairy cows, plus heifers and calves. The horizontal wind speed and direction were obtained from two vane wind monitors placed in three and ten meters high masts. Columns were measured downwind from the farms, while upwind fluxes were measured only once or twice because there were no other interfering sources.

Case study 2 (C2) - Dairy complex (USA, California)

In case study 2, the SOF method was used to measure NH_3 emissions on a large dairy complex located in Chino (California), which is a sizeable concentrated area (21 km^2) without other important NH_3 sources. Transects were collected in one day and were performed around the farm's fence line area, comprising a distance of 18 km for one transect. The area housed approximately 36,000 heads (CARB, personal communication 2015). One vane wind monitor performed wind measurements at a 10 m mast. The measurements were done by encircling the area; therefore, the emissions were calculated by estimating the flux leaving the area minus the one entering it.

Case study 3 (C3) - Dairy concentrate animal feeding operations (USA, California)

Lastly, case study 3 was conducted in dairy concentrated animal feeding operations (CAFOs) in the San Joaquin Valley (SJV), California. The results present the combination of the SOF (column) and the MeFTIR (ground concentration) instruments, to demonstrate plume height calculations using the results from this case study. These were sources with large emissions, placed in high farm-density areas. NH_3 measurements were done at the farms' fence line and one km further away from the source for one or two days for SM1 (C3a) and SM2 (C3b), respectively. A wind LIDAR was used here; its detection principle is based on the Doppler shift of the infrared pulse (~1.5µm) that the instrument sends out and is reflected by atmospheric aerosols. The instrument used in this campaign (Campbell Scientific, LIDAR ZX300) provided horizontal and vertical wind speeds and directions 10 m to 300 m above ground at 11 different heights. In this case study, the IWP_{avg} was used as wind parameter (u_t) for the emissions calculations, averaged in five-minute and three height intervals, i.e., 0-50 m, 0-100 m, and 0-300 m. As there were many CAFOs in vicinity to the farm; upwind measurements were necessary to isolate emission from the individual farm.

3. SOF uncertainty methodology

In this study, the SOF measurement uncertainty was derived based on the guide to the expression of uncertainty in measurement (GUM) methodology (Joint Committee for Guides in Metrology, 2008). For the first time, a new approach was described for NH_3 emission measurements from livestock production, although based on the principles outlined in the European measurement standard for VOC monitoring of refineries (CEN EN 17628 European standard, 2022). The random and systematic uncertainties were identified and summed up to a total standard 68% Confidence Interval (CI 68 %) or expanded uncertainty (CI 95 %). It should be noted that most scientific articles, also past SOF studies (Johansson et al., 2013; Kille et al., 2017; Mellqvist et al., 2010), only consider standard random uncertainties (CI 68 %). Thus, this paper uses a more comprehensive approach consistent with industry and metrology institutes (Joint Committee for Guides in Metrology, 2008). Additionally, a fully new method to assess the spectroscopic uncertainties is suggested and proven better to the approach commonly used when performing general spectroscopic measurements.

The random measurement uncertainty is caused by many factors, with wind turbulence as the most significant contributor. This uncertainty decreases with the number of samples taken; hence, the SOF European standard for refinery measurements recommends a minimum of 12-16 transects divided over several days (CEN EN 17628 European standard, 2022) for this type of source. In turn, systematic errors will persist, independently of transects amount. They are often correlated to the technique, instrumentation, and measurement of other important variables, such as wind speed, and best practices can reduce them. The measurement uncertainty methodology is combined with data quality requirements, which must be fulfilled for valid measurements. This includes sufficient solar height, relatively persistent wind direction and speed above 1.5 m s^{-1}, and sufficient quality of the measurements.

3.1. Spectroscopy uncertainty

Systematic spectroscopy errors can be divided into two categories, errors due to uncertainty in the strength of the absorption cross-section and errors due to imperfect spectroscopic fitting of the band shapes. An absorption strength uncertainty ($U_{abs-NH3}$) of 2 % ($|(I_{obs} - I_{cal})/ I_{obs}|$) for the NH_3 cross section was found by Kleiner et al. (2003) for the full band of 700 to 1200 cm^{-1}. Therefore, this uncertainty (U_{cros}) was calculated using the absorption strength ($U_{abs-NH3}$) (Kleiner et al., 2003), further divided by 1.96, as this error was considered a normal distribution (Eq. 5).

$$U_{cros} = \frac{U_{abs-NH3}}{1.96} \tag{5}$$

The imperfect spectroscopic fitting can have different causes, for instance, errors due to the shape of the reference cross sections used, wavelength shifts, or errors in the instrument line shape characterization. Consequently, the spectroscopic fitting routine cannot perfectly account for all the spectroscopic absorption features and may systematically over- or underestimate the column concentrations. The fitting residual, defined as the difference between the measured and fitted absorbance, captures some information of the total fitting error. The root-mean-square of the residual (RMS) is a commonly used measure of the fitting error magnitude, which could be used to estimate the column concentration uncertainty due to fitting errors. Therefore, to assess the retrieval error (U_{ret}), we calculated the ratio between the average NH_3 absorbance in 960 to 968 cm^{-1} (AVG-abs$_{960\text{-}968\mu m}$) (Fig. 1b) and the standard deviation of the fitting residual (STD) in the same wavelength range, divided by the square root of the number of points (Eq. 6). The ratio was calculated for measurement points inside and outside the plume, and the linear regression curve's slope was considered as the error.

$$U_{ret,1} = \left(\frac{\frac{STD}{\sqrt{n}}}{\overline{\mathrm{abs}}_{(960-968)\mu m}} \right) \tag{6}$$

Previous studies (Griffith, 1996) have estimated the fitting uncertainty as

$$U_{ret,2} = \frac{STD}{\overline{abs}} \tag{7}$$

Additionally, we estimated the uncertainty based on dividing the integrated area under the fitting residual A_r with the integrated area under the fitted NH_3 absorption A_{abs}.

$$U_{ret,3} = \frac{A_r}{A_{abs}} \tag{8}$$

In this study, different estimates were investigated by deliberately introducing errors in the fitted cross sections and using those cross sections in a spectral fit applied to a synthetic spectrum with absorption from a known column concentration. Different uncertainty estimates (Eq. 6, 7, and 8) were then calculated based on the residual from the fitting and compared to the error in the fitted column. The cross sections included three error types: resolution error, shifting error, and a multiplicative Gaussian noise error. For each case, a random error was chosen from each of the three types of errors within a specific range. The resolution error was a scaling factor in the range of one to four, the wavelength shift error was an offset in the range -0.2 to 0.2 cm^{-1}, and the multiplicative Gaussian noise had a standard deviation from 0 to 0.1. In total 1000 random such as these were tested and Fig.5a shows the resulting uncertainty estimates, and column error for each case. Fig. 5b shows an example of the fitted NH_3 absorbance and residual for one of the cases. The uncertainty estimate in Equation 7 was found to significantly overestimate the column concentration error. In contrast, the uncertainty estimate in Equation 6 was a better estimate, with the error being smaller than this estimate in roughly 95% of the cases. The uncertainty estimate based on the area (Eq. 8) was determined to significantly underestimate the column concentration errors in most cases.

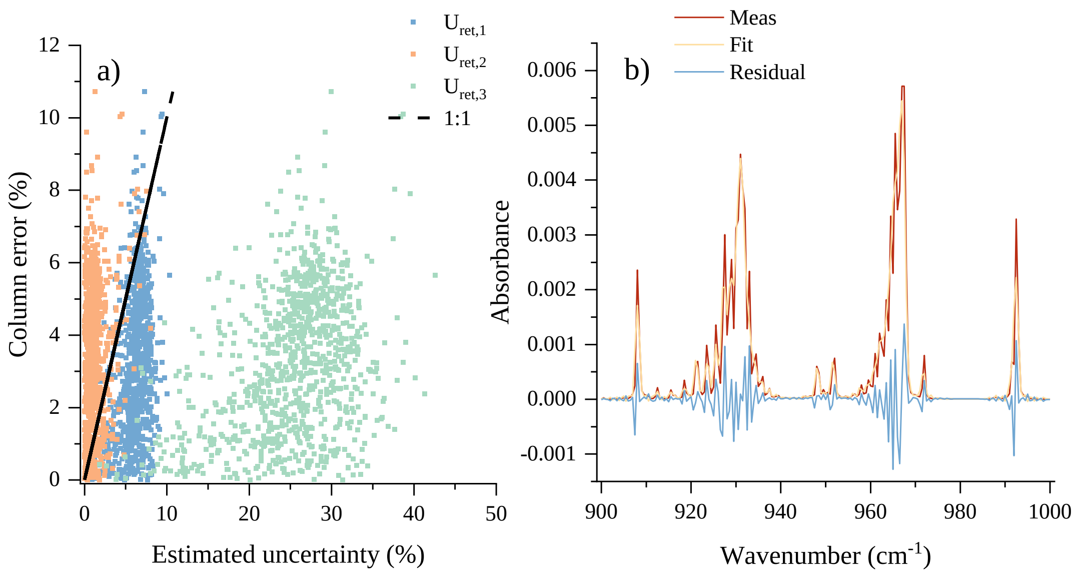

Fig. 5: a) Column concentration errors and uncertainty estimates for 1000 simulated test cases. Uncertainty estimate from Equation 6 in green, from Equation 7 in blue and from Equation 8 in orange. b) Example of the fitted NH_3 absorbance for one of the simulated cases.

3.2. Background uncertainty

The background column concentration might differ before and after the measurement when crossing an emission plume. Among other things, this might indicate the presence of a secondary source on the side or upwind of the target source (Fig. 6) or the influence of interfering background species when the solar angle changes. The background uncertainty ($\pm U_B$) corresponds to the relative difference in flux when choosing either the left or the right value as the assumed background. The uncertainty distribution is rectangular, as the background value changes within the plume, it is unknown; therefore, it should be divided by the square-root of three according to GUM (Joint Committee For Guides In Metrology, 2008) (Eq. 9).

$$\boldsymbol{U_B} = \frac{\Delta_{\boldsymbol{Background-flux}}}{\sqrt{3} \cdot \boldsymbol{flux_{avg}}} \quad (9)$$

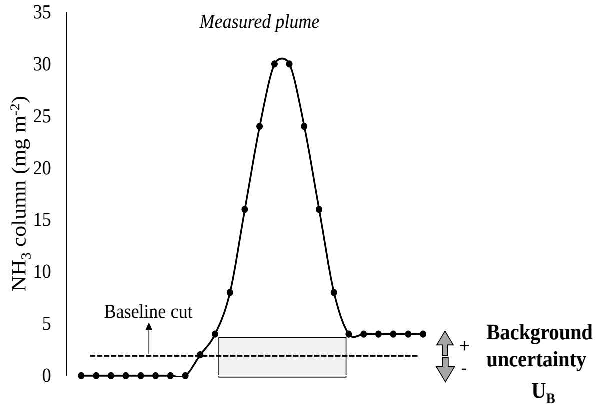

Fig. 6: Background assessment systematic uncertainty. The grey shadowed box represents the uncertainty area that is being added to the quantification.

3.3. Wind speed uncertainty

The wind speed is the largest source of uncertainty in SOF measurements (Johansson et al., 2013; Kille et al., 2017; Mellqvist et al., 2010). The wind speed parameter (u_t in Eq. 1) has to be an approximation of the plume speed, therefore the IWP_{avg} is the best estimate of this parameter. Sunny convective conditions, smooth the wind gradient convection, which together with the H_p estimation help minimizing the error. For the different case studies, the plume height was estimated according to the available information (Table 1), and only in case study C3 the plume height was measured (VCGC, Eq. 3).

In the validation test and case study C2, two wind masts held the wind monitors, one at three and the other at 10 m. The wind profile was obtained by estimating the α factor using Eq. 10, where U is a known wind speed at two different heights. Afterward, the obtained α factor is used to estimate the wind speed at the plume height (Eq. 11). Further, by using the estimated wind profile, the IWP_{avg} was obtained using Eq. 2. Furthermore, the uncertainty was estimated by the difference between the measured wind speed (10 m), which was used for the flux calculations, and the estimated IWP_{avg} from 0-plume height (Table 1, Eq. 12). For case study C1, only one 10 m mast was used, therefore, we estimated the error of choosing different vertical profiles by using information from another study at a similar geographic location. Moreover, in case study C3, we had a LIDAR as a wind sensor, therefore, the IWP_{avg} were directly calculated at different height ranges (Eq. 2). Because the wind speed profile was measured instead of estimated, the error estimation in case study C3 is a better prediction of wind speed error (Table 1, Eq. 12).

$$\alpha = \frac{\log(U_2/U_1)}{\log(z_2/z_1)} \tag{10}$$

$$U_{(z)} = U_2 \left(\frac{z}{z_2}\right)^{\alpha} \tag{11}$$

Table 1: Parameters used on the calculation of the wind speed error uncertainty

	Validation	Case study C1	Case study C2	Case study C3
Wind speed data (u_t)	10 m	10 m	10 m	Measured IWP_{avg} (0-50, 0-100, 0-300 m)
Plume height (H_P)	Estimated (Eq. 4)	Estimated (Eq. 4)	Estimated (Eq. 4)	Measured (Eq. 3)
Integrated Wind profile (IWP_{avg})	Estimated (Eq. 2, 10 and 11)	Estimated (Eq. 2, 10 and 11)	Estimated (Eq. 2) using C3 data	Measured (Eq. 2)
Error estimation (Eq. 12)	$U_{wind} = \frac{\left(1-\frac{IWP_{Avg}}{u_t}\right)}{1.96}$	$U_{wind} = \frac{\left(1-\frac{IIWP_{Avg}}{u_t}\right)}{1.96}$	$U_{wind} = \frac{\left(1-\frac{IIWP_{Avg}}{u_t}\right)}{1.96}$	$U_{wind} = \frac{\left(\frac{IWP_{Avg\ (0-300)}}{IWP_{Avg\ (0-50)}}\right)}{1.96}$

Furthermore, the wind direction error was not considered for this type of measurement because the location of the source is well-known; therefore, the wind direction was corrected according to the visual evaluation of the data processing operator. In cases where the source's location is unknown, the wind direction uncertainty should be added to the analysis, similar to other assessment errors of SOF (Johansson et al., 2014).

3.4. Calculation of standard and expanded total uncertainty

For each measurement campaign, random uncertainties were calculated as the standard error of the mean. We assumed that some other potential sources of error, for example, random wind direction would be further minimized with the increase in transects, therefore, comprising part of the random error.

$$U_{rand} = \frac{(STD)}{\sqrt{n}} \tag{13}$$

Systematic and random campaign errors were combined in a root-sum-square, resulting in the standard uncertainty (CI 68 %). Furthermore, the effective degrees of freedom were considered, and the expanded uncertainty (CI 95 %) was also calculated. The methodology followed GUM methodology (Joint Committee For Guides In Metrology, 2008) using Eq. (14), where U_{tot} is total relative uncertainty and k is coverage factor (ranging 1.96 – 3.00), depending on N degrees of freedom and the confidence interval.

$$U_{tot} = k\sqrt{\left(U_{cros}{}^{2} + U_{ret}{}^{2} + U_{B}{}^{2} + +U_{wind}{}^{2} + U_{rand}{}^{2}\right)} \tag{14}$$

4. Results

4.1. Uncertainty analysis

Each estimated uncertainty for the different campaigns is shown in Table 2. The expanded uncertainty (CI 95 %) ranged from 15.1 to 37.4 %, and the U_{wind} was one of the largest error sources (Table 2). Although, it should be noted that the wind turbulence causes a considerable part of the random uncertainty. The estimated U_{wind} was particularly high in C1b and C2 because of the relatively high H_P (130 - 500 m), which was estimated by the PTVS method (Eq. 4), while the wind information was obtained at 10 m high. This was a limitation of the available field instrumentation. In contrast, in C3, despite the large H_P (400 m), wind speed measurements were done using LIDAR, which obtains data up to 300 m, resulting in an U_{wind} smaller than at C1b and C2. Additionally, H_P could be better estimated on C3 than in the other campaigns, using the VCGC method (Eq. 3), decreasing U_{wind}, consequently, the total uncertainty. H_P is discussed in more detail in the flowing section. Moreover, for most case studies, the number of transects was large; therefore, the random uncertainty; U_{rand} was low, except for C2, which had only three transects; however, the standard deviation between them was low, and consequently the random uncertainty.

Table 2: Overview of the estimated uncertainties and the validation and in the other case studies.

	Validation	C1a	C1b	C2	C3a	C3b
Systematic – U_{cros} (%)	2.0	2.0	2.0	2.0	2.0	2.0
Systematic – $U_{ret,1}$ (%)	4.4	4.4	4.4	4.4	4.4	4.4
Systematic – U_b (%)	1.8	5.0	9.0	0.9	1.5	0.4
Systematic – U_{wind} (%)	3.0 – 6.0	3.0	32.0	23.5	11.0	11.0
Systematic – Gas release (%)	2.0	NA	NA	NA	NA	
Random – U_{rand} (%)	3.3 – 6.9	9.0	7.1	4.6	9	12
Standard uncertainty (CI 68 %)	**6.5 – 8.7**	**10.6**	**19.1**	**13.6**	**12**	**14**
Expanded uncertainty (CI 95 %)	**12.7 – 17.5**	**21.0**	**37.4**	**27.0**	**25**	**29**
Estimated H_p (m)	11 – 40	~30	~130	> 500	~ 500	~ 400

4.1.1. Plume height (H_P)

The MeFTIR and SOF were operated simultaneously in the vehicle, making it possible to estimate the H_p using the VCGC method according to Eq. 3 and comparing this to estimating H_P using the PTVS method (Eq. 4). Fig. 7a shows examples of NH_3 columns (left-axis) and ground concentrations (right-axis) measured in three distinct plumes (P1, P2, P3). In the first peak, P1, the ground concentrations were similar to P2 (right-axis), while column measurements were lower than P2 (left-axis), which indicated that P1 was located close to the ground. At the same time, P2 was at a higher height (Fig. 7a, Fig. 3c). Similarly, for P3, column concentrations (left-axis) were lower than P2. In contrast, ground concentrations (right-axis) were much higher, indicating again a plume close to the ground (Fig. 7a). Furthermore, the second method (PTVS, Eq. 4) was used and compared to the VCGC method, showing slightly lower but similar results (Fig. 7b). However, the latter is more accurate because it does not need to make assumptions about the vertical plume speed. Additionally, in more complex cases, for instance, where the NH_3 source is spread and heterogeneous (farm 8), the PTVS approach has not obtained similar values as in the VCGC method (Fig. 7b).

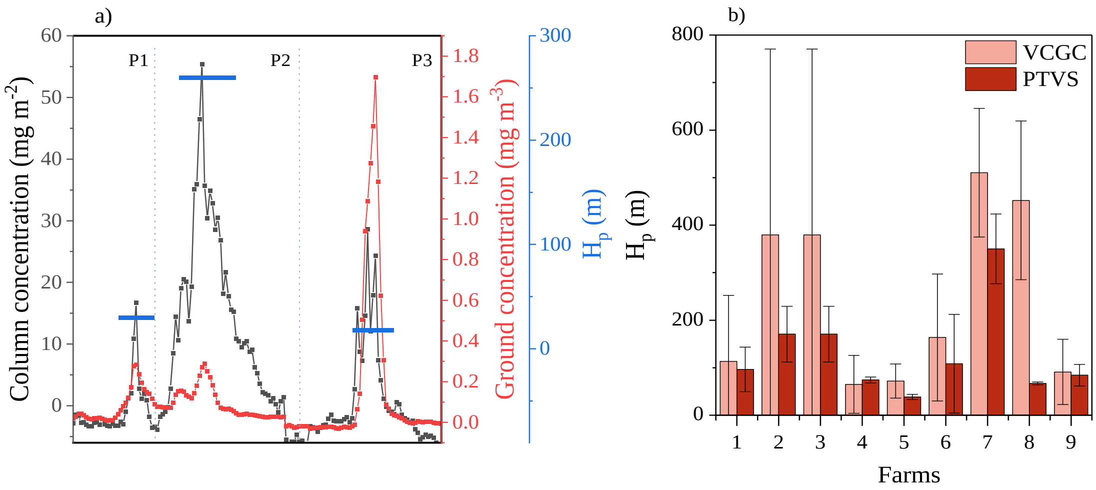

Fig. 7: a) Simultaneous measurements of NH_3 columns and ground concentrations. P1 and P3 were ground sources (Fig. Case III) b) Examples of plume height calculation using the two methods (VCGC), (light red bar), the error bars correspond to the variation in the plume height calculation, and the estimated values using vertical wind speed (PTVS) (dark red bar), the error bars correspond to the variation of the H_P calculation (variations in wind speed and measured distance).

4.2. Validation

In the NH_3 validation test, the controlled gas releases varied from 0.48 to 1.1 kg h^{-1}, while the SOF NH_3 quantified emissions varied from 0.41 to 1.27 kg h^{-1} (Fig. 8, Table 3). On average, the wind speed varied from 3.8 to 5.9 m s^{-1}, and the direction changed from weak north-easterly winds on 22-September to stronger and south-westerly winds on the two last measurement days. The weather conditions were sunny with low cloud coverage on 28-September and 1-October, while on 22-September the presence of clouds was more considerable, although measurements were still possible.

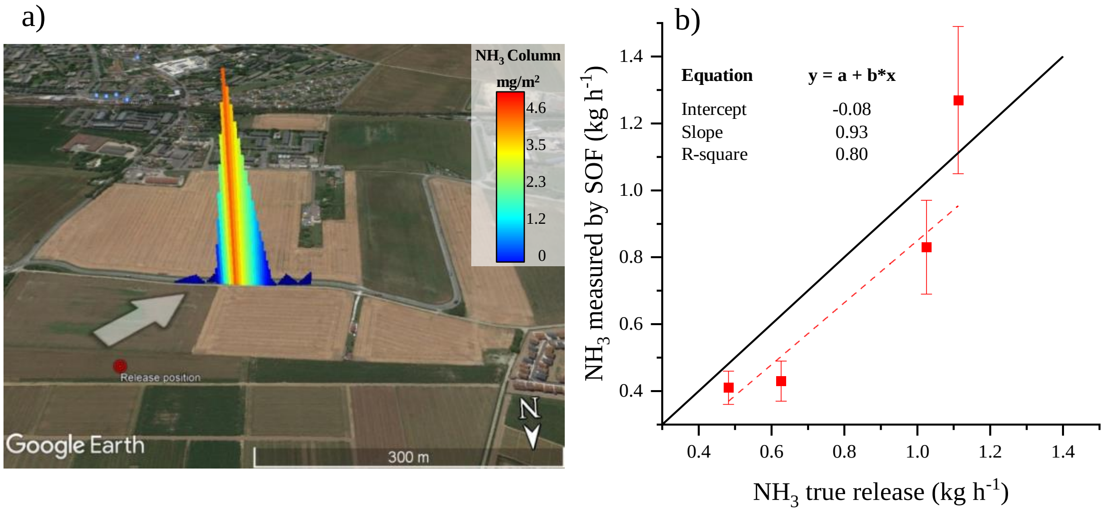

Fig. 8: a) Example of measured plume on the day 22-September at 14:55. The read circle indicated the NH_3 release point, and the arrow shows the wind direction b) True release rates and SOF quantified rates (average ± expanded uncertainty (CI 95 %)). Map source: Google Earth ©

The relative error was between a minimum of -31 % and a maximum of +14 % (Table 3). Additionally, the calculated standard uncertainty (CI 68 %) ranged from 6.4 to 8.7%, and the CI 95% was from 12.7 to 17.5 % (Table 2). The estimated uncertainty explained the error observed only in the first release (Table 3, Fig. 8b), however, within a 5 % difference in the last two releases (last two releases, 1-October). A possible error source is the wind speed measurements as the estimated plume height (Eq. 4) is around 11 to 40 m (Table 3); while the wind data is collected at 10 m high. The wind uncertainty was considered in the budget estimation; however, the vertical wind profile was not measured, which might have limited the analysis.

Table 3: Overview of NH_3 validation experiment.

Date	Measurement distance (m)	Wind speed (m s^{-1}) – Direction	Number of transects	True release rate (kg h^{-1})	SOF emission (kg h^{-1})	Error (%)[a]	Total expanded uncertainty (%)	Estimated H_P (m)
22-September	180-320	3.8 - NE	17	1.11	1.27	14	17.5	~ 40
28-September	180-220	4.2 - SW	34	0.63	0.43	-31	12.7	~ 20
1-October	150-180	5.8 - SW	26	0.48	0.41	-15	12.9	~ 12
1-October	150-180	5.9 - SW	22	1.03	0.83	-19	17.2	~ 11

[a] The error estimated from: 100·(SOF emissions - True release)/True release.

In 75 % of the measurements, the NH_3 SOF quantifications were lower than the actual release, possibly due to NH_3 dry deposition or gas loss in the release system. The NH_3 dry deposition depends on factors such as wind speed, source height, atmospheric stability, surface roughness length, and surface concentrations (Asman, 1998). However, a deep analysis of NH_3 dry deposition was outside the scope. Furthermore, only the measurements in 22-September were higher than the actual release; however, the cloud conditions were not ideal during the measurements in this campaign, which could impact the measurements affecting the light intensity measured.

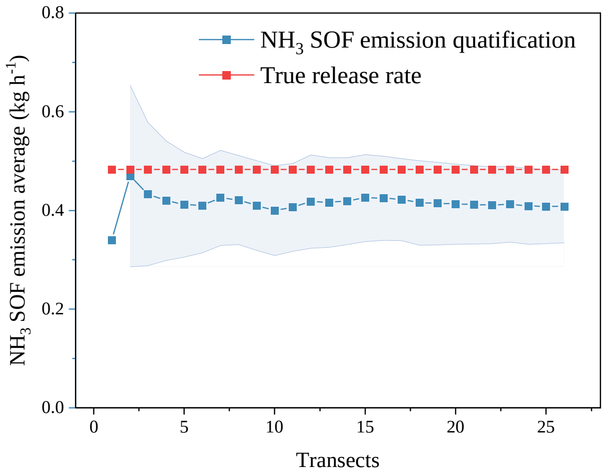

Fig. 9: The differences between measured mean and true emission, in the controlled release performed on 1-October, and the standard deviation (blue shadowed area) according to the number of measured transects.

In Fig. 9, we observe the effect of increasing the number of transects in the averaged measured flux. Random errors are canceled out by increasing the number of transects. After five to six transects, the standard deviation becomes lower and constant. However, there is still a difference between the measured flux (Fig. 9

blue dots) and the actual release (Fig. 9 red line). This error remains even with 25 transects, indicating potential systematic errors.

4.3. Case studies

These case studies were used to demonstrate the applicability of the SOF method for measurements of NH_3 emissions from livestock, considering different production systems and further describing the uncertainty methodology. Table 4 shows a measurement overview, and Fig. 10 shows examples of transects from each measurement campaign. These emissions are snapshots, thus representing only one or two days; therefore, they would not reflect annual emissions.

Table 4: Overview of results for the SOF NH_3 measurements

	C1a	**C1b**	**C2**	**C3a**	**C3b**
Month	October	October	October	May	May
Distance from the center of source (m)	220	800	2500	2000	1000
Measurement interval	09:40-14:30	12:10-16:20	13:30-16:00	12:20-14:00	14:20-17:30
Number of transects	20	14	3	7	13
Avg. wind speed (m s^{-1})	3.1	3.1	4.0	3.0	5.7
Number of animals	600 sows	700 cows	36000[b] cows	-[a]	-[a]
Avg. emission (kg h^{-1})	1.1	2.2	245.0	166.0	142.2
Uncertainty (CI 95 %)	**21.0**	**37.4**	**27.0**	**25.0**	**29.0**
Emission factor (g LU^{-1} h^{-1})	2.4	2.5	6.8		

[a] Unknown numbers. [b] Number of animals obtained from personal correspondence with the California Air and Resources Board (CARB).

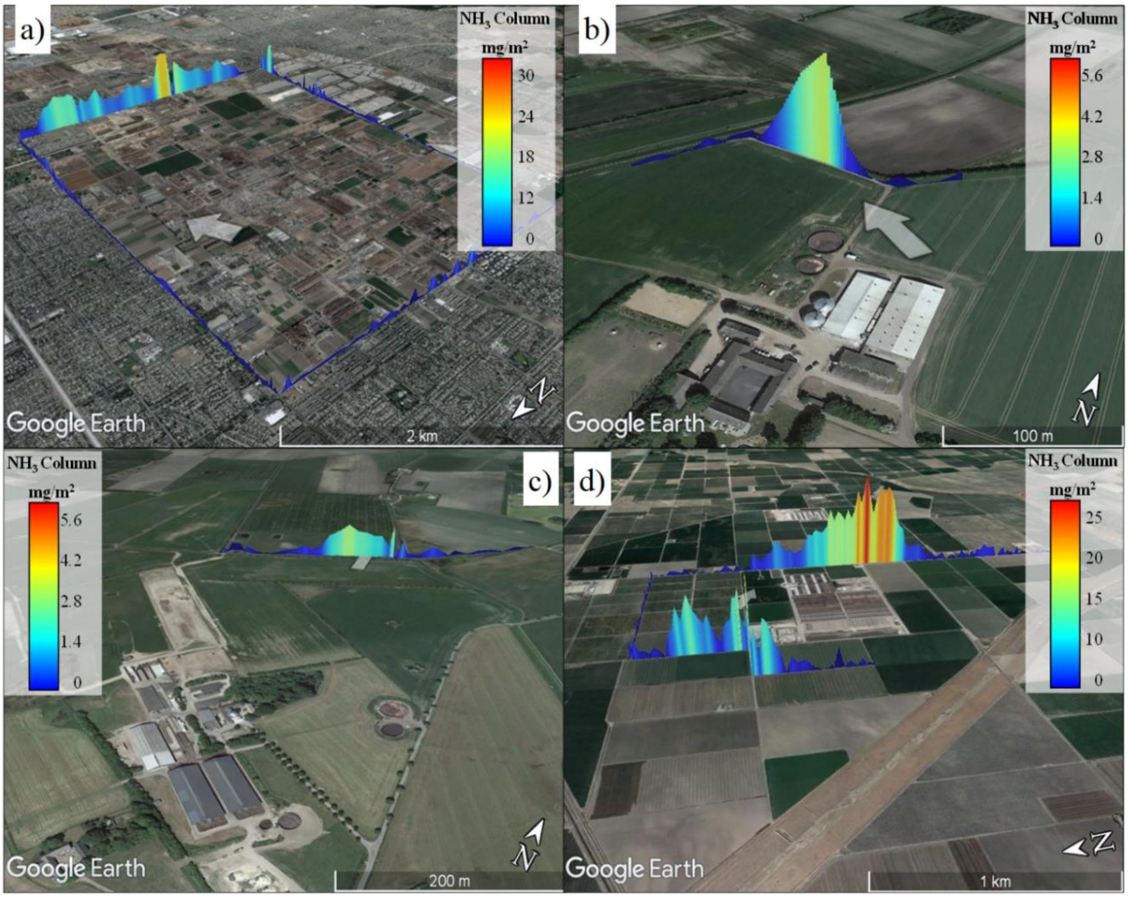

Fig. 10: a) (C2) NH_3 columns measured at Chino made by encircling the feedlots area in a box, the arrow indicates the wind. b) (C1a) Pig farm example (Total farm), flux on the figure corresponded to 0.55 kg/h. c) (C1b) Dairy farm plume example, corresponded flux of 2.52 kg/h. d) (C3) Example of measurement from individual CAFOs, on the upwind from the farm there was emissions from the field. Map source: Google Earth ©

4.3.1. C1 - Small and isolated sources - Pig and dairy single farms (Denmark)

Emissions from small and isolated farms are challenging to measure primarily because of the low emissions, and thus low concentrations that are difficult to measure at a distance from the farm. Total farm NH_3 emissions averaged 1.07 ± 0.23 kg h^{-1} (Avg. and CI 95 %) for pig farms (C1a, Fig. 10b). Thus, SOF could measure concentrations as low as 1 kg/h with an uncertainty of ~ 21%. Emissions were normalized by livestock unit (1 LU = 500 kg of body weight) to obtain an emission factor (EF) of 2.4 ± 0.5 g LU^{-1} h^{-1}, while literature has reported EFs of 1.88 g LU^{-1} h^{-1} for the house only (Rzeźnik and Mielcarek, 2016).

The dairy farm (C1b, Fig. 10c) had averaged emissions of 2.3 ± 0.9 kg h^{-1}, corresponding to an EF of 2.5 ± 0.9 g LU^{-1} h^{-1}. Based on the literature, EF dairy farm houses are expected to have around 1.1 g LU^{-1} h^{-1}, for the house only (Rzeźnik and Mielcarek, 2016). However, the uncertainty on wind speed measurements was relatively high (U_{wind} 32 %) due to limited wind instrumentation. Additionally, there is also the possibility of dry-deposition, due to the large distance between the source and the measurements road (800 m). Furthermore, the obtained rates for C1a and C1b only reflect day-time emissions.

4.3.2. C2 – Box measurements of several sources – Dairy complex (USA)

In case study C2 (Fig. 10a), SOF quantified NH_3 emissions from the Chino dairy complex located in California (USA). The magnitude of emissions was large; however, due to their size (18 km perimeter), it took almost one hour to measure one box transect. Additionally, changes in the wind speed and direction during this time interval will likely increase the measurements' uncertainty.

NH_3 emissions averaged 245.0 ± 66 kg h^{-1}, while the EF was 6.8 g $head^{-1}$ h^{-1}. In comparison with the NH_3 fluxes estimations for this area using IASI retrievals (Van Damme et al., 2018) is similar SOF 4.3 g $head^{-1}$ h^{-1}, ranging from 1.1 - 51 g $head^{-1}$ h^{-1}. In contrast, other studies showed larger EFs as 18.5 to 42 g/head/h (Leifer et al., 2017, 2018) and 14.9 to 79.7 g $head^{-1}$ h^{-1} (Nowak et al., 2012). High fluctuation in NH_3 emissions is expected because they depend on meteorological factors (wind speed, temperature, solar radiation), although some variability might also result from the different techniques used. Here, the measurements estimated uncertainty was 27 %, with the U_{wind} being the largest source of errors.

4.3.3. C3 – Large source surrounded by other sources – Dairy CAFOs (USA)

Another challenging type of facility that the SOF can measure is large-scale individual farms in high farm density areas. The difficulty lies in the interfering sources in the surroundings of the target farms. Therefore upwind or box (encircling the source) measurements were necessary in order to isolate the measured source.

The dairy CAFOs averaged 142 kg h^{-1} for C3b and 165 kg h^{-1} for C3a. The number of animals was unknown; therefore, EFs could not be calculated. Nonetheless, NH_3 emission rates and EFs from this type of facility have been published elsewhere (Vechi et al., 2023).

In C3, the IWP_{avg} and H_p were measured differently from the other campaigns, where these parameters were estimated based on more uncertain calculations. The total expanded uncertainty ranged from 25 to 29 %, and although U_{wind} was lower than the other campaign (11 %), the random uncertainty had a large contribution (9 to 12 %).

5. Conclusions and method application perspective

NH_3 emissions are challenging to quantify due to their high stickiness, which makes it difficult to sample without losses. Additionally, NH_3 quantification might be hampered by interference from fertilizer application and transport emissions or by dry deposition, meaning that concentration is lost within a few meters from the source. These issues must be considered when designing and applying new instruments and methods. The SOF method has advantages over current NH_3 quantification techniques because it offers a contact-free measurement, avoiding issues with the gas adsorption into the gas inlet and instrument interior. Additionally, it has a fast-time response (~5 s) that, combined with the mobility given by the mobile platform, allows for coverage of large areas in a measurement day. Furthermore, SOF measures vertical columns, which is better than ground concentrations, as these might be affected by NH_3 deposition (Lassman et al., 2020). Additionally, SOF columns measured by SOF can be used to validate satellite column measurements, as recently done (Guo et al., 2021). The estimation of measurement uncertainty is essential because it indicates the measurement precision, therefore, when comparing the obtained rates with other literature and models the uncertainty can better indicates whether values are significant different or not.

Nonetheless, measurements are limited by the required weather conditions (sunny sky and low cloud cover); hence, nighttime and weather with heavy clouds are not covered. Additionally, the solar angle required for the measurements leads to limitations on winter measurements at certain latitudes. NH_3 emissions are higher during daytime and sunny conditions; therefore, when using this method to estimate annual emissions or compare to other studies and inventories, the diurnal emission variation must be considered (Lonsdale et al., 2017; Zhu et al., 2015a). This can be done using models that estimate the daily NH_3 variation using meteorological information or other parallel measurements.

Here, the validation test and case studies have shown the SOF method's applicability and the accuracy level that the method can reach as long as best practices are followed. This study demonstrates that wind speed vertical profile is a crucial parameter, which is more easily measured using LIDAR instrument. Additionally, to improve the measurement accuracy and the choice of wind parameters, the plume height should be estimated by combining measurements of ground and column concentrations. Furthermore, the technique was demonstrated to be suitable for large concentrate areas and smaller sources with emissions as low as 1 kg/h, obtaining an uncertainty ranging from 21 to 37 %.

References

Asman, W. A. H.: Factors influencing local dry deposition of gases with special reference to ammonia, Atmos. Environ., 32(3), 415–421, doi:10.1016/S1352-2310(97)00166-0, 1998.

Van Damme, M., Clarisse, L., Whitburn, S., Hadji-Lazaro, J., Hurtmans, D., Clerbaux, C. and Coheur, P. F.: Industrial and agricultural ammonia point sources exposed, Nature, 564(7734), 99–103, doi:10.1038/s41586-018-0747-1, 2018.

EDGAR database: EDGAR - Emissions Database for Global Atmospheric Research Air and Toxic pollutants, [online] Available from: https://edgar.jrc.ec.europa.eu/air_pollutants, 2023.

Eilerman, S. J., Peischl, J., Neuman, J. A., Ryerson, T. B., Aikin, K. C., Holloway, M. W., Zondlo, M. A., Golston, L. M., Pan, D., Floerchinger, C. and Herndon, S.: Characterization of Ammonia, Methane, and Nitrous Oxide Emissions from Concentrated Animal Feeding Operations in Northeastern Colorado, Environ. Sci. Technol., 50(20), 10885–10893, doi:10.1021/acs.est.6b02851, 2016.

European standard: EN 17628:2022, [online] Available from: https://www.sis.se/api/document/preview/80034943/, 2022.

Galle, B. O., Samuelsson, J., Svensson, B. H. and Borjesson, G.: Measurements of methane emissions from landfills using a time correlation tracer method based on FTIR absorption spectroscopy, Environ. Sci. Technol., 35(1), 21–25, doi:10.1021/es0011008, 2001.

Galloway, J. N., Aber, J. D., Erisman, J. W., Seitzinger, S. P., Howarth, R. W., Cowling, E. B. and Cosby, B. J.: The nitrogen cascade, Bioscience, 53(4), 341–356, doi:10.1641/0006-3568(2003)053[0341:TNC]2.0.CO;2, 2003.

Golston, L. M., Pan, D., Sun, K., Tao, L., Zondlo, M. A., Eilerman, S. J., Peischl, J., Neuman, J. A. and Floerchinger, C.: Variability of Ammonia and Methane Emissions from Animal Feeding Operations in Northeastern Colorado, Environ. Sci. Technol., 54(18), 11015–11024, doi:10.1021/acs.est.0c00301, 2020.

Griffith, D. W. T.: Synthetic calibration and quantitative analysis of gas-phase FT-IR spectra, Appl. Spectrosc., 50(1), 59–70, doi:10.1366/0003702963906627, 1996.

Guo, X., Wang, R., Pan, D., Zondlo, M. A., Clarisse, L., Van Damme, M., Whitburn, S., Coheur, P. F., Clerbaux, C., Franco, B., Golston, L. M., Wendt, L., Sun, K., Tao, L., Miller, D., Mikoviny, T., Müller, M., Wisthaler, A., Tevlin, A. G., Murphy, J. G., Nowak, J. B., Roscioli, J. R., Volkamer, R., Kille, N., Neuman, J. A., Eilerman, S. J., Crawford, J. H., Yacovitch, T. I., Barrick, J. D. and Scarino, A. J.: Validation of IASI Satellite Ammonia Observations at the Pixel Scale Using In Situ Vertical Profiles, J. Geophys. Res. Atmos., 126(9), doi:10.1029/2020JD033475, 2021.

Hristov, A. N., Hanigan, M., Cole, A., Todd, R., McAllister, T. A., Ndegwa, P. M. and Rotz, A.: Review: Ammonia emissions from dairy farms and beef feedlots, Can. J. Anim. Sci., 91(1), 1–35, doi:10.4141/CJAS10034, 2011.

Huang, X., Song, Y., Li, M., Li, J., Huo, Q., Cai, X., Zhu, T., Hu, M. and Zhang, H.: A high-resolution ammonia emission inventory in China, Global Biogeochem. Cycles, 26(1), 1–14, doi:10.1029/2011GB004161, 2012.

Johansson, J., Mellqvist, J., Samuelsson, J., Offerle, B., Andersson, P., Lefer, B., Flynn, J. and Zhuoyan, S.: Quantification of industrial emissions of VOCs, NO2 and SO2 by SOF and Mobile DOAS during DISCOVER-AQ., , (2), 1–71 [online] Available from: http://aqrp.ceer.utexas.edu/projectinfoFY12_13%5C13-005%5C13-005%0AFinal%0AReport.pdf, 2013.

Johansson, J., Mellqvist, J., Samuelsson, J., Offerle, B., Lefer, B., Rappenglück, B., Flynn, J. and Yarwood, G.: Emission measurements of alkenes, alkanes, SO2 and NO2 from stationary sources in southeast Texas over a 5 year period using SOF and Mobile DOAS, J. Geophys. Res., (x), 1–8, doi:10.1002/2013JD021350.Received, 2014.

Joint Committee For Guides In Metrology: Evaluation of measurement data — Guide to the expression of uncertainty in measurement, Int. Organ. Stand. Geneva ISBN, 50(September), 134 [online] Available from: http://www.bipm.org/en/publications/guides/gum.html, 2008.

Kihlman, M.: Application of Solar FTIR Spectroscoy for Quantingfying Gas Emissions, Chalmers University of Technology, Gothenburg, Sweden., 2005.

Kille, N., Baidar, S., Handley, P., Ortega, I., Sinreich, R., Cooper, O. R., Hase, F., Hannigan, J. W., Pfister, G. and Volkamer, R.: The CU mobile Solar Occultation Flux instrument: Structure functions and emission rates of NH3, NO2 and C2H6, Atmos. Meas. Tech., 10(1), 373–392, doi:10.5194/amt-10-373-2017, 2017.

Kleiner, I., Tarrago, G., Cottaz, C., Sagui, L., Brown, L. R., Poynter, R. L., Pickett, H. M., Chen, P., Pearson, J. C., Sams, R. L., Blake, G. A., Matsuura, S., Nemtchinov, V., Varanasi, P., Fusina, L. and Di Lonardo, G.: NH3 and PH3 line parameters: The 2000 HITRAN update and new results, J. Quant. Spectrosc. Radiat. Transf., 82(1–4), 293–312, doi:10.1016/S0022-4073(03)00159-6, 2003.

Lassman, W., Collett, J. L., Ham, J. M., Yalin, A. P., Shonkwiler, K. B. and Pierce, J. R.: Exploring new methods of estimating deposition using atmospheric concentration measurements: A modeling case study of ammonia downwind of a feedlot, Agric. For. Meteorol., 290(April 2019), doi:10.1016/j.agrformet.2020.107989, 2020.

Leifer, I., Melton, C., Tratt, D. M., Buckland, K. N., Clarisse, L., Coheur, P., Frash, J., Gupta, M., Johnson, P. D., Leen, J. B., Van Damme, M., Whitburn, S. and Yurganov, L.: Remote sensing and in situ measurements of methane and ammonia emissions from a megacity dairy complex: Chino, CA, Environ. Pollut., 221, 37–51, doi:10.1016/j.envpol.2016.09.083, 2017.

Leifer, I., Melton, C., Tratt, D. M., Buckland, K. N., Chang, C. S., Frash, J., Hall, J. L., Kuze, A., Leen, B., Clarisse, L., Lundquist, T., Van Damme, M., Vigil, S., Whitburn, S. and Yurganov, L.: Validation of mobile in situ measurements of dairy husbandry emissions by fusion of airborne/surface remote sensing with seasonal context from the Chino Dairy Complex, Environ. Pollut., 242, 2111–2134, doi:10.1016/j.envpol.2018.03.078, 2018.

Lonsdale, C. R., Hegarty, J. D., Cady-pereira, K. E., Alvarado, M. J., Henze, D. K., Turner, M. D., Capps, S. L., Nowak, J. B., Neuman, J. A., Middlebrook, A. M., Bahreini, R., Murphy, J. G., Markovic, M. Z., Vandenboer, T. C. and Russell, L. M.: Modeling the diurnal variability of agricultural ammonia in Bakersfield , California , during the CalNex campaign, , 3, 2721–2739, doi:10.5194/acp-17-2721-2017, 2017.

Mellqvist, J., Samuelsson, J. and Rivera, C.: HARC Project H-53 Measurements of industrial emissions of VOCs , NH 3 , NO 2 and SO 2 in Texas using the Solar Occultation Flux method and mobile DOAS, , 2007(2), 1–69, 2007.

Mellqvist, J., Samuelsson, J., Johansson, J., Rivera, C., Lefer, B., Alvarez, S. and Jolly, J.: Measurements of industrial emissions of alkenes in Texas using the solar occultation flux method, J. Geophys. Res., 115, D00F17, doi:10.1029/2008JD011682, 2010.

Miller, D. J., Sun, K., Tao, L., Pan, D., Zondlo, M. A., Nowak, J. B., Liu, Z., Diskin, G., Sachse, G., Beyersdorf, A., Ferrare, R. and Scarino, A. J.: Ammonia and methane dairy emission plumes in the San Joaquin valley of California from individual feedlot to regional scales, J. Geophys. Res., 120(18), 9718–9738, doi:10.1002/2015JD023241, 2015.

Nowak, J. B., Neuman, J. A., Bahreini, R., Middlebrook, A. M., Holloway, J. S., McKeen, S. A., Parrish, D. D., Ryerson, T. B. and Trainer, M.: Ammonia sources in the California South Coast Air Basin and their impact on ammonium nitrate formation, Geophys. Res. Lett., 39(7), 6–11, doi:10.1029/2012GL051197, 2012.

Rzeźnik, W. and Mielcarek, P.: Greenhouse gases and ammonia emission factors from livestock buildings for pigs and dairy cows, Polish J. Environ. Stud., 25(5), 1813–1821, doi:10.15244/pjoes/62489, 2016.

Sun, K., Tao, L., Miller, D. J., Zondlo, M. A., Shonkwiler, K. B., Nash, C. and Ham, J. M.: Open-path eddy covariance measurements of ammonia fluxes from a beef cattle feedlot, Agric. For. Meteorol., 213, 193–202, doi:10.1016/j.agrformet.2015.06.007, 2015a.

Sun, K., Cady-Pereira, K., Miller, D. J., Tao, L., Zondlo, M. A., Nowak, J. B., Neuman, J. A., Mikoviny, T., Müller, M., Wisthaler, A., Scarino, A. J. and Hostetler, C. A.: Validation of TES ammonia observations at the single pixel scale in the san joaquin valley during DISCOVER-AQ, J. Geophys. Res.,

120(10), 5140–5154, doi:10.1002/2014JD022846, 2015b.
Tucker, S. C., Brewer, W. A., Banta, R. M., Senff, C. J., Sandberg, S. P., Law, D. C., Weickmann, A. M. and Hardesty, R. M.: Doppler lidar estimation of mixing height using turbulence, shear, and aerosol profiles, J. Atmos. Ocean. Technol., 26(4), 673–688, doi:10.1175/2008JTECHA1157.1, 2009.
Twigg, M. M., Berkhout, A. J. C., Cowan, N., Crunaire, S., Dammers, E., Ebert, V., Gaudion, V., Haaima, M., Häni, C., John, L., Jones, M. R., Kamps, B., Kentisbeer, J., Kupper, T., Leeson, S. R., Leuenberger, D., Lüttschwager, N. O. B., Makkonen, U., Martin, N. A., Missler, D., Mounsor, D., Neftel, A., Nelson, C., Nemitz, E., Oudwater, R., Pascale, C., Petit, J. E., Pogany, A., Redon, N., Sintermann, J., Stephens, A., Sutton, M. A., Tang, Y. S., Zijlmans, R., Braban, C. F. and Niederhauser, B.: Intercomparison of in situ measurements of ambient NH3: Instrument performance and application under field conditions, Atmos. Meas. Tech., 15(22), 6755–6787, doi:10.5194/amt-15-6755-2022, 2022.
Vechi, N. T., Mellqvist, J., Samuelsson, J., Offerle, B. and Scheutz, C.: Ammonia and methane emissions from dairy concentrated animal feeding operations in California, using mobile optical remote sensing, Atmos. Environ., 293, 119448, doi:10.1016/j.atmosenv.2022.119448, 2023.
Wyer, K. E., Kelleghan, D. B., Blanes-Vidal, V., Schauberger, G. and Curran, T. P.: Ammonia emissions from agriculture and their contribution to fine particulate matter: A review of implications for human health, J. Environ. Manage., 323(July), 116285, doi:10.1016/j.jenvman.2022.116285, 2022.
Zhu, L., Henze, D., Bash, J., Jeong, G. R., Cady-Pereira, K., Shephard, M., Luo, M., Paulot, F. and Capps, S.: Global evaluation of ammonia bidirectional exchange and livestock diurnal variation schemes, Atmos. Chem. Phys., 15(22), 12823–12843, doi:10.5194/acp-15-12823-2015, 2015a.
Zhu, L., Henze, D. K., Bash, J. O., Cady-Pereira, K. E., Shephard, M. W., Luo, M. and Capps, S. L.: Sources and Impacts of Atmospheric NH3: Current Understanding and Frontiers for Modeling, Measurements, and Remote Sensing in North America, Curr. Pollut. Reports, 1(2), 95–116, doi:10.1007/s40726-015-0010-4, 2015b.

Supplementary material

An uncertainty methodology for Solar Occultation Flux measurements: ammonia emissions from agriculture

Johan Mellqvist[1], Nathalia T. Vechi[1,2], Charlotte Scheutz[2], Marc Durif[4], Francois Gautier[4], John Johansson[3], Jerker Samuelsson[3], Brian Offerle[3] and Samuel Brohede[3]

[1]Department of Space, Earth and Environment, Chalmers University of Technology, Göteborg, Sweden
[2]Department of Environmental Engineering, Technical University of Denmark, Lyngby, Denmark
[3]Fluxsense AB, Göteborg, Sweden
[4]INERIS, Verneuil-en-Halatte, France

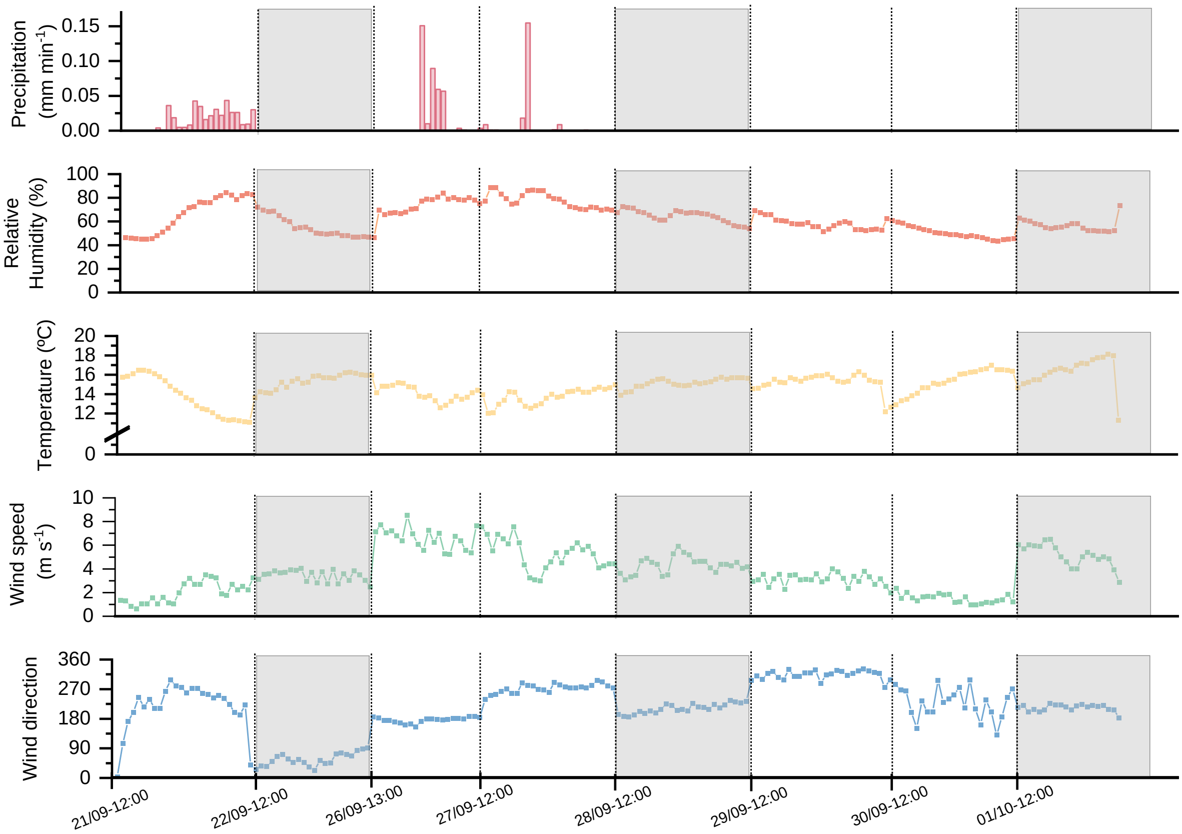

Figure S1: Weather information in the validation campaign. The information corresponds to measurements from only 12:00 to 18:00, approximately. The shadowed graphs corresponds to the measurement days.

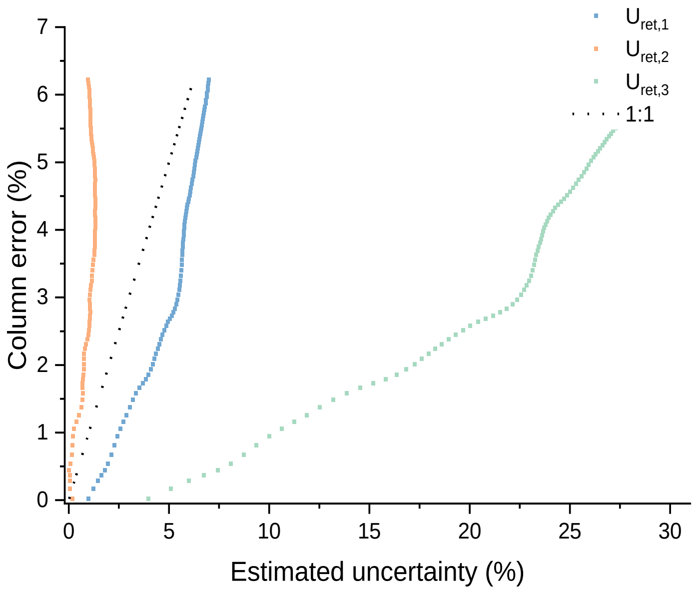

Figure S2: Error introduced by varying the wavenumber shift of -0.2 + 0.2 cm^{-1}.

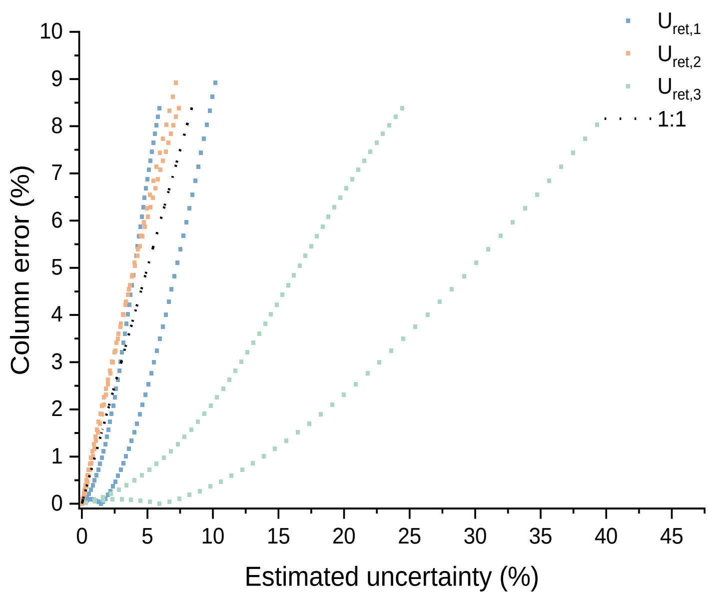

Figure S3: Error introduced by varying the resolution scale.

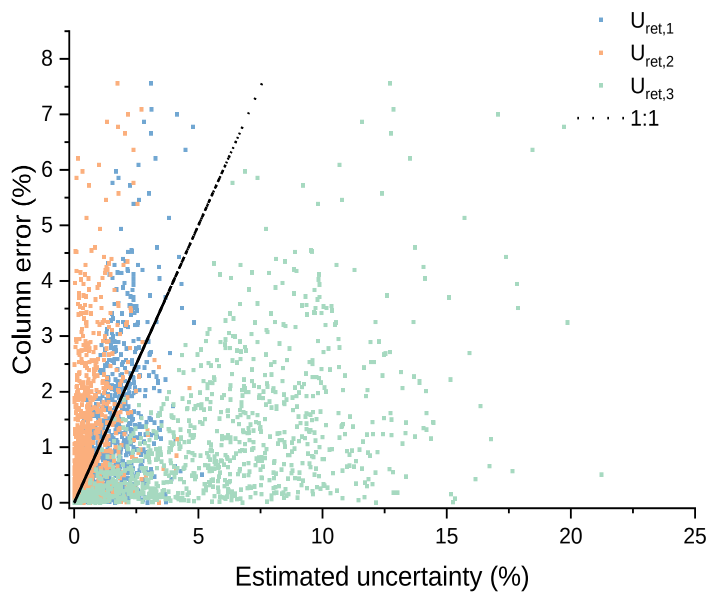

Figure S4: Error introduced by multiplying the cross sections by 1 + normal distributed noise with the standard deviation varied from 0 to 0.1.

Department of Environmental and Resource Engineering is one of the largest university departments specializing in environmental and resource engineering in Europe. The department conducts research, development & scientific advice and provides educational programs and service to society. We are working to develop new environmentally friendly and sustainable technologies, methods and solutions, and to disseminate this knowledge to society and future generations of engineers. The Department has approximately 300 staff of more than 30 nationalities.

Department of Environmental and Resource Engineering

Bygningstorvet, Building 115
2800 Kgs. Lyngby
Tlf. +45 4525 1600

www.sustain.dtu.dk